2018

Neural Circuits Controlling Circadian Rhythms

Anna King
University of Pennsylvania, annakk2@gmail.com

Neural Circuits Controlling Circadian Rhythms

Abstract
A central question in the circadian biology field is how ~24-hour oscillations of the molecular clock are translated into overt rhythms of behavior and physiology. Drosophila melanogaster is a powerful system that provided the first understanding of how molecular clocks are generated, and now the neural basis of circadian rhythms. In the Drosophila brain, there are about ~150 clock neurons that collectively are responsible for timekeeping. This thesis addresses how time-of-day signals are transmitted from the clock neurons to output circuits that drive overt rhythms. This work used a genetic approach to identify genes and circuits that regulate two output rhythms: peripheral transcriptional rhythms and brain-controlled behavioral rhythms. We showed that a specific group of clock neurons, LNds, and neuropeptide F signaling regulate transcriptional rhythms in a peripheral tissue called the fat body. We also built on previous work to map a multisynaptic circuit that regulates behavioral rest:activity rhythms. The rest:activity circuit extends from the central clock neurons, s-LNvs, through multiple neuropeptidergic output neurons to motor centers. The circadian output circuit we have mapped not only receives circadian (time-of-day) signals but also signals that drive the need to sleep. This thesis provides neural bases for the regulation of circadian rhythms and highlights the different and intersecting circuits that ensure behavior and physiology occur at optimal times of day.

Degree Type
Dissertation

Degree Name
Doctor of Philosophy (PhD)

Graduate Group
Cell & Molecular Biology

First Advisor
Amita Sehgal

Subject Categories
Genetics | Neuroscience and Neurobiology

NEURAL CIRCUITS CONTROLLING CIRCADIAN RHYTHMS

Anna King

A DISSERTATION

in

Cell and Molecular Biology

Presented to the Faculties of the University of Pennsylvania

in

Partial Fulfillment of the Requirements for the

Degree of Doctor of Philosophy

2018

Supervisor of Dissertation

_____

Amita Sehgal, Ph.D.
John Herr Musser Professor of Neuroscience
Investigator, HHMI

Graduate Group Chairperson

_____

Daniel Kessler, Ph.D.
Associate Professor of Cell and Developmental Biology

Dissertation Committee

Thomas Jongens, Ph.D.; Associate Professor of Genetics

Greg Bashaw, Ph.D.; Professor of Neuroscience

Marc Fuccillo, M.D., Ph.D.; Assistant Professor of Neuroscience

David Raizen, M.D., Ph.D.; Associate Professor of Neurology

NEURAL CIRCUITS CONTROLLING CIRCADIAN RHYTHMS

ACKNOWLEDGMENT

I am indebted to my thesis advisor, Amita Sehgal. Thank you for your guidance, support, and encouragement throughout my PhD studies. Her enthusiasm in our work helped keep me going through difficult spots. Thanks for allowing me to come up with my ideas and answers but also providing me the answers sometimes. Thanks for thinking I am worthwhile and that my work is worthwhile. To me, Amita is my professional role model, and I am truly lucky to have her as an outstanding mentor.

I want to thank my lab mates. Thanks to Renske Erion for our collaboration on Chapter 2. My gratitude extends to Daniel Cavanaugh for our collaboration and for providing me mentorship and training during my early years in the lab. Thanks to Annika Barber for our collaboration and discussions on all things related circadian circuits. Thanks to Lei Bai for training in fly genetics. Thanks to Paula Haynes for help with functional imaging experiments. To all Sehgal lab members, past and present, thank you for the years of mutual support, insightful discussions, and fun growing sundews.

I want to thank the members of my thesis committee, Thomas Jongens, Greg Bashaw, Marc Fucillio, and David Raizen for their advice and encouragement over the years.

Thanks to Steve DiNardo for being an outstanding leader of the DSRB program and for providing thoughtful advice that has helped me navigate my PhD. Thanks to Doug Epstein for his mentorship and leading the training grant in Genetics that I was lucky to be part of.

During my PhD, I was supported in part by funding from the National Institute of Health.

Finally, thanks to my parents for their continuous support throughout my studies.

ABSTRACT

NEURAL CIRCUITS CONTROLLING CIRCADIAN RHYTHMS

Anna King

Amita Sehgal

A central question in the circadian biology field is how ~24-hour oscillations of the molecular clock are translated into overt rhythms of behavior and physiology. *Drosophila melanogaster* is a powerful system that provided the first understanding of how molecular clocks are generated, and now the neural basis of circadian rhythms. In the *Drosophila* brain, there are about ~150 clock neurons that collectively are responsible for timekeeping. This thesis addresses how time-of-day signals are transmitted from the clock neurons to output circuits that drive overt rhythms. This work used a genetic approach to identify genes and circuits that regulate two output rhythms: peripheral transcriptional rhythms and brain-controlled behavioral rhythms. We showed that a specific group of clock neurons, LNds, and neuropeptide F signaling regulate transcriptional rhythms in a peripheral tissue called the fat body. We also built on previous work to map a multisynaptic circuit that regulates behavioral rest:activity rhythms. The rest:activity circuit extends from the central clock neurons, s-LNvs, through multiple neuropeptidergic output neurons to motor centers. The circadian output circuit we have mapped not only receives circadian (time-of-day) signals but also signals that drive the need to sleep. This thesis provides neural bases for the regulation of circadian rhythms and highlights the different and intersecting circuits that ensure behavior and physiology occur at optimal times of day.

TABLE OF CONTENTS

LIST OF TABLES

LIST OF FIGURES

Chapter 1 : Introduction

This introduction consists of two parts. The first part will cover current knowledge of molecular and circuit mechanisms underlying circadian clock output in the *Drosophila* brain. The second part will briefly review our understanding of how central circadian clocks control circadian rhythms in peripheral tissues.

Part 1 : Circadian output circuits in *Drosophila* brain

Submitted as: Anna N. King and Amita Sehgal (2018) “Molecular and circuit mechanisms mediating circadian clock output in the *Drosophila* brain.” *European Journal of Neuroscience.*

Abstract

A central question in the circadian biology field concerns the mechanisms that translate ~24-hour oscillations of the molecular clock into overt rhythms. *Drosophila melanogaster* is a powerful system that provided the first understanding of how molecular clocks are generated and is now illuminating the neural basis of circadian behavior. The identity of ~150 clock neurons in the *Drosophila* brain and their roles in shaping circadian rhythms of locomotor activity have been described before. This review summarizes mechanisms that transmit time-of-day signals from the clock, within the clock network as well as downstream of it. We also discuss the identification of functional multisynaptic circuits between clock neurons and output neurons that regulate locomotor activity.

Introduction

Circadian (~24 hour) rhythms allow animals to anticipate daily changes in their environment and coordinate their behavior and physiology with time of day. These rhythms are generated by an internal timing mechanism, which is synchronized to environmental cycles of light and temperature imposed by the rotation of earth. In its simplest form, a circadian system is modeled with three basic components: the clock, input pathways, and output pathways. The clock maintains ~24-hour rhythms even in constant darkness. Input pathways synchronize the clock to external signals such as light. Output pathways receive and translate circadian signals from the clock to produce biological rhythms.

Much of our molecular knowledge of circadian clocks came from genetic studies in the fruit fly, *Drosophila melanogaster*. In flies, circadian rhythms are typically studied using locomotor activity as the output. Under a 12-hour light:12-hour dark cycle, the fly exhibits a bimodal pattern in locomotor activity, with activity peaks anticipating the light-to-dark (evening) and dark-to-light (morning) transitions. Locomotor activity rhythms are dependent on internal clocks and persist in constant darkness (DD), albeit with a different pattern. In DD, the fly's locomotor activity free-runs with the periodicity of the endogenous clock, which is about (but usually not exactly) 24-hours,

such that activity each day generally occurs during the subjective day and rest occurs during the subjective night. Besides rest:activity rhythms, flies also exhibit rhythms in eclosion (emergence of adult flies from pupae), feeding, temperature preference, and sleep. Besides behavior, there are circadian rhythms at the cellular level, such as electrical activity of neurons, gene expression, and metabolic processes. A basic molecular clock mechanism regulates all output rhythms. One of the mysteries in circadian biology is how molecular clock oscillations are translated into diverse behavioral and physiological rhythms.

Here, we review output mechanisms of the circadian clock in the *Drosophila* brain. We will start by describing the circadian clock network and the output mechanisms that occur within the network. Then, we will move beyond the circadian clock network and review recent work that identified output circuits regulating circadian rhythms of behavior and physiology.

The circadian clock network in *Drosophila* brain

The basic molecular oscillator in eukaryotes consists of transcriptional activators and repressors in a feedback loop. In *Drosophila*, the co-activator complex, CLOCK-CYCLE, drives transcription of the co-repressors, *period* (*per*) and *timeless* (*tim*). Accumulated PER and TIM proteins feed back to inhibit CLOCK-CYCLE activity. Delays are built into the basic molecular oscillator at multiple steps, and include post-transcriptional and post-translational mechanisms, which ensure 24-hr rhythms in PER and TIM expression [reviewed in (Zheng and Sehgal 2012)].

Oscillations in the circadian clock are self-sustained. However, the clock is usually synchronized to external cues through a process called entrainment, which is crucial for adaption to the environment [reviewed in (Yoshii, Hermann-Luibl, and Helfrich-Förster 2016)]. Light is the primary entrainment cue, and in flies it involves a dedicated circadian photoreceptor, Cryptochrome (CRY). Upon light exposure, CRY binds TIM and targets TIM for ubiquitination by the E3 ligase, JETLAG, and then degradation. In addition to the CRY mechanism, light-input circuits from the visual system to the central clock neurons are also important for light entrainment.

In the *Drosophila* brain, there are ~150 clock neurons subdivided into six groups based on neuroanatomy. The six groups of PER-TIM-expressing neurons include the large and small ventral lateral neurons (l-LNvs and s-LNvs), the dorsal lateral neurons (LNds), the lateral posterior neurons (LPN), and three groups of dorsal neurons (DN1, DN2 and DN3) (Figure 1.1) (M. Kaneko and Hall 2000; Charlotte Helfrich-Förster, Yoshii, et al. 2007). Clock neurons between and within groups use a heterogenous set of neuropeptides and neurotransmitters for signaling [reviewed in (Beckwith and Ceriani 2015)].

The LNvs are comprised of two groups of neurons, s-LNvs and l-LNvs, and are genetically identified by expression of neuropeptide Pigment-Dispersing Factor (PDF) (Charlotte Helfrich-Förster 1995). There are four s-LNvs and four l-LNvs in each hemisphere of the fly brain. An additional pair of cells called the "5th s-LNvs" also expresses a molecular clock but is PDF-negative. The *Pdf*$^{+}$ LNvs hold an important role in regulating rest:activity rhythms. Flies with ablated or electrically silenced LNvs have arrhythmic rest:activity behavior in DD (Renn et al. 1999; Nitabach, Blau, and Holmes 2002; Depetris-Chauvin et al. 2011), and *per* null mutant flies with *per* restored in LNvs display normal rest:activity rhythms in DD (Grima et al. 2004).

Although the *Pdf*$^{+}$ LNvs appear to have the primary role, robust rest:activity rhythms are a result of clock network coordination. When molecular clocks in the network are mismatched with one another, arrhythmicity, complex rhythms (comprised of multiple rhythmic components of different period lengths), or weak rest:activity rhythms emerge in the fly behavior (Yao and Shafer 2014). The network is often simply modeled as a system of dual oscillators, where oscillators in *Pdf*$^{+}$ LNvs control the morning peak of locomotor activity, and oscillators in LNds and the 5th s-LNv control the evening peak (Grima et al. 2004; Stoleru et al. 2004; Guo et al. 2014). The LNd group is comprised of six neurons per hemisphere. Blocking neurotransmission from a LNd subset results in a large proportion of arrhythmic flies in DD (Guo et al. 2014). In addition, molecular clocks in a subset of LNds drive transcriptional rhythms of a set of metabolic genes in the fat body, a peripheral tissue analogous to adipose/liver tissue, through Neuropeptide F signaling (Erion et al. 2016).

The DN1 group is comprised of 2 anterior (DN1a) and 15 posterior (DN1p) neurons. DN1ps serve diverse functions as integrators of light, temperature, and circadian cues as well as effectors of locomotor activity, sleep, and mating. DN1s have molecular clocks that can be entrained to temperature (Yoshii, Hermann, and Helfrich-Förster 2010). Calcium (Ca^{2+}) activity in DN1ps is also regulated by temperature (Guo et al. 2016; Yadlapalli et al. 2018). DN1ps integrate temperature and light information to promote robust rest:activity rhythms (L. Zhang et al. 2010; Y. Zhang et al. 2010) and also regulate sleep at specific times of day, through different circuits using either DH31 neuropeptide or glutamate signaling (Kunst et al. 2014; Guo et al. 2016). In addition, DN1ps mediate rhythms in male sex drive (Fujii, Emery, and Amrein 2017).

The DN2s also have temperature-entrainable molecular clocks and regulate rhythms of temperature preference, namely the tendency of flies to seek different temperatures at different times of day (Yoshii, Hermann, and Helfrich-Förster 2010; H. Kaneko et al. 2012). A circuit for temperature preference at dawn has been mapped from the thermosensory anterior cells to s-LNvs to DN2s (Tang et al. 2017). The molecular clocks in LPNs are also strongly synchronized to temperature cycles (Miyasako, Umezaki, and Tomioka 2007).

Finally, glial cells in the brain also express PER and TIM (Zerr et al. 1990). Astrocytes are important for rest:activity rhythms, although the molecular clock in these cells is dispensable (Ng, Tangredi, and Jackson 2011). Glial cells are proposed to regulate outputs of clock neurons, but the signaling mechanisms remain to be uncovered (Ng and Jackson 2015; Herrero, Duhart, and Ceriani 2017). In the *Drosophila* blood-brain barrier (BBB), molecular clocks in glial cells drive circadian rhythms in BBB permeability (S. L. Zhang et al. 2018).

PDF is an important clock output factor in the clock network

In the clock network, pigment-dispensing factor (PDF) is an important clock output factor [reviewed in (Shafer and Yao 2014)]. Loss or overexpression of *Pdf* causes arrhythmic rest:activity behavior (Renn et al. 1999; Charlotte Helfrich-Förster et al. 2000), and mutations in the PDF receptor (PDFR) phenocopy *Pdf* mutants (Mertens et al. 2005; Lear, Merrill, et al. 2005; Hyun et al. 2005). PDFR is a G-protein coupled receptor that activates cAMP production upon

binding of PDF peptide. An important function of PDF/PDFR signaling is to maintain coherent and synchronized molecular oscillations in the clock network (Yoshii et al. 2009; Lin, Stormo, and Taghert 2004). All the groups of clock neurons, except the l-LNvs, express PDFR and respond to PDF application (Shafer et al. 2008; Im and Taghert 2010). Since PDFR in also expressed in *Pdf*$^{+}$ s-LNv, PDF may feed back to cell-autonomously regulate the clock itself or output from the clock (Choi et al. 2012). Outside the clock network, PDFR expression is low (Im and Taghert 2010). PDF does signal to non-clock neurons implicated in behavior (Pírez, Christmann, and Griffith 2013; J. Chen et al. 2016), but it is unclear whether PDF signaling in these circuits confers circadian timing to behavior.

PDF levels cycle across the day at s-LNv terminals in the dorsal protocerebrum, indicating that PDF may be secreted in a circadian manner (Park et al. 2000). In addition, *Pdf* mRNA levels are regulated by the molecular clock (Blau and Young 1999; Mezan et al. 2016; Gunawardhana and Hardin 2017). However, it is unclear whether rhythmic PDF levels or secretion are important for rest:activity rhythms (Kula et al. 2006). Instead, rhythmic PDF levels in the s-LNv terminals may be a secondary consequence of rhythmic neuronal firing or remodeling of the projections (discussed below). Furthermore, rhythmic PDF signaling may also occur through circadian-gated sensitivity to PDF in target neurons, mediated by PDFR and a small GTPase, Ral A (Klose et al. 2016). In summary, PDF is important for circadian rhythms, and its effect on circadian behavior is largely localized within the clock network.

Glycine and glutamate mediate reciprocal inhibition between the s-LNvs and DN1ps

Compared to neuropeptides, less is known about fast neurotransmitters in the clock network. However, within the s-LNv-DN1p circuit, the inhibitory neurotransmitter, glycine, is used in addition to PDF (Frenkel et al. 2017). Knockdown of the glycine transporter or disrupting glycine synthesis in the *Pdf*$^{+}$ LNvs lengthens the period of rest:activity rhythms, suggesting LNvs are glycinergic. In addition, glycine application on DN1ps reduces their firing frequency, and knockdown of glycine receptors subunits in the DN1ps reduces the power of rest:activity rhythms in flies, confirming functional glycine signaling in the s-LNv to DN1 circuit.

In the reciprocal direction, DN1ps signal to the s-LNvs through glutamate, an inhibitory neurotransmitter in flies (Hamasaka et al. 2007; Guo et al. 2016). A subset of the DN1ps expresses vesicular glutamate transporter (VGlut), and s-LNvs and LNds express the metabotropic glutamate receptor, mGluRA. Consistent with an inhibitory effect, glutamate application decreases Ca^{2+} in s-LNvs and LNds. Glutamate signaling is also relevant for behavioral rhythms—glutamate from non-LNv clock neurons is required for robust rest:activity rhythms and knockdown of *mGluRA* in *Pdf*$^{+}$ LNvs lengthens the period of rest:activity rhythms (Hamasaka et al. 2007; Collins et al. 2012)

Neuropeptides sNPF and PDF set different phases of Ca^{2+} rhythms in clock network

Intercellular signaling is not only essential for synchronizing molecular clock rhythms but also coordinating neuronal activity rhythms in the clock network. It is thought that the molecular clock regulates the excitability of clock neurons, such that the neurons are more active at certain times of day than other times. Electrophysiological recordings from s-LNv, l-LNv, and DN1 have shown that the molecular clock drives these cells to be more active at dawn than at dusk (Table 1.1) (Sheeba, Gu, et al. 2008; Cao and Nitabach 2008; Flourakis et al. 2015). Recent studies use genetically encoded Ca^{2+} sensors to perform longitudinal imaging of neuronal activity in the entire clock network over 24 hours, with the added advantages of obtaining more temporal information and precise determination of when clock neurons are most active (Liang, Holy, and Taghert 2016; Liang, Holy, and Taghert 2017). We review this work reported in a pair of papers by Liang, Holy, and Taghert.

Intracellular calcium (Ca^{2+}) ions are important secondary messengers for many signaling pathways, and Ca^{2+} levels rise during electrical activity in neurons. In circadian regulation, Ca^{2+} signaling is both an input and output of the molecular clock (Harrisingh et al. 2007; Ikeda 2004), with all groups of clock neurons displaying 24-hr Ca^{2+} rhythms. Despite synchrony of the molecular oscillator across the clock network, Ca^{2+} rhythms are asynchronous among the different groups of clock neurons (Table 1.1) (Liang, Holy, and Taghert 2016). Ca^{2+} peaks in clock neurons occur at times that match with their roles in behavior. For example, s-LNvs control

morning locomotor activity and have peak Ca^{2+} levels at dawn, and LNds control evening locomotor activity and have peak Ca^{2+} levels preceding the evening.

How does the clock network coordinate different phases of Ca^{2+} rhythms? To discover the mechanisms, Liang et al. focused on neuropeptides, such as PDF (Liang, Holy, and Taghert 2017). In the absence of PDF, the Ca^{2+} peaks in LNds and DN3s are shifted from ~CT 8 and ~CT 16, respectively, to dawn (~CT 0). (CT or Circadian Time is the circadian time defined by an organism's endogenous circadian clock in constant conditions; CT 0 corresponds to the start of subjective day and CT 12 to the start of subjective night). To determine if the shift in Ca^{2+} rhythms is a phase advance or delay, they applied synthetic PDF and found that Ca^{2+} levels decreased in LNds and DN3s, and importantly, the Ca^{2+} levels remained depressed for several hours. Therefore, PDF delays the Ca^{2+} peaks in LNds and DN3s and does so by staggering their Ca^{2+} peaks to two different times of the day. How one neuropeptide produces two different effects on phase is not known. The authors also determined that sNPF (short Neuropeptide F) inhibits Ca^{2+} and delays the Ca^{2+} peak in DN1s. sNPF in the clock network is required for rhythmic Ca^{2+} rhythms but not molecular clock oscillations in DN1s. Therefore, for certain clock neurons, circuit mechanisms may dominate over the cell-autonomous molecular clock in shaping Ca^{2+} rhythms. This study reported an inhibitory effect for PDF, which previously was shown to acutely depolarize or increase Ca^{2+} in cells (Mertens et al. 2005; Seluzicki et al. 2014; Vecsey, Pírez, and Griffith 2014). However, an important experimental difference is that Taghert and colleagues observed long-term effects of neuropeptides on Ca^{2+} levels. Neuropeptides have complex roles in the clock network, as they synchronize the phases of molecular clocks and Ca^{2+} rhythms; in addition, acute and long-term effects of neuropeptides on target neurons may be different. How neuropeptides serve diverse functions is the clock network is still not well understood but likely involves divergent downstream signaling mechanisms (Seluzicki et al. 2014; Duvall and Taghert 2013).

Circadian regulation of structural plasticity in s-LNvs

Circadian structural plasticity in the fly brain was first reported in the lamina, the first optic neuropil of the visual system [reviewed in (Górska-Andrzejak, Damulewicz, and Pyza 2015)]. In the lamina, many structures undergo circadian rhythms in morphological plasticity, including the retinal photoreceptor terminals, monopolar cells, and synapses (Weber, Kula-Eversole, and Pyza 2009; Górska-Andrzejak et al. 2013). Circadian plasticity of these structures is complex and involves multiple inputs from phototransduction pathways, clock neurons, and peripheral clocks in glia and photoreceptor cells.

Circadian structural plasticity has also been extensively studied in the terminal projections of s-LNvs in the dorsal protocerebrum. The s-LNv projections include both presynaptic and postsynaptic sites and are near most other clock neurons, implicating s-LNv projections as major sites for communication in the clock network (Charlotte Helfrich-Förster, Yoshii, et al. 2007; Yasuyama and Meinertzhagen 2010). In the morning, the s-LNv terminals display greater complexity, with more arbors, branching, and volume, than at night (M. P. Fernández, Berni, and Ceriani 2008; Petsakou, Sapsis, and Blau 2015). Presumably, the increased terminal complexity indicates more synaptic connections. Indeed, using the GRASP (GFP reconstitution across synaptic partners) assay, which labels synaptic contacts between two populations of neurons, contacts between s-LNv and their partners were found to be higher during the day than in the evening (Gorostiza et al. 2014; Tang et al. 2017). As such, the structural plasticity of s-LNv projections is a circadian output rhythm, regulated by the molecular clock and maintained in constant darkness (M. P. Fernández, Berni, and Ceriani 2008).

Circadian remodeling of s-LNv projections appears to be important for behavior, since mutants that have comprised overt rest:activity rhythms may also have disrupted remodeling of the s-LNv projections. When the *Pdf*$^{+}$ LNvs are acutely silenced, the s-LNv projections do not undergo circadian remodeling, and the flies display arrhythmic rest:activity behavior (Depetris-Chauvin et al. 2011). With this manipulation, the s-LNv molecular clock still runs with a normal 24-hr schedule, demonstrating that electrical activity is an output of the molecular clock and

regulates circadian remodeling of projections. The circadian remodeling of s-LNv projections is also regulated by cell-autonomous expression of PDF and Mmp1, a matrix metalloproteinase that processes PDF (Depetris-Chauvin et al. 2014). Other genes also affect rest:activity rhythms by dysregulating circadian remodeling of s-LNv projections, promoting either their branching or retraction.

Mef2 (Myocyte enhancer factor 2) is a transcriptional factor that is expressed in all groups of clock neurons (Blanchard et al. 2010). *Mef2* transcription is directly regulated by the CLOCK-CYCLE transcription factor complex, and Mef2, in turn, regulates transcription of many genes, including Fasciclin 2 (Fas2), the *Drosophila* ortholog of neural cell adhesion molecule, NCAM (Sivachenko et al. 2013). In s-LNvs, Mef2 promotes branching of the dorsal projection, while Fas2 promotes retraction. A clock output mechanism emerges for circadian remodeling of s-LNv projections: CLOCK-CYCLE → Mef2 → Fas2 → s-LNv remodeling (Sivachenko et al. 2013). Dysregulation of *Mef2* in *Pdf*$^{+}$ LNvs leads to decreased power of rest:activity rhythms or complex rhythms (Blanchard et al. 2010; Sivachenko et al. 2013). These behavioral changes are also correlated with altered molecular clocks in s-LNvs, suggesting Mef2 may also feedback onto the molecular clock (Blanchard et al. 2010).

Rho1 is a member of the Rho family of GTPase signaling proteins and a key regulator of the actin cytoskeleton. Rho1 activity cycles in the s-LNv projections and is highest in the evening (ZT12), when the projections are most condensed, which is consistent with its role in promoting retraction of projections. A Rho Guanine Nucleotide Exchange Factor (GEF), Puratrophin-1-like (Pura), activates Rho1 by promoting its association with GTP rather than GDP. *Pura* transcription cycles in s-LNvs and may be a direct target of CLOCK. Petsakou et al. proposed that clock-regulated *Pura* imposes rhythms in Rho1 activity, and the *Rho-ROCK*-myosin light chain (*MLC*) pathway regulates actomyosin retraction of s-LNv projections in a circadian manner. When *Rho1* is overexpressed in the *Pdf*$^{+}$ LNv, the s-LNv projections do not branch in the morning, and flies have arrhythmic rest:activity behavior. At the molecular level, the s-LNv molecular clocks are normal, but in downstream DN1s, the molecular clocks are phase-shifted by up to 12 hours.

Thus, remodeling of the s-LNvs has effects on other clock neurons (Petsakou, Sapsis, and Blau 2015).

Clock output genes

Less is known about the circadian output pathways that transmit timekeeping signals from central clock cells to other parts of the brain to produce rest:activity rhythms. An output component is defined as a molecule or cell population that is regulated by the circadian clock but is not an intrinsic part of the clock mechanism. Several output genes have been implicated in behavioral rhythms, including *na*, *slo, miR-279, Nf1, wake,* and *ebony*. Dysregulation of these genes disrupts behavioral rhythms in animals but does so without affecting oscillations of the molecular clock. Many of these clock output genes exhibit clock-dependent diurnal variation in expression or function.

Na (*narrow abdomen*) encodes an ion channel with homology to the mammalian NALCN sodium leak channel, and is required broadly in the clock network for normal rest:activity rhythms (Lear, Lin, et al. 2005). In the posterior DN1 (DN1p) and l-LNv clock neurons, *na* is required for cycling of a sodium leak current, which contributes to oscillations in firing frequency and resting membrane potential (Flourakis et al. 2015). *Nlf-1* (also known as *Mid1*) is a NA localization factor that is rhythmically expressed and clock-controlled. *Nlf-1* is also required for robust rest:activity rhythms (Ghezzi et al. 2014; Flourakis et al. 2015). Together, NLF-1/NA are part of a cell-autonomous clock output mechanism to ensure robust rhythms of neuronal activity.

The *slo* (*slowpoke*) potassium channel was identified as an output factor, because its binding partner, *Slob* (*slowpoke binding protein*), is a clock-controlled gene with robust transcriptional rhythms (Claridge-Chang et al. 2001; McDonald and Rosbash 2001; Ceriani et al. 2002). *slo* mutants are arrhythmic in constant darkness but have intact s-LNv molecular clocks. Instead*, slo* mutants have altered levels of PDF in s-LNv projections and desynchronized clocks in the DN1s (M. de la P. Fernández et al. 2007). *slo* may also have an important role outside the clock network, since clock neuron-specific rescue of *slo* only partially rescues rest:activity

rhythms. Furthermore, *dyschronic,* a factor that regulates SLO expression, is required in non-clock neurons for rest:activity rhythms (Jepson et al. 2012).

miR-279 is a microRNA that regulates rest:activity rhythms by targeting and downregulating expression of *Unpaired 1* (*Upd1*), a ligand of the JAK/STAT pathway (Luo and Sehgal 2012). JAK/STAT signaling constitutes a critical pathway for development and immunity, but disrupting this pathway only in adulthood impairs rest:activity rhythms. *miR-279* and *Upd1* were found to be required in clock neurons for rest:activity rhythms, although their cellular requirements were not precisely mapped. Given findings that UPD1 is a fly analog of leptin and expressed in the *Pdf*$^{+}$ LNvs, UPD1 could be an output of the s-LNvs (Beshel, Dubnau, and Zhong 2017).

Wake (*wide awake*) is a clock output molecule that regulates the timing of sleep onset. *wake* mutants have a delayed sleep onset at night but normal rest:activity rhythms (S. Liu et al. 2014). WAKE levels cycle in the l-LNvs, peaking near dusk, when they are required to promote sleep. Previously, the l-LNvs were shown to promote arousal and respond to inhibition by GABA (Sheeba, Fogle, et al. 2008; Shang, Griffith, and Rosbash 2008; Parisky et al. 2008). In l-LNvs, WAKE upregulates membrane localization of RDL, a GABA(A) receptor, which would inhibit the excitability of arousal-promoting l-LNvs. Indeed, in *wake* mutants, the l-LNvs show decreased GABA sensitivity and increased excitability (S. Liu et al. 2014). RDL also cycles in l-LNvs and is regulated by rhythmic degradation though the E3 ligase Fbxl4, whose transcription is clock-controlled. As expected, *Fbxl4* mutants have the opposite phenotype of *wake* mutants, with a shorter latency to sleep onset at dusk (Q. Li et al. 2017).

Nf1 (*neurofibromatosis-1*) encodes a Ras-specific GTPase activating protein required for rest:activity rhythms (Williams et al. 2001). *Nf1* mutants have increased Ras/mitogen-activated protein kinase (MAPK) signaling, and loss-of-function mutations in the MAPK pathway can rescue rest:activity rhythms in *Nf1* mutants. Restoring *Nf1* in clock cells does not rescue the behavioral deficits. Instead, *Nf1* is required broadly in the brain, presumably in multiple circadian neurons that regulate rest:activity rhythms (Bai et al. 2018). Not only does *Nf1* regulate PDF levels in the

s-LNv projections, it regulates Ca^{2+} and neuropeptide levels in circadian output neurons that are downstream of clock neurons (discussed below).

Ebony encodes a β-alanyl-biogenic amine synthase that controls the levels of free biogenic amines. EBONY is expressed exclusively in glial cells, where it functions to regulate rest:activity rhythms (Suh and Jackson 2007). At least some of the glial expression of EBONY co-localizes with PER and TIM clock proteins, suggesting that *ebony* is an output molecule of glial clock cells.

Circadian output circuits that regulate rhythms of behavior/physiology

The output genes described above primarily regulate the outputs of clock cells, such as firing or cell signaling, and none were definitively mapped to non-clock cells. Only in the last 5 years, with advances in circuit mapping tools, we have identified multisynaptic output circuits that regulate circadian rhythms (Figure 1.1). These circuits consist of non-clock neurons that convey circadian timing information from clock neurons to sites that control behavior or physiology. Output neurons receive inputs from clock neurons, either directly or indirectly through another group of output neurons. To date, assays of output neurons have revealed cycling of neural/cellular activity in a clock-dependent fashion (Table 1.1). Disruption of this neuronal activity disrupts the output rhythm without affecting the molecular clock. Therefore, most phenotypes from manipulating circadian output neurons are effects on rhythmicity of rest:activity rather than changes in circadian period, which is an intrinsic property of the clock. However, output neurons could feedback onto the clock to affect periodicity. As output circuits identified thus far are peptidergic and neuromodulatory in nature, and possibly also redundant, their disruption tends to weaken the amplitude of the rest:activity rhythm and not eliminate it altogether as would loss of molecular clock oscillations.

The pars intercerebralis (PI) has been proposed as a clock output region for many years. For one, ablation studies in cockroaches showed that the PI is required for locomotor activity rhythms (Nishiitsutsuji-Uwo, Petropulos, and Pittendrigh 1967; Matsui et al. 2009). Furthermore, in *Drosophila,* nearly all the circadian clock neurons, except for the l-LNvs, project to the PI

(Charlotte Helfrich-Förster 1995; Charlotte Helfrich-Förster, Yoshii, et al. 2007; M. Kaneko and Hall 2000). The PI is a major neurosecretory center with a high degree of neurochemical heterogeneity, as such functionally analogous to the mammalian hypothalamus (de Velasco et al. 2007). PI neurons regulate various behaviors in flies including sleep (Foltenyi, Greenspan, and Newport 2007; Crocker et al. 2010), feeding (Zhan, Liu, and Zhu 2016), nutrient sensing (Dus et al. 2015), courtship (Terhzaz et al. 2007), and aggression (Davis et al. 2014). Thus, the PI may be a major output center for regulating circadian timing of behaviors.

Our group identified populations of PI neurons relevant for circadian rhythms. Three different PI groups, those that express DH44 (Diuretic hormone 44), SIFa (SIFamide), or DILP2 (Drosophila insulin-like peptide 2), synapse with DN1p clock neurons (Cavanaugh et al. 2014; Barber et al. 2016). The three PI groups are largely distinct from one another, with the exception that a pair of the *Dh44*$^{+}$ neurons expresses low levels of DILP2 (Ohhara et al. 2018). Currently, it is not known whether s-LNvs or other clock neurons directly signal to the PI. Furthermore, we do not know the identity of the signaling molecules that mediate the DN1p to PI communication.

DH44→Hugin: A neuropeptidergic output circuit regulates rest:activity rhythms

The six *Dh44*$^{+}$ neurons of the PI receive clock input through a multisynaptic circuit comprised of s-LNv → DN1 → *Dh44*$^{+}$ PI (Cavanaugh et al. 2014). Activation or ablation of *Dh44*$^{+}$ PI neurons reduces the power (or amplitude) of rest:activity rhythms without affecting the molecular oscillation of clock proteins in s-LNvs, demonstrating that *Dh44*$^{+}$ PI neurons are output neurons downstream of the clock. In *Dh44*$^{+}$ PI neurons, Ca^{2+} levels cycles across the 24-hr day, with peak activity occurring around evening and trough activity in the morning. Ca^{2+} cycling in *Dh44*$^{+}$ neurons requires the *Pdf*$^{+}$ LNvs, suggesting that cycling in Ca^{2+} levels propagates from the s-LNvs to *Dh44*$^{+}$ neurons (Cavey et al. 2016). In addition, the *Nf1* circadian output gene cell-autonomously regulates Ca^{2+} cycling in *Dh44*$^{+}$ neurons (Bai et al. 2018).

What about the role of the DH44 neuropeptide in rest:activity rhythms? DH44 and one of its receptors, DH44-R1, are required for strong rest:activity rhythms (Cavanaugh et al. 2014; King et al. 2017). Our group also mapped the circuit downstream of *Dh44*$^{+}$ PI neurons to another set of

neuropeptidergic neurons in the subesophageal zone. Knockdown of *Dh44-R1* in *hugin*$^{+}$ neurons reduces the power of rest:activity rhythms. In addition, *hugin* and its encoded neuropeptides, Hugin-γ and/or Prokynin-2, are required for robust rest:activity rhythms. *hugin*$^{+}$ neurons themselves display clock-dependent cycling of neuropeptide vesicle release from their axon termini. A subset of *hugin*$^{+}$ neurons projects back to the PI, potentially providing feedback regulation, while another subset of *hugin*$^{+}$ neurons projects to the ventral nerve cord (VNC), where the circuit potentially modulates motor circuits driving locomotor activity (King et al. 2017). For the first time, we have a minimal, linear circuit between clock neurons and output neurons regulating locomotor activity.

SIFa^{+} PI neurons regulate rest:activity rhythms

In the same screen that identified *Dh44*$^{+}$ PI neurons, the *SIFa*$^{+}$ PI neurons were also found to regulate rest:activity rhythms (Cavanaugh et al. 2014). Ablation of all four *SIFa*$^{+}$ neurons in the brain disrupts rest:activity rhythms but spares the s-LNv molecular clock. Loss of SIFa peptide itself produces a weaker effect on rest:activity rhythms than neuronal ablation, suggesting that other or co-neurotransmitters from *SIFa*$^{+}$ neurons regulate rest:activity rhythms (Bai et al. 2018). Finally, circadian phenotypes in *Nf1* mutants may be due to dysregulation of *SIFa*$^{+}$ neurons. In *Nf1* mutants with arrhythmic rest:activity behavior, both Ca^{2+} levels in *SIFa*$^{+}$ neurons and mRNA levels of *SIFa* are increased (Bai et al. 2018).

Dilp2^{+} PI neurons integrate circadian timing and metabolic signals

The fourteen *Dilp2*$^{+}$ PI neurons and the insulin-like peptides have well-described roles in feeding and metabolism (Nässel et al. 2013). Similar to the *Dh44*$^{+}$ and *SIFa*$^{+}$ neurons, *Dilp2*$^{+}$ neurons receive inputs from DN1p clock neurons (Barber et al. 2016). However, unlike their PI counterparts, *Dilp2*$^{+}$ neurons do not appear to control rest:activity rhythms. Activation of *Dilp2*$^{+}$ neurons in the adult fly is not sufficient to impair rest:activity rhythms (Cavanaugh et al. 2014). However, *Dilp2*$^{+}$ neurons and insulin signaling may be important for development of circadian output circuits (Monyak et al. 2017). A set of *Dilp2*$^{+}$ neurons project out of the brain and into the aorta, where circulating insulin-like peptides may be released to affect peripheral tissues, like the

fat body. *Dilp2*$^{+}$ neurons and insulin signaling regulate transcriptional rhythms of *sxe2*, a lipase in the fat body (Barber et al. 2016). As circadian output neurons, *Dilp2*$^{+}$ neurons show cycling in electrical activity (Barber et al. 2016). *Dilp2*$^{+}$ neurons exhibit higher electrical activity in the morning compared to the night, specifically increased firing frequency and burst firing events. These differences in electrical activity are lost in a *period* null mutant, demonstrating that cycling of *Dilp2*$^{+}$ neuronal activity is clock-dependent. Cycling of electrical activity in *Dilp2*$^{+}$ neurons is in phase with cycling in upstream clock neurons, DN1s and LNvs (Sheeba, Gu, et al. 2008; Cao and Nitabach 2008; Flourakis et al. 2015). In addition to clock-regulation, firing in *Dilp2*$^{+}$ neuron is regulated by feeding, since restricted feeding can shift the nighttime firing pattern of *Dilp2*$^{+}$ neurons to the daytime firing pattern (Barber et al. 2016). Thus, *Dilp2*$^{+}$ PI neurons integrate both circadian timing and metabolic signals.

Leucokinin regulates rest:activity rhythms

Leucokinin (*Lk*)-expressing neurons in the lateral horn are circadian output neurons that regulate sleep and rest:activity rhythms (Cavey et al. 2016). Both *Lk* and *Lk receptor* (*Lk-R*) mutants have reduced power of rest:activity rhythms. s-LNv clock neurons project to *Lk*$^{+}$ lateral horn neurons, and firing of *Pdf*$^{+}$ LNv neurons indirectly inhibits Ca^{2+} in *Lk*$^{+}$ lateral horn neurons. While the inhibitory transmitter is unknown, PDF neuropeptide appears to be involved in an indirect circuit between *Pdf*$^{+}$ LNv and *Lk*$^{+}$ lateral horn neurons. LK-R is expressed broadly in the brain, including the lateral horn, ellipsoid body, and fan-shaped body, which are all areas implicated in locomotor control. The cellular requirement of LK-R for rest:activity rhythms has not been mapped. However, both *Lk*$^{+}$ and *Lk-R*$^{+}$ neurons in the lateral horn display cycling of Ca^{2+} levels that is dependent on the molecular clock and *Pdf*$^{+}$ LNvs. Cycling of Ca^{2+} levels occurs with opposite phases in *Lk*$^{+}$ and *Lk-R*$^{+}$ neurons, since LK peptide inhibits Ca^{2+} in *Lk-R*$^{+}$ neurons. *Lk*$^{+}$ and *Lk-R*$^{+}$ lateral horn neurons also exhibit rhythms in excitability to carbachol, a cholinergic receptor agonist, that tracks with baseline Ca^{2+} rhythms. In summary, rhythmic neuronal activity can propagate to output neurons that are at least two synapses removed from clock neurons.

PTTH^{+} neurons regulate eclosion rhythms

Eclosion (adult emergence from pupae) occurs only once in the life of a fly, but rhythms of eclosion can be monitored in a population, with peaks of emerging flies typically observed around dawn. The prothoracic gland (PG) is an endocrine gland that produces ecdysone, the steroid hormone that controls molting. Eclosion rhythms are controlled by central brain clocks and peripheral clocks in the PG (Myers, Yu, and Sehgal 2003), but the brain clock has a dominant role over the PG clock (Selcho et al. 2017). The central clock transmits timing information to the PG clock through a s-LNv → *PTTH*$^{+}$ neurons → PG circuit (Selcho et al. 2017). PTTH (prothoracicotropic hormone) is expressed in two pairs of brain neurons that receive input from s-LNvs via short Neuropeptide F. In turn, PTTH from the brain signals onto the PG through the PTTH receptor, *torso*. Knockdown of *torso* in the PG disrupts eclosion rhythms but has no effect on adult rest:activity rhythms (Selcho et al. 2017). These works highlight that s-LNvs control rest:activity rhythms and eclosion rhythms through different output circuits.

Conclusion

The molecular mechanism of the circadian oscillator has been worked out in detail. For many years, we knew much less about how oscillations of molecular clock are translated into overt rhythms in behavior and physiology. Only recently has the field begun to identify functional connections within and downstream of the clock network, thus providing a neural basis for circadian rhythms. The primary focus of the field has been dissecting functional circuits that control rest:activity rhythms, and so the circuits that control other rhythmic behaviors in adult flies are underexplored. For all circadian circuits, clock-regulated cycling of neuronal activity appears to be the output mechanism for timekeeping and can propagate from clock neurons to output neurons along multisynaptic circuits. Longitudinal recording of neuronal activity over 24 hours remains a challenge in flies but will be informative for precisely studying how cycling of activity in circadian circuits is shaped by the molecular clock and neurotransmission.

Figure 1.1

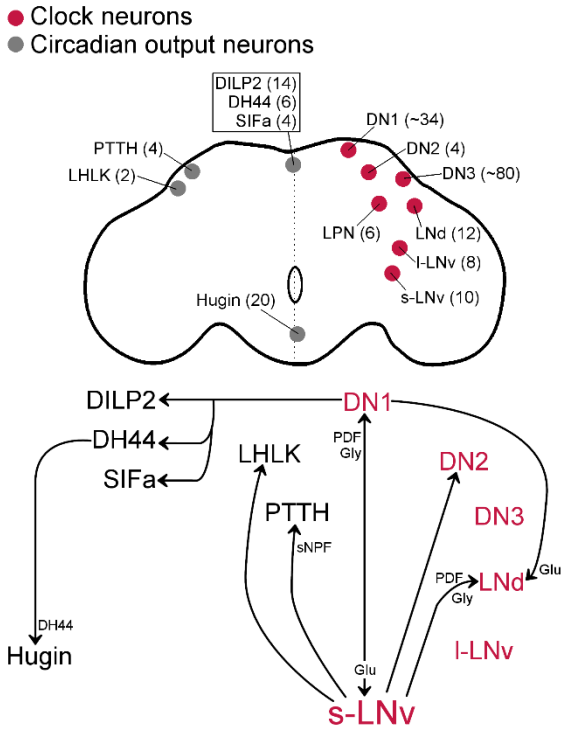

Circadian circuits in the fly brain. **Top.** Schematic representation of a fly brain with neuroanatomical locations of clock neurons (red, right hemisphere) and circadian output neurons (gray, left hemisphere or midline). Bilaterally represented neurons are labeled in only one of the hemispheres. Approximate total number of cells in the brain is indicated in parentheses. **Bottom.** Arrows represent the paths of communication between groups of circadian neurons. Circuits were mapped using neuronal activation and functional imaging and/or GRASP (GFP reconstitution across synaptic partners) methods. The neuropeptide/neurotransmitters that signal in the circuits were genetically identified by removing the peptide or neurotransmitter transporter in the presynaptic neuron and removing the receptor in the postsynaptic neuron. PDF mediates s-LNv communication to LNd, DN1, and LHLK (indirectly) (Leucokinin^{+} lateral horn). Glycine (Gly) also signals from s-LNv to DN1 and LNd. Short neuropeptide F (sNPF) signals in the s-LNv to PTTH circuit. Glutamate (Glu) signals from the DN1 to s-LNv and LNd. The molecules that signal between DN1 and PI neurons (DH44/SIFa/Dilp2) are unknown. DH44 neuropeptide signal from *Dh44*$^{+}$ to *hugin*$^{+}$ neurons.

Table 1.1

Cycling in Circadian Circuits

Neuronal group:	Cycling:	Highest at: (hours since lights-on)	Cycles in constant darkness?	Cycle lost in a clock mutant?:	Reference
Clock neurons					
s-LNv	Electrical activity	~0	N.d.	N.d.	(Cao and Nitabach 2008)
	Intracellular calcium (Ca^{2+}) levels	23-24	Yes	Yes	(Liang, Holy, and Taghert 2016)
	Complexity of projections	~0	Yes	Yes	(M. P. Fernández, Berni, and Ceriani 2008)
	Synapse contacts	~2	Yes	N.d.	(Gorostiza et al. 2014)
	Rho1 activity	~12	Yes	Yes	(Petsakou, Sapsis, and Blau 2015)
	PDF levels in projections	0-6	Yes	Yes	(Park et al. 2000)
	PDF and dopamine sensitivity	~0	Yes	N.d.	(Klose et al. 2016)
l-LNv	Electrical activity	1-6	No (DD day 1); Yes (DD day 14)	Yes	(Sheeba, Gu, et al. 2008; Cao and Nitabach 2008)
	Ca^{2+} levels	5-6	Yes	Yes	(Liang, Holy, and Taghert 2016)
	GABA sensitivity	Evening	N.d.	N.d.	(Q. Li et al. 2017)
LNd	Ca^{2+} levels	~12	Yes (highest at CT 8-9)	Yes	(Liang, Holy, and Taghert 2016)
DN1	Electrical activity	0-4 or 20-24	N.d.	Yes	(Flourakis et al. 2015)
	Ca^{2+} levels	18-20	Yes	Yes	(Liang, Holy, and Taghert 2016)
DN2	Synaptic contacts with s-LNvs	22-24	N.d.	N.d.	(Tang et al. 2017)
DN3	Ca^{2+} levels	17-18	Yes	Yes	(Liang, Holy, and Taghert 2016)
Circadian output neurons					
$DILP2^{+}$ PI	Electrical activity	0-4	No	Yes	(Barber et al. 2016)
$DH44^{+}$ PI	Ca^{2+} levels	7-12	Yes	Yes	(Cavey et al. 2016; Bai et al. 2018)
$Hugin^{+}$ SEZ	Neuropeptide vesicle release	Night	N.d.	Yes	(King et al. 2017)
LK^{+} LH	Ca^{2+} levels	Night	Yes	Yes	(Cavey et al. 2016)
	Carbachol sensitivity	Night	Yes	Yes	(Cavey et al. 2016)
LK $Receptor^{+}$ LH	Ca^{2+} levels	Day	Yes	Yes	(Cavey et al. 2016)
	Carbachol sensitivity	Day	Yes	Yes	(Cavey et al. 2016)

N.d. = not determined

CT = circadian time

DD = constant darkness

LH = lateral horn

PI = pars intercerebralis

SEZ = subesophageal zone

Part 2 : Central clocks regulate circadian rhythms in peripheral tissues

The circadian system is arranged in a hierarchy, where the central clock in the brain can regulate clocks and rhythms in peripheral tissues (Albrecht 2012). The central clock is unique, since it is primarily synchronized with light:dark cycles and resistant to other external cues. Although peripheral clocks can be self-sustained and cell autonomous (the degree of autonomy varies from clock to clock), they are synchronized with the central clock to ensure circadian synchrony within the animal. Peripheral clocks are also influenced by external cues, such as feeding, temperature, and behavior. In addition, in *Drosophila*, several tissues have photosensitive peripheral clocks which can directly entrain to light (Giebultowicz et al. 2000). External cues such as restricted feeding or jet lag can differentially phase shift peripheral clocks, leading to circadian desynchrony, a factor that contributes to the pathophysiology of many diseases (Roenneberg and Merrow 2016; Damiola 2000). Not only is central clock-to-peripheral tissue signaling an important area of study from the human health perspective, the neural basis for peripheral circadian rhythms is relatively understudied. Here, I will highlight a few works that provide a mechanistic understanding of how the central clock influences rhythms in peripheral tissues. In general, endocrine signaling is an important mechanism that can mediate brain-to-periphery communication. Neurohormones may serve as internal timing cues that synchronize peripheral circadian rhythms (E Challet 2015). In addition to identifying neuroendocrine signals, several studies have mapped circuits between the central clock neurons and neuroendocrine centers.

Neural clock to oenocyte clock signaling regulates pheromone rhythms

In the first part of the introduction, I introduced a circuit through which the central clock communicates with the peripheral clock of the prothoracic gland to regulate eclosion rhythms in flies. The s-LNv clock neurons signal to $PTTH^{+}$ neuroendocrine cells, which then signal directly to the clock in the prothoracic gland. Another peripheral tissue, oenocytes, also have molecular clocks influenced by central clocks. In insects, oenocytes produce cuticular hydrocarbon pheromones, which are important for mediating social interactions such as mating. Since PDF is

an important output factor of the central clock, Krupp et al. asked whether PDF signaling is required for oenocyte clock function (Krupp et al. 2013). They found that in *Pdf* mutants, the oenocyte clock still oscillates but runs with a period that is longer than 24 hours. Thus, PDF signaling acts to modulate the period of the oenocyte clock. The study also found that PDF signaling is required for rhythmic expression of *desat1*, an oenocyte-expressed enzyme involved in the biosynthesis of male *Drosophila* sex pheromones. PDF is expressed in two different groups of neurons, the LNv central clock neurons in the brain and abdominal ganglion neurons (AbNs) in the ventral nerve cord. Unlike LNvs, AbNs do not have molecular clocks. Krupp et al. found that PDF from both LNvs and AbNs is required for normal 24-hour oscillations of *desat1*. However, only PDF from AbNs regulates levels of male sex pheromones. Therefore, oenocyte clocks are regulated by both central clock neurons and non-clock neurons, with PDF neuropeptide as the circulating hormone communicating between the CNS and peripheral clocks in oenocytes (Krupp et al. 2013; Shafer and Yao 2014).

Central clocks drive peripheral transcriptional rhythms

Circadian clocks and transcriptional rhythms are ubiquitous throughout an animal. In mice, 43% of all protein coding genes show circadian rhythms in mRNA expression (transcriptional rhythms) in at least one tissue (R. Zhang et al. 2014). For a majority of transcripts, transcriptional rhythms are driven by the local tissue clock, either directly as a clock-controlled gene or indirectly through a clock-controlled gene regulatory mechanism (Kornmann, Schaad, Bujard, et al. 2007). However, there are subsets of rhythmic transcripts that are independent of the local tissue clock. This phenomenon is evident in the murine liver, where cycling of about 30-90 liver genes is regulated by the central clock (brain clock) and not by the local clock (Kornmann, Schaad, Bujard, et al. 2007; Hughes et al. 2012). The factors that drive cycling of liver clock-independent genes are not known. One study found that glucocorticoid from the adrenal gland regulates a subset of transcriptional rhythms in the liver (Oishi et al. 2005). Circadian rhythm of glucocorticoids depends on adrenocorticotropic hormone from the anterior pituitary, which is in turn regulated by corticotropin-releasing hormone rhythms from the

hypothalamus (E Challet 2015). Thus, the hypothalamic-pituitary-adrenal axis could be a potential neuroendocrine mechanism that regulates peripheral liver rhythms.

In flies, the fat body is a major regulator of metabolism and a functional analog of mammalian liver and adipose tissue (Arrese and Soulages 2010). The fat body contains a molecular clock that locally drives cycling of gene expression. However, about 40% of cycling genes in the fat body are not regulated by the fat body clock but by other factors, which may include signals from the central clock (Xu et al. 2011). A study from our lab followed up on *sxe2*, a rhythmically expressed fat body gene independent of the local clock (Barber et al. 2016). Instead, *Dilp2*$^{+}$ neurons and insulin-like peptides from the brain are required for *sxe2* cycling in the fat body. Earlier, I introduced *Dilp2*$^{+}$ neurons as circadian output neurons that receive clock signals from DN1ps. *Dilp2*$^{+}$ neurons project out of the brain and into the aorta, where circulating insulin-like peptides are released to affect peripheral tissues, like the fat body. In addition to possible other effects, insulin-like peptides signal through the insulin receptor on the fat body to regulate *sxe2* cycling. Thus, a circuit from DN1p central clocks to fat body tissue via *Dilp2*$^{+}$ neuroendocrine cells can explain rhythmic expression of *sxe2*. Several other fat body clock-independent cyclic genes remain to be studied. As the central clock has an important role in orchestrating peripheral rhythms (Izumo et al. 2014), it is likely that central clocks and neuroendocrine signals regulate several fat body genes. In Chapter 2 of this thesis, I describe another mechanism that links the central clock to rhythmically expressed genes, *sxe1* and *Cyp6a21*, in the fat body.

Chapter 2 : Neural Clocks and Neuropeptide F/Y Regulate Circadian Gene Expression in a Peripheral Metabolic Tissue

Published: Erion, Renske*, Anna N. King*, Gang Wu, John B. Hogenesch, and Amita Sehgal. "Neural Clocks and Neuropeptide F/Y Regulate Circadian Gene Expression in a Peripheral Metabolic Tissue." ELife 5 (2016). doi:10.7554/elife.13552.

*equal contributions

Abstract

Metabolic homeostasis requires coordination between circadian clocks in different tissues. Also, systemic signals appear to be required for some transcriptional rhythms in the mammalian liver and the *Drosophila* fat body. Here we show that free-running oscillations of the fat body clock require clock function in the PDF-positive cells of the fly brain. Interestingly, rhythmic expression of the cytochrome P450 transcripts, *sex-specific enzyme 1* (*sxe1*) and *Cyp6a21*, which cycle in the fat body independently of the local clock, depends upon clocks in neurons expressing neuropeptide F (NPF). NPF signaling itself is required to drive cycling of *sxe1* and *Cyp6a21* in the fat body, and its mammalian ortholog, Npy, functions similarly to regulate cycling of cytochrome P450 genes in the mouse liver. These data highlight the importance of neuronal clocks for peripheral rhythms, particularly in a specific detoxification pathway, and identify a novel and conserved role for NPF/Npy in circadian rhythms.

Introduction

Circadian clocks constitute an endogenous timekeeping system that synchronizes behavior and physiology to changes in the physical environment, such as day and night, imposed by the 24 hour rotation of the earth (Zheng and Sehgal 2012). A coherent circadian system is composed of a cooperative network of tissue-specific circadian clocks, which temporally coordinate and compartmentalize biochemical processes in the organism (Wijnen and Young 2006). Clock disruption is associated with numerous deleterious health consequences including cancer, cardiovascular disease, and metabolic disorders (Marcheva et al. 2010; Marcheva et al. 2013; Turek et al. 2005).

In the fruit fly, *Drosophila melanogaster*, the neuronal clock network is comprised of roughly 150 circadian neurons, which are grouped based on their anatomical location and function in the brain (Allada and Chung 2010). The lateral neurons include the small and large ventral lateral neurons (LN_vs), the dorsal lateral neurons (LN_ds) and the lateral posterior neurons (LPNs). The dorsal neurons are divided into three subgroups, dorsal neurons (DN) 1, 2, and 3. The small LNvs (sLN_vs) have traditionally been referred to as the central clock because they are

necessary and sufficient for rest:activity rhythms under constant conditions (Grima et al. 2004; Stoleru et al. 2004), but recent studies also indicate an important role for the LN_ds (Guo et al. 2014). The LN_vs express the neuropeptide pigment dispersing factor (PDF), which is important for rest:activity rhythms (Renn et al. 1999; Stoleru et al. 2005; Lin, Stormo, and Taghert 2004; Yoshii et al. 2009) and for the function of circadian clocks in some peripheral tissues (Myers, Yu, and Sehgal 2003; Krupp et al. 2013). The LN_ds constitute a heterogeneous group of neurons differentiated by the expression of peptides and receptors (G. Lee, Bahn, and Park 2006; Johard et al. 2009; Yao and Shafer 2014). Thus far, these peptides, which include Neuropeptide F (NPF), have only been implicated in behavioral rhythms (C. He et al. 2013; Hermann et al. 2012; Hermann-Luibl et al. 2014).

Most physiological processes require clocks in peripheral tissues, either exclusively or in addition to brain clocks. For instance, a peripheral clock located in the fat body, a tissue analogous to mammalian liver and adipose tissue (Arrese and Soulages 2010), regulates feeding behavior (Xu, Zheng, and Sehgal 2008; Seay and Thummel 2011) and nutrient storage (Xu, Zheng, and Sehgal 2008) and drives the rhythmic expression of genes involved in metabolism, detoxification, innate immunity, and reproduction (Xu et al. 2011). Molecular clocks in the brain and fat body have different effects on metabolism, suggesting that clocks in these two tissues complement each other to maintain metabolic homeostasis (Xu, Zheng, and Sehgal 2008). Such homeostasis requires interaction between organismal clocks, but how this occurs, for example whether neuronal clocks regulate fat body clocks, as they do for some other tissue-specific clocks, is not known. In addition, the fat body clock does not regulate all circadian fat body transcripts. 40% of rhythmically expressed fat body transcripts are unperturbed by the absence of a functional fat body clock (Xu et al. 2011), suggesting these genes are controlled by rhythmic external factors, which could include light, food, and/or signals from clocks in other tissues (Wijnen et al. 2006). Likewise in the mammalian liver, where circadian gene regulation has been well-studied, cyclic expression of many genes persists when the liver clock is ablated (Kornmann, Schaad, Bujard, et al. 2007). Brain specific rescue of clock function in *Clock$^{\Delta 19}$* animals partially restored liver gene expression rhythms (~40%), albeit with compromised amplitude (Hughes et al.

2012). The specific signals that mediate this rescue, however, were not identified, although systemic signals that regulate peripheral clocks have been identified (Cailotto et al. 2009; Kornmann, Schaad, Bujard, et al. 2007; Reddy et al. 2007; Oishi et al. 2005).

The relative simplicity of fly neuroanatomy and physiology, the vast array of genetic tools, and the conservation of molecular mechanisms with mammals make the fly an ideal organism to dissect complex interactions between physiological systems. In this study, we found that neural clocks regulate circadian gene expression in the fly fat body, a peripheral metabolic tissue. We demonstrate that cycling of the core clock gene, *period (per*), requires PDF-expressing cells in constant darkness. Interestingly, however, clocks in the NPF-expressing subset of LN_ds, as well as NPF itself, are important for driving rhythmic expression of specific cytochrome P450 genes that cycle independently of the fat body clock. Lastly, we show that Npy, the mouse homolog of NPF, regulates transcriptional circadian output in the mouse liver. Microarray analyses reveal that Npy contributes to the rhythmic expression of hundreds of transcripts in the liver, including a subset of cytochrome P450 genes. In summary, we identified a conserved role for NPF/Npy neuropeptides in the circadian system in coupling neuronal clocks to transcriptional output in peripheral tissues in flies and mice.

Methods

Fly Genetics

Flies were grown on standard cornmeal-molasses medium and maintained at 25°C. The following strains were used: Iso31 (isogenic *w1118* stock; (Ryder et al. 2004)), *Pdf*-GAL4 (Renn et al. 1999), 911-GAL4 (InSITE Library; (del Valle Rodríguez, Didiano, and Desplan 2011)), *Dvpdf*-GAL4*; pdf*-GAL80 (Guo et al. 2014), *Clk*^{Jrk} (Allada et al. 1998), and UAS-*npf* RNAi (Vienna Drosophila Resource Center #108772). The following flies were obtained from Bloomington Drosophila Stock Center: *Npf*-GAL4 (#25681), UAS-CLKΔ (#36318), UAS-CYCΔ (#36317), *tub*-GAL80^{ts} (#7018), and *npfr* mutant (#10747).

Locomotor Activity

The previously described Drosophila Activity Monitoring Systems (Trikinetics, Waltham, MA) were used to monitor rest:activity rhythms under constant conditions. Roughly 1 week old male flies were entrained for at least 3 days to 12 hour light: 12 hour dark cycles (LD) and then transferred to constant darkness for at least 7 days. Data were analyzed using ClockLab software (Actimetrics) and rhythmicity of individual male flies was determined for days 2-7 of DD as described previously (Williams et al. 2001).

Adult Fat Body Collection

Male flies (roughly 4-7 days old) were entrained to a 12:12 LD cycle at 25°C for at least 3 days before they were harvested. The abdominal fat body was obtained by separating the fly abdomen from the rest of the body and then removing all internal organs, leaving the fat body attached to the cuticle to be collected on dry ice for RNA extraction. For *tub*-Gal80^{ts} experiments, flies were raised at 18°C. Control flies were kept at 18°C, while the experimental flies were shifted to 30°C, the restrictive temperature for Gal80^{ts}, for at least 4 days before collection.

Mice Husbandry and Liver Collection

Npy knockout mice were obtained from The Jackson Laboratory (004545) along with their background strain for controls (002448). Genotyping primers are listed on the Jackson website. 8-12 weeks old male mice were entrained to 12:12 LD cycles and fed a standard ad lib diet. Livers from *Npy* knockouts and their background controls were collected every 4 hours starting at lights on (ZT0) and immediately frozen in liquid nitrogen. 3-4 male mouse livers were collected at every timepoint for each genotype. All procedures were approved by the University of Pennsylvania Institutional Animal Care and Use Committee.

Real-Time Quantitative PCR and Statistical Analyses

For each time point, fat bodies from 12 male flies were collected for RNA preparation. Total RNA was extracted using Trizol reagent (Life Technologies, Grand Island, NY) and purified using RNeasy Mini Kit (Qiagen Inc., Valencia, CA) according to manufacturer's protocol. All RNA samples were treated with RNase-free DNase (Qiagen Inc.). RNA was reverse transcribed to generate cDNA using a High Capacity cDNA Reverse Transcription kit (Life Technologies, Grand Island, NY). Quantitative RT-PCR was performed on a 7900HT Fast-Real-Time PCR (Applied Biosystems) using SYBR Green (Life Technologies). The following primer sequences were used for qPCR: *αtubulin* (Forward 5' CGTCTGGACCACAAGTTCGA 3' and reverse 5' CCTCCATACCCTCACCAACGT 3'), *per* (Forward 5' CGTCAATCCATGGTCCCG 3' and reverse 5' CCTGAAAGACGCGATGGTG 3'), *Cyp4d21/sxe1* (Forward 5' CTCCTTTGGTTTATCGCCGTT 3' and reverse 5' TTATCAGCGGCTTGTAGGTGC), *sxe2* (Forward 5' TGCGGTACGATCTTTATACGCC 3' and reverse 5' CTAACTGGCCATTTCGGATTGA 3'), *CG14934* (Forward 5' GGAAATCACGACAATCCTCGA 3' and reverse 5' CCCAACTCCTCGCCATTATAAG 3'), *Cyp6a21* (Forward 5' GTTGTATCGGAAACCCTTCGATT 3' and reverse 5' AACCTCATAGTCCTCCAGGCATT 3'), and *CG117562* (Forward 5'ACCACAGAGGTGAAACGCATCT 3' and reverse 5'CAGCAGCAGTTCAAATACCGC 3'). Transcript levels were normalized to those of *αtubulin* to control for the total RNA content in each sample.

Kits and procedures to isolate RNA and generate cDNA from mouse livers are the same as described above for fly fat bodies. The following primer sequences were used for qPCR: *Cyp2b10* (Forward 5' GACTTTGGGATGGGAAAGAG 3' and reverse 5' CCAAACACAATGGAGCAGAT 3'), *36B4* (Forward 5' TCCAGGCTTTGGGCATCA 3' and reverse 5' CTTTATCAGCTGCACATCACTCAGA 3'), *Rev-erb alpha* (Forward 5' GTCTCTCCGTTGGCATGTCT 3' and reverse 5' CCAAGTTCATGGCGCTCT 3') and *Alas1* (PrimerBank ID 23956102a1) (Spandidos et al. 2008; Spandidos et al. 2010; Wang and Seed 2003). Transcript levels were normalized to the housekeeping gene, *36B4*.

Significant circadian rhythmicity of transcript levels was determined using the JTK_Cycle algorithm (Hughes, Hogenesch, and Kornacker 2010). *P* values of less than 0.05 were considered significant. We also used two-way ANOVA for repeated measures and a Tukey's *post hoc* test for differences across time (GraphPad Prism). P-values are reported in Table 2.2.

Microarray Analysis

Liver samples from *Npy* KO and wild type mice were collected every 4h over 24h (n = 2 per genotype and timepoint). RNA was purified as described above. Expression profiling was done at the Penn Molecular Profiling Facility using Mouse Gene 2.0 ST Arrays (Affymetrix, Santa Clara, CA, which also provided the annotation files). For extracting expression values of transcripts, raw CEL files were analyzed with the RMA algorithm (Irizarry et al. 2003) implemented in the affy package in Bioconductor in R (R 2.14.2) (Gautier et al. 2004). The newly developed MetaCycle (version 1.0.0; https://github.com/gangwug/MetaCycleV100.git) was used to detect circadian transcripts from time-series expression data in the wild type (WT) and *Npy* knockout (KO) groups, respectively. Key parameters in MetaCycle were the periodicity detection algorithms, JTK_CYCLE (Hughes, Hogenesch, and Kornacker 2010) and Lomb-Scargle (Glynn, Chen, and Mushegian 2006), the period length (set at exactly 24 hr), and the p-value integration method (Fisher's method, Fisher 1956). Using MetaCycle, we calculated two new features of circadian transcripts, baseline expression level (bEXP) and relative amplitude (rAMP). The former one is defined as the average expression level of a cycling transcript within one period length, and the

latter one is a normalized amplitude value with bEXP. Based on analysis results from MetaCycle, expressed transcripts (bEXP larger than 101.6) with a p-value < 0.01 in WT and > 0.8 in the KO group were considered WT-specific rhythmic transcripts and shown in the heatmap. To generate the heatmap, expression values from replicate libraries in each group were averaged, median normalized by transcript, sorted by phase, and plotted as a heatmap using pheatmap in R.

Results

The Central Clock Regulates the Fat Body Clock in Constant Darkness

While some peripheral clocks in *Drosophila* are completely autonomous, e.g. malphigian tubules (Hege et al. 1997), others rely upon cell-extrinsic factors, in particular the clock in the brain. For example, PDF-positive LN_vs are required for rhythmic expression of clock components in the prothoracic gland, a peripheral tissue that gates rhythmic eclosion (Myers, Yu, and Sehgal 2003). In addition, PDF released by neurons in the abdominal ganglion is necessary to set the phase of the clock in oenocytes (Krupp et al. 2013), which regulate sex pheromone production and mating behavior (Krupp et al. 2008). We investigated whether clocks in PDF-positive LN_vs were necessary for clock function in the abdominal fat body. The molecular clock in *Drosophila* consists of an autoregulatory loop in which the transcription factors, CLOCK (CLK) and CYCLE (CYC), activate expression of the genes *period* (*per*) and *timeless* (*tim*), and PER and TIM proteins feedback to inhibit the activity of CLK-CYC (Zheng and Sehgal 2012). To disrupt the molecular clock exclusively in PDF-positive cells, we used the GAL4/UAS system to express a dominant-negative version of the CLK transcription factor, CLKΔ. CLKΔ lacks regions of its DNA-binding domain, preventing it from binding DNA and activating transcription of genes, including components of the molecular clock. However, CLKΔ can still heterodimerize with its partner, CYC, through its protein interaction domain (Tanoue et al. 2004). Behavioral assays of *Pdf*-GAL4/UAS-CLKΔ flies showed that a majority of the flies had arrhythmic locomotor activity in constant darkness (DD) (Figure 2.1A and Table 2.1), confirming that CLKΔ expression in the LN_vs disrupts circadian rhythms.

To assess functionality of the molecular clock in fat body tissue, we measured transcript levels of the core clock gene *per* in abdominal fat bodies over the course of the day (Figure 2.1B). We found that circadian expression of *per* in the fat body was not altered in flies with a disrupted central clock (*Pdf*-GAL4/UAS-CLKΔ) under a 12-hour light: 12-hour dark (LD) cycle (Figure 2.1C). Unlike mammals, peripheral clocks in *Drosophila* can detect light, which acts as the dominant entrainment signal (Plautz et al. 1997; Oishi et al. 2004). Therefore, under LD conditions, light may directly synchronize oscillations in *per* transcript levels in fat body cells, masking the effects

of ablating the central clock. Consequently, we evaluated *per* rhythms in the absence of light. Since rhythmic gene expression dampens under constant conditions and is undetectable in the fat body by the sixth day of DD (Xu et al. 2011), we tested rhythmic expression of *per* on the second day in DD (DD2). *per* levels were rhythmic in the fat body of control flies on DD2. In contrast, flies expressing CLKΔ in the LNvs showed an apparent lack of *per* rhythms in the fat body (Figure 2.1D; see Discussion). This suggests that the clock in PDF-positive LN_vs influences the peripheral fat body clock in the absence of external environmental cues.

Rhythmic Expression of Fat Body Transcripts that Cycle Independently of the Local Tissue Clock Requires Organismal Circadian Function

The fat body clock regulates roughly 60% of circadian genes in the fat body; the mechanisms that drive daily cycling of the other 40% of circadian genes in this tissue are unknown (Xu et al. 2011). Several potential mechanisms could explain rhythmic gene expression in the absence of the local tissue-specific clock, for example, light, nutrients, or clocks located in other tissues. As noted above, many tissues in *Drosophila* have photoreceptors. Therefore, in addition to entraining clocks to the external environment, LD cycles can drive rhythmic transcription via clock-independent pathways (Wijnen et al. 2006). LD cycles can even drive a rhythm of feeding (Xu, Zheng, and Sehgal 2008), which could lead to cyclic expression of metabolic genes. Nutrients are known to be strong entrainment signals in peripheral tissues; in fact, rhythmic or restricted feeding, even in the absence of a clock, can drive cyclic expression of several fat body genes (Xu et al. 2011). Another possibility is that rhythmic expression of specific fat body transcripts requires a clock in another tissue.

To differentiate between light, nutrient, and clock control, we measured daily expression of genes that cycle independently of the fat body clock in Clk^{jrk} mutants. Clk^{jrk} mutants lack functional clocks in all tissues due to a premature stop codon that eliminates the CLK activation domain (Allada et al. 1998). Although Clk^{jrk} mutants cannot sustain feeding rhythms under constant conditions, LD cycles can drive feeding rhythms in Clk^{jrk} flies albeit with a delayed phase relative to wild type flies (Xu, Zheng, and Sehgal 2008). We predicted that transcripts driven by

light, or even nutrient intake driven by light, would oscillate in *Clk^{jrk}* mutants in LD with the same or altered phase, while clock-dependent transcripts would not oscillate at all. The genes we tested were selected based on the robustness of their rhythms in the absence of the fat body clock (Xu et al. 2011). We found that none of these genes displayed circadian rhythms in *Clk^{jrk}* mutants, suggesting that although these genes do not require an intact fat body clock, they do require an intact clock in some other tissue (Figure 2.2). In addition to the loss of rhythmic expression in *Clk^{jrk}* mutants, there were also differences in baseline expression levels. Rhythmic gene expression of *sex-specific enzyme 2* (*sxe2*), a lipase and *CG17562*, an oxidoreductase was eliminated in *Clk^{jrk}* mutants to produce an intermediate level of gene expression throughout the day (Figure 2.2A-B). In contrast, rhythmic expression as well as overall levels of *sex-specific enzyme 1* (*sxe1*), a cytochrome P450, and *CG14934*, a purported glucosidase involved in glycogen breakdown, were greatly reduced in *Clk^{jrk}* mutants (Figure 2.2C-D).

Clocks in NPF-Positive Neurons Drive Daily Oscillations in Expression of Fat Body Transcripts

Having established that circadian expression of genes cycling independently of the fat body clock requires an intact molecular clock elsewhere in the organism, we sought to identity the specific clock population involved. We chose to focus on the regulation of *sxe1* because it has the most robust cycling profile of all the rhythmic fat body clock-independent genes. *sxe1* was named on the basis of its regulation by the sex determination pathway in fly heads and is enriched in the non-neuronal fat body tissue of males (Fujii and Amrein 2002). Early microarray studies looking for cycling transcripts in *Drosophila* heads also indicated that *sxe1* is regulated by the circadian system (Claridge-Chang et al. 2001; McDonald and Rosbash 2001; Ceriani et al. 2002). However, the nature and function of the circadian control of *sxe1* are unclear. *sxe1* is a cytochrome P450 gene and implicated in xenobiotic detoxification and male courtship behavior (Fujii, Toyama, and Amrein 2008) and may confer cyclic regulation to either or both of these processes.

Rhythms of *sxe1* expression are abolished in *Clk*^{irk} mutants in LD, and so we evaluated *sxe1* regulation by other clocks in the presence of light cycles rather than under constant darkness (Figure 2.2C). Our initial discovery that PDF neurons regulate the fat body clock in constant darkness led us to hypothesize that these neurons may also regulate fat body clock-independent genes. Abolishing the clock in PDF cells by expressing CLKΔ under *Pdf*-GAL4, slightly decreased *sxe1* transcript levels in the abdominal fat body, but did not abolish rhythmic expression (Figure 2.3A). This suggests that although the PDF neurons regulate the fat body clock, these neurons are not the primary drivers of rhythmic *sxe1* expression.

DN1 and LN_d clusters have been implicated in the regulation of circadian behavior (L. Zhang et al. 2010; Y. Zhang et al. 2010; Stoleru et al. 2004; Grima et al. 2004). In fact, DN1s were recently shown to be part of an output circuit regulating rest:activity rhythms (Cavanaugh et al. 2014), and clocks in the DN1s are known to mediate other circadian behaviors, such as aspects of the male sex drive rhythm (Fujii and Amrein 2010). However, aside from behavioral rhythms, little is known about the functional significance of the DN1 and LN_d clusters in regulating circadian outputs. We investigated whether rhythmic *sxe1* expression requires clocks in the DN1 cluster by using the 911-GAL4 driver to target the DN1s (Cavanaugh et al. 2014). Since expressing CLKΔ in the DN1s was lethal, we expressed dominant negative CYCLE, CYCΔ, in the DN1s and found the manipulation did not alter *sxe1* rhythms or expression levels in the fat body (Figure 2.3B).

The six LN_ds express NPF (neuropeptide F), sNPF (short neuropeptide F), and ITP (ion transport peptide) in different cells, with some overlap (Muraro, Pírez, and Ceriani 2013). In adult males, NPF is expressed in 3 out of 6 LN_ds, as well as a subset of the LNvs and some non-clock neurons in the brain (G. Lee, Bahn, and Park 2006; Hermann et al. 2012). NPF is also expressed in endocrine cells in the midgut, although the role of NPF in these cells is not known (Brown et al. 1999). We first used *Npf*-GAL4 to target the LN_ds. Interestingly, we found that expressing CLKΔ under *Npf*-GAL4 severely disrupted expression of *sxe1* (Figure 2.3C). This effect was not specific to the CLKΔ transgene, because *sxe1* expression was also abolished using CYCΔ to disrupt clocks in NPF cells (Figure 2.3D). Since it was possible that expression of CLKΔ or CYCΔ in non-

clock NPF cells was disrupting *sxe1* expression, we sought other ways to ablate the clock in LN_d neurons. A subset of the LN_d cluster can also be targeted with the *Dvpdf*-GAL4 driver in combination with *pdf*-GAL80 (Guo et al. 2014). Expressing CLKΔ under *Dvpdf*-GAL4;*pdf*-GAL80 reduced *sxe1* levels throughout most of the day, particularly at ZT16, the time of peak *sxe1* expression (Figure 2.3E). The manipulation did not completely abolish rhythmic expression of *sxe1,* presumably because the *Dvpdf*-GAL4 driver does not target all the NPF clock neurons.

We also assessed the circadian expression profile of another fat body clock-independent cytochrome P450 gene, *Cyp6a21*. Fat body expression of *Cyp6a21* robustly cycles in wild type flies but rhythmic expression was dampened in *Npf*-GAL4/UAS-CLKΔ flies, with a relatively small reduction in its overall expression level (Figure 2.3F). This suggests that clocks in NPF-positive neurons have a broader role in regulating the expression of cytochrome P450 genes in the fat body. Furthermore, ablating clocks in NPF-positive cells did not alter rhythmic expression of *per*, indicating that while rhythmic transcriptional output was impaired, the fat body clock remained intact (Figure 2.3G). Together, these data suggest that a subset of LN_ds expressing NPF drive rhythmic expression of specific fat body genes.

Next we tested whether overexpressing CLKΔ in NPF-positive neurons in adulthood is sufficient to alter circadian gene expression in the fat body. To limit the expression of CLKΔ to adulthood, we used flies with a tubulin-GAL80ts transgene (*tub*-GAL80ts) in addition to *Npf*-GAL4 and CLKΔ transgenes. Tub-GAL80ts ubiquitously expresses a temperature-sensitive GAL80 protein, which represses GAL4 activity at the permissive temperature of 18°C (McGuire et al. 2003). All *Npf*-GAL4/UAS-CLKΔ; *tub*-$GAL80^{ts}$/+ flies were raised at 18°C and upon reaching adulthood, control flies were kept at 18°C, while experimental flies were shifted to the restrictive temperature (30°C) to induce CLKΔ expression. We found that after shifting flies to 30°C, expression of *sxe1* remained rhythmic and similar to 18°C controls, suggesting adult-specific clock ablation in NPF-positive neurons is either incomplete or insufficient to affect *sxe1* rhythms (Figure 2.3H). However, this manipulation had a different effect on cyclic expression of *Cyp6a21*. Robust cycling of *Cyp6a21* cycling was maintained in control flies kept at the permissive temperature, although the phase was shifted, perhaps due to the different temperature (18^{o}C)

required for this assay. Importantly though, rhythmic expression of *Cyp6a21* was dampened by adult-specific clock ablation in LN_d neurons (Figure 2.3I). Together these data indicate that clocks in NPF-expressing neurons have differential effects on the expression of cycling fat body genes.

NPF-NPF Receptor Axis Regulates Rhythmic Expression of sxe1 and Cyp6a21

After identifying NPF-positive clock neurons as relevant for rhythmic gene expression in the fat body, we reasoned NPF itself might act as a circadian signal. Indeed, NPF was reported to cycle in a subset of NPF-positive neurons, including LN_ds and LN_vs (C. He et al. 2013). NPF regulates a variety of behavioral processes in *Drosophila* including feeding (Wu et al. 2003; Wu, Zhao, and Shen 2005; Lingo, Zhao, and Shen 2007; Itskov and Ribeiro 2013), courtship (Kim, Jan, and Jan 2013), aggression (Dierick and Greenspan 2007), and sleep (Chunxia He et al. 2013). Therefore, we asked if molecular clocks in NPF-positive neurons mediate free-running behavioral rhythms. We found that flies expressing CLKΔ with *Npf*-GAL4 as well as flies carrying a null mutation in *nfpr*, the gene encoding the receptor for NPF, display normal rhythms of rest:activity (Table 2.1). In contrast, *Dvpdf*-GAL4;*pdf*-GAL80 driving UAS-CLKΔ increased the number of arrhythmic flies and slightly lengthened the period of rhythmic flies, further indicating that *Dvpdf*-GAL4;*pdf*-GAL80 and *Npf*-GAL4 do not represent the exact same population of LN_ds (Table 2.1). These data suggest that NPF plays at best a minor role in regulating rhythmic locomotor behavior. However, NPF might play a role in other aspects of circadian rhythms, such as circadian control of energy homeostasis.

To determine whether NPF drives rhythmic *sxe1* expression in the fat body, we began by knocking down *npf* in all NPF-positive cells with RNA interference (RNAi), as *npf* mutants are not available. Driving UAS-*npf* RNAi under *Npf*-GAL4 resulted in dampened but still rhythmic *sxe1* expression (Figure 2.4A). Although this manipulation vastly reduced *npf* levels in fly heads (Figure 2.4B), it is possible that very small amounts of NPF can drive some level of cycling; alternatively, knockdown efficiency may have been limited in the NPF-positive clock cells. Thus we tested the null mutant of the sole NPF receptor in *Drosophila*, *npfr* (Garczynski et al. 2002). Our results show *sxe1* levels do not cycle and are dramatically reduced in *npfr* mutants, which

phenocopies the daily *sxe1* expression profile of flies expressing either CLKΔ or CYCΔ under *Npf*-GAL4 (Figure 2.4C). Rhythmic expression of *Cyp6a21* was also lost in the fat body of *npfr* mutants (Figure 2.4D). We speculate that expressing CLKΔ under *Npf*-GAL4 alters the circadian production or release of NPF. Indeed, mRNA analysis of *Npf*-GAL4/UAS-CLKΔ heads showed that *npf* levels were reduced compared to controls (Figure 2.4E) while cyclic *per* expression, which arises from clock function in many different cells, was unaffected (Figure 2.4F). This result is consistent with reports of loss of NPF expression in LN_ds of Clk^{irk} brains (G. Lee, Bahn, and Park 2006). Taken together, these data suggest circadian clocks in NPF-positive cells regulate NPF expression to subsequently drive *sxe1* and *Cyp6a21* rhythms in the fat body.

Npy Regulates Circadian Expression of Cytochrome P450 genes in the Mammalian Liver

In mammals, liver-specific circadian clocks play an important role in liver physiology via contributions to glucose homeostasis and xenobiotic clearance (Gachon et al. 2006; Lamia, Storch, and Weitz 2008). Liver clock ablation in mice resembles fat body clock ablation in flies; in particular, ablating liver clocks eliminates rhythmic expression of most, but not all, circadian liver transcripts (Kornmann, Schaad, Bujard, et al. 2007). Furthermore, rescuing clock function specifically in the brains of $Clock^{\Delta 19}$ mutant mice restores rhythmic expression of roughly 40% of circadian liver transcripts (Hughes et al. 2012). These data suggest that some circadian transcripts in the liver are driven by systemic signals, perhaps emanating from the master pacemaker in the suprachiasmatic nuclei (SCN) of the hypothalamus (Mohawk, Green, and Takahashi 2012).

Since we identified NPF in the regulation of circadian gene expression in the fly fat body, we reasoned that the mammalian homolog, Npy, might regulate circadian gene expression in the liver. Thus, we isolated RNA from the livers of male *Npy* knockout (*Npy* KO) mutant mice and wild type controls over the course of an entire day. Although there is no direct mammalian homologue of *sxe1*, we noticed that a similar P450 enzyme involved in xenobiotic detoxification, *Cyp2b10*, also continues to cycle in animals lacking functional liver clocks (Kornmann, Schaad, Bujard, et al. 2007). We measured *Cyp2b10* levels in *Npy* KO and wild type mice and found that *Cyp2b10*

transcript levels did not display a circadian rhythm in *Npy* KOs (Figure 2.5A). However, circadian expression of the core clock gene *Rev-erb alpha* was unaffected in the livers of *Npy* KOs confirming that the liver clock is still intact (Figure 2.5B). We wondered whether other enzymes involved in xenobiotic detoxification are also regulated by Npy. *Aminolevulinic acid synthase 1* (*Alas1*), is required for P450 synthesis (Furuyama, Kaneko, and Vargas 2007) and was also reported to cycle in the absence of the liver clock (Kornmann, Schaad, Bujard, et al. 2007). Unlike *Cyp2b10*, circadian expression of *Alas1* was unaffected in *Npy* KOs, suggesting that NPY does not regulate global rhythmic detoxification in the liver (Figure 2.5C).

To determine the extent to which loss of Npy impacts gene expression in the liver, we performed genome-wide expression analysis on wild type control and *Npy* KO livers collected at 4-hr intervals over a day in LD. Using the newly developed MetaCycle package (see Materials and Methods) and a stringent *P*-value cutoff of $p<0.01$ to detect cyclic transcripts, we found that 289 transcripts were cyclic in controls but not in *Npy* KO, indicating that the oscillation of these transcripts is under the regulation of Npy signaling (Figure 2.5D). Furthermore, the loss of transcript cycling was generally not accompanied by differences in expression levels; in other words, the median transcript abundance in wild type animals correlated with that in *Npy* KO (Figure 2.5E). Based on our *Drosophila* data and also the fact that Npy regulates *Cyp2b10* expression, we speculated that Npy might have a broader role in regulating cytochrome P450 gene expression. We examined the microarray data for cyclic P450 transcripts and found several of these genes were not cyclic in *Npy* KOs. Notably, the microarray data confirmed our qPCR data for *Cyp2b10* and indicated that *Cyp2r1, Cyp17a1*, and *Cyp2c70* transcripts also cycle in wild type but not in *Npy* KO liver. In contrast, *Cyp3a13* and *Cyp7a1* transcripts cycle robustly in both genotypes.

Lastly, we compared our *Npy* KO data to the previously reported set of liver transcripts whose expression oscillates independently of the liver clock (Kornmann, Schaad, Bujard, et al. 2007; Kornmann, Schaad, Reinke, et al. 2007). Among that set, we discovered nine additional liver clock-independent transcripts— *Rbl2*, *Ddx46*, *Cirbp*, *Sqle*, *Ldb1*, *Actg1, Hmgcs1*, *Heca*, and *Ctgf*— that require Npy for robust rhythmic expression (Table 2.3). As only a subset of liver-clock

independent transcripts requires Npy for oscillations, other mechanisms likely contribute to rhythmic expression of these genes (further discussed below). Although many genes, including clock genes, continued to cycle in *Npy* knockout livers, the overall phases and amplitudes of expression for cycling transcripts in *Npy* KO slightly differed from those in wild type (Figure 2.S1). Overall, we found that diverse liver circadian transcripts, including cytochrome P450 genes, are influenced by Npy signaling. This report is the first to describe a role for Npy in the circadian regulation of peripheral gene expression in mammals.

Discussion

In this report we dissect the role of neural clocks in the regulation of circadian gene expression in a peripheral tissue. We find that clocks in PDF-positive neurons influence cycling of the *per* clock gene in the *Drosophila* fat body in the absence of external cues. More importantly, we identify the non-cell autonomous mechanism that underlies cycling of specific fat body transcripts in *Drosophila* and specific liver transcripts in mice. We show that clocks in *Drosophila* NPF-positive neurons drive daily expression of *sxe1* and *Cyp6a21*, fat body genes not controlled by the fat body clock. Likewise, mammalian Npy drives rhythmic expression of specific liver transcripts, indicating a conserved role of NPF/Npy in the control of peripheral circadian rhythms.

Prior to this report, it was proposed that clocks in the brain and fat body interact, but the extent of the interaction and the mechanisms driving it were not identified (Xu, Zheng, and Sehgal 2008). Our data suggest that in light:dark cycles, the central clock is not required for cycling of the fat body clock, although we cannot exclude an effect on the phase of cycling. However, in constant conditions, the clock in PDF cells influences the fat body clock, as it does the prothoracic gland clock. Why the central clock regulates only some peripheral clocks in the fly is unclear. Unlike other peripheral clocks, the fat body clock modulates behavioral rhythms, specifically the phase of feeding rhythms, in addition to its own physiology (Xu, Zheng, and Sehgal 2008; Xu et al. 2011; Seay and Thummel 2011). Thus, synchrony between clocks in the brain and fat body is likely essential for metabolic homeostasis.

The circadian system controls behavior and physiology in large part through its regulation of circadian gene expression (Zheng and Sehgal 2012). Tissue-specific gene expression patterns are thought to be generated primarily by local clocks; however, few studies have comprehensively evaluated rhythmic expression driven by local clocks versus external factors. A previous comparison of gene expression profiles of flies containing or lacking an intact fat body clock found that the fat body clock only regulates ~60% of all circadian fat body genes (Xu et al. 2011). Here we report that at least some of the other 40% of circadian fat body genes are regulated by clocks located in other tissues. We found that disrupting clocks in NPF-positive cells abolished rhythmic expression of two cytochrome P450 genes, *sxe1* and *Cyp6a21*. Since we specifically disrupted the molecular clock by expressing CLKΔ or CYCΔ, only NPF-positive cells containing circadian clock components should have been targeted (LN_ds). We cannot formally exclude the possibility that expression of CLKΔ or CYCΔ in non-clock cells or even in the gut (Brown et al. 1999) contributes to this phenotype; however, the effect of targeting CLKΔ to specific LN_ds with the *Dvpdf* driver suggests that these cells contribute to the peripheral rhythm phenotype. In addition, even though NPF expression has been reported in both the LN_ds and LN_vs (Hermann et al. 2012), it is unlikely the LN_vs regulate *sxe1* rhythms, because disrupting clocks in PDF-positive LN_vs does not abolish *sxe1* oscillations. LN_ds can be synchronized by inputs from LN_vs (Guo et al. 2014), but cell-autonomous entrainment mechanisms in the LN_ds may limit the influence of LN_vs in light:dark cycles, which may explain why ablating clocks in LN_vs has a small effect on *sxe1* expression. Thus, we suggest that the clocks in LN_ds are required for cycling of *sxe1* and *Cyp6a21* expression in the fat body.

NPF neuropeptide reportedly modulates rest:activity rhythms in *Drosophila* (Hermann et al. 2012; C. He et al. 2013). We did not detect a role for clocks in NPF cells, nor for the single known NPF receptor, in the regulation of rest:activity rhythms, but it is possible that other mechanisms are utilized. However, we show that NPF regulates the expression of circadian genes in the fat body. Consistent with the assertion that NPF is the relevant output for fat body rhythms from NPF-positive cells, we also found that flies lacking functional clocks in these cells display significantly reduced *npf* levels (Figure 2.4D). Interestingly, Lee *et al*. previously showed

that *npf* mRNA is absent in the LN_ds of adult male *Clk*^{jrk} mutant brains (G. Lee, Bahn, and Park 2006). This further supports our hypothesis that NPF is regulated by the circadian clock in LN_ds, and its release from these neurons is necessary for mRNA rhythms of specific fat body genes. However, the effect of NPF on the fat body is likely not direct. Some insect species release NPF into the hemolymph to reach other tissues, but this does not appear to be the case in *Drosophila* (Nässel and Wegener 2011). The NPF receptor may function in clock neurons in the dorsal fly brain (i.e. DN1s), neurons in the suboesophageal ganglion, or neurons innervating the mushroom body (Krashes et al. 2009; C. He et al. 2013). Alternatively, NPF could signal through recently identified neurons downstream of the clock network, which are part of the circadian output circuit driving rest:activity rhythms (Cavanaugh et al. 2014). Although much is known about the neuronal clock network, very little is known about the neurons and signals downstream of the clock network, which make up the output pathways leading to rhythms in behavior and physiology. Our discovery that NPF-positive clock neurons drive rhythmic gene expression in the fat body provides a unique opportunity to investigate the pathway(s) that convey circadian information from the brain to peripheral tissues.

We report a striking parallel in the mammalian system, where the NPF ortholog, Npy, drives cyclic expression of specific liver genes, notably several in the cytochrome P450 pathway. Npy is not required for free-running rest:activity rhythms in mice, but it promotes phase shifts in these rhythms in response to non-photic stimuli (Yannielli and Harrington 2004; Maywood, Okamura, and Hastings 2002; Besing et al. 2012). Behavioral effects of Npy are likely mediated by its brain expression, but as Npy is also expressed in the periphery, it is possible that a peripheral source contributes to cycling in the liver. Regardless, Npy has a profound effect on circadian gene expression in the liver.

Since NPF promotes feeding in *Drosophila* larvae (Wu et al. 2003; Wu, Zhao, and Shen 2005; Lingo, Zhao, and Shen 2007) and Npy does so in mice, it is possible NPF/Npy drive cycling in the fat body/liver through the regulation of feeding. Feeding is known to be a potent stimulus for metabolic clocks, with circadian gene expression in peripheral tissues driven by restricted feeding cycles in both flies and mammals (Xu et al. 2011; Gill et al. 2015; Vollmers et al. 2009). However,

under conditions of *ad lib* food, feeding rhythms in flies are of low amplitude and likely insufficient to drive robust cycling. Consistent with this, while cyclic expression of *Cyp6a21* can be driven by a restricted feeding paradigm, as can the clock in the fat body, cycling is more robust when this paradigm is conducted in wild type versus clockless animals (Xu et al. 2011), indicating that its regulation is not through feeding alone. Finally, time restricted feeding experiments of mice do not support the idea that restricted feeding drives cycling of *Cyp2b10* in clockless mice, even though it is sufficient to maintain rhythms of many other liver genes (Vollmers et al. 2009). Thus, while feeding cannot be discounted as an important factor, which may contribute to the cycling of the genes reported here, these genes are unique in their dependence on Npy. Only a limited subset of liver transcripts previously shown to be independent of the liver clock require Npy for cyclic expression (Kornmann, Schaad, Bujard, et al. 2007). Similarly, several fly genes, for example *sxe2* and *CG17562*, continue to oscillate when CLKΔ is expressed under *Npf*-GAL4 (data not shown). These results suggest there are additional mechanisms regulating circadian rhythms in the fat body/liver. Why would more than one mechanism exist to couple rhythmic gene expression in a specific peripheral tissue to other clocks? One possibility is that different mechanisms regulate distinct phases of circadian gene expression. Alternatively, different mechanisms may couple gene expression to different cell populations, processes, or behaviors.

The functional importance of the interaction between NPF/Npy and fat body/liver genes in the circadian system is unclear. Cytochrome P450 genes, such as *Cyp6a21*, *sxe1 and Cyp2b10*, are associated with detoxification (King-Jones et al. 2006; Fujii, Toyama, and Amrein 2008), which is likely rhythmic, although not yet reported. Overexpression of NPFR in larvae increases foraging behavior as well as consumption of noxious or bitter compounds (Wu, Zhao, and Shen 2005). Indeed, NPF/Npy signaling is generally associated with an increase in feeding (Wu et al. 2003; Wu, Zhao, and Shen 2005; Lingo, Zhao, and Shen 2007; Beck 2006), which can lead to ingestion of toxic substances. Thus, coordination of feeding with expression of detoxification enzymes, such as *sxe1*, *Cyp6a21* and *Cyp2b10,* through NPF/Npy may have evolved to promote survival. Large delays between consumption of noxious substances and their removal could affect an animal's health; thus, the need for coordination between clocks in processing such

substances. Conservation of cytochrome P450 regulation from flies to mammals supports the idea that neural control of detoxification in the periphery promotes organismal fitness (Figure 2.6).

In this study we exclusively evaluated males, because the initial studies reporting rhythmic gene expression in the presence and absence of the fat body or liver clock in flies or mammals respectively, were based on males (Xu et al. 2011; Kornmann, Schaad, Bujard, et al. 2007). Interestingly, NPF/Npy and *sxe1*/*Cyp2b10* expression is sexually dimorphic in *Drosophila* (G. Lee, Bahn, and Park 2006; Fujii, Toyama, and Amrein 2008) and mammals (Lu et al. 2013; Karl, Duffy, and Herzog 2008; Urban, Bauer-Dantoin, and Levine 1993), suggesting there may be some gender specificity to this entire pathway. The functional significance of sex-specific regulation is unclear, but indicates that other mechanisms could contribute to such coordination in females.

This work has implications for chronopharmacology, which is based on the circadian timing of drug metabolism, transport, tolerance, and efficacy. Rhythmic expression of genes involved in drug breakdown and absorption in the liver influences drug efficacy and toxicity (Dallmann, Brown, and Gachon 2014), and loss of such rhythms can have long-term effects on health and lifespan (Gachon et al. 2006). Therefore, expression of these genes may be tightly coordinated to optimize drug metabolism, and speaks to the importance of controlling the timing of drugs that have toxic side effects. The role for Npy reported here suggests it could be a potential target for improving drug efficacy and toxicity. Ultimately, understanding circadian rhythms at a systems level, including interactions between tissues and other physiological systems, will be useful from biological and clinical perspectives.

Acknowledgements

We thank members of the Sehgal laboratory for input and advice throughout this project. We are also grateful for the services provided by the Neurobehavioral Testing core at the UPenn Smilow Center. The work was supported by NIH grant R37NS048471. RE and ANK were supported in part by a Predoctoral Training Grant in Genetics (T32 GM008216).

Author Contributions

RE, Conception and design, Acquisition of data, Analysis and interpretation of data, Drafting or revising the article. ANK, Acquisition of data, Analysis and interpretation of data, Drafting or revising the article. GW, Analysis and interpretation of data, Drafting or revising the article. J BH, Analysis and interpretation of data, Drafting or revising the article. AS, Conception and design, Analysis and interpretation of data, Drafting or revising the article

Figures

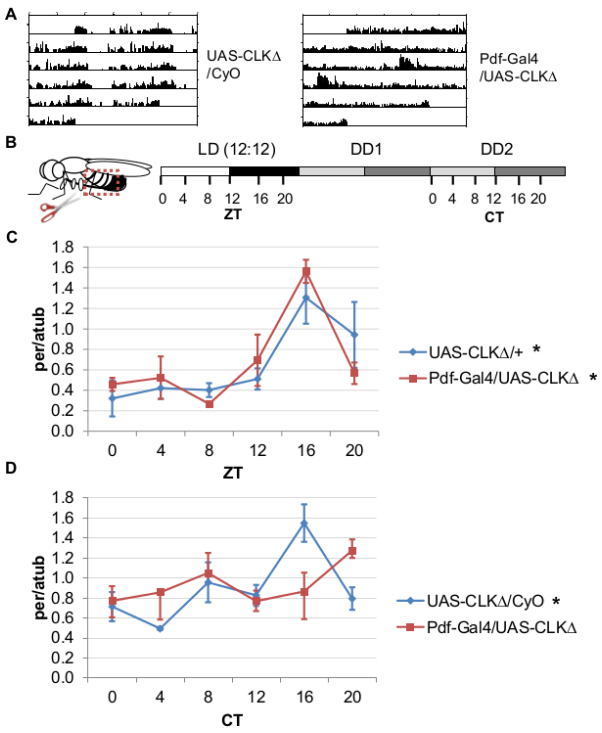

Figure 2.1

Oscillations of *per* in the fat body require an intact central clock in the absence of external cues. (A) Representative double-plotted activity records of individual control UAS-CLKΔ/CyO (left) and *Pdf*-GAL4/UAS-CLKΔ (right) flies over the course of 5 days in constant darkness. **(B)** Schematic of experimental design. Male flies, aged 7-10 days, were entrained for several days in 12 hour light: 12 hour dark cycles (LD). Male flies were dissected to obtain abdominal fat bodies (dotted red box) either on the last day in LD or on the second day of constant darkness (DD2). Graphs depict mRNA levels, normalized to α−tubulin (atub), over the course of the day in the presence of light (LD; Zeitgeber Time, ZT) or in constant darkness (DD2; Circadian Time, CT). Ablating the central clock (*Pdf*-GAL4/UAS-CLKΔ) (red line) does not affect *per* rhythms in LD **(C)** but abolishes *per* rhythms in DD2 **(D)** compared to controls (blue line). Each experiment was repeated independently three times, and average ± standard error of the mean (SEM) is reported for each timepoint. Significant rhythmicity was determined using JTK_cycle. Asterisk (*) adjacent to genotype label indicates JTK_cycle $p<0.05$. See Table 2.2 for JTK cycle values.

Figure 2.1 contributions: R.E. generated data; A.N.K. and R.E analyzed data.

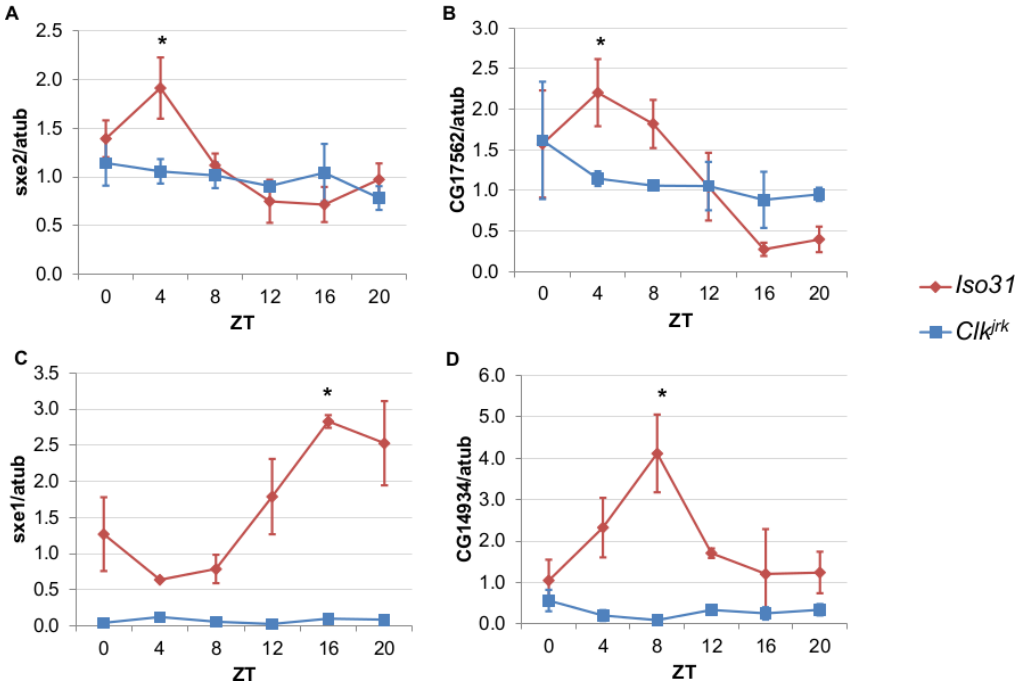

Figure 2.2

Rhythmic expression of genes that cycle independently of the fat body clock requires clocks in other tissues.

Daily oscillations of several fat body clock-independent genes were tested in male mutants lacking functional clocks in all tissues, *Clk*^{jrk} mutants, in LD. Rhythmicity of *sxe2* **(A)**, *CG17562* **(B)**, *sxe1* **(C)**, and *CG14934* **(D)** is abolished in *Clk*^{jrk} mutants but is intact in Iso31 wild type controls. All genes were normalized to α−tubulin (atub) levels. Each experiment was repeated independently three times. The average value for each timepoint is plotted with error bars denoting SEM. JTK_cycle p value <0.05 is indicated by an asterisk (*) at the time of peak expression. See Table 2.2 for JTK_cycle p values. ZT- Zeitgeber Time

Figure 2.2 contributions: R.E. generated data; A.N.K. and R.E analyzed data.

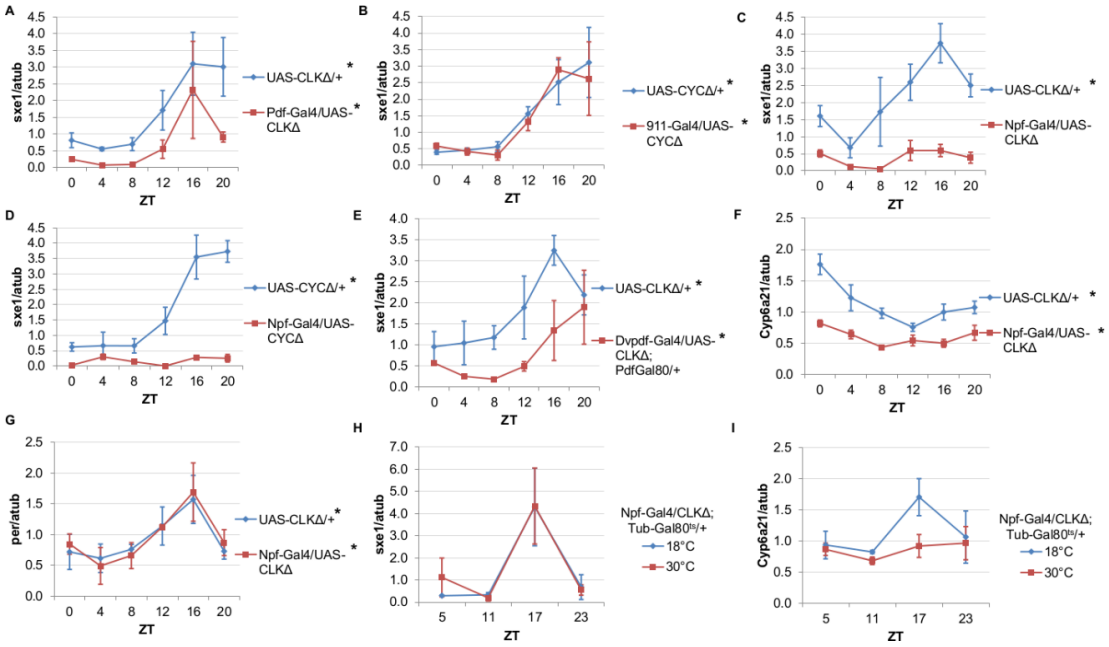

Figure 2.3

NPF-expressing clock neurons regulate rhythmic expression of fat body genes, *sxe1* and *Cyp6a21*. (A,B) Ablating the molecular clock by expressing CLKΔ or CYCΔ in either the LN_vs (*Pdf*-GAL4) **(A)** or DN1s (911-GAL4) **(B)** does not eliminate rhythmic *sxe1* expression in the fat body. **(C,D)** Expressing CLKΔ **(C)** or CYCΔ **(D)** using *Npf*-GAL4 abolishes rhythmic *sxe1* expression in the fat body. **(E)** Expressing CLKΔ in a subset of LN_ds (*Dvpdf*-GAL4;*Pdf*-GAL80) also does not eliminate cycling but reduces *sxe1* expression in the fat body. **(F)** *Npf*-GAL4>UAS-CLKΔ abolishes rhythmic *Cyp6a21* expression in the fat body. **(G)** *per* expression is rhythmic in flies expressing UAS-CLKΔ under *Npf*-GAL4. **(H, I)** CLKΔ expression in NPF cells is restricted to adulthood using *Tub*-GAL80^{ts}. **(H)** *sxe1* expression is not affected with adult-specific clock ablation in NPF cells. **(I)** Rhythmic *Cyp6a21* expression is affected in the fat body when *Npf*-GAL4>UAS-CLKΔ expression is induced in adult at 30°C. Each experiment was repeated independently at least twice. The average value for each timepoint is plotted with error bars denoting SEM. JTK_cycle p value <0.05 is indicated by an asterisk (*) next to the genotype label. See Table 2.2 for JTK_cycle p values. ZT- Zeitgeber Time. Figure 2.3 contributions: R.E. generated and analyzed data in panels A-E, F; A.N.K. generated data for panels F, H, I and analyzed all data.

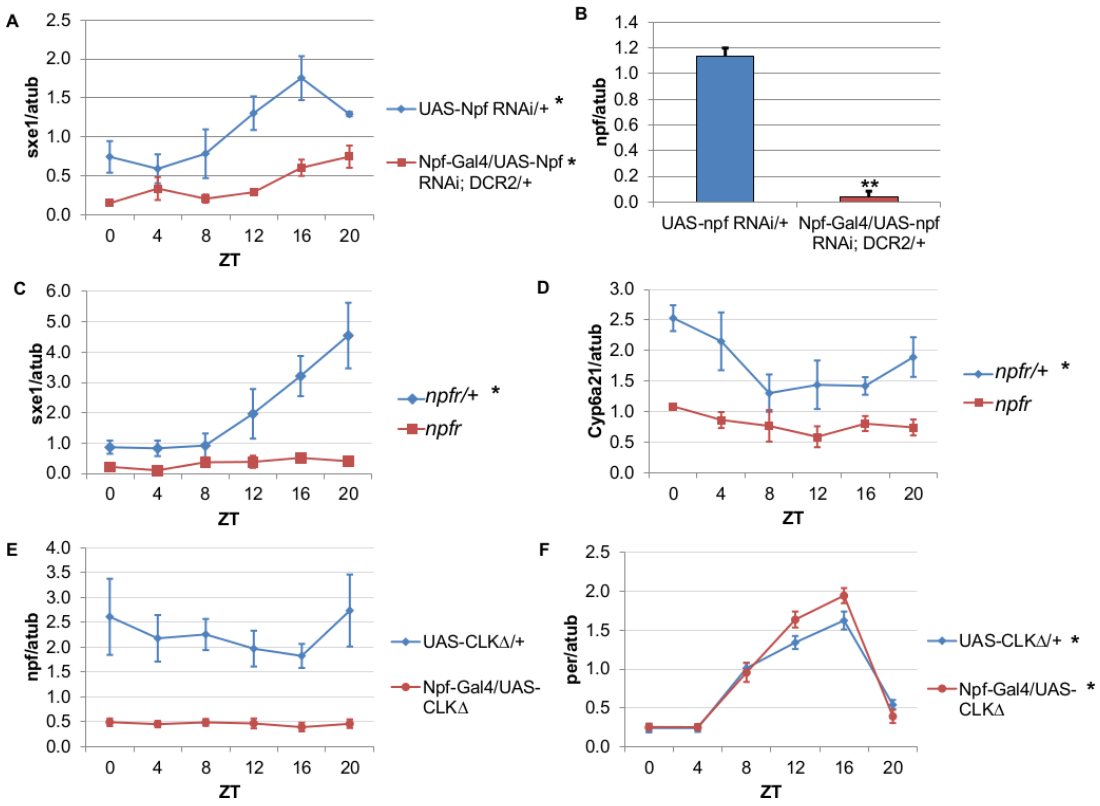

Figure 2.4

NPF is a critical circadian signal for *sxe1* and *Cyp6a21* rhythms in the fat body.

(A) Knockdown of *npf* in all NPF-positive cells does not eliminate rhythmicity but reduces expression of *sxe1* in the fat body at all times. **(B)** Analysis of *npf* knockdown efficiency in heads of *Npf*-GAL4/UAS-*npf* RNAi; DCR2 (UAS-Dicer2) flies showed a significant reduction in *npf* levels by Student's t-test (**= p<0.001). **(C,D)** *sxe1* and *Cyp6a21* expression in the fat body are reduced and do not cycle in homozygous *npfr* mutants compared to heterozygous controls. **(E)** *npf* levels in the heads of *Npf*-GAL4/UAS-CLKΔ are reduced compared to controls (UAS-CLKΔ/+). **(F)** Total *per* levels are not altered in the heads of *Npf*-GAL4/UAS-CLKΔ compared to controls. Each experiment was repeated independently three times except for (B) which n=6 for each genotype. The average value ± SEM for each timepoint is plotted. JTK_cycle p<0.05 is indicated by an asterisk (*) next to the genotype label. See Table 2.2 for JTK_cycle p values. ZT- Zeitgeber Time.

Figure 2.4 contributions: R.E. generated and analyzed data in panels A-C, E, F; A.N.K. generated data for panel D and analyzed all data.

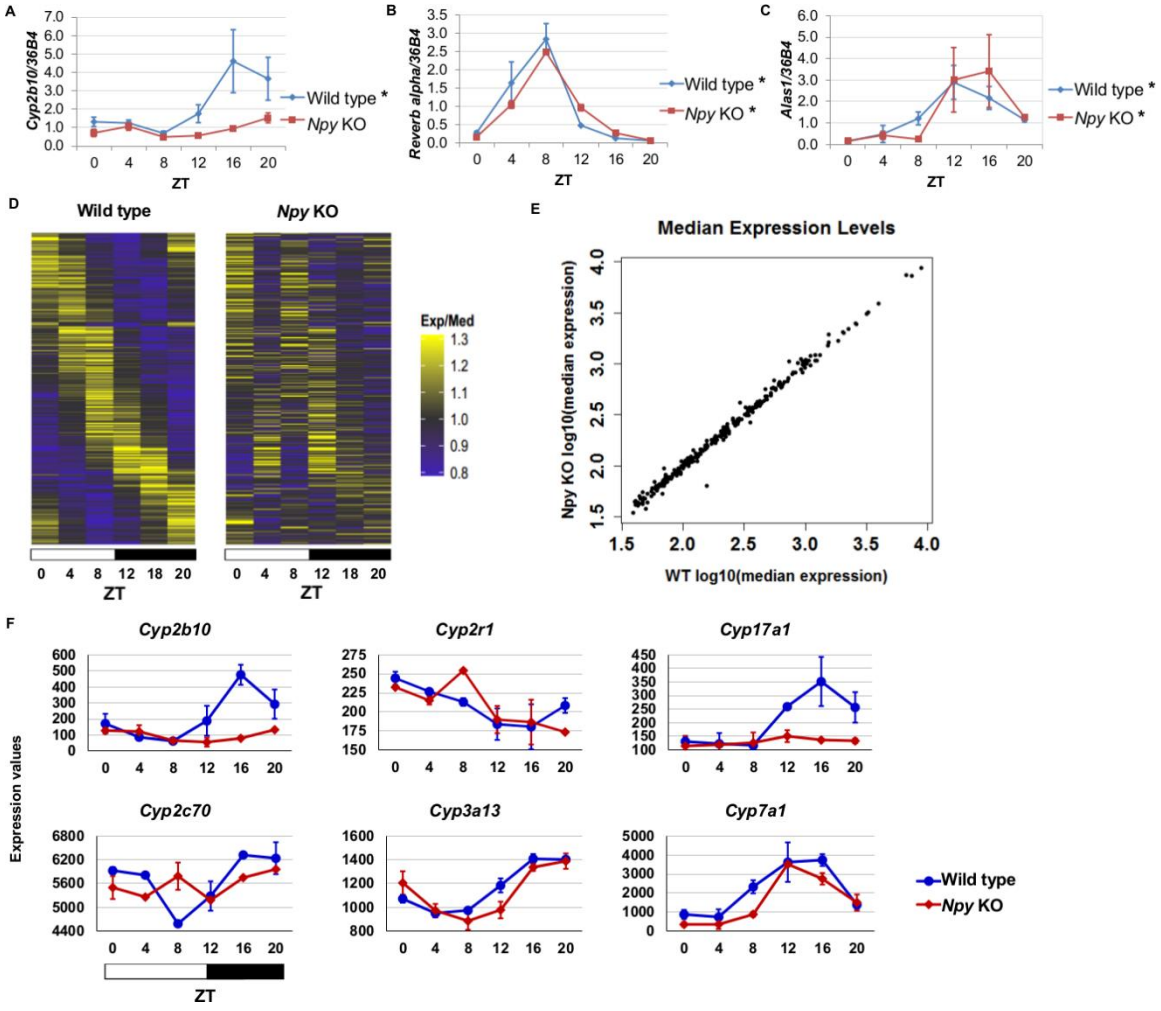

Figure 2.5

Npy regulates circadian expression of cytochrome P450 genes in the murine liver. (A-C) Quantitative PCR analysis in murine livers. Daily oscillations of *Cyp2b10* expression **(A)** are abolished in *Npy* KOs compared to their background controls (wild type), while oscillations of the circadian gene, *Reverb alpha* **(B)**, are unaffected. **(C)** Levels of another liver clock-independent gene, *Alas1,* are similar in wild type and *Npy* KO, suggesting Npy does not regulate its rhythmicity. For qPCR data, *n*=3-4 mice for each genotype and time point. Transcript levels were normalized to the housekeeping gene *36B4*. **(D-F)** Microarray analysis was used to detect transcript expression in livers of *Npy* KO and their background controls collected over the course of 24 hours in LD. **(D)** The heatmap includes transcripts that oscillate in wild type but not in *Npy* KO liver. Data represent the average transcript abundance from *n*=2 samples for each genotype

and timepoint. Here, the MetaCycle *p*-value cutoff of p<0.01 was used to identify cyclic transcripts; p>0.8 was considered not cyclic. **(E)** The median expression values of the wild type-only cyclic transcripts are not different between *Npy* KO and wild type. **(F)** Daily expression values of cytochrome P450 genes from microarrays. Cytochrome P450 genes *Cyp2b10, Cyp2r1, Cyp17a1,* and *Cyp2c70* are cylic in wild type liver but are not cyclic in *Npy* KO liver. *Cyp3a13* and *Cyp7a1* cycle robustly in both wild type and *Npy* KO. Graphs show average ± SEM. ZT- Zeitgeber Time

Figure 2.5 contributions: R.E. generated and analyzed data in panels A-C; A.N.K. generated data for panels D-F and analyzed all data; G.W. analyzed data for panels D-F.

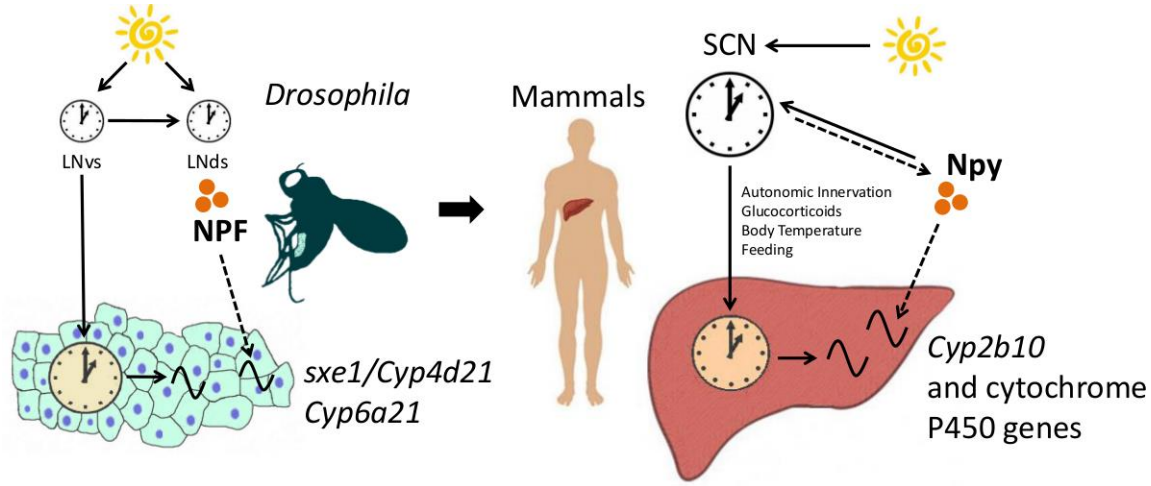

Figure 2.6

NPF/Npy regulate rhythmically expressed P450 enzymes in the periphery of flies and mammals.

A model of brain clock regulation of peripheral cycling. Brain clocks regulate clocks in peripheral tissues. In *Drosophila*, clocks in PDF-positive neurons (LN_vs) regulate the clock in the fat body. Similarly, in mammals, clocks in the suprachiasmatic nuclei (SCN) have been shown to regulate peripheral clocks such as the liver clock via autonomic innervation, glucocorticoids, body temperature, and feeding. In both the fat body and liver, not all circadian transcripts depend on the local-tissue clock. Clocks in NPF-positive LN_ds and NPF itself regulate circadian expression of cytochrome P450 enzymes in the fly fat body. The LN_vs can influence other brain clocks (such as the LN_ds), but are not required for rhythms of fat body transcripts in LD as LN_ds may entrain directly to light. In mammals, Npy was previously known to be a non-photic signal involved in entraining the SCN. However, the SCN could also influence Npy production or release, which in turn drives rhythmic expression of cytochrome P450 enzymes in the liver.

Figure 2.6 contributions: R.E. produced figure.

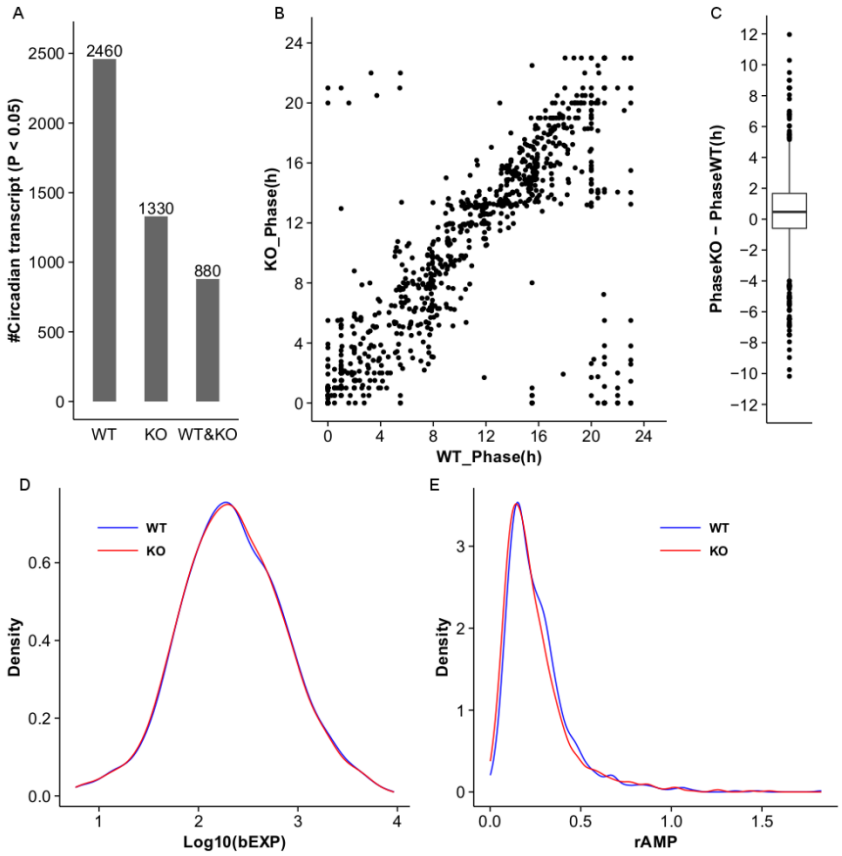

Figure 2.S1 (related to Figure 2.5)

MetaCycle analysis of cycling liver transcripts in wild type and *Npy* KO.

(A) Microarray analysis detects 2,460 and 1,330 cycling transcripts (MetaCycle p<0.05) in WT and *Npy* KO liver datasets respectively. 880 cycling transcripts are common between the two datasets. **(B,C)** Scatter plot and box plot graph the phase in *Npy* KO relative to WT for the 880 genes with cycling expression patterns in both datasets. In general, the phase in *Npy* KO is delayed compared to that in WT. **(D)** Density plot graphs the distribution of baseline expression levels, bEXP (see Materials and Methods), for the 880 cycling transcripts in WT and KO datasets. X-axis graphs the log base 10 of bEXP value. **(E)** Density plot graphs the distribution of relative amplitudes, rAMP (see Materials and Methods), for the 880 cycling transcripts in WT and KO datasets.

Figure 2.S1 contributions: A.N.K. generated and analyzed data and G.W. analyzed data.

Tables

Table 2.1

Analysis of locomotor activity rhythms in flies under DD conditions.

Clock ablation in *Pdf*+ neurons (*Pdf*-GAL4/UAS-CLKΔ) or in LN_d neurons (*Dvpdf*-GAL4/UAS-CLKΔ; *pdf*-GAL80/+) disrupts free-running behavioral rhythms in flies. Flies with clock ablation in *Npf*+ neurons (*Npf*-GAL4/UAS-CLKΔ) and *npfr* mutants have normal free-running rhythms.

Genotype	n	% Rhythmic	Period	FFT
Pdf-GAL4/UAS-CLKΔ	39	36	23.51	0.04
UAS- CLKΔ/CyO	48	90	23.71	0.06
Npf-GAL4/UAS-CLKΔ	62	98	24.01	0.06
UAS-CLKΔ/+	58	100	23.70	0.05
npfr	39	95	23.66	0.05
npf/+	46	100	23.44	0.11
Dvpdf-GAL4/UAS-CLKΔ; *pdf*-GAL80/+	63	68	25.51	0.06
UAS-CLKΔ/+	63	100	23.91	0.08

Table 2.1 contributions: R.E. produced and analyzed data.

Table 2.2

Analysis of cycling in gene expression with JTK_Cycle statistics and two-factor ANOVA test.

All qPCR data were tested for circadian rhythmicity with JTK_cycle test and two-way ANOVA for repeated measures with a Tukey's *post hoc* test. P-values from these tests are summarized.

Figure	Genotpye	Gene	Tissue	JTK_cycle P-value	Time P-value	Genotype P-value	TimeXGenotype P-value
1C	[ZT] UAS-CLKΔ/+	*per*	Fat Body (FB)	0.0194	< 0.0001	0.7826	0.4679
1C	[ZT] Pdf-Gal4/UAS-CLKΔ	*per*	FB	0.0094			
1D	[CT] UAS-CLKΔ/+	*per*	FB	0.0041	0.0313	0.665	0.0281
1D	[CT] Pdf-Gal4/UAS-CLKΔ	*per*	FB	1			
2A	*Iso31*	*sxe2*	FB	0.0014	0.0131	0.1852	0.0843
2A	*Clk^{irk}*	*sxe2*	FB	1			
2B	*Iso31*	*CG17562*	FB	0.0014	0.0223	0.6409	0.1746
2B	*Clk^{irk}*	*CG17562*	FB	0.6945			
2C	*Iso31*	*sxe1*	FB	0.002	0.0019	<0.0001	0.002
2C	*Clk^{irk}*	*sxe1*	FB	1			
2D	*Iso31*	*CG14934*	FB	0.082	0.1146	<0.0001	0.0266
2D	*Clk^{irk}*	*CG14934*	FB	0.5429			
2E	*Iso31*	*cyp6a21*	FB	0.1769	0.2791	0.9816	0.6328
2E	*Clk^{irk}*	*cyp6a21*	FB	0.3837			
3A	UAS-CLKΔ/+	*sxe1*	FB	0.0007	0.0003	0.0049	0.7061
3A	Pdf-Gal4/UAS-CLKΔ	*sxe1*	FB	9.00E-07			
3B	UAS-CYCΔ/+	*sxe1*	FB	0.0363	0.0006	0.7995	0.9592
3B	911-Gal4/UAS-CYCΔ	*sxe1*	FB	0.0044			
3C	UAS-CLKΔ/+	*sxe1*	FB	0.0014	0.006	<0.0001	0.0749
3C	Npf-Gal4/UAS-CLKΔ	*sxe1*	FB	0.1969			
3D	UAS-CYCΔ/+	*sxe1*	FB	0.0029	<0.0001	<0.0001	<0.0001
3D	Npf-Gal4/UAS-CYCΔ	*sxe1*	FB	1			
3E	UAS-CLKΔ/+	*sxe1*	FB	0.0196	0.0038	0.0017	0.5326
3E	Dvpdf-Gal4/UAS-CLKΔ;Pdfgal80/+	*sxe1*	FB	0.0001			
3F	UAS-CLKΔ/+	*cyp6a21*	FB	0.0009	<0.0001	<0.0001	0.0574
3F	Npf-Gal4/UAS-CLKΔ	*cyp6a21*	FB	0.0259			
3G	UAS-CLKΔ/+	*per*	FB	0.0568	0.0057	0.8767	0.9902
3G	Npf-Gal4/UAS-CLKΔ	*per*	FB	0.0441			
4A	UAS-Npf RNAi/+	*sxe1*	FB	0.002	0.0005	<0.0001	0.1421
4A	Npf-Gal4/UAS-Npf RNAi	*sxe1*	FB	0.0441			
4B	UAS-Npf RNAi/+	*cyp6a21*	FB	1	0.1525	0.0085	0.9349
4B	Npf-Gal4/UAS-Npf RNAi	*cyp6a21*	FB	1			
4BC	Not analyzed with JTK	*npf*	Head	-			
4CD	*npfr*/+	*sxe1*	FB	0.0128	0.0008	<0.0001	0.0038
4CD	*npfr*	*sxe1*	FB	0.1969			

4DE	*npfr*/+	*cyp6a21*	FB	0.0916	0.0319	<0.0001	0.4182
4DE	*npfr*	*cyp6a21*	FB	0.115			
4EF	UAS-CLKΔ/+	*npf*	Head	1	0.7588	<0.0001	0.846
4EF	Npf-Gal4/UAS-CLKΔ	*npf*	Head	1			
4FG	UAS-CLKΔ/+	*per*	Head	0.0001	<0.0001	0.141	0.042
4GF	Npf-Gal4/UAS-CLKΔ	*per*	Head	1.19E-05			
5A	Wild type	*Cyp2b10*	Liver	0.001	0.0209	0.0034	0.164
5A	NPY Knockout (KO)	*Cyp2b10*	Liver	0.051			
5B	Wild type	*Reverbα*	Liver	7.46E-12	<0.0001	0.4979	0.0661
5B	NPY KO	*Reverbα*	Liver	7.17E-09			
5C	Wild type	*Alas1*	Liver	9.81E-06	0.0007	0.8476	0.8202
5C	NPY KO	*Alas1*	Liver	0.0018			

Table 2.2 contributions: R.E. and A.N.K. analyzed data.

Table 2.3

Cycling of liver clock-independent genes in wild type and *Npy* KO liver.

Microarray and MetaCycle analysis of liver clock-independent genes in wild type (WT) and *Npy* null (KO) liver. Cycling of liver clock-independent gene expression is eliminated, phase shifted, or unaffected in *Npy* KO liver. List of liver clock-independent genes from Kornmann et al. 2007 *Cold Spring Harbor Symposia on Quantitative Biology*. Median Exp = median expression level, Relative Amp = amplitude of gene expression cycling.

Liver clock-independent genes with disrupted cycling of expression in *Npy* KO

Affymetrix transcript ID	Gene	WT MetaCycle P value	WT Phase	WT Median Exp	WT Relative Amp	KO MetaCycle P value	KO Phase	KO Median Exp	KO Relative Amp
17503756	Rbl2	0.0003	8.94	367.0	0.217	0.0753	9.20	338.7	0.132
17287733	Ddx46	0.0007	7.77	264.2	0.229	0.1756	11.46	262.8	0.158
17235227	Cirbp	0.0037	6.28	58.1	0.188	0.0924	7.83	54.3	0.056
17311807	Sqle	0.0039	21.00	193.4	0.790	0.7685	9.43	229.9	0.310
17365314	Ldb1	0.0067	10.38	234.1	0.164	0.1503	12.05	216.2	0.171
17475360	Cyp2b10	0.0102	17.75	155.9	0.869	0.0782	0.00	85.7	0.486
17331429	Actg1	0.0153	18.56	155.7	0.470	0.3570	1.52	124.5	0.512
17290173	Hmgcs1	0.0230	0.50	751.5	0.687	0.1625	4.83	695.2	0.083
17239493	Heca	0.0265	9.30	255.6	0.132	0.1921	10.93	258.6	0.086
17232235	Ctgf	0.0331	13.18	37.9	0.364	0.9984	11.52	42.8	0.152

Liver clock-independent gene with altered phase of expression in NPY KO

Affymetrix transcript ID	Gene	WT MetaCycle P value	WT Phase	WT Median Exp	WT Relative Amp	KO MetaCycle P value	KO Phase	KO Median Exp	KO Relative Amp
17268729	Fbxl20	0.0001	7.66	72.8	0.338	0.0287	3.35	74.6	0.024

Other liver clock-independent genes

Affymetrix transcript ID	Gene	WT MetaCycle P value	WT Phase	WT Median Exp	WT Relative Amp	KO MetaCycle P value	KO Phase	KO Median Exp	KO Relative Amp

17441490	Fbxo21	0.0000	7.47	389.4	0.528	0.0040	7.63	417.3	0.405
17323838	Klhl24	0.0003	7.95	655.8	0.393	0.0154	7.89	733.9	0.207
17348840	Rnf125	0.0003	1.00	1876.3	0.498	0.0003	1.00	1782.6	0.485
17239817	Enpp3	0.0006	3.52	705.3	0.276	0.0397	2.00	691.8	0.154
17224540	Tuba4a	0.0007	0.00	553.8	0.496	0.0041	0.00	495.7	0.311
17397426	Ccrn4l	0.0014	13.21	67.5	0.912	0.0055	13.13	61.4	0.862
17225506	Per2	0.0015	15.94	100.4	0.568	0.0016	18.31	95.1	0.196
17530653	Alas1	0.0018	14.17	2348.8	0.686	0.0433	15.23	1613.2	0.791
17322289	Calcoco1	0.0022	7.63	238.0	0.234	0.0105	7.81	212.3	0.113
17284002	Hsp90aa1	0.0028	19.45	163.3	0.342	0.0020	20.00	170.9	0.224
17397240	Hspa4l	0.0032	20.00	116.8	0.356	0.0060	20.00	121.8	0.386
17455507	Hsph1	0.0077	17.26	172.2	0.596	0.0104	17.69	210.7	0.368
17516365	Hspa8	0.0080	15.90	2249.3	0.220	0.0145	15.95	2414.1	0.138
17362240	Stip1	0.0096	20.00	334.7	0.241	0.0104	1.71	330.8	0.210
17514871	Chordc1	0.0152	18.03	249.2	0.297	0.0029	17.12	247.0	0.363
17371059	March7	0.0167	7.64	108.5	0.134	0.0100	6.20	118.1	0.110
17236003	Tcp11l2	0.0183	7.56	88.2	0.335	0.0281	5.03	107.8	0.216
17246231	Erbb3	0.0403	6.31	741.6	0.186	0.0355	5.39	634.6	0.079
17483546	Fus	0.0427	6.42	138.1	0.164	0.0092	8.12	120.6	0.137
17285056	Idi1	0.0570	0.00	324.4	0.409	0.9922	7.35	327.1	0.001
17445308	Cyp51	0.0573	0.50	245.0	0.570	0.2233	4.74	275.0	0.194
17406908	Fdps	0.0574	5.99	381.0	0.572	0.4333	4.77	423.2	0.118
17421972	Errfi1	0.0688	11.69	3378.1	0.240	0.6534	13.17	3415.2	0.119
17234552	Lss	0.1491	0.50	115.3	0.607	0.3760	3.98	131.2	0.117
17406990	Efna1	0.1893	0.50	291.1	0.248	1.0000	6.58	304.3	0.109
17479596	Hddc3	0.2322	2.00	138.0	0.030	0.1139	8.05	139.9	0.082
17509629	Msmo1	0.4935	16.88	472.2	0.269	1.0000	9.50	503.5	0.137
17467799	Tgoln1||Tgoln2	0.7122	1.00	883.7	0.028	0.0055	0.77	922.2	0.140
17508036	Slc25a15	0.7439	18.63	1960.6	0.054	0.7151	0.00	1816.9	0.047
17262621	Hspa4	0.8215	0.88	731.2	0.075	0.9913	12.82	694.9	0.011
17351465	Tubb6	0.8380	17.26	50.4	0.122	0.2040	6.99	49.2	0.066
17383905	Slc25a25	1.0000	11.90	370.3	0.131	0.9952	12.51	309.2	0.278
17455234	Rnf6	1.0000	10.76	95.2	0.001	0.8039	9.29	92.5	0.063

Table 2.3 contributions: A.N.K. and G.W. analyzed data.

Chapter 3 : A Peptidergic Circuit Links the Circadian Clock to Locomotor Activity

Published: King, Anna N., Annika F. Barber, Amelia E. Smith, Austin P. Dreyer, Divya Sitaraman, Michael N. Nitabach, Daniel J. Cavanaugh, and Amita Sehgal. "A Peptidergic Circuit Links the Circadian Clock to Locomotor Activity." Current Biology 27, no. 13 (2017): 1915-927. doi:10.1016/j.cub.2017.05.089.

Abstract

The mechanisms by which clock neurons in the *Drosophila* brain confer a ~24-hour rhythm onto locomotor activity are unclear, but involve the neuropeptide Diuretic hormone 44 (DH44), ortholog of corticotropin-releasing factor. Here, we identified DH44 receptor 1 as the relevant receptor for rest:activity rhythms and mapped its site of action to *hugin*-expressing neurons in the subesophageal zone (SEZ). We traced a circuit that extends from *Dh44*-expressing neurons in the pars intercerebralis (PI) through *hugin*+ SEZ neurons to the ventral nerve cord. Hugin neuropeptide, a neuromedin U ortholog, also regulates behavioral rhythms. The DH44 PI-Hugin SEZ circuit controls circadian locomotor activity in a daily cycle but has minimal effect on feeding rhythms, suggesting that the circadian drive to feed can be separated from circadian locomotion. These findings define a linear peptidergic circuit that links the clock to motor outputs to modulate circadian control of locomotor activity.

Introduction

Drosophila melanogaster has been instrumental for understanding the molecular and cellular basis of circadian clocks. At the molecular level, a transcription-translation feedback loop keeps the circadian clock running at a ~24-hour pace. At the cellular level, ~150 clock-expressing neurons in the *Drosophila* brain synchronize as a network to coordinate behavioral rhythms (Yao and Shafer 2014; Peng et al. 2003). Of these clock neurons, the ventrolateral neurons (LNvs) are the most important for driving locomotor activity rhythms in free-running conditions of constant darkness (Renn et al. 1999; Grima et al. 2004). In addition, the LNvs maintain the phase and amplitude of molecular oscillations among different clock neurons through neuropeptide pigment-dispersing factor (PDF) signaling (Peng et al. 2003; Lin, Stormo, and Taghert 2004; Yoshii et al. 2009). While we have some understanding of the signaling mechanisms within the central clock network that generate circadian rhythms, the mechanisms for relaying circadian timing information from the clock to neural circuits controlling behavior are poorly understood.

A screen for circadian output neurons in *Drosophila* identified *Dh44*-expressing neurons in the pars intercerebralis (PI), a functional homolog of the mammalian hypothalamus (de Velasco

et al. 2007), as relevant for rest:activity rhythms (Cavanaugh et al. 2014). *Dh44*+ PI neurons lack clocks themselves but are indirectly connected to the small LNvs (sLNvs), the central pacemaker neurons, through DN1 (dorsal neurons) clock neurons. The DH44 neuropeptide is the fly ortholog of corticotropin-releasing factor (CRF) and modulates rest:activity rhythms (Cavanaugh et al. 2014). To identify signals downstream of DH44 that regulate rest:activity rhythms, we sought to identify the relevant receptor and its site of action. Here, we find that a null mutation in *Dh44 receptor 1* (*Dh44-R1*) disrupts the amplitude of free-running rest:activity rhythms. We find that DH44-R1 acts in neurons expressing *hugin,* a neuropeptide ortholog of neuromedin U (Melcher et al. 2006), which also regulates rest:activity rhythms. *Dh44*+ PI neurons are anatomically and functionally connected to *hugin*+ neurons in the subesophageal zone, a sensorimotor control center in flies (McKellar 2016). *hugin*+ neurons display cyclic neuropeptide release that is controlled by the clock and have descending projections into the ventral nerve cord, where they potentially regulate motor circuits driving locomotion. Although *Dh44-R1* and *hugin* modulate circadian locomotor activity, manipulations of the Dh44 PI-Hugin SEZ circuit have little to no effect on feeding rhythms. We propose that the sLNv→DN1→DH44 PI→Hugin SEZ→VNC pathway defines a linear circuit that modulates rest:activity rhythms.

Methods

Experimental Model and Subject Details

Drosophila lines

Flies were maintained on cornmeal-molasses medium at 25°C. The w^{1118} iso31 strain was used as wild type. When tested as controls, UAS and GAL4 fly lines were tested as heterozygotes after crossing to iso31. Most of the GAL4 lines used in the screen were selected for their restricted expression in the brain from the Janelia Fly Light collection (Jenett et al. 2012) at the Bloomington Drosophila Stock Center (BDSC) and the Vienna Tiles collection (Kvon et al. 2014) at the Vienna Drosophila Resource Center (VDRC). See Table 3.2 for a list of the complete genotype for the animals used in each experiment.

Method Details

Generating *Dh44-LexA* driver

Dh44-LexA was generating using the same ~2.2 kb *Dh44* enhancer fragment (chr3R:9639799-9641976 from dm6) in *Dh44-GAL4* (VT039046 from VDRC). The *Dh44* fragment was directionally cloned into a pBPLexA::p65Uw plasmid (Addgene 26231) between two attR sites using the Gateway TOPO cloning kit (Thermo Fisher Scientific, Inc.). Flies were generated by site-specific PhiC31 integration at an attP40 site (Pfeiffer et al. 2010). Despite using the same enhancer fragment as *Dh44-GAL4*, we observed that *Dh44-LexA* was expressed in other neurons, in addition to the six *Dh44*+ pars intercerebralis neurons. Therefore, *Dh44-LexA* was only used in experiments where anatomical analysis could exclude the spurious expression pattern. Transgenic fly injections were done by Rainbow Transgenic Flies, Inc. (Camarillo, CA).

Generating *Dh44-R1* and *Dh44-R2* mutants

Dh44-R1^{DsRed} and *Dh44-R2*^{174} mutants were generated with the CRISPR/CAS9 system. Guide RNA sequences to target *Dh44-R1* and *Dh44-R2* were determined using a target finder (http://flycrispr.molbio.wisc.edu/tools). Guide RNAs were cloned into the pCFD4 plasmid (Port et al. 2014). For the *Dh44-R1* mutation, a homology directed repair template (HDR) was also used.

5’ and 3’ homology arms spanning 1 Kb upstream and downstream of the desired deletion were cloned into the pHD-DsRed-attP plasmid (Gratz et al. 2014). Primers and guide RNA sequences used are listed below. Guide RNAs and HDR template were injected into *vasa-Cas9* flies at Rainbow Transgenic Flies, Inc. Mutations were identified with PCR screening and sequencing (see Table 3.3 for primer sequences). To PCR identify mutations at the CRISPR target site in *Dh44-R2*, two forward primers and one reverse primer were used. One forward primer primes outside the CRISPR target site, referred as Primer outside (Po), and another forward primer overlaps the CRISPR target site, referred as Primer indel (Pi). Thus, Po amplifies from both wild type and mutant alleles. Pi can only amplify from the wild type allele, and any mutation will disrupt the binding of Pi. To PCR verify HDR insertion at *Dh44-R1*, one primer was targeted against a genomic region outside of the HDR template and the other primer was targeted against a region within the HDR template. Thus, a PCR product can only be produced when the HDR template has been integrated into the genomic *Dh44-R1* locus.

Generating *UAS-t-Dh44*

t-Dh44 cDNA was chemically synthesized using optimal *Drosophila* codon usage and with an optimal *Drosophila* Kozak translation initiation site upstream of the start methionine (CAAA) as described in (Choi et al. 2009). *t-Dh44* cDNA and encoded peptide sequence are as follows:

cDNA:

GAATT CCAAA ATGTC CGCCC TGCTC ATCTT GGCTT TGGTC GGTGC TGCAG TTGCC AACAA ACCCT CCCTG AGCAT CGTGA ATCCG CTAGA TGTCC TGCGT CAACG CCTGC TACTT GAGAT AGCCC GTCGC CAGAT GAAGG AGAAT AGCCG ACAGG TGGAG CTGAA TCGAG CCATC CTGAA GAACG TGGGC AACGA GCAGA AGCTC ATCAG TGAGG AGGAT CTGGG AAACG GAGCT GGCTT TGCTA CTCCA GTGAC ACTAG CCCTT GTGCC TGCAC TGTTG GCAAC CTTCT GGTCG CTCCT GTAAT CTAGA

Peptide:

MSALLILALVGAAVANKPSLSIVNPLDVLRQRLLLEIARRQMKENSRQVELNRAILKNVGNEQKLIS EEDLGNGAGFATPVTLALVPALLATFWSLL

The cDNA was cloned into pJFRC7-20XUAS-IVS plasmids using NotI and NheI, and cloned vectors were injected into fly strains carrying the attP40 landing site to obtain transgenic flies (Pfeiffer et al. 2010).

Behavior experiment: circadian rest:activity rhythm

Rest:activity rhythm assays were performed with the Drosophila Activity Monitoring System (Trikinetics, Waltham MA) as described previously (Cavanaugh et al. 2014; Williams et al. 2001). Flies were entrained to a 12 h light: 12 h dark (LD) cycle for > 3 days at 25°C. ~7 d old male flies were individually placed into glass tubes with 5% sucrose/2% agar food and monitored in constant darkness (DD) for 7 d at 25°C. For TrpA1 experiments, flies were raised at 18°C. ~7 d old male flies were entrained to an LD cycle for 3 days at 21°C, then transferred to DD for 5 days at 21°C, followed by 5 days DD at 28°C. The GAL4 screen was initially performed with 8-16 flies. All other behavioral experiments were performed at least 2 independent times with at least 16 flies/genotype each.

Immunohistochemistry, GRASP, and microscopy

Fly brains from ~4-7 d old males were dissected in phosphate-buffered saline with 0.1% Triton-X (PBST) and fixed in 4% formaldehyde for 20 min at room temperature. Brains were rinsed 3 x 10 min with PBST, blocked for 60 min in 5% Normal Donkey Serum in PBST (NDST), and incubated in primary antibody diluted in NDST for >16 h at 4°C. Brains were rinsed 3 x 10 min in PBST, incubated 2 h in secondary antibody diluted in NDST, rinsed 3 x 10 min in PBST, and mounted with Vectashield (Vector Laboratories Inc.). Primary antibodies used are rabbit anti-GFP at 2µg/mL (Thermo Fisher Scientific Inc. A-11122), rat anti-RFP at 1µg/mL (ChromoTek 5F8), and mouse anti-brp at 1:100 (Developmental Studies Hybridoma Bank nc82). Secondary antibodies used are FITC donkey anti-rabbit (Jackson ImmunoResearch 711-095-152), Cy3 donkey anti-rat (712-165-153), and Cy5 donkey anti-mouse (715-175-151) at 1:500. For GRASP experiments, endogenous signal without antibody labeling was imaged. Eight-bit images were acquired using a Leica TCS SP5 laser scanning confocal microscope with a 40x/1.3 NA or 20x/0.7 NA objective and a 1-µm z-step size. Maximum intensity z-projection images were generated in Fiji, a distribution of ImageJ software (Schindelin et al. 2012).

P2X2 activation and calcium imaging

Adult male flies ~7–9 d old were anesthetized on ice and dissected in hemolymph-like saline (HL3) consisting of (in mM): 70 NaCl, 5 KCl, 1.5 CaCl2, 20 MgCl2, 10 NaHCO3, 5 trehalose, 115 sucrose, 5 HEPES, pH 7.1 (Yao et al. 2012). Imaging experiments were performed using a naked brain preparation in a small bath of HL3 in a perfusion chamber (AutoMate Scientific Inc., Berkeley CA). The brain was stabilized under nylon fibers attached to a platinum wire frame. Solutions were perfused over the brain at a rate of ~5 mL/min with a gravity-fed ValveLink perfusion system (Automate Scientific Inc.). After 1 min of baseline GCaMP6s imaging, ATP was delivered to the chamber by switching perfusion flow from the channel containing HL3 to another channel containing 5 mM ATP (Sigma–Aldrich, St Louis, MO) in HL3, pH 7.1. ATP was perfused for 1 min. GCaMP6 calcium imaging was performed on a Leica TCS SP5 confocal microscope. Twelve-bit images were acquired with a 40×/0.8 water immersion objective at 256 × 256 pixel resolution. Z-stacks were acquired every 5 or 10 s.

ANF-GFP

Adult males were entrained to a LD cycle. For each time point, ventral nerve cords were dissected in PBST and fixed in 4% PFA/PBS for 20 m at room temperature. Tissues were washed 3 times in PBST, mounted in Vectashield media, and imaged on a Leica TCS SP5 confocal microscope using identical laser power and scan settings for all samples. Eight-bit images were acquired using a Leica TCS SP5 laser scanning confocal microscope with a 20x/0.7 NA objective and a 1-μm z-step size.

Behavior experiment: locomotor activity

The number of beam crossings (activity counts) per 30 min was measured using the Drosophila Activity Monitoring System. ~7 d old individual male flies were monitored for 3 d in LD and then 3 d in DD. Locomotor activity analysis was performed 2 or 3 independent times with 16 flies per genotype with similar results.

Feeding behavior experiment: FLIC

Feeding rhythm analysis was performed using the Fly Liquid-food Interaction Counter (FLIC) (Ro, Harvanek, and Pletcher 2014). Liquid food for the *Dh44-R1*^{DsRed} experiments was prepared as a 10% sucrose (w/v) solution. Liquid food for the *hugin>Kir2.1* experiments was a 10% sucrose solution plus 45 mg/L MgCl2 · 6H2O as an additional source of ions for a more robust signal. ~2-3 d old male flies were entrained in a LD cycle for >3 d at 25°C, then transferred to DD 25°C for 8 d. Feeding events, measured as constant food contact for a minimum of 1 s, were monitored for 8 d in DD.

Quantitative reverse transcription PCR (qPCR)

Total RNA was extracted from 3–7 d old male flies (30 heads or 5 whole bodies) using TRIzol reagent (Thermo Fisher Scientific Inc.). RNA was reverse transcribed to generate cDNA using a High Capacity cDNA Reverse Transcription kit (Thermo Fisher Scientific Inc.). qPCR was performed on a ViiA™ 7 Real-Time PCR System (Applied Biosystems) using SYBR Green PCR master mix (Thermo Fisher Scientific Inc.). Primers (5' to 3') for qPCR used in the study are: actin-F: GCGCGGTTACTCTTTCACCA; actin-R: ATGTCACGGACGATTTCACG; Dh44-F: GCAGGCAAATGAAGGAGAAC; Dh44-R: CCACGTTCTTCAGGATGG; Dh44-R1-F: CAGCACCCCCGAAAAGTACG; Dh44-R1-R: ATTAGCACCGCACAGACAGG; Dh44-R2-F: CCGGAACAGGGTATCAGTCG; Dh44-R2-R: AGAAGCCCTGCGTGCTTATG; hugin-F: ATGTGTGGTCCTAGTTATTGCAC; hugin-R: TCCCAAATCCAGTTTGCTCGT. Because the region targeted by the *Dh44-R1* primers above was deleted in the *Dh44-R1*^{DsRed} mutant, the following primers were used to measure mRNA levels of *Dh44-R1*: Dh44-R1-CRISPR-F: CCTGATGAGGCAAGGACTCG and Dh44-R1-CRISPR-R: AGATCTGCGACACGGAAGTG.

Quantification and Statistical Analysis

The statistical details of experiments can be found in the figure legends. All statistical tests were performed in GraphPad Prism (version 7.03). Tukey's boxplots were generated in R (version 3.3.1) using ggplot2 package. In the boxplots, the line inside the box indicates the median, and the bottom and top lines represent the 1st and 3rd quartiles (the 25th and 75th percentiles). The

upper whisker extends to the highest value that is within 1.5 * IQR above the 3rd quartile, where IQR is the inter-quartile range (the distance between the 25th and 75th percentiles). The lower whisker extends to the lowest value within 1.5 * IQR below the 1st quartile. Data beyond the end of the whiskers are outliers and plotted as points.

Behavior experiment: circadian rest:activity rhythm

Circadian rhythms was analyzed with ClockLab software (Actimetrics, Wilmette IL). Period and rhythm strength were determined for each individual fly using activity data collected from days 2–7 of DD. Period length was determined using $\chi 2$ periodogram analysis, and relative power (or amplitude) of circadian rhythm was determined using fast Fourier transform (FFT). Fly activity was considered rhythmic if the $\chi 2$ periodogram showed a peak above the 95% confidence interval and the FFT value was >0.01 (Cavanaugh et al. 2014). Data from flies that survived the duration of the experiments were pooled and analyzed. Behavioral data were analyzed with one-way analysis of variance (ANOVA). Tukey's test was used as the post hoc test in Figure 1B-E. Sidak's test was used as the post hoc test in all other experiments to compare means between the two control genotypes (flies containing GAL4 or UAS only) and experimental genotype (flies containing both GAL4 and UAS). Differences between groups were considered significant if $P < 0.05$ by the post hoc test. TrpA1 data were analyzed with two-way repeated-measures ANOVA followed by a Sidak's test. Differences in FFT power between temperatures and within a genotype were considered significant if $P < 0.05$ by Sidak's test.

Calcium imaging

Image processing and fluorescence intensity measurement was performed in Fiji. A summed intensity Z-projection at each time point was used for analysis. StackReg plugin for Fiji was used to correct for xy movements over time in the projected image (Thevenaz, Ruttimann, and Unser 1998). Regions of interest (ROIs) were manually drawn to encompass individual GCaMP-positive cell bodies, and mean fluorescence intensities was measured from a ROI at each time point. For each individual cell, fluorescence traces over time were normalized using this equation: $\Delta F/F = (F_n - F_0)/F_0$, where F_n is the fluorescence intensity recorded at time point n, and F_0 is the average

fluorescence value during the 30 s-baseline preceding ATP application. Maximum ΔF/F was calculated by subtracting the average ΔF/F in the 30 s preceding ATP delivery from the largest ΔF/F value during the 60 s of ATP application. Brains with cells that have unstable baselines were discarded from quantification. The sample sizes, including the total number of cell bodies and number of brains, quantified are indicated in legend. We used two-tailed Mann-Whitney U test (for 2 group comparison) or Kruskal-Wallis test followed by Dunn's multiple comparison test (for 3 group comparison) to compare differences in maximum ΔF/F between groups. A responding cell was defined as a cell with a maximum ΔF/F greater than 2*SD(ΔF/F of the negative control group). The onset of response for a cell was defined as the time where ΔF/F cross a threshold corresponding to 2*SD(ΔF/F during the 30 s baseline preceding ATP).

ANF-GFP experiments

FIJI software was used to measure fluorescent signal in axon terminal. Background subtraction was performed using the "rolling ball" method, then a max intensity Z-projection was generated. To create a selection mask of the axons, a 1.5 pixel range Gaussian blur was applied to a Z projected image of the myr-RFP signal, and the threshold was adjusted to select for the brightest myr-RFP signal. Fluorescent artifacts, such as autofluorescent puncta in the T3 and abdominal segments, were removed from the mask and not measured. The mask was transferred to the max Z-projected images and used to measure the mean pixel intensity of the ANF-GFP and myr-RFP signals. We also took a background signal for each ventral nerve cord. Normalized GFP/RFP signal was determined as (mean ANFGFP - mean background GFP) ÷ (mean myrRFP - mean background RFP) for each ventral nerve cord. ANF-GFP data were analyzed with two-way ANOVA. After determining the interaction effect between time and genotype variables was significant ($P < 0.05$), Tukey's post hoc test was used to compare the means between time points within a genotype.

Behavior experiment: locomotor activity

Each fly's 24-h activity profile was determined from the average of 3 d of data. Locomotor activity profiles for each genotype were then generated from the average of 15-16 flies' activity profiles.

We defined light or day activity as cumulative activity counts occurring between ZT or CT 0-11.5 (inclusive of start and end times), dark or night activity between ZT/CT 12-23.5, evening activity between ZT/CT 9.5-12.5, and morning activity between ZT/CT 21.5-23.5 and 0-0.5. Statistical tests were done with one-way ANOVA followed by a Tukey post hoc test. Differences between groups were considered significant if $P<0.05$ by the Tukey test. Tukey's boxplots were generated in R.

Feeding behavior

Period and rhythm strength of feeding behavior were determined from feeding events during days 2-7 of darkness (DD) using ClockLab software. Only flies that survived the duration of the experiment were included in the data analysis. Period length was determined using $\chi 2$ periodogram analysis, and ~24-hour rhythm strength was determined by subtracting the corresponding $P = 0.01$ $\chi 2$ significance value from the amplitude of the maximum period. Flies were categorized as rhythmic (power >10) or arrhythmic (power <10). Normalized feeding activity was calculated within each fly for comparison across flies and experiments. Feeding activity of a fly for a given 30 min period was divided by the average behavioral count of 30 min over the duration of the experiment. Plots of normalized feeding activity begin at day 2 of the experiment after flies have acclimated to the FLIC monitor enclosure.

Quantitative reverse transcription PCR (qPCR)

Two-tailed Welch's t test was used to compare differences in gene expression between experimental and control groups. We used one-way ANOVA test and JTK_CYCLE algorithm (version 3) (Hughes, Hogenesch, and Kornacker 2010) to determine if there was cycling in gene expression.

Results

DH44-R1 is the predominant DH44 receptor regulating circadian rhythms of rest:activity

DH44 neurons as well as the peptide itself are required for normal rest:activity rhythms in constant darkness (Cavanaugh et al. 2014). As DH44 can signal through two G-protein coupled receptors, DH44-R1 and DH44-R2, we asked which receptor was necessary for rhythmic behavior (Johnson, Bohn, and Taghert 2004; Hector et al. 2009). Using CRISPR/CAS9-mediated genome editing, we generated mutant alleles of both *Dh44 receptor* genes, *Dh44-R1^{DsRed}* and *Dh44-R2^{174}*. The *Dh44-R1^{DsRed}* allele is a deletion of the entire protein coding region and replaces exons 2 to 11 with a DsRed selection marker, which decreases mRNA levels of *Dh44-R1* (Figure 3.1A and 2.S1A). *Dh44-R2^{174}* allele is a 5-base-pair deletion in exon 6 of the gene (Figure 3.1A). *Dh44-R2^{174}* mutants have normal levels of *Dh44-R2* mRNA (Figure 3.S1A); however, the frameshift mutation is predicted to result in a non-functional truncated protein with only two transmembrane domains (Figure 3.S1B).

We assessed circadian rhythms of locomotor activity in *Dh44-R1^{DsRed}* and *Dh44-R2^{174}* mutants under constant darkness (DD). Both *Dh44-R1^{DsRed}* and *Dh44-R2^{174}* mutants displayed rest:activity rhythms with wild type period length (Figure 3.S1C-S1E and Table 3.1). However, the amplitude of the behavioral rhythm was affected in *Dh44-R1^{DsRed}* mutants (Figure 3.1B), as assayed by fast Fourier transform (FFT) (Cavanaugh et al. 2014). *Dh44-R2^{174}* mutants were largely normal, although FFT analysis shows that they had modestly weaker rest:activity rhythms compared to control heterozygotes (Figure 3.1C). Both *Dh44-R1^{DsRed}* and *Dh44-R2^{174}* failed to complement large chromosomal deficiencies that remove the respective genes, consistent with *Dh44-R1^{DsRed}* and *Dh44-R2^{174}* being null alleles (Figure 3.1B-1C). To investigate the relationship between the two DH44 receptors, we tested the behavior of flies mutant for both receptors. Double heterozygotes, *Dh44-R1^{DsRed},Dh44-R2^{174}*/+, had strong rest:activity rhythms similar to those of single heterozygous mutants. In contrast, flies homozygous for both mutations (*Dh44-R1^{DsRed},Dh44-R2^{174}*) exhibited weak rest:activity rhythms like those seen in *Dh44-R1^{DsRed}* mutants (Figure 3.1D and S1F). Since loss of *Dh44-R2* does not modify the phenotype of the *Dh44-*

R1^{DsRed} mutant, we conclude that DH44-R1 is the primary DH44 receptor regulating rest:activity rhythms.

The phenotype of *Dh44-R1*^{DsRed} mutants suggests a modulatory role of DH44 signaling, which is generally the case for peptide signaling. Indeed, while flies lacking core clock genes, such as *period* (*per*), are completely arrhythmic, this is not the case for mutants of PDF, the major neuropeptide in the clock circuit, or PDF receptor (Renn et al. 1999; Lear, Merrill, et al. 2005; Hyun et al. 2005; Mertens et al. 2005; Wülbeck, Grieshaber, and Helfrich-Förster 2008; Shafer and Taghert 2009). We found that 54% of *Pdf*^{01} mutants, but none of the *per*^{0} flies, were rhythmic (Table S1). Nevertheless, rest:activity rhythms of *Dh44-R1*^{DsRed} flies were stronger than those of *Pdf*^{01} and *Pdfr*^{han5304} mutants (Figure 3.1E), suggesting that DH44 is not the only signal downstream of PDF relevant for rest:activity rhythms. We examined expression levels of the DH44 receptors across the day, but did not see any evidence for cycling of *Dh44-R1* or *Dh44-R2* mRNA (Figure 3.S1F).

To verify a role for *Dh44-R1* in neurons, we pan-neuronally knocked it down using RNA interference (RNAi). *elav*-GAL4-driven expression of two different RNAi lines reduced mRNA levels of *Dh44-R1* to approximately 50% of the levels in controls (Figure 3.S2A-S2B). Compared to control flies, *elav>Dh44-R1 RNAi* flies showed lower amplitude of rest:activity rhythms (Figure 3.1F). Interestingly, knockdown of *Dh44-R2* also dampened rest:activity rhythms (Figure 3.1G), more so than the genetic mutant, perhaps because of compensation with the global knockout. Nevertheless, simultaneous knockdown of both receptors in neurons resulted in the same rhythm phenotype as knockdown of a single DH44 receptor (Figure 3.1H). These data are consistent with the results from genetic mutant analysis and suggest that effects of *Dh44-R1* and *Dh44-R2* on circadian rhythms are not additive or synergistic; thus, any role of DH44-R2 is not independent of DH44-R1. Because of the stronger phenotype of the *Dh44-R1* mutant, we conclude that DH44-R1 is the more relevant receptor for rest:activity rhythms.

Dh44-R1-expressing neurons regulate rest:activity rhythms

To identify the site of DH44-R1 action relevant for rest:activity rhythms, we first examined expression of a *Dh44-R1*^{R21A07}-GAL4 driver (which includes 3.65 kb from *Dh44-R1* promoter). *Dh44-R1*^{R21A07}-GAL4 is expressed broadly in the brain and in a pattern similar to an *in situ* characterization of *Dh44-R1* mRNA expression (Figure 3.1I) (K.-M. Lee et al. 2015). RNAi-mediated knockdown of *Dh44-R1* in *Dh44-R1*^{R21A07}-GAL4+ neurons reduced the strength of rest:activity rhythms (Figure 3.S2C-S2D), supporting the idea that the driver targets neurons that mediate effects of DH44-R1.

We next determined whether activating *Dh44-R1*-expressing neurons is sufficient to degrade rest:activity rhythms. We expressed the *Drosophila* temperature-activated cation channel, TrpA1 (Pulver et al. 2009), in *Dh44-R1*-expressing neurons and tested rest:activity rhythms of individual flies at 21°C and then at 28°C. At 21°C, 93.5% of the *Dh44-R1*^{R21A07}*>TrpA1* flies were rhythmic. However, after transitioning the flies to 28°C to activate TrpA1, only 31% of the flies were rhythmic. FFT power for *Dh44-R1*^{R21A07}*>TrpA1* flies also decreased after transitioning to 28°C (Figure 3.1J-K). Sustained activation of *Dh44-R1*-expressing neurons is sufficient to disrupt rest:activity rhythms, indicating these neurons have a role in regulating rest:activity rhythms.

Effects of *Dh44-R1* on rest:activity rhythms are mediated by *hugin*+ neurons in the SEZ

To identify the specific neurons requiring *Dh44-R1* for rest:activity rhythms, we targeted RNAi knockdown of *Dh44-R1* to random subsets of brain cells using 168 independent GAL4s (Figure 3.S3) (Jenett et al. 2012; Kvon et al. 2014). We found that 15 GAL4s driving *Dh44-R1* RNAi weakened rest:activity rhythms comparable to the phenotype observed with pan-neuronal *nsyb*-GAL4 or *elav*-GAL4 targeted knockdown (Figure 3.2A and S3). Of the GAL4 hits, three are regulated by *Dh44-R1* genomic sequences: *Dh44-R1*-GAL4 (K.-M. Lee et al. 2015), R21A07-GAL4, and R57E06-GAL4. We examined the expression of GAL4 hits in the brain and found that the subesophageal zone (SEZ) stood out as a region of overlap, labeled by five candidate GAL4 drivers (Figure 3.2B). Interestingly, axons of *Dh44*+ PI neurons terminate in the SEZ.

We focused on *hugin*-GAL4, because its expression is restricted to about 20 *hugin*+ neurons in the SEZ (Melcher and Pankratz 2005). *Hugin* (*hug*) encodes a prepropeptide that produces two neuropeptides, Pyrokinin-2 and Hugin-γ, one of which (Pyrokinin-2) is homologous to mammalian neuromedin U (NMU) (Melcher et al. 2006). We followed up on the initial phenotype and found that knockdown of *Dh44-R1* in *hugin*+ neurons weakens rest:activity rhythms. While only one of the two *Dh44-R1* RNAi transgenes significantly reduced circadian rhythmicity in a wild type background, both yielded a consistent weak rhythm phenotype in a sensitized *Dh44-R1*^{DsRed}/+ heterozygous background, suggesting incomplete knockdown in wild type flies (Figure 3.2C).

To verify circadian relevance of DH44 expression in *hugin*+ neurons, we expressed a membrane-tethered form of DH44 (t-DH44) in *hugin*+ neurons. Membrane-tethered peptides cell-autonomously and constitutively activate their cognate receptors, and were used previously to study PDF signaling in the circadian network (Choi et al. 2009; Choi et al. 2012). Expression of t-DH44 in *hugin*+ neurons, weakened rest:activity rhythms (Figure 3.2D), supporting the idea that *Dh44-R1* functions in *hugin*+ SEZ neurons to modulate rest:activity rhythms.

Hugin+ neurons in the SEZ receive inputs from _Dh44_+ neurons in the PI

Since the function of DH44-R1 partially maps to *hugin*+ neurons, we sought to determine if *hugin*+ neurons receive synaptic inputs from *Dh44*+ neurons (Figure 3.3A). To analyze the circuitry, we labeled the projections of each neuronal subset—*hugin*+ and *Dh44*+—with fluorescent markers: syt1-GFP to identify presynaptic membranes and Denmark to identify postsynaptic membranes (Y. Q. Zhang, Rodesch, and Broadie 2000; Nicolaï et al. 2010). *Hugin*+ neurons have both presynaptic and postsynaptic components within the SEZ and near the esophagus. Interestingly, *hugin*+ axon terminals also project to the PI (Figure 3.3B). Conversely, axons from *Dh44*+ PI neurons terminate within the SEZ, and *Dh44*+ dendritic compartments are located both in the PI and near the esophagus (Figure 3.3C).

To test for synaptic connections between *Dh44*+ and *hugin*+ neurons, we used a GFP reconstitution across synaptic partners (GRASP) method that labels synaptic sites (Feinberg et

al. 2008; Y. Chen et al. 2014). We used *Dh44*-GAL4 to express neurexin-bound GFP fragment 1-10 and *hugin*-LexA to express CD4 membrane-bound GFP fragment 11. In these flies, GRASP signal was observed in the SEZ, near the esophagus, and along the midline of the brain (Figure 3.3D). To determine the polarity of the connectivity detected with GRASP and to confirm *Dh44*+ and *hugin*+ projections overlap in the same region, we simultaneously labeled the axons of one group with Rab3-GFP (Shearin et al. 2013) and the somatodendritic membrane of the other group using Denmark. We found that axons from *Dh44*+ PI neurons intersect with *hugin*+ dendrites near the esophagus and in the SEZ (Figure 3.3E). Intriguingly, *hugin*+ axon terminals also contact *Dh44*+ dendrites near the esophagus (Figure 3.3F). In addition, we detected a GRASP signal between *Dh44*+ and *hugin*+ neurons in the PI (Figure 3.3G), where *hugin*+ axon terminals contact *Dh44*+ neurons (Figure 3.3H). GRASP and polarity analysis indicate that *Dh44*+ PI and *hugin*+ SEZ neurons make extensive synaptic contacts through reciprocal projections.

To test whether *Dh44*+ and *hugin*+ neurons are functionally connected, we expressed and activated ATP-gated P2X2 receptors in *Dh44*+ neurons while imaging Ca^{2+} in *hugin*+ neurons with GCaMP6m (Lima and Miesenböck 2005; T.-W. Chen et al. 2013). Addition of ATP to activate *Dh44*+ neurons increased GCaMP signal in a subset of *hugin*+ neurons (Figure 3.3I-J). Some neurons showed a decreased GCaMP signal upon ATP application; however, this is likely an experimental artifact since we also observed decreases in the negative control group. We estimated the number of *hugin*+ neurons that responded to *Dh44*+ PI activation as the number of neurons with a GCaMP signal increase greater than 2 standard deviations from the mean response in the negative control. We found approximately 15% of the ~20 *hugin*+ neurons responded and increased GCaMP signal upon activation of *Dh44*+ PI neurons (Figure 3.3J), suggesting that *hugin*+ neurons are a heterogeneous group.

We next asked to what extent DH44 signaling is required for the Ca^{2+} response in *hugin*+ neurons following *Dh44*+ PI activation. Thus, we performed the P2X2 and GCaMP6 imaging experiments in *Dh44-R1*^{DsRed} mutants. We did not observe significant differences in the amplitude of the responses in *hugin*+ neurons between mutants and heterozygotes (Figure 3.3K-L), but the

onset of response to *Dh44*+ PI activation was delayed in *Dh44-R1*^{DsRed} mutants (Figure 3.3M). Thus, the functional connection between *Dh44*+ PI and *hugin*+ SEZ is partly dependent on DH44 signaling. It is likely that, in addition to DH44, *Dh44*+ neurons express other neurotransmitters that may signal in the circadian output circuit. Taken together, the functional and anatomical data are consistent with *hugin*+ SEZ neurons receiving inputs from *Dh44*+ PI neurons.

Hugin+ neurons are circadian output neurons with descending projections into the ventral nerve cord

The findings reported above suggested that *hugin*+ neurons regulate rest:activity rhythms. To test this idea, we expressed *Kir2.1*, an inwardly-rectifying potassium channel, with the *hugin*–GAL4 driver to hyperpolarize and silence *hugin*-expressing neurons (Baines et al. 2001). Flies expressing *hugin>Kir2.1* showed weaker rhythms (Figure 3.4A), and ablating *hugin*+ neurons using the proapoptotic gene *reaper* resulted in an even stronger phenotype (Figure 3.4A) (White, Tahaoglu, and Steller 1996).

Next, we tested whether Hugin neuropeptide is the signal from *hugin*+ neurons that controls behavioral rhythms by knocking down *hugin* expression and assaying behavior. To test for efficacy of knockdown with two different RNAi transgenes against *hugin,* we drove their expression pan-neuronally with *elav*-GAL4, and saw >90% reduction in *hugin* mRNA levels (Figure 3.S4A). Expression of the RNAi transgenes in *hugin*+ neurons resulted in weaker rest:activity rhythms (Figure 3.4B). These data show that *hugin*+ neurons and Hugin neuropeptide modulate rest:activity rhythms.

We also examined the projections of *hugin*+ neurons to identify their targets. A subset of the *hugin*+ neurons are descending neurons (Melcher and Pankratz 2005), which have cell bodies in the central brain and project to the ventral nerve cord (VNC), a region containing motor circuits responsible for locomotion (Enriquez et al. 2015). We confirmed that *hugin*+ neurons in the central brain send axonal projections to the VNC using the presynaptic marker syt1-GFP (Figure 3.4C). Double labeling experiments revealed that *hugin*+ SEZ neurons are negative for *vglut* (*vesicular glutamate transporter*)-GAL4, a marker for motor neurons (data not shown) (Mahr

and Aberle 2006). To determine whether *hugin*+ neurons contact *vglut*+ neurons in the VNC, we used the presynaptic marker Rab3-GFP and postsynaptic marker Denmark. *hugin*+ presynaptic terminals localize with *vglut*+ dendritic projections in thoracic segments T2 and T3 and the abdominal (A) segment of the VNC (Figure 3.4D). GRASP also revealed contacts between *hugin*+ and *vglut*+ neurons in the thoracic and abdominal ganglia (Figure 3.4E). We hypothesize that descending projections from the *hugin*+ neurons to the VNC signal to motor circuits.

Neuropeptide release from *hugin*+ neurons is clock-regulated

LNvs and DN1s show rhythmic electrical activity with peak spontaneous firing rates around the early morning (Sheeba, Gu, et al. 2008; Cao and Nitabach 2008; Flourakis et al. 2015). *Dh44*+ circadian output neurons also show rhythms of intracellular Ca^{2+} (Cavey et al. 2016), which is likely indicative of rhythmic neural activity and peptide release (Shakiryanova et al. 2005). To determine if peptide release is rhythmic in *hugin*+ neurons we used ANF-GFP, a transgenic neuropeptide reporter (Rao et al. 2001). We expressed *UAS-ANF-GFP* and *UAS-myr-RFP*, used to normalize the ANF-GFP signal, in *hugin*+ neurons and detected the ANF-GFP signal in cell bodies, the projections to the PI, and the descending projections in the VNC. As the ANF-GFP signal in the *hugin*+ projections to the VNC is most likely to reflect neuropeptide release that affects motor circuits, we measured ANF-GFP in these projections. We found that ANF-GFP was rhythmic in the descending projections, with ~33% reduction in levels from the peak at midday (ZT6) to the trough in the middle of the night (ZT18) (Figure 3.5). We also measured ANF-GFP levels in *hugin*+ descending projections in per^{01} mutants, which do not have a molecular clock, and found rhythms were lost, confirming that the rhythms of neuropeptide release from *hugin*+ neurons are clock-controlled. However, mRNA levels of *hugin* do not appear to cycle (Figure 3.S4B).

The DH44 PI-Hugin SEZ circuit controls locomotor rhythms without affecting feeding rhythms

All the data described above assayed the strength of rhythms in constant darkness (DD), which is the paradigm typically used to assess internal clock function. However, clocks also modulate the

daily distribution of activity, which is particularly evident in a light:dark (LD) cycle. In LD cycles flies display morning and evening peaks of locomotor activity separated by an afternoon siesta, all of which are controlled by different clock neurons (Grima et al. 2004; Stoleru et al. 2004; Stoleru et al. 2005). However, little to nothing is known about the output circuits controlling diurnal behavior. To determine the contribution of DH44 signaling to the timing of diurnal behavior, we analyzed behavior of *Dh44-R1* and *Dh44-R2* mutants under standard 12:12 LD conditions. Compared to heterozygous flies, *Dh44-R1*-deficient mutants (*Dh44-R1^{DsRed}/Df*) had a reduced evening peak of locomotor activity (Figure 3.6A). However, *Dh44-R2^{174}* mutants displayed a normal pattern of activity in LD (Figure 3.S5A-S5B). In DD, where the pattern typically consists of a single broad evening peak of activity, *Dh44-R1^{DsRed}/Df* mutants showed a strong reduction of this peak (Figure 3.6B).

Neuronal inactivation of *hugin*+ neurons with Kir2.1 expression attenuated the evening peak of activity in both LD and DD conditions (Figure 3.6C and 6D), recapitulating the phenotype of *Dh44-R1*-deficient mutants. We hypothesize that *Dh44-R1* and *hugin>Kir2.1* mutants have dampened clock output signals, which attenuates the evening peak in particular. Together, the data suggest that DH44-R1 acting in *hugin*+ neurons modulates circadian locomotor activity in LD and DD conditions.

The role of Hugin/NMU (Melcher and Pankratz 2005; Howard et al. 2000) and DH44/CRF (Dus et al. 2015; Spina et al. 1996; Stengel and Taché 2014) in feeding-related behaviors raised the possibility that the DH44 PI-Hugin SEZ circuit affects locomotor activity rhythms indirectly by driving feeding. We performed continuous, long-term monitoring of fly feeding behavior using the Fly Liquid-Food Interaction Counter (FLIC) system (Ro, Harvanek, and Pletcher 2014) to directly assess whether manipulations of the DH44 PI-Hugin SEZ circuit alter fly feeding rhythms. *Dh44-R1^{DsRed}* mutants exhibited strong feeding rhythms that were indistinguishable from those of controls (Figure 3.6E and Figure 3.S5C). Feeding rhythms in *hugin>Kir2.1* flies were also strong, although slightly reduced in strength compared to corresponding controls (Figure 3.6F and Figure 3.S5C), perhaps indicating that the *hugin*+ cells are functionally heterogeneous and the subset

unresponsive to DH44 makes a minor contribution to the modulation of feeding behavior. Overall, these results show that the degradation of rest:activity rhythms in these flies was not secondary to alterations in feeding behavior. They also suggest that distinct output circuits mediate control of feeding and rest:activity rhythms.

Discussion

The neural circuits that transmit information from clock neurons to motor outputs to control rest:activity rhythms are poorly understood. We showed previously that *Dh44*+ PI cells are circadian output neurons indirectly connected to sLNvs, the central pacemaker neurons (Cavanaugh et al. 2014). Here, we identified *hugin*+ neurons as downstream circadian neurons that modulate rest:activity rhythms. Our data suggest that information flows from the clock network, to *Dh44*+ PI neurons, to *hugin*+ SEZ neurons, and finally to the VNC, which contains motor circuitry for locomotor activity (Figure 3.6G).

While both *Dh44-R1* and *Dh44-R2* mutants showed some defects in their rest:activity rhythms, the amplitude of behavioral rhythms was significantly weaker in *Dh44-R1* mutants than in *Dh44-R2* mutants. In addition, the *Dh44-R2* mutation did not modify the *Dh44-R1* mutant phenotype, suggesting that *Dh44-R1* is the predominant DH44 receptor that regulates rest:activity rhythms. *Dh44-R1* may function both independently as well as together with *Dh44-R2,* which could explain the small circadian deficiency in *Dh44-R2* mutants. To localize the neurons where *Dh44-R1* functions to regulate rest:activity rhythms, we tested 168 GAL4 drivers and identified 15 that weaken rest:activity rhythms when used to drive RNAi targeted to *Dh44-R1* (Figure 3.2A). While no obvious area of expression was common to all GAL4 lines, several GAL4s target expression to the SEZ, specifically *hugin*+ neurons, suggesting that the SEZ is a major neuroanatomical region receiving DH44 signals. However, *Dh44-R1* may be required in multiple groups of neurons for robust rest:activity rhythms, similar to how the collective network of clock neurons is required for sustaining molecular oscillations and behavioral rhythms (Yao and Shafer 2014; Peng et al. 2003).

We also asked whether DH44-R1 and *hugin*+ neurons regulate the output of morning and evening peaks of activity under LD conditions. *Dh44-R1* mutants have a normal morning peak, suggesting that the timing signal from morning oscillators in sLNvs is propagated to motor outputs through alternative circuits. However, the evening peak of activity is reduced. An effect of DH44 on the evening peak of activity, which is the peak that persists in free-running conditions (Grima et al. 2004), is actually consistent with disrupted free-running rhythms in *Dh44-R1* mutants, but it would require a link between *Dh44*+ cells and evening oscillators in dorsal lateral neurons (LNds) (Guo et al. 2014). This may occur through direct connections, since LNds project to the region of the PI (M. Kaneko and Hall 2000). *Dh44*+ cells may also receive evening signals from DN1s, which control the evening peak of activity in addition to the morning peak (Guo et al. 2016; L. Zhang et al. 2010; Y. Zhang et al. 2010).

Several points about this study are worth noting: First, the pathway reported here does not necessarily function as a linear feedforward circuit. *Hugin*+ SEZ neurons not only project to the VNC but may also project back to the *Dh44*+ PI neurons. Indeed, GRASP revealed membrane contacts between *hugin*+ and *Dh44*+ neurons in both the PI and SEZ. Reciprocal connections between *Dh44*+ and *hugin*+ neurons may comprise a feedback circuit mechanism for propagating rhythmic signals in the output circuit. As discussed below, zebrafish orthologs of DH44 and Hugin are also linked in a circuit that regulates arousal, but in that case, Hugin acts upstream of DH44 (Chiu et al. 2016). It is possible *hugin*+ neurons signal to *Dh44*+ neurons, as they do in the *Drosophila* larval brain (Schlegel et al. 2016). Second, while we describe one discrete circuit, this circuit almost certainly integrates with other circuits involved in circadian rhythms of locomotor activity. *Leucokinin* (LK)-expressing neurons also regulate rest:activity rhythms, and the LK receptor is expressed in *Dh44*+ neurons (Cavey et al. 2016; Cannell et al. 2016). Thus, LK and DH44 may comprise another interconnected circuit for rest:activity rhythms. Third, it is clear that circadian output circuits are modulatory rather than strictly essential, since loss of one neuropeptide (ie. DH44, Hugin, or LK) does not cause complete arrhythmicity but reduces the amplitude of rest:activity rhythms. Even PDF, a neuropeptide expressed in the LNvs,

is not completely essential. Consistent with previous reports of rhythms in the absence of PDF signaling (Wülbeck, Grieshaber, and Helfrich-Förster 2008; Shafer and Taghert 2009), we found that 54.3% of the *Pdf*-null flies are still rhythmic. However, behavioral rhythms are weaker in *Pdf* mutants than in *Dh44-R1* and *hugin* loss of function mutants.

Hugin is an ortholog of mammalian neuromedin U (NMU) (Melcher et al. 2006). We find that *Drosophila* Hugin regulates circadian rhythms of locomotor activity, in particular by promoting activity at specific times of day, which is consistent with behavioral effects of NMU-related peptides in vertebrates. Although not associated with changes in rhythms, *nmu* overexpression in zebrafish larvae promotes hyperactivity and inhibits sleep during both the day and night (Chiu et al. 2016). In addition, consistent with our fly data, *nmu* mutant larval and adult zebrafish are less active during the daytime (Chiu et al. 2016). However, Hugin/NMU may even have a conserved role in circadian rhythms, because NMU injections into the rat brain can shift the phase of locomotor activity rhythms (Nakahara et al. 2004). Moreover, cells expressing a different neuromedin, Neuromedin S, are important for rest:activity rhythms controlled by the mammalian suprachiasmatic nucleus, although the peptide itself does not appear to be relevant (I. T. Lee et al. 2015).

In addition to the circadian clock, locomotor activity is regulated by various internal states, such as hunger and arousal, as well as environmental cues, such as light and temperature. These other states and inputs could modify locomotor activity through alternate circuits that access motor command centers in parallel to circadian output circuits. Alternatively, they could directly modulate circadian locomotor circuits. For example, the DH44 PI-Hugin SEZ circuit is located close to the esophagus in the brain and may be receptive to feeding signals. Indeed, *Dh44*+ PI neurons are proposed to function as a post-ingestive nutrient sensor (Dus et al. 2015), and the SEZ contains gustatory cells activated by tastants (Harris et al. 2015). We addressed whether manipulations of *Dh44-R1* or *hugin*+ SEZ neurons affect the flies' overt feeding rhythms and found that these were largely unaltered, suggesting that effects of the DH44 PI-Hugin SEZ circuit on locomotor rhythms are not mediated by an increase in hunger or food-seeking behavior.

Thus, while it is possible that the drive to eat contributes to rest:activity rhythms, the cellular basis of locomotor rhythms can be distinguished from that of feeding rhythms. Indeed, locomotor activity rhythms are also more robust than feeding rhythms (Xu, Zheng, and Sehgal 2008), likely because activity restricted to specific times of day serves many functions other than feeding.

Acknowledgements

We thank Drs. Monica Dus, Paula Haynes, Young-Joon Kim, and Kyunghee Koh for sharing fly lines. Stocks from the Bloomington Drosophila Stock Center (NIH P40OD018537) and Vienna Drosophila Resource Center were used in this study. The work was supported by NIH R37NS048471 (to A.S.). A.N.K. was supported in part by NIH grants T32GM008216 and F31NS100395.

Author Contributions

Conceptualization, A.N.K., A.F.B., D.J.C., and A.S.; Methodology, A.N.K., A.F.B., A.E.S., A.P.D., D.J.C., and A.S.; Investigation, A.N.K., A.E.S., A.P.D., and D.J.C.; Formal Analysis, A.N.K., A.E.S., and A.P.D.; Resources, A.F.B., D.S., and M.N.N.; Writing – Original Draft, A.N.K. and A.S.; Writing – Review & Editing, A.N.K., A.F.B., A.E.S., A.P.D., D.S., M.N.N., D.J.C., and A.S.; Visualization, A.N.K., A.E.S., and A.P.D.; Supervision, A.S.

Figures

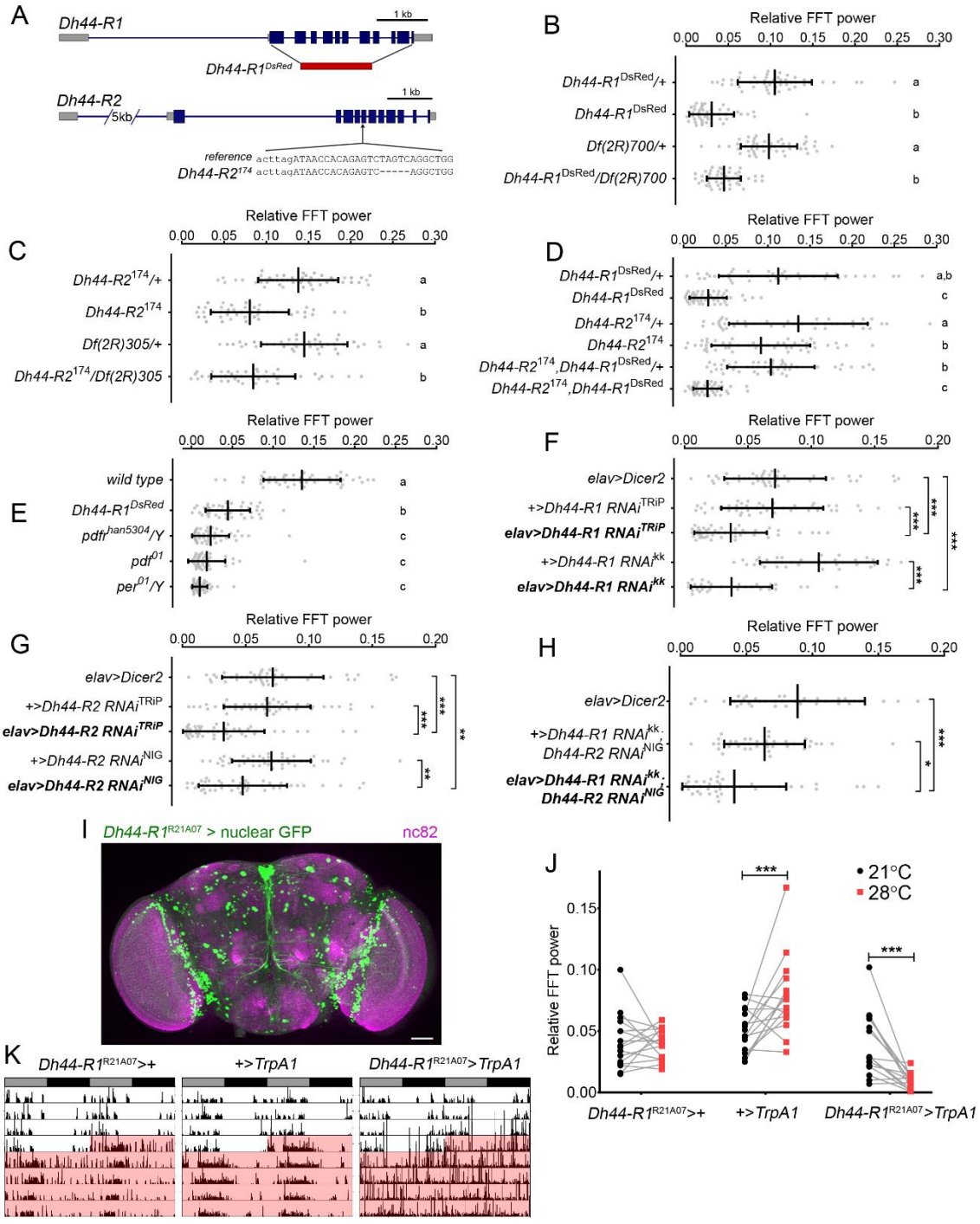

Figure 3.1

DH44 receptors regulate rest:activity rhythms.

(A) Sequence alterations to *Dh44-R1* and *Dh44-R2* loci. Blue denotes the coding DNA sequence, and red denotes the replacement of *Dh44-R1* with DsRed sequence. **(B-D)** Amplitude of circadian rest:activity rhythm under constant darkness (DD) represented by FFT power (mean±SD) for *Dh44-R1*^{DsRed} mutants (B), *Dh44-R2*^{174} mutants (C), *Dh44-R2*^{174}, *Dh44-R1*^{DsRed} double mutants (D), and their heterozygous controls. **(E)** Amplitude of rest:activity rhythms in *Dh44-R1*^{DsRed} mutants, clock output mutants (*Pdf*^{01} and *Pdfr*^{han5304}), and clock mutant (*per*^{01}). For B-E, groups with the same letter are not significantly different from each other (P>0.05 by Tukey's test following one-way ANOVA). **(F-H)** Amplitude of rest:activity rhythm under DD conditions represented by FFT power (mean±SD) for flies with RNAi-mediated knockdown of *Dh44-R1* (F), *Dh44-R2* (G), or both *Dh44-R1* and *Dh44-R2* (H) in all neurons. *P<0.05, **P<0.01, ***P<0.001 by Sidak's test following one-way ANOVA. **(I)** Brain with *Dh44-R1*^{R21A07}*-GAL4*+ neurons labeled with nuclear GFP (green) and counterstained with nc82 (anti-bruchpilot, magenta). Scale bar, 50 µm. **(J)** FFT power for rest:activity rhythms at 21°C (black) and at 28°C (red). ***P<0.00093 by Sidak's test following two-way repeated measure ANOVA. **(K)** Representative records of individual fly activity in DD for 4 days at 21°C and then for 4 days at 28°C for TrpA1 activation (red). See also Figures 3.S1-S2 and Table 3.1.

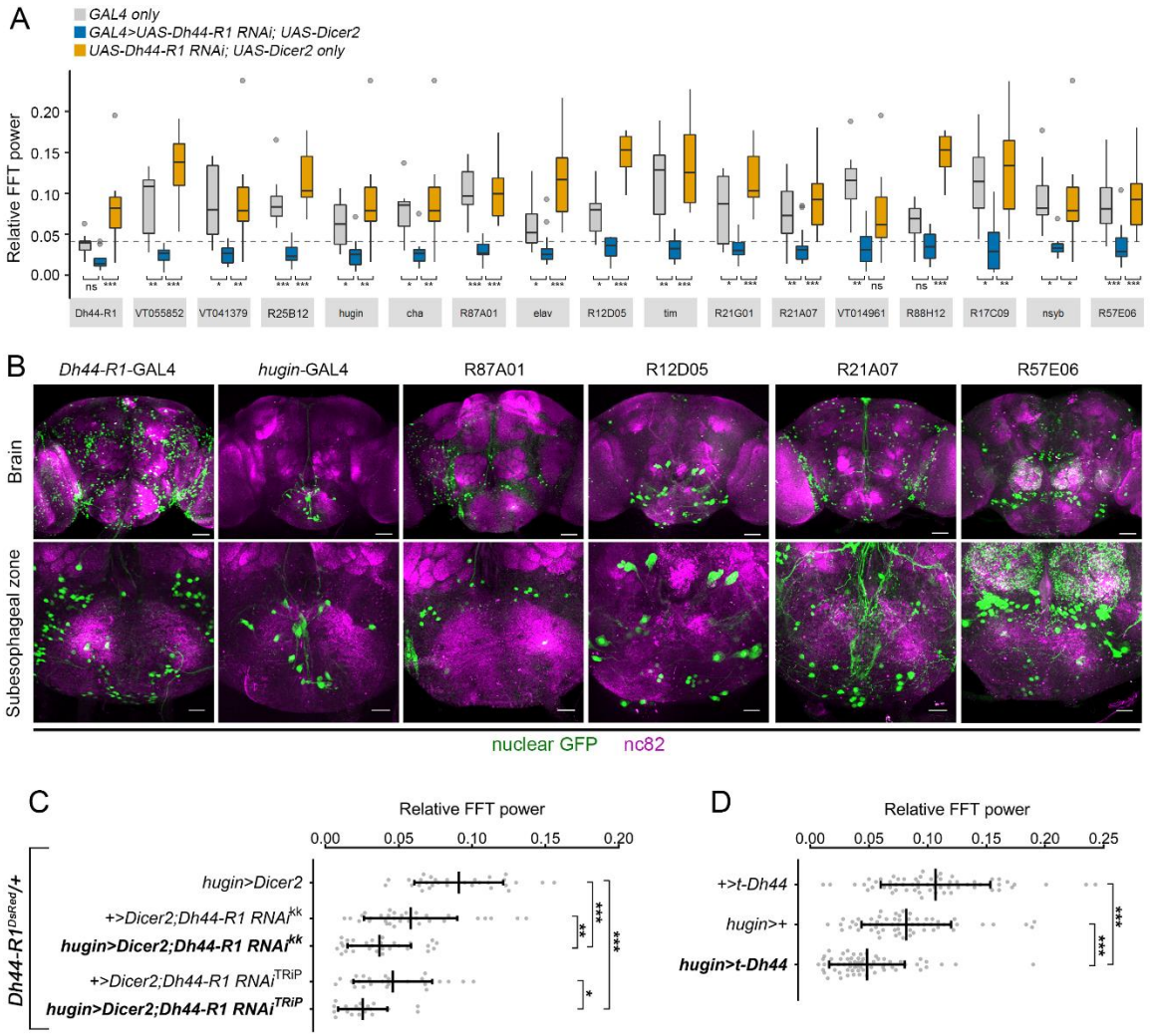

Figure 3.2

***Dh44-R1* in *hugin+* neurons regulates rest:activity rhythms.**

(A) Amplitude (FFT values) of circadian rest:activity rhythm in flies with different GAL4s driving *Dh44-R1* RNAi knockdown (blue) and GAL4 genetic controls (gray and orange). 17 GAL4 lines that yielded the weakest rhythms by FFT analysis are shown from the GAL4 screen. Data summarized with Tukey's boxplots. Gray dashed line denotes 1 SD below the average FFT value of the RNAi knockdown phenotype from all 168 GAL4 lines screened. **(B)** Images of SEZ-localized and -proximal GAL4 hits expressing nuclear GFP (green) in the brain (scale bar 50 µm) and SEZ (scale bar 20 µm). Brains counterstained with nc82 (magenta). **(C)** Amplitude of

rest:activity rhythms with *Dh44-R1* knocked down in *hugin+* neurons in a *Dh44-R1*^{DsRed} heterozygous background and genetic control flies under DD conditions. **(D)** Amplitude of rest:activity rhythms under DD conditions in flies expressing a transgenic tethered DH44 peptide in *hugin+* neurons (*hugin>t-Dh44*). For C-D, mean±SD. *P<0.05, **P<0.01, ***P<0.001 by Sidak's test following one-way ANOVA. See also Figure 3.S3.

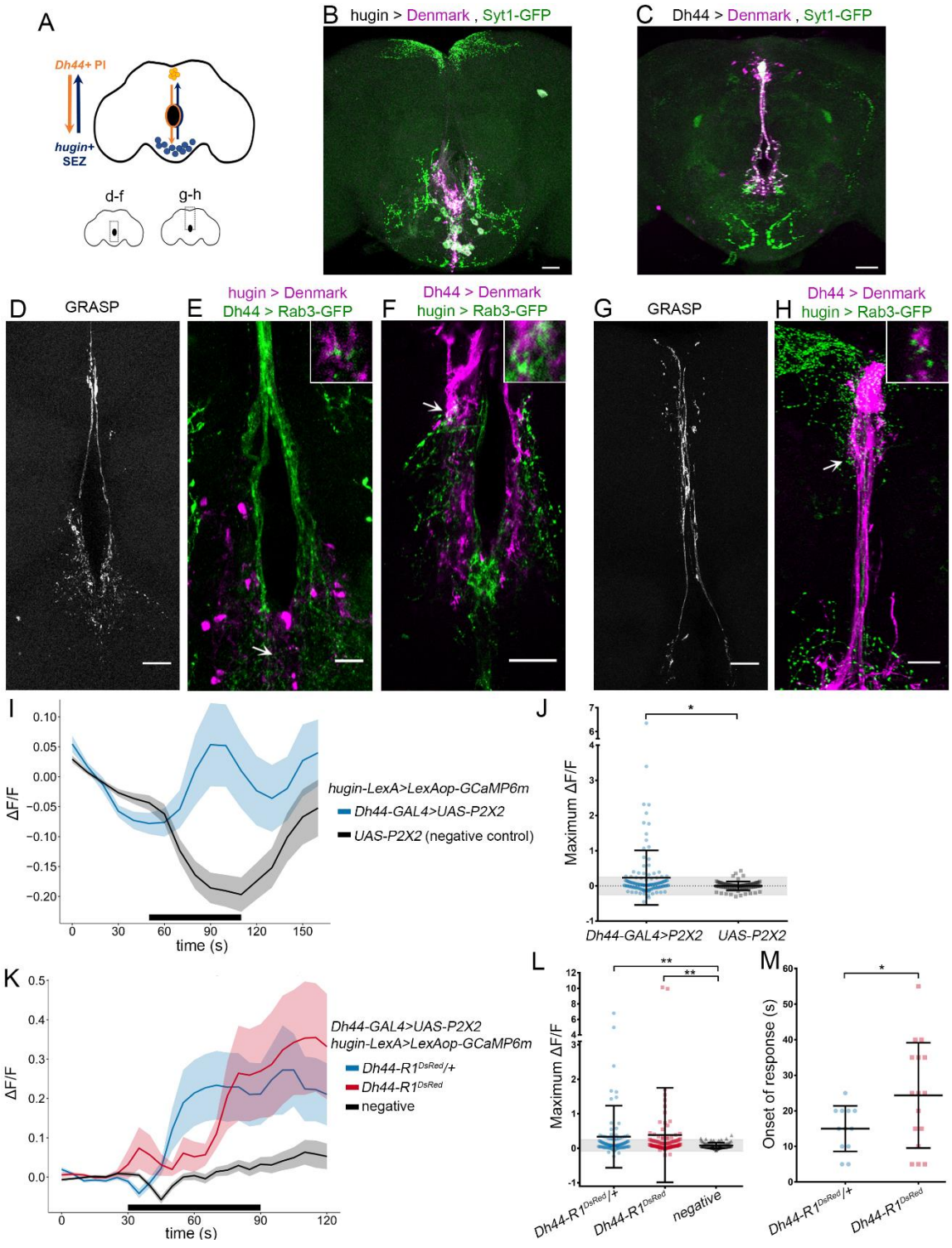

Figure 3.3

***Hugin*+ neurons in the SEZ receive inputs from *Dh44*+ PI neurons.**

(A) Schematic of a circuit between *Dh44*+ neurons in the pars intercerebralis (PI) and *hugin*+ neurons in the subesophageal zone (SEZ). **(B-C)** *Hugin*-GAL4 (B) or *Dh44*-GAL4 (C) expressing presynaptic (syt1-GFP, green) and postsynaptic markers (Denmark, magenta) in the brain. **(D)** Neurexin-GRASP signal near the esophagus in a brain expressing *Dh44-GAL4>UAS-neurexin-spGFP1-10; hugin-LexA>LexAop-CD4-spGFP11*. **(E)** *Dh44*+ axon terminals (green) and *hugin*+ dendrites (magenta) near the esophagus in the brain. **(F)** *Hugin*+ axon terminals (green) and *Dh44*+ dendrites (magenta) near the esophagus in the brain. **(G)** Neurexin-GRASP signal in the PI of a brain expressing *Dh44-GAL4>UAS-neurexin-spGFP1-10; hugin-LexA>LexAop-CD4-spGFP11*. **(H)** *hugin*+ axon terminals (green) and *Dh44*+ dendrites (magenta) in the PI. Insets in E,F,H show 3x magnification of a single confocal section from the region indicated by the arrows. Scale bars, B-C: 35 µm; D,F-H: 20 µm; E: 10 µm. **(I)** GCaMP signal over time in *hugin*+ neurons with activation of *Dh44*+ cells (blue, n = 129 cells, 11 brains) or no activation (black, n = 83 cells, 8 brains). Black bar denotes duration of ATP application. Data represented as mean±SEM. **(J)** Maximum GCaMP change (ΔF/F) in individual cells. Mean±SD. Shaded gray region indicates within 2 SD of the mean value for the *UAS-P2X2* group. *P = 0.0119, Mann-Whitney Test, U = 4259, Z = -2.51. **(K)** GCaMP signal over time in *hugin*+ neurons upon activation of *Dh44*+ cells in *Dh44-R1^{DsRed}*/+ heterozygotes (blue, n = 99 cells, 9 brains) or *Dh44-R1^{DsRed}* mutants (red, n = 108 cells, 11 brains). Negative control is *UAS-P2X2; hugin-LexA>LexAop-GCaMP6m* in *Dh44-R1^{DsRed}*/+ heterozygotes (black, n = 82 cells, 7 brains). Black bar denotes duration of ATP application. Data represented as mean±SEM. **(L)** Maximum GCaMP change (ΔF/F) in individual cells. Mean±SD. Shaded gray region indicates within 2 SD of the mean for the negative control group. **P<0.005, Kruskal-Wallis test followed by Dunn's test. **(M)** Onsets of response in *Dh44-R1^{DsRed}* mutants and heterozygotes. Mean±SD. *P = 0.0339, two-tailed Welch's t test.

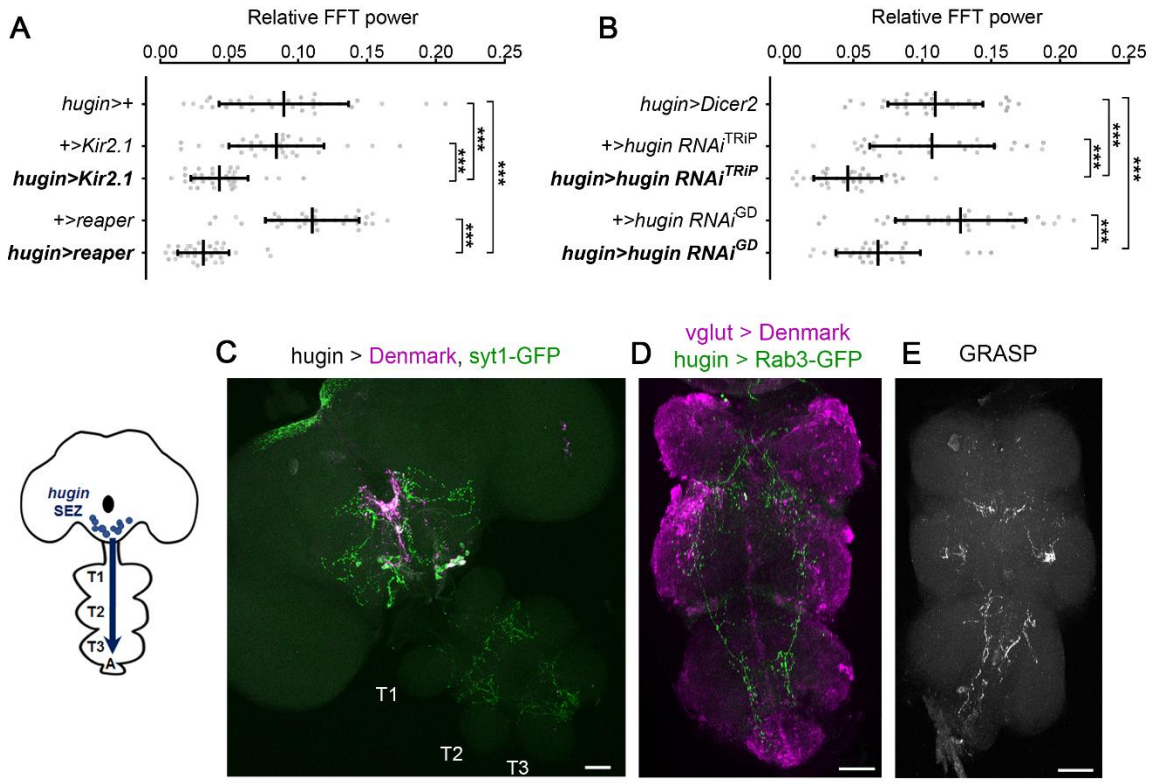

Figure 3.4

***Hugin*+ neurons are circadian output neurons that project to the ventral nerve cord.**

(A) Amplitude of rest:activity rhythm in control flies and flies with *hugin*+ neurons silenced (*hugin>Kir2.1*) or ablated (*hugin>reaper*) under DD conditions. **(B)** Amplitude of rest:activity rhythms in control flies and flies with RNAi-mediated knockdown of *hugin* in *hugin*+ neurons. For A-B, Mean±SD. ***P<0.001 by Sidak's test following one-way ANOVA. **(C)** *Hugin*-GAL4 expressing postsynaptic Denmark (magenta) and presynaptic syt1-GFP (green) markers in the central brain and VNC. The VNC is formed of first (T1), second (T2) and third (T3) thoracic and abdominal ganglia (A). **(D)** *Hugin*-LexA expressing presynaptic Rab3-GFP (green) and *vglut*-GAL4 expressing Denmark (magenta) markers in the VNC. **(E)** GRASP signal in the VNC of flies expressing *vglut-GAL4>UAS-CD4-spGFP1-10; hugin-LexA>LexAop-CD4-spGFP11*. For C-E, scale bars: 50 µm.

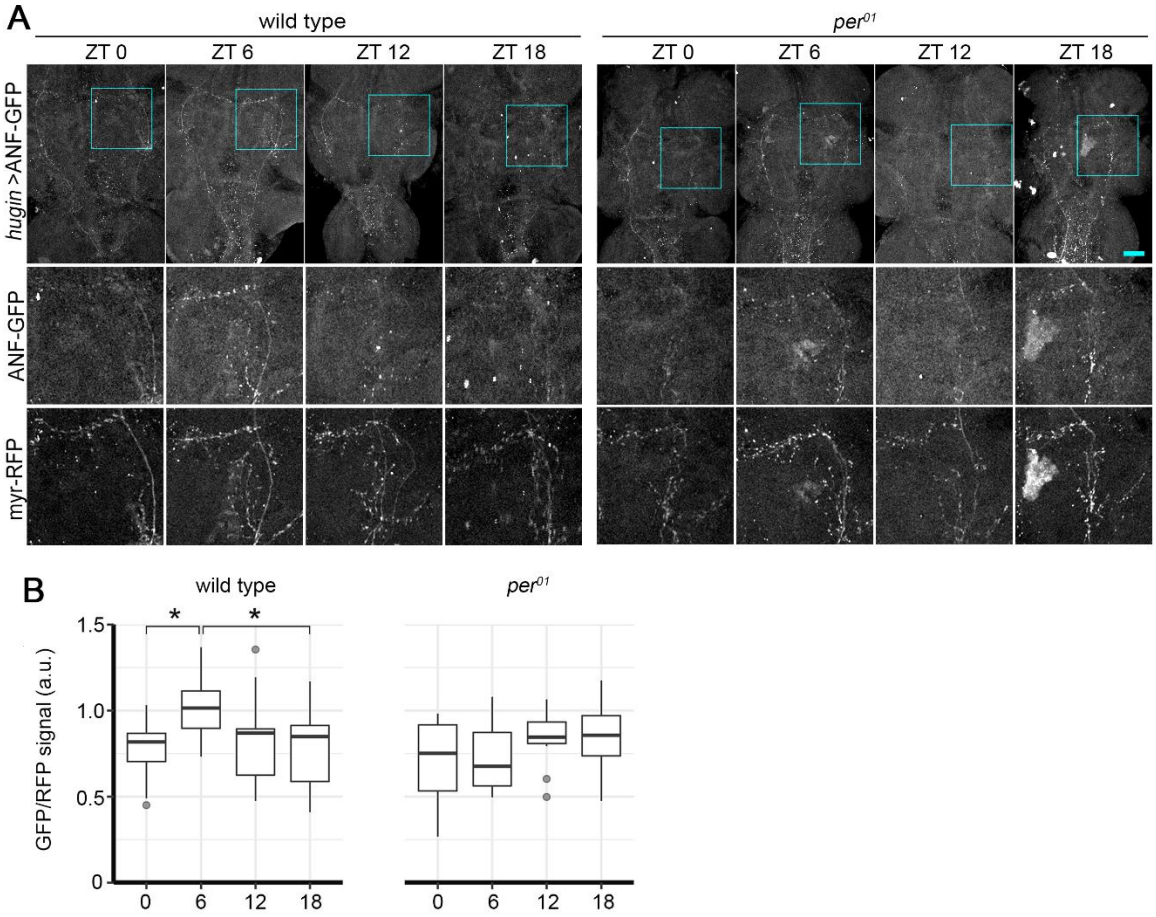

Figure 3.5

Neuropeptide levels in projections of *Hugin*+ neurons are regulated by the circadian clock. **(A)** ANF-GFP signal in VNCs from wild type or *per*^{01} flies expressing *hugin*>ANF-GFP. Scale bar, 50 µm. Close ups of the boxed regions (top) are shown in the middle and bottom rows to highlight the ANF-GFP and corresponding myr-RFP signals respectively. **(B)** Tukey's boxplots of ANF-GFP fluorescence levels in the entire VNC at ZT 0, 6, 12, and 18. (ZT is the Zeitgeber time, where ZT 0 corresponds to lights-on time and ZT 12 to lights-off time. n = 10-15 flies/timepoint and genotype *P<0.0359 by two-way ANOVA and Tukey's test for comparison within genotype. See also Figure 3.S4.

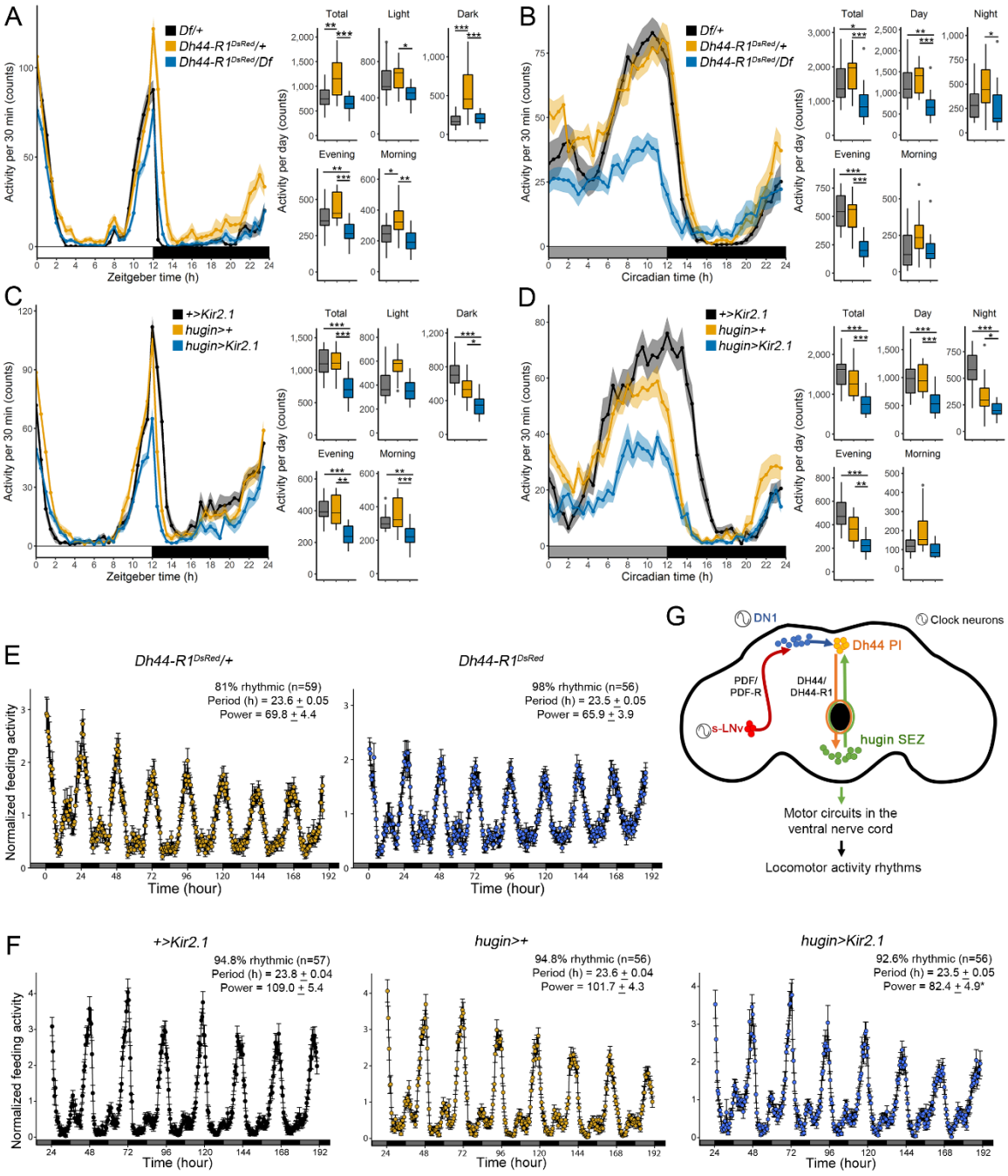

Figure 3.6

The DH44-Hugin circuit alters locomotor activity without affecting feeding.

(A)-(B) Locomotor activity profile of *Dh44-R1^{DsRed}/Df* mutants averaged over 3 days in LD (A) or DD (B). **(C)-(D)** Locomotor activity profiles of *hugin>Kir2.1* flies averaged over 3 days in LD (C) or

DD (D). For A-D, traces (left) show activity counts/30 min (mean±SEM). Tukey's boxplots (right) summarize the distribution of activity counts per day during a total 24-hr day, day (ZT or CT 0-12), night (ZT or CT 12-24), evening (ZT or CT 9-13), and morning (ZT or CT 21-1). n = 15-16/genotype. **(E)-(F)** Normalized feeding activity in *Dh44-R1*^{DsRed}/+ and *Dh44-R1*^{DsRed} flies (E) and *hugin>Kir2.1* and genetic control flies (F) in DD conditions. Period and power data summarized as mean±SEM. For A-F, *P<0.05, **P<0.01, ***P<0.001 by one-way ANOVA and Tukey's test. **(G)** Model of a circadian output circuit for locomotor activity rhythms in *Drosophila*. The circuit extends from the master pacemaker sLNvs (red), through DN1 clock neurons (blue), and to *Dh44*+ PI neurons (orange). This circadian output circuit continues through *hugin*+ SEZ neurons (green) to the VNC. See also Figure 3.S5.

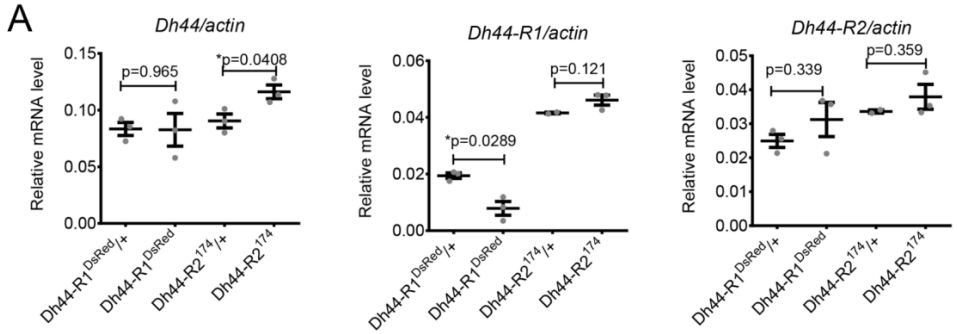

B

```
Dh44-R2 WT      MADDDLRALV DSLDDASQED LAKVIANFSV DMLQRASALI GAQQGSSGGQ LQNRTLQCQQ
Dh44-R2 174     MADDDLRALV DSLDDASQED LAKVIANFSV DMLQRASALI GAQQGSSGGQ LQNRTLQCQQ

Dh44-R2 WT      QQQREEEQAS LEALASGGKR ILQCPSSFDS VLCWPRTNAG SLAVLPCFEE FKGVHYDTTD
Dh44-R2 174     QQQREEEQAS LEALASGGKR ILQCPSSFDS VLCWPRTNAG SLAVLPCFEE FKGVHYDTTD

Dh44-R2 WT      NATRFCFPNG TWDHYSDYDR CHQNSGSIPV VPDFSPNVEL PAIIYAGGYF LSFATLVVAL
Dh44-R2 174     NATRFCFPNG TWDHYSDYDR CHQNSGSIPV VPDFSPNVEL PAIIYAGGYF LSFATLVVAL

Dh44-R2 WT      IIFLSFKDLR CLRNTIHANL FLTYITSALL WILTLFLQVI TTESSQAGCI TLVIMFQYFY
Dh44-R2 174     IIFLSFKDLR CLRNTIHANL FLTYITSALL WILTLFLQVI TTESGWLHNV GNHVSVLLPN

Dh44-R2 WT      LTNFFWMFVE GLYLYTLVVQ TFSSDNISFI IYALIGWGCP AVCILVWSIA KAFAPHLENE
Dh44-R2 174     QLFLDVCGGP LSVHAGGANI LQ*H*

Dh44-R2 WT      HFNGLEIDCA WMRESHIDWI FKVPASLALL VNLVFLIRIM WVLITKLRSA HTLETRQYYK

Dh44-R2 WT      ASKALLVLIP LFGITYLLVL TGPEQGISRN LFEAIRAFLI STQGFFVALF YCFLNSEVRQ

Dh44-R2 WT      TLRHGFTRWR ESRNIHRNSS IKNRSTEECV ICLRPSPHTR LGSLQRYHSI DITDFV*
```

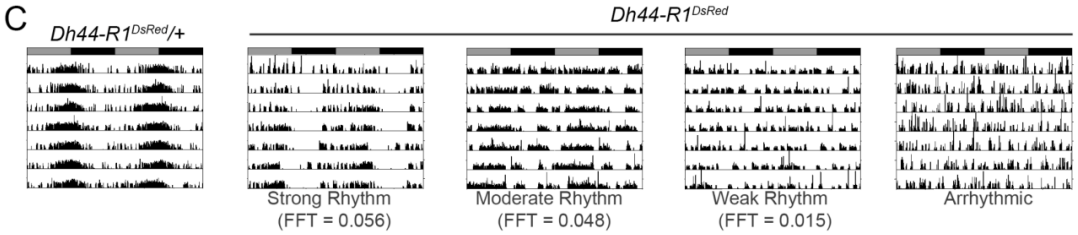

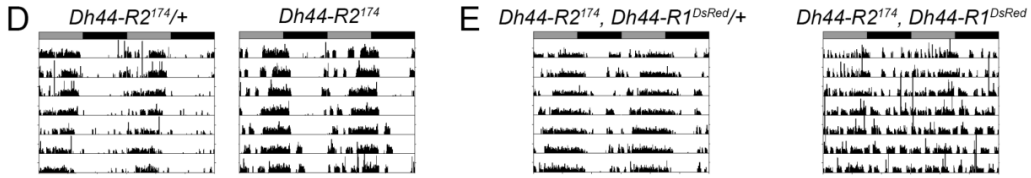

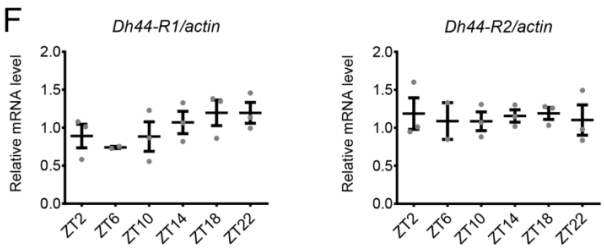

Figure 3.S1 (related to Figure 3.1)

Characterization of *Dh44-R1* and *Dh44-R2* mutants.

(A) mRNA levels for *Dh44-R1*, *Dh44-R2*, and *Dh44* in whole fly tissue from *Dh44-R1^{DsRed}* and *Dh44-R2^{174}* mutants. mRNA levels were normalized to *actin* and compared relative to their heterozygous controls. *P < 0.05 by two-tailed Welch's t-test. qPCR data expressed as mean±SEM from n = 3. **(B)** Predicted protein sequences for *Dh44-R2* wild type and *Dh44-R2^{174}* mutant alleles. *Dh44-R2^{174}* is a frameshift mutation that changes the protein sequence (indicated with bold text) and results in premature stop codons (indicated with *). Hormone binding domain (blue) and 7-transmembrane domain (orange) are annotated from NCBI's Conserved Domain Database (Marchler-Bauer et al. 2015). **(C-E**) Representative locomotor activity records from individual flies in constant darkness (DD). Records are double-plotted with gray and black bars indicating subjective day and night, respectively. **(C)** Locomotor activity of *Dh44-R1^{DsRed}*/+ and *Dh44-R1^{DsRed}* mutant flies in DD. Representative activity records show examples of *Dh44-R1^{DsRed}* homozygous mutants with strong, moderate, weak rhythms or arrhythmic behavior. **(D)** Locomotor activity of *Dh44-R2^{174}*/+ and *Dh44-R2^{174}* mutant flies in DD. **(E)** Locomotor activity of *Dh44-R2^{174},Dh44-R1^{DsRed}*/+ and *Dh44-R2^{174},Dh44-R1^{DsRed}* double mutant flies in DD. **(F)** *Dh44-R1* or *Dh44-R2* mRNA levels in fly head tissue at time points across the day. One-way ANOVA detects no difference between time points (*Dh44-R1*: $F_{5, 11} = 1.27$, P = 0.343; and *Dh44-R2:* $F_{5, 11} = 0.09308$, P = 0.992). JTK_Cycle (Hughes, Hogenesch, and Kornacker 2010) does not detect cycling (*Dh44-R1:* P = 0.272; and *Dh44-R2:* P =1). mRNA levels were normalized to *actin* levels. qPCR data expressed as mean±SEM from n = 2–3 biological replicates.

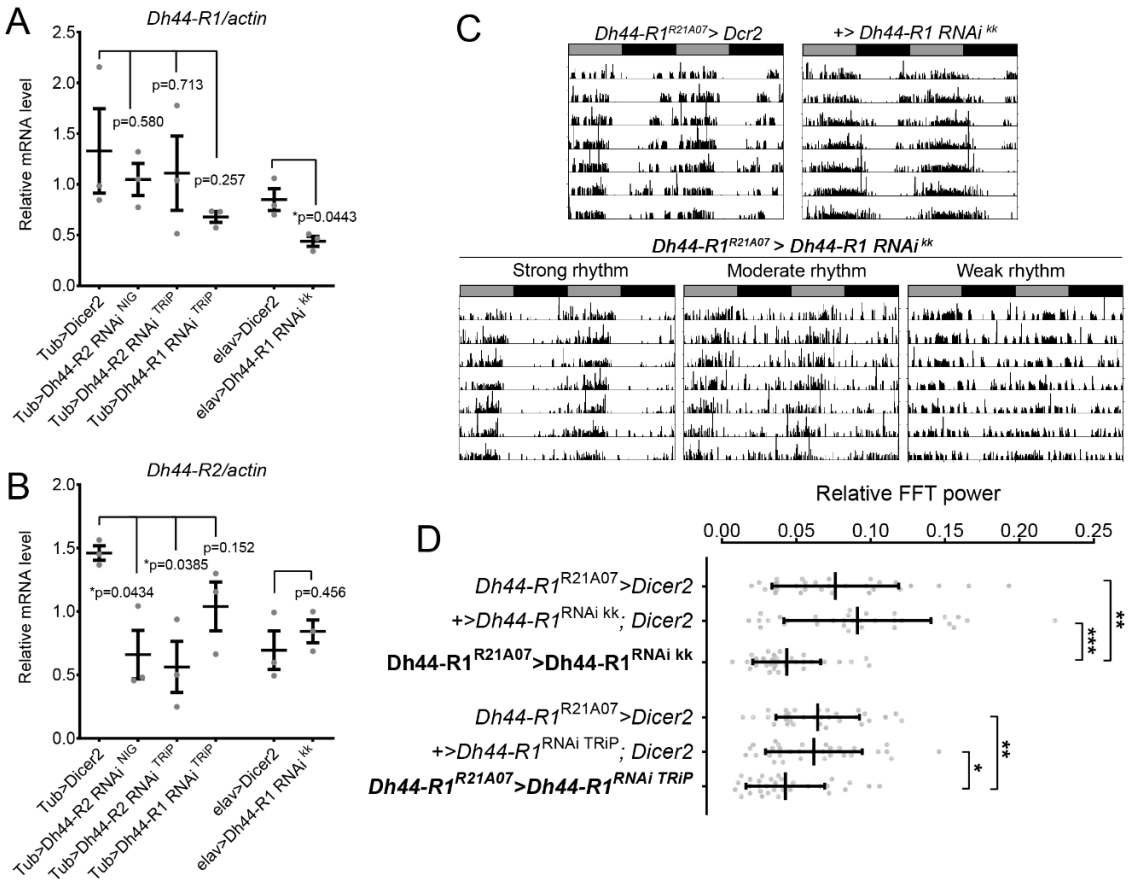

Figure 3.S2 (related to Figure 3.1)

Analysis of RNAi-mediated knockdown of *Dh44-R1*.

(A-B) *Dh44-R1* (A) and *Dh44-R2* (B) mRNA levels in whole fly tissue after knockdown of *Dh44-R1* or *Dh44-R2* using *tubulin*-GAL4 (*Tub*) or *elav*-GAL4. mRNA levels were normalized to *actin* and compared relative to GAL4>Dicer2 control. *Dh44-R1 RNAi kk* knockdown with *Tub*-GAL4 was lethal. *P<0.05 by two-tailed Welch's t-test. qPCR data expressed as mean ± SEM from n = 3. **(C)** Representative activity records show knockdown flies (*Dh44-R1R21A07>Dh44-R1 RNAikk*) can have strong, moderate, or weak rhythms. Control flies (*Dh44-R1R21A07>Dcr2* or *+>UAS-Dh44-R1 RNAikk*) have strong rest:activity rhythms. **(D)** DD amplitude of rest:activity rhythms represented by FFT analysis in the circadian range. RNAi-mediated knockdown of *Dh44-R1* in *Dh44-R1*-expressing cells lowered the amplitude of rest:activity rhythms in flies (*P < 0.05, **P < 0.01, ***P < 0.001 by One-way ANOVA with Sidak's multiple comparison test).

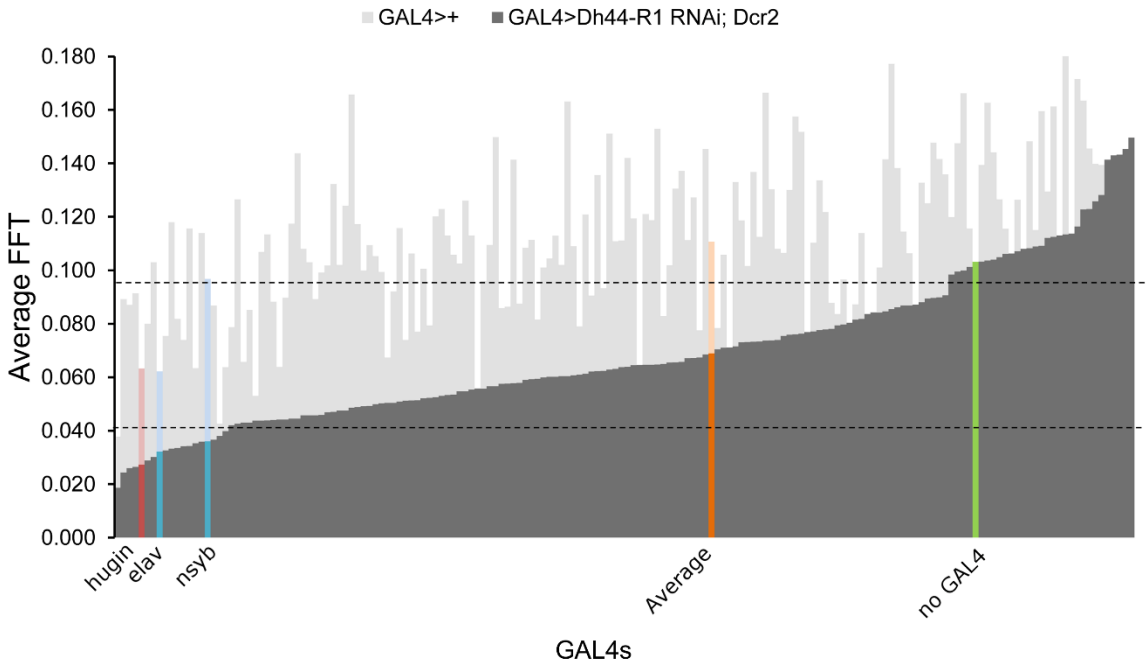

Figure 3.S3 (related to Figure 3.2)

A GAL4 screen with RNAi identifies cells requiring DH44-R1 for strong rest:activity rhythms. The mean FFT values for activity rhythms from flies carrying different GAL4 drivers along with *UAS-Dicer2; UAS-Dh44-R1*$^{RNAi\ kk}$ to knock down DH44-R1 (knockdown, dark gray) or the GAL4 alone (negative control, light gray). The average FFT values from all 168 GAL4 tested (orange), no GAL4 control (*UAS-Dicer2,UAS-Dh44-R1*$^{RNAi\ kk}$; green), and pan-neuronal GAL4s (blue) are shown. Dashed lines denote 1 standard deviation below and above the average FFT from all 168 GAL4 tested. n = 8-16 flies/GAL4, except n = 190 flies for no GAL4 control.

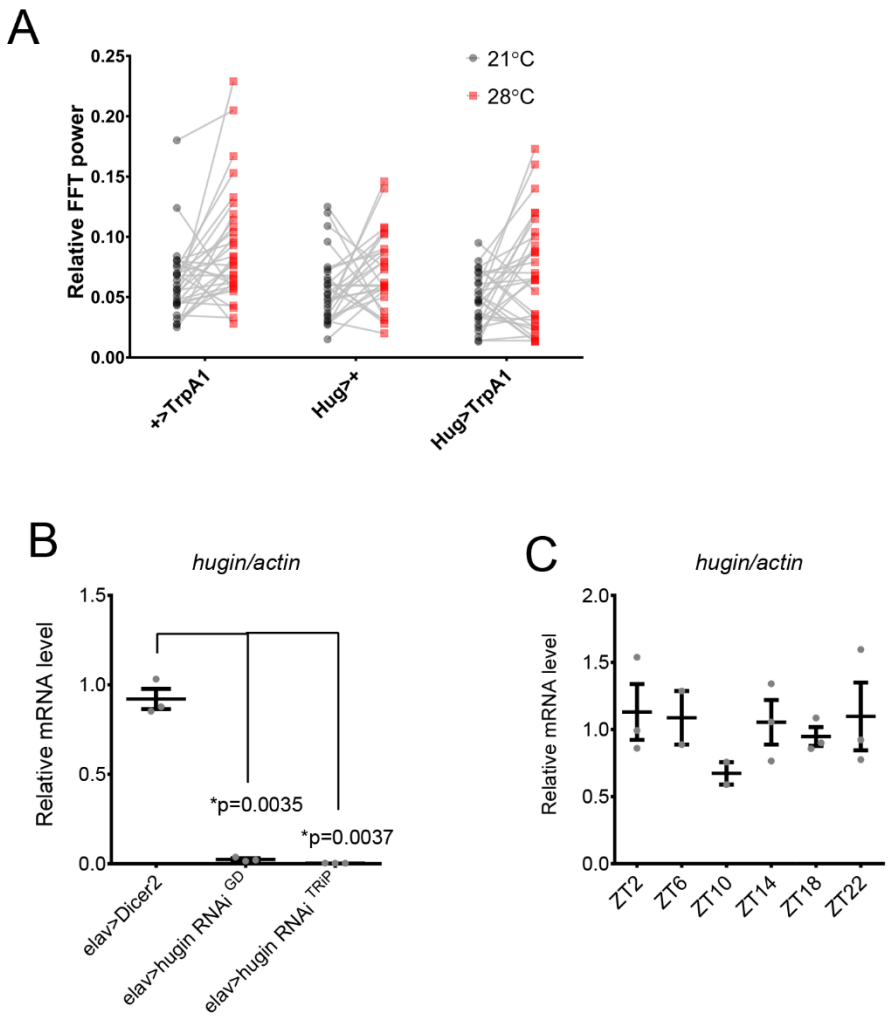

Figure 3.S4 (related to Figure 3.4-3.5)

mRNA levels of *hugin* do not cycle across the day.

(A) *hugin* mRNA levels in whole fly tissue after knockdown of hugin using *elav*-GAL4 coupled with Dicer2 to drive RNAi expression. mRNA levels were normalized to *actin* and compared relative to *elav*-GAL4>*Dicer2* control. *P<0.01, two-tailed Welch's t-test. **(B)** Expression profiling of *hugin* mRNA levels across the day in fly head tissue. One-way ANOVA detects no difference between time points ($F_{5, 10} = 0.6927$, P = 0.641). JTK_Cycle does not detect significant cycling (P = 1). mRNA levels normalized to *actin*. All qPCR data expressed as mean±SEM from n = 2-3 biological replicates.

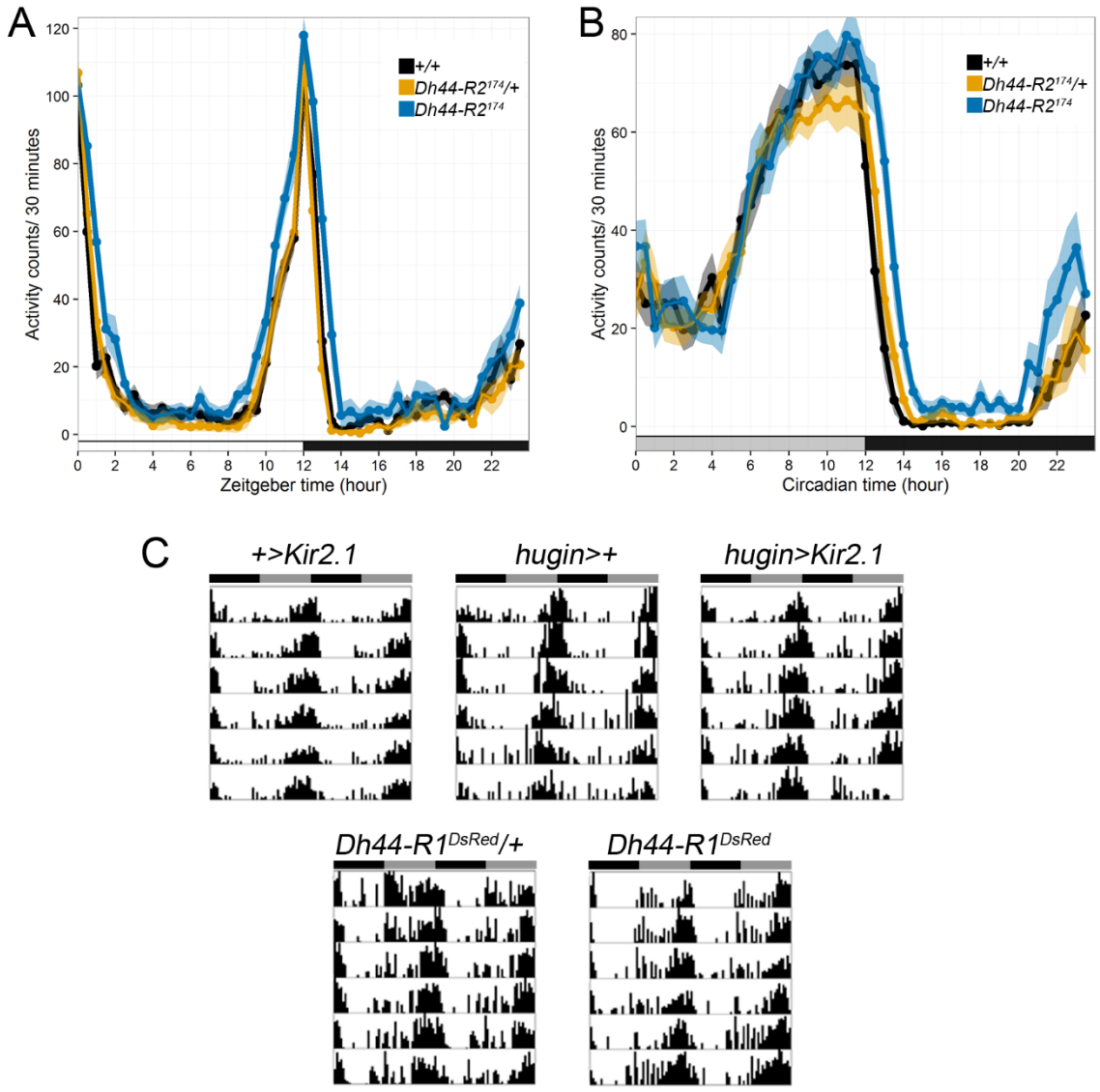

Figure 3.S5 (related to Figure 3.6)

Analysis of locomotor activity and feeding rhythms.

(A-B) Locomotor activity profile of *Dh44-R2^{174}* mutants averaged over 3 d in LD **(A)** or 3 d in DD **(B)**. n=15 flies/genotype. Mean ± SEM. **(C)** Representative plots of feeding activity for *+>Kir2.1, hugin>+,* and *hugin>Kir2.1* flies (top) and *Dh44-R1^{DsRed}/+* and *Dh44-R1^{DsRed}* flies (bottom) in DD. Behavior is double plotted with 6 days of data. Gray and black bars represent subjective day and night, respectively.

Tables

Table 3.1

Analysis of locomotor activity rhythms in flies under DD conditions.

Table shows number of flies analyzed (*n*), percentages of rhythmic flies (% R), and length of circadian period in hours as mean±SEM. Bold text indicates experimental genotype.

Genotype	**n**	**% R**	**Period (h) ± SEM**
Dh44-R1^{DsRed}/+	44	97.7	23.63 ± 0.04
Dh44-R1^{DsRed}	47	80.9	23.51 ± 0.12
Dh44-R2^{174}/+	47	100	23.75 ± 0.03
Dh44-R2^{174}	48	95.8	23.91 ± 0.03
Dh44-R2^{174}, *Dh44-R1*^{DsRed}/+	48	100	23.61 ± 0.03
Dh44-R2^{174}, *Dh44-R1*^{DsRed}	46	93.5	23.39 ± 0.28
Df(2R)BSC700/+	48	100	23.63 ± 0.03
Dh44-R1^{DsRed}/*Df(2R)BSC700*	47	100	23.53 ± 0.05
Df(2R)BSC305/+	44	100	23.78 ± 0.02
Dh44-R2^{174}/*Df(2R)BSC305*	45	97.8	23.56 ± 0.09
pdf^{01}	46	54.3	22.96 ± 1.05
pdfr^{han5304}/Y	47	68.1	22.96 ± 0.62
per^{01}/Y	46	0	N/A
wild type (*w*^{1118}/Y)	46	100	23.73 ± 0.04
elav>UAS-*Dicer2*	47	97.9	23.41 ± 0.26
+>UAS-*Dh44-R1*$^{RNAi\ kk}$	39	100	23.67 ± 0.07
elav>UAS-*Dicer2,* UAS-*Dh44*-R1$^{RNAi\ kk}$	30	80	23.46 ± 0.12
+>UAS-*Dh44-R1*$^{RNAi\ TRiP}$/+	45	97.8	23.45 ± 0.08
elav>UAS-*Dicer2,* UAS-*Dh44-R1*$^{RNAi\ TRiP}$	45	88.9	23.44 ± 0.13
+>UAS-*Dh44-R2*$^{RNAi\ TRiP}$	46	95.7	23.51 + 0.07
elav>UAS-*Dicer2*, UAS-*Dh44-R2*$^{RNAi\ TRiP}$	47	74.5	23.42 ± 0.13
+>UAS-*Dh44-R2*$^{RNAi\ NIG}$	48	100	23.91 + 0.04
elav>UAS-*Dicer2*, UAS-*Dh44-R2*$^{RNAi\ NIG}$	47	93.6	23.93 ± 0.14
+>UAS-*Dh44-R1*$^{RNAi\ kk}$, UAS-*Dh44-R2*$^{RNAi\ NIG}$	40	97.5	23.82 ± 0.05
elav>Dicer2, Dh44-R1$^{RNAi\ kk}$, *Dh44-R2*$^{RNAi\ NIG}$	39	84.6	23.63 ± 0.09
Dh44-R1^{R21A07}>UAS-*Dicer2*	31	100	23.87 ± 0.06
+>UAS-*Dh44-R1*$^{RNAi\ kk}$	32	100	23.40 ± 0.04
Dh44-R1^{R21A07}>UAS-*Dicer2*,UAS-*Dh44-R1*$^{RNAi\ kk}$	31	96.8	23.25 ± 0.07
Dh44-R1^{R21A07}>UAS-*Dicer2*	31	100	23.87 ± 0.04
+>UAS-*Dh44-R1*$^{RNAi\ TRiP}$	31	100	23.37 ± 0.06
Dh44-R1^{R21A07}>UAS-*Dicer2*, UAS-*Dh44-R1*$^{RNAi\ TRiP}$	31	96.9	23.81 ± 0.06
+>UAS-*TrpA1*/+ (21°C)	31	100	23.64 ± 0.09
+>UAS-*TrpA1*/+ (28°C)	31	100	23.68 ± 0.15
Dh44-R1^{R21A07}-GAL4>+ (21°C)	32	96.9	23.91 ± 0.33
Dh44-R1^{R21A07}-GAL4>+ (28°C)	32	100	23.70 ± 0.23
Dh44-R1^{R21A07}>UAS-*TrpA1* (21°C)	31	93.5	23.70 ± 0.18
Dh44-R1^{R21A07}>UAS-*TrpA1* (28°C)	31	31	23.39 ± 0.08
Dh44-R1^{DsRed}/+; *hugin*>UAS-*Dicer2*	30	100	23.53 ± 0.04
Dh44-R1^{DsRed}/+; +>UAS-*Dh44-R1*$^{RNAi\ kk}$	32	100	23.24 ± 0.33
Dh44-R1^{DsRed}/+; *hug*>UAS-*Dicer2*,UAS-*Dh44-R1*$^{RNAi\ kk}$	29	96.6	23.80 ± 0.45
Dh44-R1^{DsRed}/+; +>UAS-*Dh44-R1*$^{RNAi\ TRiP}$/+	24	95.8	23.78 ± 0.05
Dh44-R1^{DsRed}/+; *hug*>UAS-*Dicer2*,UAS-*Dh44-R1*$^{RNAi\ TRiP}$	19	78.9	23.67 ± 0.19
+>UAS-*t-Dh44*	62	100	23.56 ± 0.05
hugin-GAL4>+	61	100	23.58 ± 0.03
hugin>UAS-*t-Dh44*	60	96.8	23.50 ± 0.07

hugin-GAL4>+	32	100	23.64 + 0.04
+>UAS-*Kir2.1*	32	100	23.47 + 0.05
hugin>UAS-*Kir2.1*	31	96.8	23.39 ± 0.07
+>UAS-*reaper*	32	100	23.83 + 0.03
hugin>UAS-*reaper*	31	90.3	23.81 ± 0.06
hugin>UAS-*Dicer2*	47	100	24.02 ± 0.04
+>UAS-*hugin*$^{RNAI\ TRiP}$	47	100	23.45 ± 0.04
hugin>UAS-*Dicer2,* UAS-*hugin*$^{RNAI\ TRiP}$	48	91.7	23.53 ± 0.05
+>UAS-*hugin*$^{RNAI\ GD}$	48	100	23.89 ± 0.03
hugin>UAS-*Dicer2,* UAS-*hugin*$^{RNAI\ GD}$	47	100	23.89 ± 0.02

Table 3.2

Fly genotypes used in the study.

Figure	Genotype
Figure 3.1B	*w/Y; Dh44-R1^{DsRed}/+* *w/Y; Dh44-R1^{DsRed}/Dh44-R1^{DsRed}* *w/Y; Df(2R)BSC700/+* *w/Y ;Dh44-R1^{DsRed}/Df(2R)BSC700*
Figure 3.1C	*w/Y; Dh44-R2^{174}/+* *w/Y; Dh44-R2^{174}/Dh44-R2^{174}* *w/Y; Df(2R)BSC305/+* *w/Y; Dh44-R2^{174}/Df(2R)BSC305*
Figure 3.1D	*w/Y; Dh44-R2^{174},Dh44-R1^{DsRed}/+* *w/Y; Dh44-R2^{174},Dh44-R1^{DsRed}/ Dh44-R2^{174},Dh44-R1^{DsRed}*
Figure 3.1E	*w/Y; Dh44-R1^{DsRed}* *w,per^{01}/Y* *w;;pdf^{0}* *w,pdfr^{han5304}/Y* *w/Y iso31*
Figure 3.1F	*w,elav-GAL4/Y; UAS-Dicer2/+; +/+* *w/Y; UAS-Dh44-R1 RNAi kk/+; +/+* *w,elav-GAL4/Y; UAS-Dicer2/UAS-Dh44-R1 RNAi kk; +/+* *w/Y; +/+; UAS-Dh44-R1 RNAi TRiP/+* *w,elav-GAL4/Y; UAS-Dicer2/+; UAS-Dh44-R1 RNAi TRiP/+*
Figure 3.1G	*w,elav-GAL4/Y; UAS-Dicer2/+; +/+* *w/Y; +/+; UAS-Dh44-R2 RNAi NIG/+* *w,elav-GAL4/Y; UAS-Dicer2/+; UAS-Dh44-R2 RNAi NIG/+* *w/Y; +/+; UAS-Dh44-R2 RNAi TRiP/+* *w,elav-GAL4/Y; UAS-Dicer2/+; UAS-Dh44-R2 RNAi TRiP/+*
Figure 3.1H	*elav-GAL4/Y; UAS-Dicer2/+; +/+* *w/Y; UAS-Dh44-R1 RNAi kk/+; UAS-Dh44-R2 RNAi NIG/+* *elav-GAL4/Y; UAS-Dicer2/UAS-Dh44-R1 RNAi kk; UAS-Dh44-R2 RNAi NIG/+*
Figure 3.1I	*w/Y; UAS-GFP.nls/+; Dh44-R1^{R21A07}-GAL4/+*
Figure 3.1J-K.	*w/Y; +/+; Dh44-R1^{R21A07}-GAL4/+* *w/Y; UAS-dTrpA1/+; +/+* *w/Y; UAS-dTrpA1/+; Dh44-R1^{R21A07}-GAL4/+*
Figure 3.2A	*w/Y; UAS-Dh44-R1 RNAi kk/+; UAS-Dicer2/+* *w/Y; +/+; GAL4/+* or *w/Y; GAL4/+; +/+* *w/Y; UAS-Dh44-R1 RNAi kk/+; UAS-Dicer2/GAL4* or *w/Y; UAS-Dh44-R1 RNAi kk/GAL4; UAS-Dicer2/+*
Figure 3.2B	*w/Y; UAS-GFP.nls/+; GAL4/+*
Figure 3.2C	*w/Y; Dh44-R1^{DsRed}/+; hug-GAL4/UAS-Dicer2* *w/Y; Dh44-R1^{DsRed}/+,UAS-Dh44-R1 RNAi kk; UAS-Dicer2/+* *w/Y; Dh44-R1^{DsRed}/+,UAS-Dh44-R1 RNAi kk; hug-GAL4/UAS-Dicer2* *w/Y; Dh44-R1^{DsRed}/+,UAS-Dicer2; UAS-Dh44-R1 RNAi TRiP/+* *w/Y; Dh44-R1DsRed/+,UAS-Dicer2; hug-GAL4/UAS-Dh44-R1 RNAi TRiP*
Figure 3.2D	*w/Y; UAS-t-Dh44/+* *w/Y; +/+; hug-GAL4/+* *w/Y; UAS-t-Dh44/+; hug-GAL4/+*
Figure 3.3B	*w/Y; UAS-Denmark,UAS-syt-GFP/+; hug-GAL4/+*
Figure 3.3C	*w/Y; UAS-Denmark,UAS-syt-GFP/+; Dh44-GAL4/+*
Figure 3.3D,G	*w/Y; hug-LexA/LexAop-CD4-spGFP11; Dh44-GAL4/UAS-Nrx-spGFP1-10*
Figure 3.3E.	*w/Y; Dh44-LexA/UAS-Denmark; hug-GAL4/LexAop-Rab3-GFP*
Figure 3.3F,H	*w/Y; hug-LexA/UAS-Denmark; Dh44-GAL4/LexAop-Rab3-GFP*
Figure 3.3I-J	*w/Y; hug-LexA/UAS-P2X2; Dh44-GAL4/LexAop-GCaMP6m-p10* *w/Y; hug-LexA/UAS-P2X2; Dh44-GAL4/LexAop-GCaMP6m-p10* *w/Y; hug-LexA/UAS-P2X2; +/LexAop-GCaMP6m-p10*
Figure 3.3K-M	*w/Y; Dh44-R1^{DsRed},UAS-P2X2/Dh44-R1^{DsRed},hug-LexA; Dh44-GAL4/LexAop-GCaMP6m-p10* *w/Y; Dh44-R1^{DsRed},UAS-P2X2/+,hug-LexA; Dh44-GAL4/LexAop-GCaMP6m-p10* *w/Y; Dh44-R1^{DsRed},UAS-P2X2/+,hug-LexA; +/LexAop-GCaMP6m-p10*
Figure 3.4A	*w/Y; +/+; hug-GAL4/+* *w/Y; +/+; UAS-Kir2.1/+* *w/Y; +/+; hug-GAL4/UAS-Kir2.1* *yw,UAS-reaper/Y; +/+; +/+* *yw,UAS-reaper/Y; +/+; hug-GAL4/+*

Figure 3.4B	*w/Y; UAS-Dicer2/+; hug-GAL4/+* *w/Y; +/+; UAS-hugin RNAi TRiP/+* *w/Y; UAS-Dicer2/+; hug-GAL4/UAS-hugin RNAi TRiP* *w/Y; +/+; UAS-hugin RNAi GD/+* *w/Y; UAS-Dicer2/+; hug-GAL4/UAS-hugin RNAi GD*
Figure 3.4C	*w/Y; UAS-Denmark,UAS-syt-GFP/+; hug-GAL4/+*
Figure 3.4D	*w/Y; hug-LexA,vglut-GAL4/UAS-Denmark; LexAop-Rab3-GFP/+*
Figure 3.4E	*w/Y; hug-LexA,vglut-GAL4/LexAop-CD4-spGFP11; UAS-CD4-spGFP1-10/+*
Figure 3.5	*w/Y; UAS-ANF-GFP,UAS-myr-RFP/+; hug-GAL4/+* *w, per^{01}/Y; UAS-ANF-GFP,UAS-myr-RFP/+; hug-GAL4/+*
Figure 3.6A,B.	*w/Y; Df(2R)BSC700/+* *w/Y;Dh44-$R1^{DsRed}$/+* *w/Y;Dh44-$R1^{DsRed}$/Df(2R)BSC700*
Figure 3.6C, D, F.	*w/Y; +/+; hug-GAL4/+* *w/Y; +/+; UAS-Kir2.1/+* *w/Y; +/+; hug-GAL4/UAS-Kir2.1*
Figure 3.6E	*w/Y;Dh44-$R1^{DsRed}$/+* *w/Y;Dh44-$R1^{DsRed}$/Dh44-$R1^{DsRed}$*
Figure 3.S1A	*w/Y; Dh44-$R2^{174}$/+* *w/Y; Dh44-$R2^{174}$/Dh44-$R2^{174}$* *w/Y; Dh44-$R1^{DsRed}$/+* *w/Y; Dh44-$R1^{DsRed}$/Dh44-$R1^{DsRed}$*
Figure 3.S1C	*w/Y; Dh44-$R1^{DsRed}$/+* *w/Y; Dh44-$R1^{DsRed}$/Dh44-$R1^{DsRed}$*
Figure 3.S1D	*w/Y; Dh44-$R2^{174}$/+* *w/Y; Dh44-$R2^{174}$/Dh44-$R2^{174}$*
Figure 3.S1E	*w/Y; Dh44-$R2^{174}$,Dh44-$R1^{DsRed}$/+* *w/Y; Dh44-$R2^{174}$,Dh44-$R1^{DsRed}$/Dh44-$R2^{174}$,Dh44-$R1^{DsRed}$*
Figure 3.S1F	*w/Y iso31*
Figure 3.S2A, B	*w/Y; UAS-Dicer2/+; tubulin-GAL4/+* *w/Y; UAS-Dicer2/+; tubulin-GAL4/UAS-Dh44-R2 RNAi NIG* *w/Y; UAS-Dicer2/+; tubulin-GAL4/ UAS-Dh44-R2 RNAi TRiP* *w/Y; UAS-Dicer2/+; tubulin-GAL4/ UAS-Dh44-R1 RNAi TRiP* *w,elav-GAL4/Y; UAS-Dicer2/+; +/+* *w,elav-GAL4/Y; UAS-Dicer2/UAS-Dh44-R1 RNAi kk; +/+*
Figure 3.S2C, D	*w/Y; +/+; Dh44-$R1^{R21A07}$-GAL4/UAS-Dicer2* *w/Y; UAS-Dh44-R1 RNAi kk/+; UAS-Dicer2/+* *w/Y; UAS-Dh44-R1 RNAi kk/+; Dh44-$R1^{R21A07}$-GAL4/UAS-Dicer2* *w/Y; UAS-Dicer2/+; UAS-Dh44-R1 RNAi TRiP/+* *w/Y; UAS-Dicer2/+; Dh44-$R1^{R21A07}$-GAL4/UAS-Dh44-R1 RNAi TRiP*
Figure 3.S3	*w/Y; UAS-Dh44-R1 RNAi kk/+; UAS-Dicer2/+* *w/Y; +/+; GAL4/+* or *w/Y; GAL4/+; +/+* *w/Y; UAS-Dh44-R1 RNAi kk/+; UAS-Dicer2/GAL4* or *w/Y; UAS-Dh44-R1 RNAi kk/GAL4; UAS-Dicer2/+*
Figure 3.S4A	*w,elav-GAL4/Y; UAS-Dicer2/+; +/+* *w,elav-GAL4/Y; UAS-Dicer2/+; UAS-hugin RNAi TRiP/+* *w,elav-GAL4/Y; UAS-Dicer2/+; UAS-hugin RNAi GD/+*
Figure 3.S4B	*w/Y iso31*
Figure 3.S5A, B	*w/Y iso31* *w/Y; Dh44-$R2^{174}$/+; +/+* *w/Y; Dh44-$R2^{174}$/Dh44-$R2^{174}$; +/+*
Figure 3.S5C, D	w*/Y; +/+; hug-GAL4/+* *w/Y; +/+; UAS-Kir2.1/+* *w/Y; +/+; hug-GAL4/UAS-Kir2.1* *w/Y; Dh44-$R1^{DsRed}$/+ and w/Y; Dh44-$R1^{DsRed}$/Dh44-$R1^{DsRed}$*

Table 3.3

Sequences used in generating *Dh44-R1* and *Dh44-R2* CRISPR mutants.

Primer	**Sequence 5' → 3'**
gRNA sequences and primers used to generate and screen *Dh44-R1* and Dh44-R2 CRISPR mutations.	
gRNA to exon 6 of *Dh44-R2*	GATAACCACAGAGTCTAGTC AGG
gRNA to 5' end of *Dh44-R1*	GTTGTCAATTCGTAGGGAAA TGG
gRNA to 3' end of *Dh44-R1*	GGGCATTGTTGGAGCCCCGG TGG
Cloning primers for HDR template *Dh44-R1*^{DsRed}	
5'HA-Dh44-R1 Forward	CATTGCATGCGTGGAGCACCCAAGCCTTG
5'HA-Dh44-R1 Reverse	TACTGCGGCCGCCCTACGAATTGACAACGTTC
3'HA-Dh44-R1 Forward	TATAACTAGTGGGCTCCAACAATGCCCTG
3'HA-Dh44-R1 Reverse	AGTGGCGCGCCAAAGAGCCTTTATTACGAAGGAC
Primers for PCR verification of *Dh44-R2* CRISPR mutation	
Dh44-R2 Po Forward	TCAACGAAGTTTACCTTGCCAATC
Dh44-R2 Pi Forward	GATAACCACAGAGTCTAGTCAGG
Dh44-R2 P Reverse	ATGAGGGCGTAGATAATAAAGC
Primers for PCR verification of *Dh44-R1* CRISPR mutation	
5'HA Dh44-R1 far Forward	ACGAAGCCGAGCATACAGTG
5'HA HDR Reverse	CGGTCGAGGGTTCGAAATCGATAAG
3'HA HDR Forward	GTGGTTTGTCCAAACTCATC
3'HA Dh44-R1 far Reverse	GAGCGTCGGACCCAATTAGC

Chapter 4 : Sleep signals are integrated into an output arm of the circadian clock

Anna N. King and Amita Sehgal

Abstract

Sleep is controlled by homeostatic mechanisms, which regulate sleep duration and depth, and a circadian clock, which regulates the timing of sleep. Homeostatic sleep drive can sometimes override the circadian clock, such that recovery sleep after sleep deprivation can occur outside the normal circadian rest period. However, the mechanisms underlying this effect are not known. We report here that sleep-promoting dorsal fan-shaped body (dFB) neurons, an effector of a sleep homeostat circuit in *Drosophila*, are presynaptic to *hugin*+ neurons, which were previously identified as circadian output neurons that regulate locomotor activity rhythms. Sleep deprivation decreases activity of *hugin*+ neurons, which may serve to suppress circadian control and thereby promote recovery sleep driven by the dFB neurons. Indeed, removal of *hugin*+ neurons increases sleep-promoting effects of the dFB neurons. Trans-synaptic mapping reveals that *hugin*+ neurons feedback on to s-LNv central clock neurons, which also show decreased activity upon sleep loss. These findings identify a circuit-based mechanism through which sleep drive modulates the circadian clock to promote recovery sleep following deprivation.

Introduction

Sleep is a shared behavioral state observed in many animals (Joiner 2016; Bringmann 2018). Sleep behavior is characterized by a period of inactivity, reduced responsiveness to the environment, reversibility, homeostatic rebound after sleep deprivation, and a correlated change in neural activity (Dubowy and Sehgal 2017). Although the function of sleep is not clear, it appears to be important for many processes, such as memory and learning, synaptic scaling, and neurodevelopment. The functions and regulation of sleep are extensively studied in model organisms, such as *Drosophila melanogaster* (Dubowy and Sehgal 2017).

Sleep is regulated by two processes, circadian and homeostatic (Borbély et al. 2016). The circadian process consists of an endogenous molecular clock that, together with its downstream pathways, is synchronized to external day/night cycles and determines the timing of sleep to generate 24-hour rhythms in sleep and wake. The homeostatic process tracks sleep

history and generates sleep drive based on history. Sleep homeostasis can be overtly seen as an increase in sleep duration and depth after prolonged wakefulness. Generally, circadian and homeostatic processes are studied as separate pathways that regulate sleep, although they clearly intersect to provide optimal control of behavior. In addition, sleep homeostasis mechanisms can sometimes overrule clock mechanisms, such that sleep after deprivation can occur during normal activity periods. In rodents, there is evidence for homeostatic mechanisms affecting the circadian system. Sleep deprivation dampens electrical activity in the suprachiasmatic nucleus (SCN), the central pacemaker required for circadian rhythms of behavior (Deboer, Détári, and Meijer 2007), and reduces the ability of the circadian clock to phase shift by light (Mistlberger, Landry, and Marchant 1997; Etienne Challet et al. 2001).

In the *Drosophila* brain, the circadian clock is expressed in ~150 clock neurons that are organized into neuroanatomical groups: small and large ventrolateral neurons (s-LNvs and l-LNvs), dorsolateral neurons (LNds), lateral posterior neurons (LPNs), and dorsal neuron groups (DN1, DN2, and DN3) (Charlotte Helfrich-Förster, Shafer, et al. 2007). Synchronization of molecular clocks across the clock network ensures robust rest:activity rhythms, although distinct roles are served by different groups of clock neurons. Molecular clocks in LNvs have the primary role in controlling locomotor activity rhythms (C Helfrich-Förster 1998; Renn et al. 1999; Grima et al. 2004), and they do so partially through a circadian output circuit from s-LNvs → DN1s → *Dh44*+ neurons → *hugin*+ neurons. *Dh44*-expressing neurons in the pars intercerebralis regulate rest:activity rhythms, at least in part through signaling of DH44 neuropeptide to *hugin*-expressing neurons in the subesophageal zone (SEZ) (Cavanaugh et al. 2014; King et al. 2017). *Dh44*+ and *hugin*+ circadian output neurons do not contain clocks but display cycling in neuronal activity, likely under control of upstream circadian signals. Thus, intracellular Ca^{2+} levels in *Dh44*+ neurons vary across the day (Cavey et al. 2016; Bai et al. 2018), and *hugin*+ neurons display cyclic neuropeptide release that is controlled by the clock (King et al. 2017). Consistent with an origin of circadian signal, neuronal activity of clock neurons is also rhythmic, in conjunction with sleep and wake states (Sheeba, Gu, et al. 2008; Flourakis et al. 2015; Guo et al. 2016). In

addition to their critical role in the timing of sleep, some clock neurons have been implicated in arousal or in the control of sleep amount (Shang, Griffith, and Rosbash 2008; Parisky et al. 2008; Kunst et al. 2014). However, their link to the sleep circuitry is generally not understood.

Regulation of sleep homeostasis is complex and known to involve the central complex and mushroom body (Joiner et al. 2006; Pitman et al. 2006; Sitaraman et al. 2015; Donlea 2017). Recent studies have focused on a group of sleep-promoting neurons that project to the dorsal fan-shaped body in the central complex (dFB neurons). Activation of dFB neurons promotes sleep (Donlea et al. 2011; Ueno et al. 2012), and these neurons are required for sleep rebound after deprivation (Qian et al. 2017). dFB neurons receive input signals from R2 ellipsoid body neurons, which track sleep need (S. Liu et al. 2016). As sleep pressure builds, dFB neurons become more electrically active (Donlea, Pimentel, and Miesenbock 2014), and induce sleep by inhibiting Helicon cells with the neuropeptide Allatostatin A (AstA) (Donlea et al. 2018). A subset of dFB neurons expressing the 5HT2b serotonin receptor is sufficient to promote sleep (Qian et al. 2017).

Because little is known about the circuits linking clock neurons and sleep-regulatory neurons (J. Chen et al. 2016), we set out to explore the connection between sleep homeostatic and circadian circuits in *Drosophila*. We find that sleep-promoting dFB neurons are presynaptic to *hugin*+ circadian output neurons. *hugin*+ neurons are dispensable for determining daily sleep amount, but they appear to modulate sleep-promoting effects of dFB neurons, such that ablation of *hugin*+ neurons enhances sleep driven by the dFB, and activation of *hugin*+ neurons reduces recovery sleep after heat-induced nighttime sleep loss. We find that *hugin*+ neurons target PDF+ s-LNv clock neurons, and both circadian neuronal groups show decreases in intracellular Ca^{2+} levels following sleep deprivation. We propose a circuit mechanism by which a sleep homeostatic circuit counteracts the circadian clock through downregulating wake-promoting outputs of the circadian clock.

Methods

Drosophila melanogaster

Flies were maintained on cornmeal-molasses medium. For thermogenetic and *trans*-Tango experiments, flies were raised at 18°C, and all other flies were maintained at 25°C. w^{1118} iso31 strain was used as the wild type strain. For sleep behavior experiments, transgenic lines were backcrossed into the iso31 genetic background. For controls, UAS and GAL4 fly lines were tested as heterozygotes after crossing to iso31. See Table 4.1 for a list of complete genotypes used in each experiment. The following flies were from the Bloomington Drosophila Stock Center: *23E10-GAL4* (#49032) (Jenett et al. 2012), *23E10-LexA* (#52693) (Pfeiffer et al. 2010), *Hugin-GAL4* (#58769) (Melcher and Pankratz 2005), *Hugin-LexA* (#52715), *Dh44-GAL4* (#39347), *UAS-CD8::RFP* (#32219), *LexAop-Rab3::GFP* (#52239) (Shearin et al. 2013), *LexAop-6xmCherry-HA* (#52271), *UAS-nSyb::GFP1-10, LexAop-CD4::GFP11* (#64314), *UAS-reaper* (#5773) (White, Tahaoglu, and Steller 1996). *Trans*-Tango fly was a gift from G. Barnea. CaLexA fly was a gift from J.W. Wang. *UAS-TrpA1* was a gift from L.C. Griffith. *UAS-shibire^{ts}* (*20XUAS-IVS-Shibire[ts1]-p10-INS*) and *LexAop-TrpA1* (chromosome 2) were gifts from G. Rubin (Pfeiffer, Truman, and Rubin 2012). *LexAop-TrpA1* (chromosome 3) was a gift from S. Waddell (Burke et al. 2012).

Immunohistochemistry

For polarity labeling and CaLexA experiments, ~7 d old females raised at 25°C were used. For *trans*-Tango experiments, ~15-20 d old females raised at 18°C were used, as previously described (Talay et al. 2017). All fly brains were dissected in phosphate-buffered saline with 0.1% Triton-X (PBST) and fixed with 4% formaldehyde in PBS for 20 min at room temperature. Brains were rinsed 3 x 10 min with PBST, blocked in 5% Normal Goat Serum in PBST (NGST) for 60 min, and incubated in primary antibody diluted in NGST for >16 h at 4°C. Brains were rinsed 3 x 10 min in PBST, incubated 2 h in secondary antibody diluted in NGST, rinsed 3 x 10 min in PBST, and mounted with Vectashield media (Vector Laboratories Inc.). Primary antibodies used were: rabbit anti-GFP at 2µg/mL (Thermo Fisher Scientific Inc. A-11122), rat anti-RFP at 1µg/mL

(ChromoTek 5F8), mouse anti-BRP at 1:1000 (Developmental Studies Hybridoma Bank nc82), rat anti-HA at 1µg/mL (Roche clone 3F10), and mouse anti-PDF at 0.3µg/mL (Developmental Studies Hybridoma Bank c7-c). Secondary antibodies were from Thermo Fisher Scientific Inc. and used at 1:1000: Alexa Fluor 488 goat anti-rabbit, Alexa Fluor 555 goat anti-rat, Alexa Fluor 647 goat anti-rat, Alexa Fluor 647 goat anti-mouse.

nSyb-GRASP

nSyb-GRASP flies were dissected in extracellular saline (103 mM NaCl, 3 mM KCl, 1 mM NaH_2PO_4, 4 mM $MgCl_2$, 10 mM D-(+)-trehalose dehydrate, 10 mM D-(+)-glucose, 5 mM N-tris(hydroxymethyl) methyl-2-aminoethane sulfonic acid, 26 mM $NaHCO_3$, pH 7.4). Dissected brains were exposed to a high concentration of KCl to increase GRASP signal, as previously described (Macpherson et al. 2015). Dissected brains were incubated in 1 ml 70 mM KCl in saline three times (~5 s per KCl incubation), alternating with 1 ml saline (~5 s per wash), and then transferred to 1 mL saline to incubate for 10 minutes. Brains were fixed with 4% formaldehyde in PBS for 20 minutes at room temperature, rinsed 3 x 10 min in PBST, and mounted with Vectashield media. Endogenous GRASP signal without antibody labeling was imaged.

Confocal Microscopy

Eight-bit images were acquired using a Leica TCS SP5 laser scanning confocal microscope with a 40x/1.3 NA or 20x/0.7 NA objective and a 1-µm z-step size. Maximum intensity z-projection images were generated in Fiji, a distribution of ImageJ software (Schindelin et al. 2012).

Sleep Behavior Assay

Individual ~7 d old female flies were loaded into glass tubes containing 5% sucrose and 2% agar. Locomotor activity was monitored with the Drosophila Activity Monitoring system (DAMS) (Trikinetics, Waltham, MA). Flies were monitored for sleep in a 12 h:12 h (12:12) light:dark cycle at 25°C for CaLexA experiments or at 21°C for thermogenetic experiments. Incubator temperature shifts occurred at lights-on, Zeitgeber time (ZT) 0. For mechanical sleep deprivation experiments, flies were loaded into the DAMS and sleep deprived during the night by shaking on

an adapted vortex for 2 s randomly within every 20 s interval. Sleep was defined as 5 consecutive min of inactivity. Sleep analysis was performed with PySolo software (Gilestro and Cirelli 2009). Data from flies that survived the duration of the experiments were pooled and analyzed. Behavioral data were analyzed with one-way analysis of variance (ANOVA) with Tukey's test as the post hoc test to compare means between groups. Differences between groups were considered significant if $P < 0.05$ by the post hoc test.

CaLexA Analysis

Fluorescence intensity measurement was performed in Fiji. Regions of interest (ROIs) were manually drawn to encompass individual RFP-positive cell bodies, and mean pixel intensities of RFP and GFP signals were measured from the ROI. For each cell, the CaLexA-GFP/RFP signal (arbitrary unit, a.u.) was calculated as a ratio between the mean pixel intensities of GFP and RFP. For each brain, CaLexA-GFP/RFP signals from all cells were averaged and served as one biological replicate. Welch's *t*-test was used to compare differences in CaLexA-GFP/RFP signal between sleep-deprived and control groups.

Statistical Analysis

The statistical details of experiments can be found in figure legends. All statistical tests were performed in R (version 3.3.1). Graphs were generated in R using ggplot2 package, except for sleep profiles, which were generated in Pysolo. In Tukey's boxplots, the line inside the box indicates the median, and the bottom and top lines represent the 1st and 3rd quartiles. The upper whisker extends to the highest value that is within 1.5 * IQR above the 3rd quartile, where IQR is the inter-quartile range (the distance between the 25th and 75th percentiles). The lower whisker extends to the lowest value within 1.5 * IQR below the 1st quartile. Data beyond the end of the whiskers are outliers and plotted as points.

Results

Sleep-promoting dFB neurons are presynaptic to *hugin*+ circadian output neurons

We previously described that *hugin*+ subesophageal zone (SEZ) neurons innervate the pars intercerebralis in the most dorsal part of the brain (King et al. 2017). We also noticed that the *hugin*+ projections extend beyond the pars intercerebralis into the superior medial protocerebrum (SMP). The SMP is the target of many sleep-regulatory neurons, including the mushroom body (MB), mushroom body output neurons (MBON), dopamine neurons (DAN), and dorsal fan-shaped body (dFB) (Artiushin and Sehgal 2017). We focused on the dFB, since it is the best characterized sleep-regulatory region to date. Several GAL4 drivers target dFB neurons, but we focused on the ~24 sleep-promoting dFB neurons labeled with the 23E10-GAL4 driver, which we will refer to as *23E10*+ dFB neurons (Donlea, Pimentel, and Miesenbock 2014; Pimentel et al. 2016; Qian et al. 2017; Donlea et al. 2018).

We doubled labeled the membranes of *23E10*+ dFB neurons and *hugin*+ neurons and found that both sets of projections localized to the SMP (Figure 4.1A). In *23E10*+ dFB neurons, expression of *brp-short*^{GFP}, a nonfunctional 754-residue portion of BRP that localizes to presynaptic active zones (Schmid et al. 2008; Fouquet et al. 2009), labels projections in both the dFB and SMP (Figure 4.1B). In addition, using *23E10-LexA* to express *Rab3::GFP*, another presynaptic marker, reveals *23E10*+ presynaptic terminals in the dFB and SMP (Figure 4.1A). While previous studies reported that the presynaptic sites of dFB neurons are primarily in a single dorsal layer of the fan-shaped body, additional presynaptic sites are visible in the SMP in published images (W. Li et al. 2009; Donlea et al. 2018). However, the signal of the presynaptic markers is weaker in the SMP than the dFB, suggesting the presence of more presynaptic sites in the dFB than in the SMP.

We also used a trans-synaptic GFP fluorescence reconstitution assay (nSyb-GRASP) to look for a possible synaptic connection between *23E10*+ and *hugin*+ neurons. This system uses the expression of a split version of GFP, one part tethered to neuronal Synaptobrevin (nSyb::spGFP1-10) in the putative presynaptic cells and the complement tethered to the

membrane (CD4::spGFP11) in the putative postsynaptic neurons (Macpherson et al. 2015). Split GFP fragments only reconstitute at close membrane contacts, which are identified by GFP fluorescence (Feinberg et al. 2008). Since nSyb is trafficked to the presynaptic vesicle membrane, nSyb-GRASP identifies membrane contacts specifically at synapses. We first tested that nSyb-GRASP works by co-expressing presynaptic nSyb::spGFP1-10 and complementary CD4::spGFP11 in *23E10*+ dFB neurons. In these flies, GFP reconstituted in both the dFB and SMP (Figure 4.1C left), confirming that *23E10*+ dFB neurons have presynaptic sites in both these sites. In flies with the presynaptic nSyb::spGFP1-10 expressed in *23E10*+ dFB neurons and complementary CD4::spGFP11 expressed in *hugin*+ neurons, fluorescent GFP reconstituted in the SMP but not in the dFB (Figure 4.1C middle). We also performed the reciprocal experiment, with nSyb::spGFP1-10 expressed in the *hugin*+ neurons and complementary CD4::spGFP11 expressed in *23E10*+ dFB neurons, but did not observe any GFP fluorescence in the brain (Figure 4.1C right). Also, no GFP fluorescence was also observed in brains expressing either half of the GRASP components and imaged under the same conditions (data not shown). These results suggest that *23E10*+ dFB neurons are presynaptic to *hugin*+ neurons in the SMP.

Disrupting activity of *hugin*+ neurons is not sufficient to alter sleep amount or recovery sleep

The connection between *23E10*+ dFB and *hugin*+ neurons led to the question of whether *hugin*+ neurons also regulate sleep. To test this, we expressed temperature-sensitive *TrpA1* channel in *hugin*+ neurons and activated them with high temperature while measuring sleep behavior (Pulver et al. 2009). In other experiments, we expressed temperature-sensitive *shibire^{ts}*, a dominant-negative dynamin gene, to inhibit synaptic transmission from *hugin*+ neurons at high temperature (Kitamoto 2001). As previously reported (Donlea et al. 2011; Ueno et al. 2012), activation of *23E10*+ dFB neurons at high temperature with TrpA1 led to sleep increase (data not shown). We did not observe changes in sleep amount when *hugin*+ neurons were activated with *TrpA1* or inhibited with *shibire^{ts}* (Figure 4.2A-2B). While there were no changes to sleep, *hugin>shibire^{ts}* flies were less active than control flies, as measured by number of beam

crossings per day, which confirms our previous findings that *hugin*+ neurons regulate locomotor activity (King et al. 2017).

Since mechanisms that participate in baseline and sleep recovery may be different, we asked whether *hugin*+ neurons play a role in regulating sleep homeostasis. We used the same thermogenetic approach to activate or inhibit the *hugin*+ neurons, while simultaneously sleep depriving the flies using a mechanical method. After sleep deprivation, recovery sleep was monitored in the flies. We found no significant difference in recovery sleep between the experimental and control genotypes when *hugin*+ neurons were activated or inhibited. As sleep is a vital behavior regulated by redundant pathways, it is possible that disrupting the activity of *hugin*+ neurons alone does not affect sleep amount or homeostasis.

Sleep deprivation decreases Ca^{2+} levels in *hugin*+ neurons

Sleep is correlated with changes in neuronal activity in sleep-regulatory circuits, including the MB, dFB, and R2 ellipsoid body (Bushey, Tononi, and Cirelli 2015; Sitaraman et al. 2015; Yap et al. 2017; S. Liu et al. 2016). For example, sleep-promoting dFB neurons tend to be more electrically active after sleep deprivation, when sleep pressure is high, than dFB neurons in rested flies (Donlea, Pimentel, and Miesenbock 2014). If the *hugin*+ neurons receive signals from sleep-promoting dFB neurons, activity of *hugin*+ neurons may change with sleep pressure. To address this question, we measured intracellular Ca^{2+} levels as a readout of neuronal activity in *hugin*+ neurons using CaLexA (Calcium-dependent nuclear import of LexA) (Masuyama et al. 2012). The CaLexA system drives expression of GFP in response to sustained increases in intracellular Ca^{2+} levels. We used *hugin-GAL4* to express CaLexA-GFP transgenes and *UAS-CD8:RFP* for normalizing the GFP signal. We completely deprived *hugin>CaLexA-GFP,RFP* flies of sleep for nine hours at the end of the night (ZT 15-24) and subsequently collected flies for CaLexA measurements (Figure 4.3A). A control group, flies of the same genotype that were not sleep deprived, was assayed at the same time of day as the deprived group. CaLexA-dependent GFP signal intensity was lower in *hugin*+ cell bodies in the sleep-deprived flies as compared to controls (Figure 4.3B-C). To rule out a general effect of sleep deprivation on Ca^{2+}, we also tested

whether sleep deprivation affects Ca^{2+} levels in *Dh44*+ neurons, another group of circadian output neurons (Cavanaugh et al. 2014). However, the CaLexA-GFP signal in *Dh44*+ neurons was not significantly different between the sleep-deprived and control flies (Figure 4.3D). These data show that Ca^{2+} levels of *hugin*+ neurons is decreased following sleep deprivation, suggesting that the homeostat engages *hugin*+ neurons.

hugin+ neurons are effectors of *23E10*+ sleep-promoting dFB neurons

If *hugin*+ neurons are downstream of *23E10*+ sleep-promoting dFB neurons, they could affect the sleep-promoting output of *23E10*+ neurons. To test this hypothesis, we activated *23E10*+ neurons in flies where *hugin*+ neurons were either ablated or simultaneously activated. We used the GAL4/UAS system to express the proapoptotic gene, *reaper*, to genetically ablate *hugin*+ neurons, and used the LexA/LexAop system to express 2 copies of *TrpA1* to activate *23E10*+ dFB neurons. Thermogenetic activation of the *23E10*+ neurons using the LexA/LexAop system (*23E10-LexA>LexAop-TrpA1(2x); +>UAS-reaper* in blue) led to sleep increase, especially at night (Figure 4.4A-B). The sleep increase was not as large as the one observed in *23E10-GAL4>UAS-TrpA1* flies (Figure 4.4D), because we suspect 23E10-LexA is less effective than 23E10-GAL4 as a transcriptional activator. When *23E10*+ neurons were activated in flies with *hugin*+ neurons ablated (*23E10-LexA>LexAop-TrpA1(2x); hugin-GAL4>UAS-reaper* in red), the sleep gain was enhanced during the day (Figures 4.4A-B). This result is consistent with *23E10*+ neurons promoting sleep through inhibiting *hugin*+ neurons. When the *23E10*+ and *hugin*+ neurons were simultaneously activated using the GAL4/UAS system, there was no change to the sleep-promoting effects of *23E10*+ dFB neurons, perhaps because *23E10*+ dFB neurons can use other output circuits, such as the Helicon cells, to induce sleep (Donlea et al. 2018).

In the thermogenetic sleep experiments, we also observed significant heat-induced sleep loss during the night, independent of *23E10*+ dFB activation (Figure 4.4B right). Temperature reorganizes sleep behavior in flies, and the heat-induced nighttime sleep loss engages the homeostat, resulting in sleep increase the next day (Parisky et al. 2016). To determine if *hugin*+ neurons affect recovery sleep after heat-induced nighttime sleep loss, we maintained flies for a

day at 31°C (high temperature), after which they were returned to 21°C (low temperature) to recover sleep. Recovery sleep was determined by comparing sleep at Day 3 with Day 1, both at 21°C. Ablation of *hugin*+ neurons did not affect the amount of sleep loss at 31°C or the amount of recovery sleep at 21°C after heat-induced sleep loss (Figure 4.4B-C). Thermogenetic activation of *hugin*+ neurons also did not affect the amount of sleep loss at 31°C, when compared to the controls (Figure 4.4E). However, after return to 21°C, recovery sleep was decreased in flies where *hugin*+ cells were activated with *TrpA1,* compared to control groups or flies with *23E10>TrpA1* activation alone (Figure 4.4F). Despite having increased sleep during the high temperature, flies with activation of *23E10*+ dFB neurons recovered sleep after the transition from high to low temperature. However, flies subjected to simultaneous activation of *23E10*+ and *hugin*+ neurons showed decreased sleep recovery at 21°C, similar to that seen with *hugin>TrpA1* activation. We hypothesize that heat-induced sleep loss engages the homeostat, which normally inhibits activity of *hugin*+ circadian neurons to generate sleep drive that manifests overtly as recovery sleep.

***Pdf*+ clock neurons are targets of *hugin*+ neurons**

We next sought to map neurons downstream of *hugin*+ neurons by using *trans*-Tango, a pan-neuronal trans-synaptic labeling system (Talay et al. 2017). In the *trans*-Tango method, a tethered ligand is expressed at the synapses of a set of genetically defined neurons. The ligand activates a synthetic signaling pathway in postsynaptic partners to express tdTomato fluorescent protein (Talay et al. 2017). Presynaptic neurons are simultaneously labeled with myr::GFP, a different fluorescent protein. We expressed the *trans*-Tango ligand in *hugin*+ neurons and observed *trans*-Tango-dependent signal in many brain regions, including the pars intercerebralis, mushroom body lobes, mushroom body calyx and pedunculus, SMP, subesophageal zone, and accessory medulla (Figure 4.5A). In addition, we found that *hugin*+ neurons have bilateral projections into the accessory medulla, which track with the *trans*-Tango signal (Figure 4.5A'', magenta, arrowheads). Postsynaptic neurons in the accessory medulla were reminiscent of *Pdf*+ small ventrolateral neurons (s-LNvs), prompting us to label for PDF peptide and confirm that that

a subset of the postsynaptic partners observed in *hugin>trans-Tango* flies is PDF-positive. *Pdf*+ neurons are subdivided into the small (s-LNv) and large (l-LNv) ventrolateral neurons, each group containing 4-5 neurons per hemisphere. The *trans*-Tango-dependent signal was more intense in the s-LNvs than in the l-LNvs (Figure 4.5B), indicating that s-LNvs are primary targets of *hugin*+ neurons.

Our data demonstrate a circuit that links sleep homeostasis centers to circadian clock neurons (*23E10*+ dFB → *hugin*+ SEZ → *Pdf*+ s-LNvs) and suggest a potential mechanism for homeostatic components to regulate outputs of the circadian clock. To test whether the activity of *Pdf*+ neurons themselves is altered with sleep deprivation, we again used the CaLexA system to measure Ca^{2+} level changes in *Pdf*+ neurons during sleep deprivation. With mechanical sleep deprivation, the CaLexA-GFP signal in both *Pdf*+ s-LNv and l-LNv cell bodies was lower in the sleep-deprived flies as compared to controls (Figure 4.6). Therefore, sleep deprivation suppresses an additional clock output, the activity of LNvs.

Discussion

The circadian clock and homeostat both regulate sleep, but it is not clear how the two processes functionally interact. We identify a circuit-based mechanism in the fly brain that links output arms of a sleep homeostat and the circadian clock. *23E10*+ sleep-promoting dFB neurons signal through *hugin*+ circadian neurons to suppress circadian outputs and, thereby, allow for sleep at times when the circadian system typically promotes wake (Figure 4.6C). We also find that *hugin*+ circadian output neurons feedback to s-LNvs, the central clock neurons. Thus, a sleep homeostat circuit influences outputs of the circadian clock by modulating the activity of circadian output neurons and clock neurons.

The circadian clock can regulate sleep by cell-intrinsically controlling the neuronal activity of clock neurons, such as the LNvs. The wake-promoting effect of the LNvs is light-dependent and largely comes from the l-LNv subset (Sheeba, Fogle, et al. 2008; Shang, Griffith, and Rosbash 2008; Parisky et al. 2008). While s-LNvs alone are not sufficient to promote wake,

downregulation of PDF receptor in s-LNvs increases sleep, suggesting PDF signaling to s-LNvs modulates wake-promoting effects of l-LNvs (Shang, Griffith, and Rosbash 2008; Parisky et al. 2008). In addition, the downregulation of short Neuropeptide F signaling between s-LNvs and l-LNvs decreases nighttime sleep (Shang et al. 2013). Notably, both s-LNvs and l-LNvs show more depolarized resting membrane potentials during the day than during the night, supporting the idea that LNvs are more active during times of increased arousal (Sheeba, Gu, et al. 2008; Cao and Nitabach 2008).

Does sleep homeostasis influence the neuronal activity of LNvs, and if so, how? It was previously reported that sleep loss due to social enrichment is associated with an increased number of synapses in the LNv projections into the medulla, a brain region that processes visual information from the eyes (Donlea, Ramanan, and Shaw 2009). Here, we report Ca^{2+} levels in LNvs decrease with sleep deprivation, which we hypothesize dampens the wake-promoting effects of LNvs to allow for recovery sleep. It is possible that decreased Ca^{2+} levels in LNvs with sleep deprivation precedes synaptic downscaling that occurs with sleep recovery. While we have only mapped a connection from *23E10*+ dFB to the LNv wake-promoting clock neurons through *hugin*+ neurons, it is likely that other sleep homeostat pathways also modulate LNvs. Notably, GABA and myoinhibitory peptide signal to LNvs to regulate sleep, although the source of these neuromodulators is not known yet (Parisky et al. 2008; B. Y. Chung et al. 2009; Oh et al. 2014).

We suggest that a sleep homeostat effector, *23E10*+ dFB neurons, also influences circadian-regulated locomotor activity through *hugin*+ circadian output neurons. Previously, we showed that a circuit from s-LNvs → DN1 → *Dh44*+ neurons → *hugin*+ neurons controls locomotor activity rhythms. *hugin*+ neurons are locomotor activity-promoting, especially during the evening (day-to-night transition) peak of activity (Cavanaugh et al. 2014; King et al. 2017). Our data suggest the *23E10*+ sleep-promoting dFB neurons inhibit *hugin*+ activity-promoting neurons. One, the sleep-promoting effect of *23E10*+ dFB neurons is enhanced during the daytime when the *hugin*+ neurons are removed. Second, neuronal activity of *hugin*+ neurons is suppressed with sleep deprivation, while dFB neurons become more active after sleep deprivation (Donlea, Pimentel, and Miesenbock 2014). In our behavior experiments, we find that

activating *hugin+* neurons during a period of heat-induced sleep loss leads to less recovery sleep. More experiments are required to explore this idea, but perhaps during sleep deprivation, the homeostat not only generates sleep drive but also actively disengages activity-promoting circuits.

In *Drosophila,* there is limited previous evidence for influences of sleep homeostatic mechanisms on the circadian system. As we previously introduced, in rodents, sleep deprivation affects circadian functions. Sleep deprivation reduces electrical activity of SCN neurons to approximately 60% of baseline activity, and the suppression lasts for 7 hours (Deboer, Détári, and Meijer 2007). We find a similar effect in flies, where neuronal activity is depressed in LNv central clock neurons and remained depressed even 5 hours after the deprivation ended (data not shown). In the rodent model, the mechanism mediating the reduced SCN activity is not clear but may involve serotonin signaling from the raphe dorsalis (Deboer 2018). Importantly, sleep deprivation does not appear to affect the core clock mechanism in the rodent SCN (Curie et al. 2015), and in flies, sleep deprivation does not shift the phase of the rest:activity rhythm in freerunning conditions, suggesting that the clock is unperturbed (Hendricks et al. 2001). Therefore, sleep homeostasis appears to influence primarily clock outputs.

Acknowledgements

Stocks from the Bloomington Drosophila Stock Center (NIH P40OD018537) were used in this study. We thank Drs. Gilad Barnea, Jing Wang, Leslie Griffith, Gerald Rubin, and Scott Waddell for generously providing fly lines. The work was supported by NIH R37NS048471 (to A.S.). A.N.K. was supported in part by NIH T32GM008216 and F31NS100395.

Author Contributions

Conceptualization, A.N.K. and A.S.; Methodology, A.N.K. and A.S.; Investigation, A.N.K.; Formal Analysis, A.N.K.; Writing – Original Draft, A.N.K. and A.S.; Supervision, A.S.

Figures

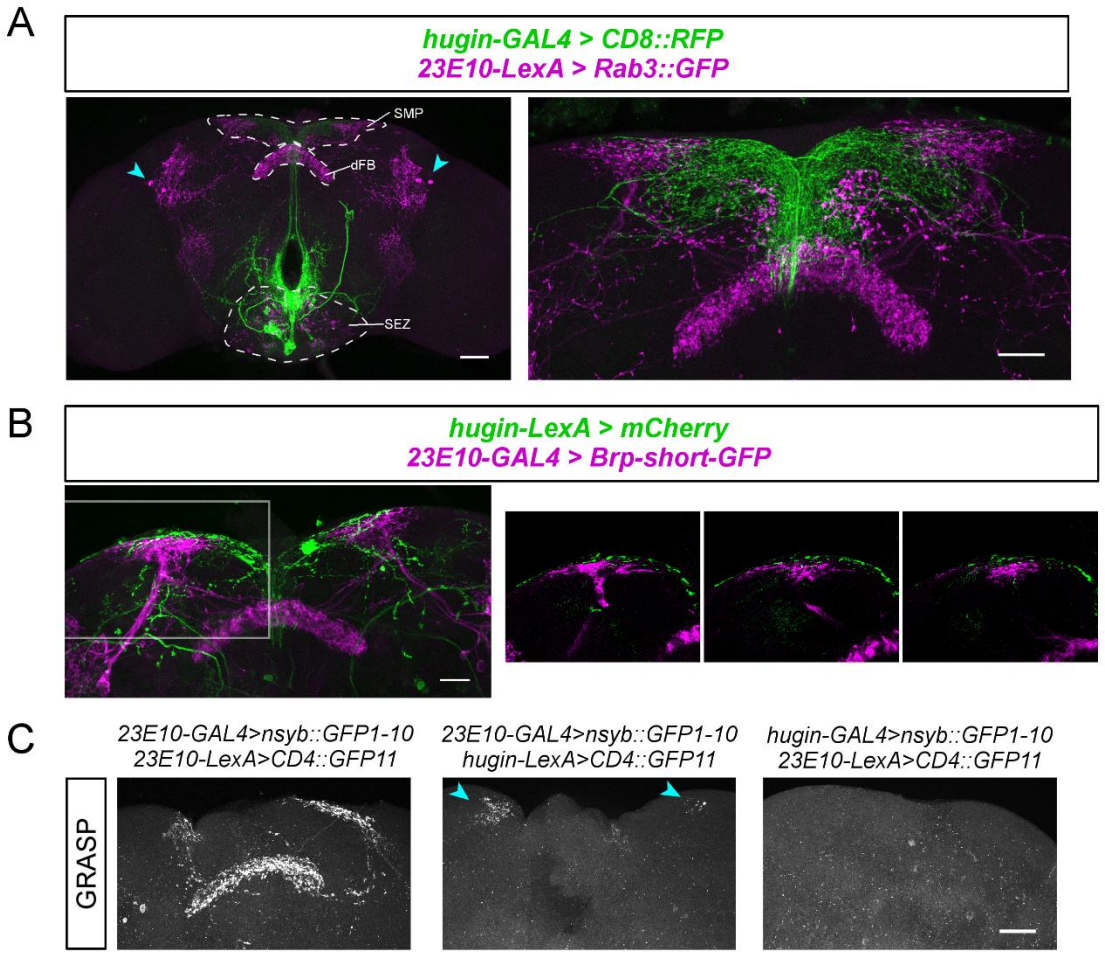

Figure 4.1

Sleep-promoting dFB (dorsal fan-shaped body) neurons contact *hugin*+ circadian output neurons.

(A) Co-labeling of *hugin*+ neurons with membrane marker (green) and *23E10*+ dFB neurons with RAB3::GFP, a presynaptic marker (magenta). The left image shows co-labeling of neurons in the whole fly brain; arrowheads indicate *23E10*+ cell bodies. Superior medial protocerebrum (SMP), dorsal fan-shaped body (dFB), and subesophageal zone (SEZ) regions are labeled. The right image shows the dorsal protocerebrum, where *hugin*+ projections intermingle with *23E10*+ projections in the SMP. **(B)** Co-labeling of *hugin*+ neurons with membrane marker (green) and *23E10*+ dFB neurons with BRP-short^{GFP}, a presynaptic marker (magenta). The left image shows

co-labeling of neurons in the dorsal brain. The right series of images show single confocal sections of the region indicated by white box, where *hugin*+ projections intermingle with *23E10*+ projections in the SMP. **(C)** Synaptic nSyb::spGFP1-10 is expressed in presynaptic neurons and complementary spGFP11 expressed in putative postsynaptic neurons. GFP reconstitution occurs only if synaptic connectivity exists. C, Left: When both nSyb::spGFP1-10 and spGFP11 is expressed in *23E10*+ dFB neurons, GFP reconstitution occurs in the dFB and SMP. C, Middle: Cyan arrowheads point to the GFP reconstitution in the SMP when nSyb::spGFP1-10 is expressed in *23E10*+ dFB neurons and spGFP11 is expressed in *hugin*+ neurons. C, Right: No GFP reconstitution when nSyb::spGFP1-10 is expressed in *hugin*+ neurons and spGFP11 is expressed in *23E10*+ dFB neurons. Scale bars, A(left): 50 µm; A(right), B, C: 25 µm.

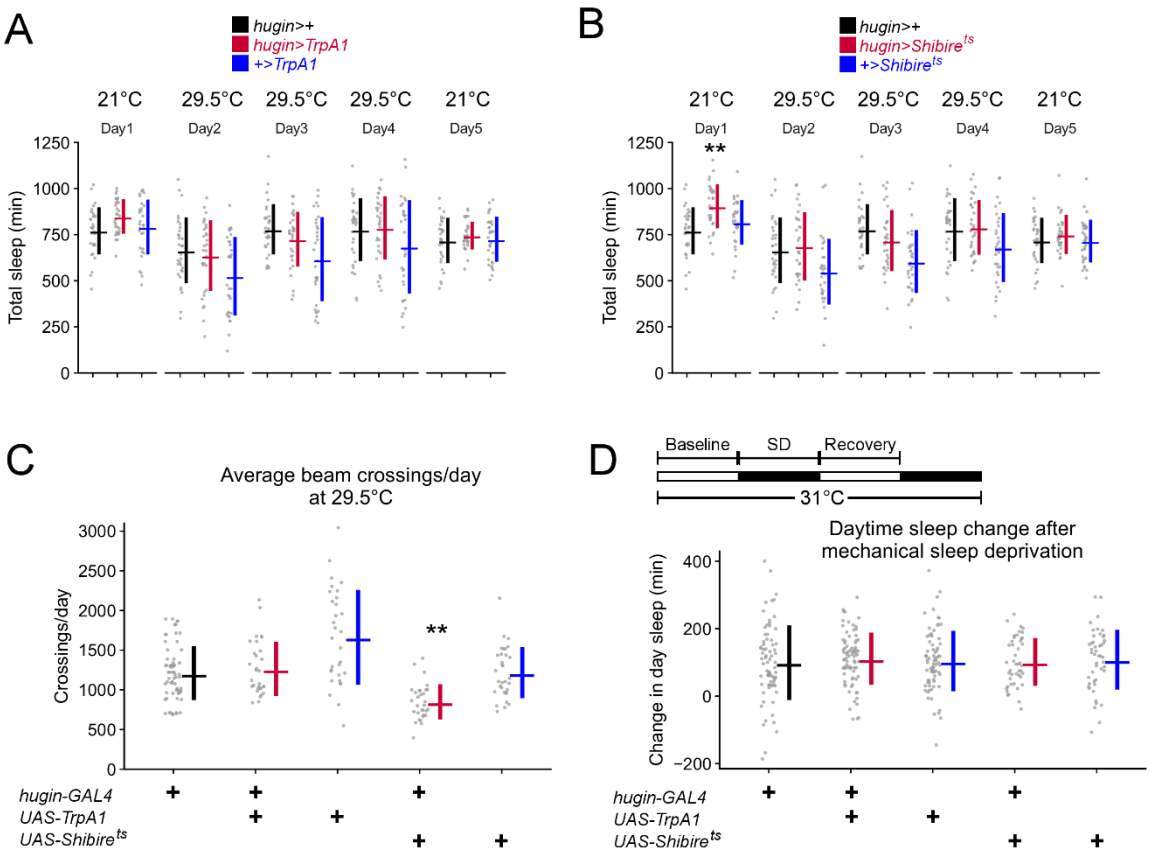

Figure 4.2

Disrupting activity of *hugin*+ neurons does not alter normal sleep amount or recovery after mechanical sleep deprivation.

(A) Thermogenetic activation of *hugin*+ neurons does not alter total amount of sleep. **(B)** Thermogenetic inhibition of synaptic transmission from *hugin*+ neurons does not alter total amount of sleep. Data for *hugin*>+ control are shared between panels A and B. **(C)** Blocking synaptic transmission in *hugin*+ neurons reduces the number of beaming crossing, a measure of locomotor activity. **(D)** Thermogenetic activation or inhibition of *hugin*+ neurons does not alter sleep recovery after mechanical sleep deprivation. Experimental setup: Flies were kept at 31°C for the entire duration of experiment. Flies were sleep deprived (SD) by mechanical shaking during the nighttime on day 1 and allowed to recover during the daytime on day 2. Change in day sleep was based upon sleep during 12 hours of the Recovery day and 12 hours of Baseline day. **p<0.01 by Tukey's test after one-way ANOVA. Circles are individual fly data points, and summary statistics displayed as mean ± SD.

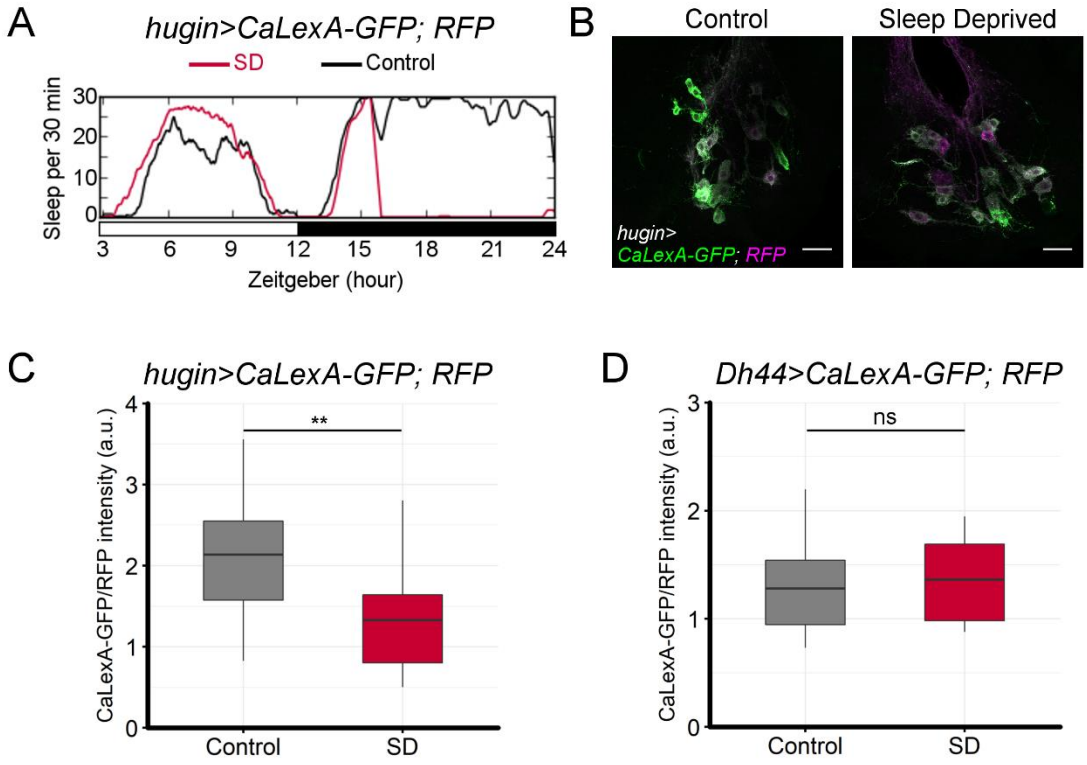

Figure 4.3

Ca^{2+} levels of *hugin*+ neurons are suppressed with sleep deprivation.

(A) Sleep profiles of *hugin>CaLexA-GFP; RFP* flies subjected to no sleep deprivation (Control, black, n = 8 flies) or 9-hr sleep deprivation (SD, red, *n* = 8 flies). Sleep graphed as minutes per 30-minute bin over 21 hours. **(B)** Representative images show GFP reporting Ca^{2+} levels via CaLexA system and RFP normalizer signals in *hugin>CaLexA-GFP; RFP* fly from Control or SD groups. Max intensity projection images show *hugin*+ neurons in subesophageal zone. Scale bar, 25 µm. **(C)** Tukey's boxplot comparing relative levels of GFP signal normalized to RFP signal in *hugin*+ cell bodies from Control (*n* = 21 flies) and SD (*n* = 18 flies) groups. **p = 0.00116, Welch's *t*-test. **(D)** Tukey's boxplot comparing relative levels of GFP signal normalized to RFP signal in *Dh44*+ cell bodies from Control (*n* = 11 flies) and SD (*n* = 18 flies) groups. n.s., p = 0.818 by Welch's *t*-test.

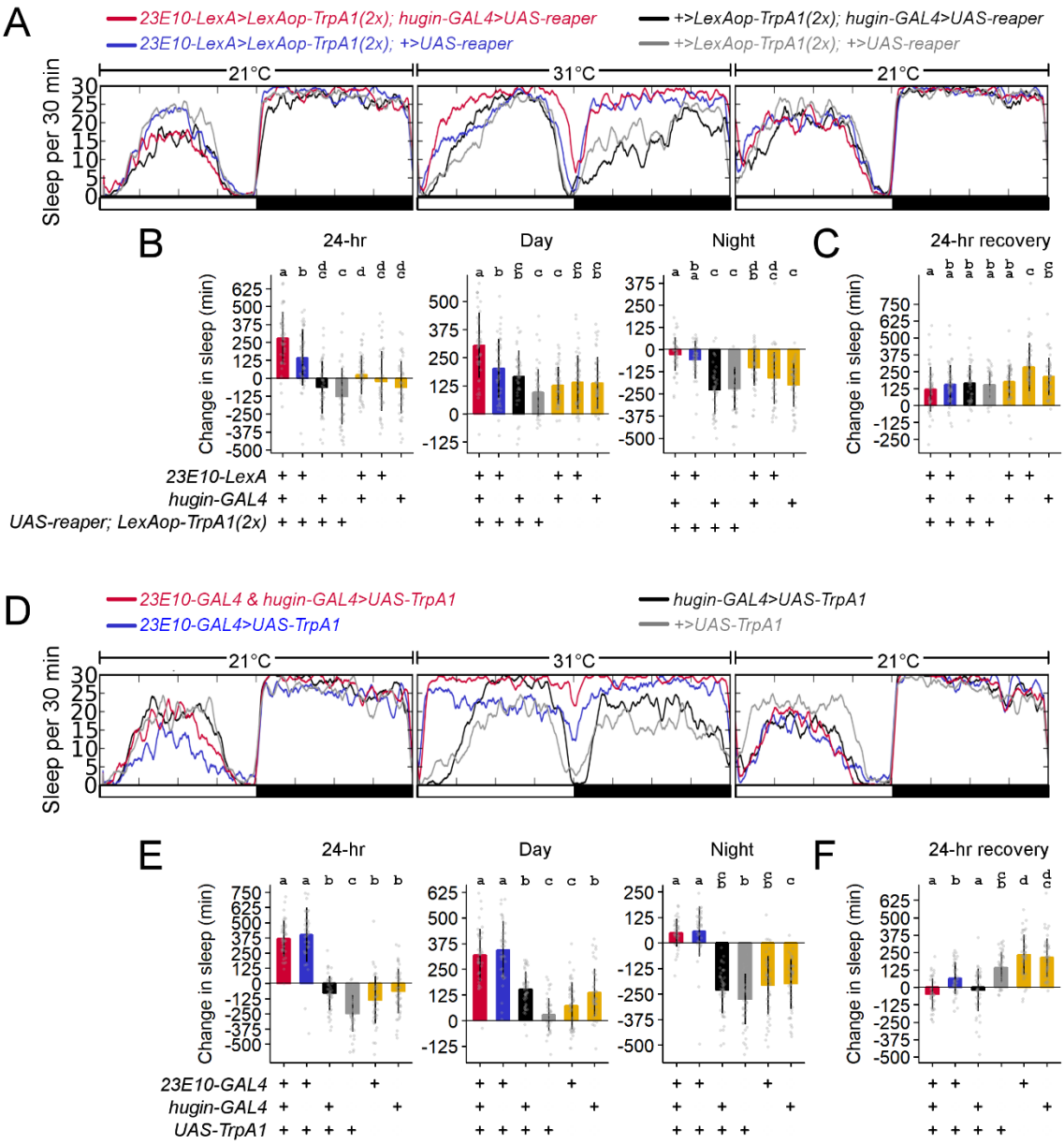

Figure 4.4

***hugin*+ neurons are effectors of *23E10*+ sleep-promoting dFB neurons.**

(A) *23E10*+ dFB neurons activated with *TrpA1* in flies with ablated *hugin*+ neurons using *reaper*. Sleep graphed as minutes per 30-minute bin over 3 days (A representative experiment is shown with *n* = 14 or 16 flies/genotype). Experimental setup: Baseline sleep at 21°C was monitored on day 1. A temperature shift from 21°C to 31°C occurred at ZT0 on day 2 to measure sleep gain from *23E10*+ activation. A temperature shift from 31°C to 21°C occurred at ZT0 on day 3 to

measure sleep recovery after heat-induced nighttime sleep loss. **(B)** *23E10*+ dFB neurons activated with *TrpA1* in flies where *hugin*+ neurons were ablated using *reaper*. Changes in sleep amount between Day 1 of baseline and Day 2 of *23E10*+ activation are shown. **(C)** *23E10*+ dFB neurons activated with *TrpA1* in flies where *hugin*+ neurons were ablated using *reaper*. Changes in sleep amount between Day 1 of baseline and Day 3 of recovery from heat-induced nighttime sleep loss are shown. **(D)** Simultaneous activation of *23E10*+ dFB neurons and *hugin*+ neurons with *TrpA1* (a representative is experiment shown with *n* = 11-16 flies/genotype). Experimental setup is as described for panel A. **(E)** Simultaneous activation of *23E10*+ dFB neurons and *hugin*+ neurons with *TrpA1*. Changes in sleep amount between Day 1 of baseline and Day 2 of *23E10*+ activation are shown. **(F)** Simultaneous activation of *23E10*+ dFB neurons and *hugin*+ neurons with *TrpA1*. Changes in sleep amount between Day 1 of baseline and Day 3 of recovery from heat-induced nighttime sleep loss are shown. For panels B, C, E, F: Means compared with one-way ANOVA and Tukey's test. Means sharing the same letter are not significantly different from each other ($P > 0.05$, Tukey's test). Circles are individual fly data points, and summary statistics are displayed as mean $\pm$ SD.

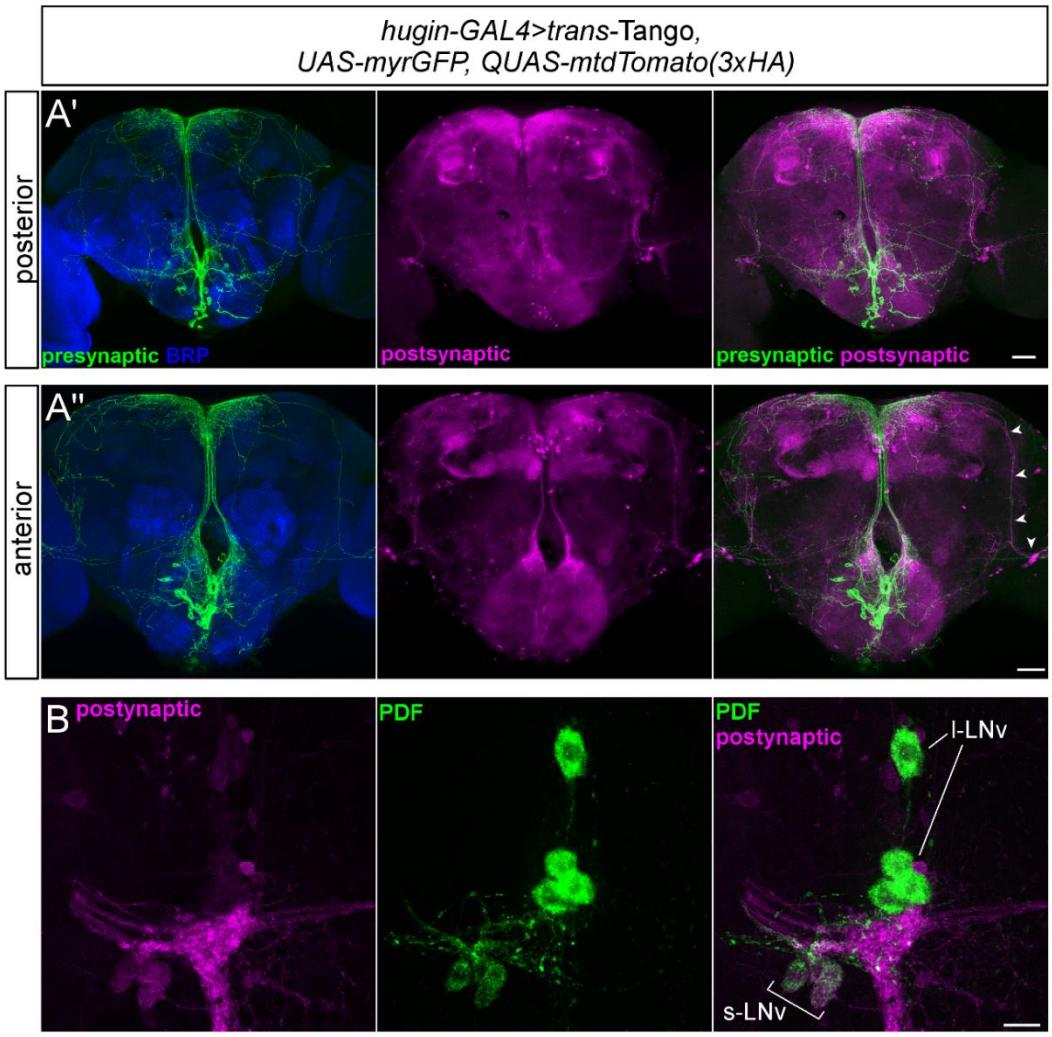

Figure 4.5

***hugin*+ neurons target PDF-expressing clock neurons.**

(A) *trans*-Tango ligand is expressed in *hugin*+ neurons (green). *trans*-Tango system reveals the synaptic partners (magenta) of *hugin*+ neurons in the brain. Panel A' image is a max intensity projection from the posterior side. Panel A'' image is a max intensity projection from the anterior side, and arrowheads indicates postsynaptic signal that resembles the projections of PDF+ neurons. Neuropil counterstained with anti-BRP (blue). **(B)** Co-labeling of PDF peptide (green) and postsynaptic signal (magenta) in flies with *trans*-Tango ligand expressed in *hugin*+ neurons. PDF+ s-LNvs are postsynaptic to *hugin*+ neurons. s-LNv, small ventrolateral neurons, l-LNv, large ventrolateral neurons. Scale bars, A: 50 μm; B: 15 μm.

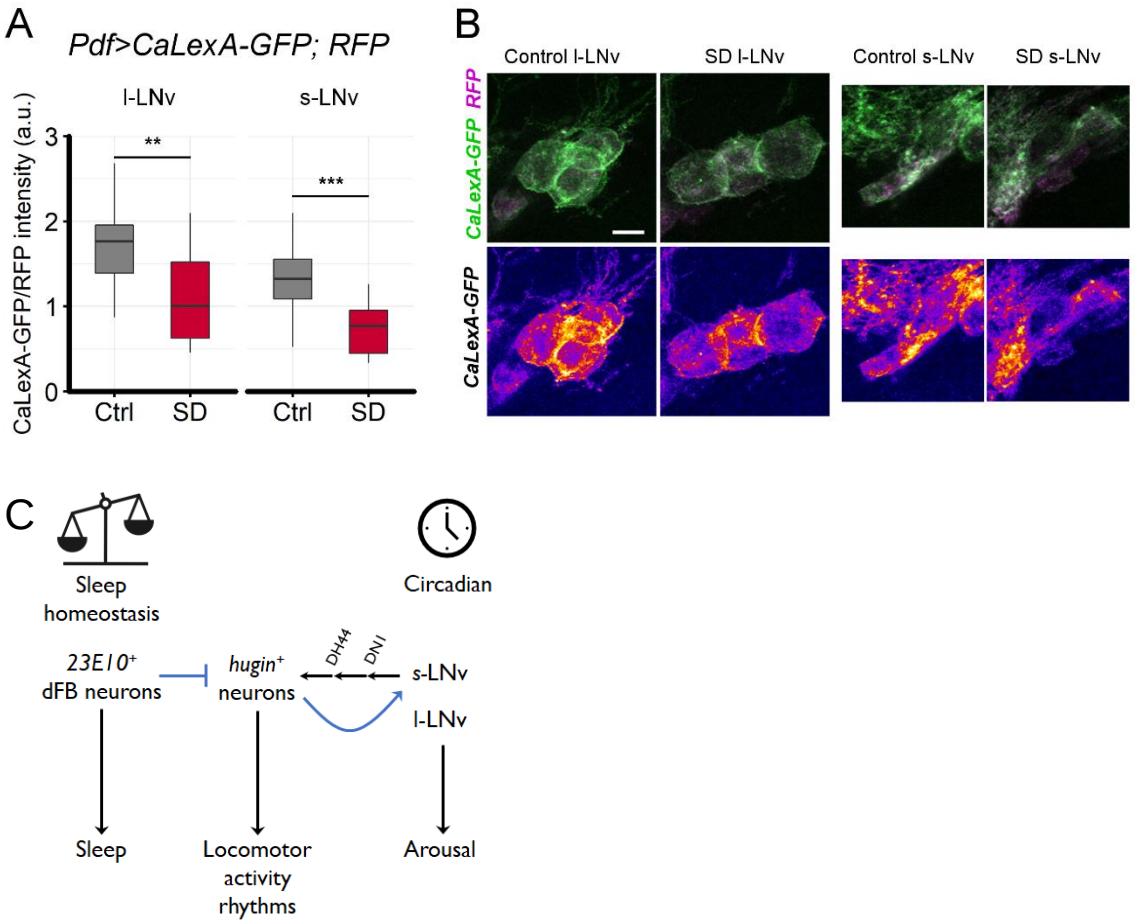

Figure 4.6

Ca^{2+} levels of *Pdf*-expressing clock neurons are suppressed with sleep deprivation.

(A) *Pdf>CaLexA-GFP; RFP* flies were subjected to no sleep deprivation (Ctrl, gray) or 9-hr sleep deprivation (SD, red). Tukey's boxplot compares relative levels of GFP signal normalized to RFP signal in cell bodies of *Pdf*+ large ventrolateral neurons (l-LNv) or small ventrolateral (s-LNv) from Control (*n* = 18 flies) and SD (*n* = 19 flies) groups. **p = 0.00910, ***p = 0.000655 by Welch's *t*-test. **(B)** Representative images of l-LNvs or s-LNvs from a *Pdf>CaLexA-GFP; RFP* fly in Control or SD group. Top row shows merged images of GFP signal reporting Ca^{2+} levels with CaLexA system and RFP normalizer signal. Bottom row shows "Fire" pseudocolor image of CaLexA-GFP signal (blue/purple=low intensity and yellow/white=high intensity). Scale bar, 10 µm applies for all panels. **(C)** Proposed model for regulation of a circadian output circuit by sleep homeostatic drive**.** *23E10*+ dorsal fan-shaped body (dFB) neurons are effectors of a sleep homeostatic circuit and

promote sleep. During high sleep drive, the *23E10+* dFB neurons promote sleep and dampen the output activities of the circadian system through inhibiting *hugin+* circadian output neurons and LNv clock neurons.

Table 4.1

Fly genotypes used in the study.

Figure	Genotype
Figure 4.1	*w; 23E10-LexA/UAS-CD8::RFP; hugin-GAL4/LexAop-Rab3::GFP* *w; hugin-LexA/UAS-brp-short-GFP; 23E10-GAL4/LexAop-6xmCherry-HA* *w; 23E10-LexA/UAS-nSyb::GFP1-10, LexAop-CD4::GFP11; 23E10-GAL4/+* *w; hugin-LexA/UAS-nSyb::GFP1-10, LexAop-CD4::GFP11; 23E10-GAL4/+* *w; 23E10-LexA/UAS-nSyb::GFP1-10, LexAop-CD4::GFP11; hugin-GAL4/+*
Figure 4.2	*w; UAS-TrpA1/+; hugin-GAL4/+* *w;; UAS-shibire^{ts}/hugin-GAL4*
Figure 4.3	*w, UAS-reaper/w; 23E10-LexA/LexAop-TrpA1; hugin-GAL4/LexAop-TrpA1* *w, UAS-reaper/w; 23E10-LexA/LexAop-TrpA1; +/LexAop-TrpA1* *w, UAS-reaper/w; +/LexAop-TrpA1; hugin-GAL4/LexAop-TrpA1* *w, UAS-reaper/w; +/LexAop-TrpA1; +/LexAop-TrpA1* *w; 23E10-LexA/+; hugin-GAL4/+* *w; 23E10-LexA/+; +* *w;; hugin-GAL4/+* *w; UAS-TrpA1/+; hugin-GAL4/23E10-GAL4* *w; UAS-TrpA1/+; 23E10-GAL4/+* *w; UAS-TrpA1/+; hugin-GAL4/+* *w; UAS-TrpA1/+* *w;; 23E10-GAL4/+*
Figure 4.4	*w; UAS-CD8::RFP, LexAop-CD8::GFP-2A-CD8::GFP/+; hugin-GAL4/UAS-mLexA-VP16-NFAT, LexAop-CD2::GFP* *w; UAS-CD8::RFP, LexAop-CD8::GFP-2A-CD8::GFP/+; Dh44-GAL4/UAS-mLexA-VP16-NFAT, LexAop-CD2::GFP*
Figure 4.5	*w,UAS-myrGFP.QUAS-mtdTomato(3xHA)/w; trans-Tango/+; hugin-GAL4*
Figure 4.6	*w; UAS-CD8::RFP, LexAop-CD8::GFP-2A-CD8::GFP/pdf-GAL4; UAS-mLexA-VP16-NFAT, LexAop-CD2::GFP/+*

Chapter 5 : Conclusions and Future Directions:

My central thesis question is: “How are molecular oscillations of the clock translated into rhythms of behavior and physiology”. The molecular basis of circadian rhythms has been extensively studied, but relatively little is known about the neural basis of circadian rhythms. There is considerable interest in studying the neural basis of circadian rhythms in flies, given that only about 150 brain neurons that express molecular clocks are collectively responsible for timekeeping. For many years, research was primarily focused on clock neurons, and the targets of clock neurons were unknown. As a result, we did not understand how time-of-day information is transmitted from the clock network to output circuits. To address this question, I set out to identify genes, neurons, and circuits that are downstream of the clock network and regulate circadian rhythms (summarized in Figure 5.1). In my thesis work, I studied the neural basis of peripheral transcriptional rhythms and behavioral rhythms.

Transcriptional rhythms in a peripheral tissue

Circadian clocks and transcriptional rhythms are numerous and prevalent throughout the body. In both mammals and flies, the central clock (i.e. brain clock) is considered the primary clock that drives circadian rhythms and coordinates oscillations of secondary clocks in peripheral tissues. In flies, the central clock has a dominant role under freerunning conditions over clocks in the fat body or prothoracic gland (Erion et al. 2016; Selcho et al. 2017; Myers, Yu, and Sehgal 2003). However, the central clock not only influences peripheral clocks but also peripheral output rhythms, such as transcription. Understanding how the central clock communicates with peripheral tissues is a significant question in the field. In Chapter 2, we used flies to study the mechanisms by which the central clock influences rhythms in peripheral tissues. This work was prompted by the finding that some transcriptional rhythms in the fat body depend upon clocks in other tissues. To identify the drivers of these fat body transcriptional rhythms that are independent of the local clock, we assayed for a role of brain clock neurons. We found that molecular clocks in LNds drive transcriptional rhythms of cytochrome P450 genes, *Cyp6a21* and

sxe1 (as known as *Cyp4d21*), in the fat body. Furthermore, we found signaling of NPF, a neuropeptide expressed in LNd, drives transcriptional rhythms of *Cyp6a21* and *sxe1*. Finally, we identified a similar mechanism in mice, where NPY (the NPF homolog) is required for rhythmic expression of a subset of liver genes, in particular those of the cytochrome P450 family. Our work is a start at addressing how central clocks influence peripheral transcriptional rhythms. It is likely that the brain communicates to peripheral tissue using endocrine signaling mechanisms, and NPF is probably not the hormone that directly signals to the peripheral tissue, since NPF+ LNds arborize exclusively within the brain and NPF receptors are not found in the fat body. Therefore, future studies are needed to identify the neuroendocrine signal between the brain and fat body, as well as the circuit between the LNds and the neuroendocrine center (target of NPF action).

In addition to neural clocks, feeding influences circadian rhythms in metabolic tissues. Indeed, restricted feeding schedules drive cycling of some fat body genes in *Drosophila* and some liver genes in mice (Vollmers et al. 2009; Xu et al. 2011). It is possible that LNd clocks and NPF signaling drive behavioral rhythms of feeding, which then drive transcriptional rhythms in the fat body. While we have not tested if LNds are involved in feeding rhythms, feeding alone cannot drive the normal robust rhythmic expression of *Cyp6a21* and *sxe1* in the fat body. Time-restricted feeding does not drive *Cyp6a21* cycling in clockless mutants to the extent seen in wild type flies (Xu et al. 2011), and flies display similar *sxe1* cycling regardless of whether feeding was time-restricted or ab libitum (Gill et al. 2015). However, the question remains unanswered: how much of the fat body transcriptome is shaped by feeding, the central clock, or a combination of both?

Our work supports the idea that the circadian system is hierarchical, with the central clock orchestrating peripheral clocks (Albrecht 2012). We showed that the fat body clock does not rely upon the central clock in the presence of light:dark cycles, presumably because it has its own photoreceptors, but it is sensitive to the loss of the central clock under freerunning conditions. A similar situation occurs in mice; under freerunning conditions, the central clock is required for synchronous and high amplitude clock oscillations in peripheral tissues (Izumo et al. 2014). Notably, peripheral tissues in mammals do not express photoreceptors, so their entrainment to

light is driven entirely by the central clock. In addition, peripheral clocks may need to be coupled to the central clock so that the peripheral clock can reset to changes in behavioral rhythms. Because of this hierarchical system, all peripheral output rhythm, to varying extents are coupled to the central clock. This leads to the question: why are some cycling genes independent of the local clock and instead tightly coupled to the central clock? In our study, we looked at *Cyp6a21* and *sxe1*, which both belong to the cytochrome P450 gene family of detoxification enzymes (H. Chung et al. 2009). While we did not test the importance for *Cyp6a21* and *sxe1* cycling for metabolic function, we speculate that coupling of detoxification rhythms with feeding behavioral rhythms is advantageous, as it allows detoxification enzymes to be expressed in anticipation of feeding rather than as a response to feeding. Understanding how the neural circuits for metabolic rhythms and behavioral rhythms intersect is another future direction of study.

Neural basis for behavioral rhythms: beyond the circadian clock network

In Chapter 3, I studied the neural basis of rest:activity rhythms (i.e. locomotor activity rhythms). Locomotor activity is the most used behavioral output to study the molecular and neural basis of circadian rhythms in flies. Since the identification of the clock neurons, researchers have speculated about the targets of clock neurons, but it was only recently that we have mapped a circadian output circuit. Previous work in the Sehgal lab demonstrated that *Dh44*+ and *SIFa*+ neurons are circadian output neurons for rest:activity rhythms. In my thesis work, I extended the circuit from *Dh44*+ neurons to *hugin*+ neurons and motor circuits in the ventral nerve cord. Our work only provides a minimal pathway, and more circuits need to be mapped to fully explain rhythmic rest:activity behavior. To my knowledge, our work is the first account of a continuous linear pathway from clock neurons to neurons involved in locomotive behavior. A first step in the field, the circuit that we have mapped provides a framework for future studies to address other questions, such as how different behavioral rhythms are coordinated at the circuit level, what neurotransmitters function in a circadian output circuit, what neurotransmitters and molecular mechanisms generate cycling of neuronal activity in a circadian output circuit, and how is cycling

of neuronal activity coordinated across a circadian output circuit? I explore these questions in more depth in the following paragraphs.

Locomotor activity is a robust and easy behavior to monitor, which allows us to effectively map circuits involved in locomotor activity rhythms. Since locomotor activity is influenced by many other behaviors, does the circuit we have mapped regulate timing of locomotor activity in general or a specific behavior? We showed that *hugin*+ neurons regulate locomotor activity rhythms but do not affect feeding/drinking bout rhythms. Is there a shared circadian output circuit for timekeeping, or are there rather dedicated output circuits for each behavior? Compared to rest:activity rhythms, relatively less is known about the neural basis of feeding rhythms or courtship rhythms (Xu, Zheng, and Sehgal 2008; Sakai and Ishida 2001). Courtship rhythms may share a similar initial circuit as locomotor activity rhythms. Male-sex drive rhythms are locomotor patterns of courtship that appear in co-housed female and male flies. Like solitary locomotor activity rhythms, male sex-driven rhythms depend on LNv and DN1 clocks in males. However, altering DN1s has different effects on solitary rhythms and locomotor rhythms in male sex-drive, suggesting that different output circuits regulate solitary locomotor activity rhythms and courtship rhythms (Fujii and Amrein 2010).

Informative circuit maps require the identification of not only the neurons but also the neurotransmitters. Neuropeptides play a prominent role in circadian biology, and our work adds DH44 and Hugin to a list of neuropeptides involved in circadian behavior, which include Leucokinin, an output molecule for rest:activity rhythms, PTTH, an output molecule for eclosion rhythms, and ITP, sNPF, NPF, and PDF, molecules that synchronize the clock network (Cavey et al. 2016; Selcho et al. 2017; Hermann et al. 2012; Hermann-Luibl et al. 2014; Yao and Shafer 2014). Unlike small molecule neurotransmitters, neuropeptides can signal by paracrine and endocrine mechanisms, both of which can affect multiple target sites. Neuropeptides also confer circuit flexibility and can modulate activity of neurons by affecting presynaptic and postsynaptic properties and intrinsic electrical properties. In addition, neuropeptides are often co-released with other neurotransmitters, such as bioaminergic and classical small-molecule neurotransmitters,

which adds additional circuit flexibility (Nusbaum, Blitz, and Marder 2017; Nässel 2018). However, bioaminergic and classical small-molecule neurotransmitters are not well-studied in *Drosophila* circadian output circuits. In the clock network, glutamate and glycine have been identified as small-molecule neurotransmitters that regulate rest:activity rhythms (Collins et al. 2012; Hamasaka et al. 2007; Guo et al. 2016; Frenkel et al. 2017). The s-LNvs co-release PDF and an unknown classical neurotransmitter to promote the morning peak of locomotor activity (Choi et al. 2012); the s-LNv neurotransmitter may be glycine (Frenkel et al. 2017). DN1ps use glutamate and DH31 to influence different postsynaptic target neurons and regulate sleep (Kunst et al. 2014; Guo et al. 2016); although, it has not been demonstrated that a single DN1p cell co-expresses both DH31 and glutamate. Outside the clock network, co-transmitters are likely expressed in peptidergic circadian output neurons but have not been investigated. Loss of *Dh44* or either DH44 receptor (*Dh44-R1*/*Dh44-R2*) does not completely phenocopy *Dh44*+ neuronal ablation. In *Dh44-R1* mutants, activation of *Dh44*+ neurons still produces a delayed Ca^{2+} response in *hugin*+ neurons. These data suggest that other co-transmitters in *Dh44*+ neurons are involved in the circadian output circuit, although, it is possible the co-transmitters are other neuropeptides. In larva, *hugin*+ neurons also use acetylcholine as a key transmitter, but whether acetylcholine is maintained in adults is unknown (Schlegel et al. 2016). While we have identified multisynaptic circuits, we have yet to identify all the neurotransmitters that the circuits use to regulate rest:activity rhythms.

Circuit mapping can only take us so far in explaining how rhythmic behavior is generated. The next steps are to determine what drives activity in the neurons of a circuit, how are signals processed through a circuit, and why the physiological activity of neurons is a useful correlate for behavior (Olsen and Wilson 2008). While the last question is challenging to address, the field may be able to address the first two questions. In circadian circuits, cycling of neuronal activity across the 24-hour day is a general output mechanism that is dependent on the circadian clock (reviewed in Chapter 1 and Table 1.1). Here, I broadly define neuronal activity. Neuronal activity can be electrical firing events but also include Ca^{2+} activity, cAMP activity, neuropeptide release,

response to a neurotransmitter, or structural synaptic remodeling. The output circuit that we have mapped appears to be no exception, and almost all known circadian output neurons exhibit cycling of one or more of these activities. I showed that *hugin*+ neurons exhibit time-of-day differences in neuropeptide vesicle release that is dependent on the molecular clock. *Lk*+ and *Dh44*+ circadian output neurons show cycling in intracellular Ca^{2+} levels, and *Dilp2*+ neurons have time-of-day differences in firing frequency and burst firing (Cavey et al. 2016; Barber et al. 2016). While circadian cycling of activity has been demonstrated in output neurons, we do not understand how cycling is generated and maintained in output neurons. Since every clock neuron has a 24-hour molecular oscillator, it is assumed that the cell-autonomous clock drives cycling of neuronal activity (Flourakis et al. 2015), although, cycling of activity in some clock neurons may be shaped more by neuropeptide signaling than by the cell-autonomous clock mechanism (Liang, Holy, and Taghert 2017). Circadian output neurons do not have a canonical molecular clock and probably have cycling of activity shaped primarily through intercellular signals. Output neurons may also have rhythmically expressed ion channels, such as the potassium channel *slowpoke*, that regulate intrinsic currents (M. de la P. Fernández et al. 2007). Future studies will dissect the mechanisms that shape circadian cycles of activity in output neurons.

Fluorescence-based activity sensors or readouts are instrumental tools for studying circadian cycles of activity in circuits. In the field, circadian cycling of neuronal activity is mostly determined by sampling time points from groups of flies (our studies included). However, I recognize the challenges in interpreting circadian rhythms using fluorescence-based activity sensors and time point sampling. First, without normalization, it is not useful to compare fluorescence-based readouts of activity between samples. Second, there are likely differences in baseline levels of activity and/or fluorescent intensity between samples, and population sampling can dampen any rhythm. Third, the time resolution is important for determining precise peak of activity cycling, and time point analyses of appropriate resolution requires a lot of work. However, with advances in fluorescent microscopy for live imaging, the field would benefit from performing 24-hr continuous recording of circuit activity in a single animal (Liang, Holy, and Taghert 2016).

Continuous data collection addresses many of the challenges of time point sampling. In addition, longitudinal imaging will be useful to study the molecular or intercellular signaling mechanisms that generate cycling of activity in non-clock neurons. In addition, the field would may benefit from network-wide recording, since behavior is a result of activity in a network of neurons. In the future, once we have identified more circadian output circuits, we may study how cycling of neural activity is processed through a circuit and coordinated across a network of circadian neurons.

Neural basis of sleep regulation: interactions between the homeostat and circadian clock

Sleep is another area of study that benefited from the circuit-mapping approaches I described above. In its simple form, sleep regulation involves a clock and a homeostatic component (Borbély et al. 2016). Over the years, researchers have identified neurons and circuits for sleep regulation in the fly brain. Many if not all clock neurons regulate sleep at specific times of day (Sheeba, Fogle, et al. 2008; Parisky et al. 2008; Shang, Griffith, and Rosbash 2008; Guo et al. 2016; Kunst et al. 2014; S. Liu et al. 2014). While some studies point to possible effectors, the downstream circuits that mediate circadian-gated sleep effects still need to be mapped out (Cavanaugh et al. 2016; J. Chen et al. 2016). Cavanaugh et al. 2016 identified neurons whose activation effectively increases sleep during the middle of the day and night but not during the day-to-night transition. These time-of-day effects are clock-dependent, as a clock mutant showed similar increases at all times. While the clock neurons involved were not mapped, the work suggests that the circadian system acts upstream of the sleep-promoting neurons to prevent premature sleep onset in the evening, even when sleep drive is high. Chen et al. showed that activation of Allatostatin A+ (AstA) neurons increases sleep, and PDF from LNv clock neurons partially mediates the sleep-promoting effects. Expression of membrane-tethered PDF in AstA+ neurons slightly increases sleep. Interestingly, PDF neuropeptide in the LNv to AstA circuit is thought to increase sleep, but loss of PDF (in null mutants) also increases sleep (Parisky et al. 2008). This discrepancy may be due to time-of-day specific actions of PDF and downstream PDF signaling mechanisms.

Remarkably, there has been rapid progress in mapping multisynaptic circuits that regulate sleep homeostasis, promote sleep and/or inhibit waking when sleep pressure is high (Donlea, Pimentel, and Miesenbock 2014; Donlea et al. 2018; Q. Liu et al. 2012; Ueno et al. 2012; S. Liu et al. 2016; Haynes, Christmann, and Griffith 2015; Seidner et al. 2015; Oh et al. 2014). Circadian and homeostatic sleep circuits have largely been studied independently, and my final piece of work aims to understand how the two types of circuits interact to generate sleep:wake cycles.

In Chapter 3, I identified an output circuit that regulates locomotor activity rhythms, primarily by promoting locomotor activity during the evening. The *Dh44-Hugin* circuit does not appear to regulate baseline sleep, because ablation of *Dh44*+ or *hugin*+ neurons does not affect sleep amount (Cavanaugh et al. 2014). In Chapter 4, I found that *hugin*+ circadian output neurons also receive sleep homeostatic information. Sleep deprivation alters the Ca^{2+} levels in at least two nodes in the circadian output circuit: *hugin*+ neurons and LNv clock neurons. I hypothesize that the homeostatic component directly dampens the activity-promoting effects of the circadian output circuit. While I did not test the effect of sleep deprivation on all known circadian circuits, sleep deprivation does not affect the Ca^{2+} activity of *Dh44*+ circadian output neurons, suggesting some specificity to how sleep homeostasis modulates circadian output circuits. DN1ps are another node of the circadian output circuit and comprised of both sleep-promoting and activity-promoting neurons. It would be interesting to determine if sleep deprivation affects sleep-promoting and activity-promoting clock neurons differently.

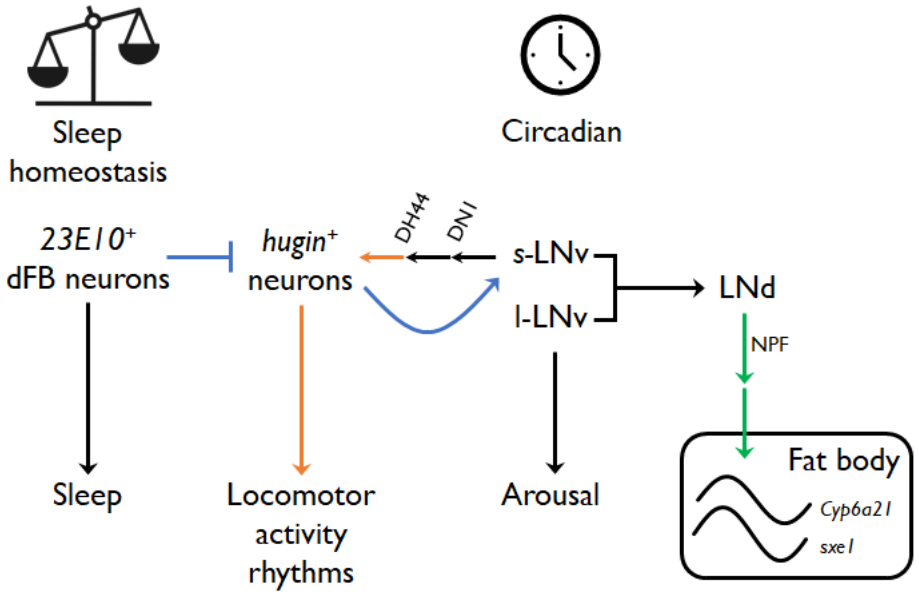

Figure 5.1

A schematic of circuits related to thesis work. Color coded circuits were identified in this thesis work. Green circuits: LNd clock neurons control transcriptional rhythms of cytochrome P450 genes, *sxe1* and *Cyp6a21* in the fat body through NPF signaling (Chapter 2). Orange circuits: *hugin*$^{+}$ circadian output neurons regulate locomotor activity rhythms and are downstream of the s-LNv → DN1 → *DH44*$^{+}$ circadian circuit. *hugin*$^{+}$ neurons project into the ventral nerve cord, where they can modulate locomotor circuits (Chapter 3). Blue circuits*:* *hugin*$^{+}$ neurons also receive signals from a group of sleep-promoting neurons (*23E10*$^{+}$ dFB). *hugin*$^{+}$ neurons modulate the sleep-promoting effects of dFB activation. *hugin*$^{+}$ neurons also feed back to the central clock neurons, s-LNvs (Chapter 4). Abbreviations: dFB (dorsal fan-shaped body neurons), DH44 (Diuretic hormone 44), DN1 (dorsal neuron group 1), LNd (dorsolateral neurons), l-LNv (large ventrolateral neurons), LNv (ventrolateral neurons), NPF (Neuropeptide F), s-LNv (small ventrolateral neurons), sxe1 (sex-specific enzyme 1, Cyp4d21).

Bibliography

Albrecht, Urs. 2012. “Timing to Perfection: The Biology of Central and Peripheral Circadian Clocks.” *Neuron* 74 (2): 246–60. doi:10.1016/j.neuron.2012.04.006.

Allada, Ravi, and Brian Y. Chung. 2010. “Circadian Organization of Behavior and Physiology in Drosophila.” *Annual Review of Physiology* 72 (January): 605–24. doi:10.1146/annurev-physiol-021909-135815.

Allada, Ravi, Neal E. White, W. Venus So, Jeffrey C. Hall, and Michael Rosbash. 1998. “A Mutant Drosophila Homolog of Mammalian Clock Disrupts Circadian Rhythms and Transcription of Period and Timeless.” *Cell* 93 (5): 791–804. doi:10.1016/S0092-8674(00)81440-3.

Arrese, Estela L., and Jose L. Soulages. 2010. “Insect Fat Body: Energy, Metabolism, and Regulation.” *Annual Review of Entomology* 55: 207–25. doi:10.1146/annurev-ento-112408-085356.

Artiushin, Gregory, and Amita Sehgal. 2017. “The Drosophila Circuitry of Sleep-Wake Regulation.” *Current Opinion in Neurobiology* 44 (June): 243–50. doi:10.1016/j.conb.2017.03.004.

Bai, Lei, Yool Lee, Cynthia T Hsu, Julie A Williams, Daniel Cavanaugh, Xiangzhong Zheng, Carly Stein, et al. 2018. “A Conserved Circadian Function for the Neurofibromatosis 1 Gene.” *Cell Reports* 22 (13). Elsevier: 3416–26. doi:10.1016/j.celrep.2018.03.014.

Baines, Richard A., Jay P. Uhler, Annemarie Thompson, Sean T. Sweeney, and Michael Bate. 2001. “Altered Electrical Properties in Drosophila Neurons Developing without Synaptic Transmission.” *J. Neurosci.* 21 (5): 1523–31.

Barber, Annika F., Renske Erion, Todd C Holmes, and Amita Sehgal. 2016. “Circadian and Feeding Cues Integrate to Drive Rhythms of Physiology in Drosophila Insulin-Producing Cells.” *Genes & Development* 30 (23). Cold Spring Harbor Laboratory Press: 2596–2606. doi:10.1101/gad.288258.116.

Beck, B. 2006. “Neuropeptide Y in Normal Eating and in Genetic and Dietary-Induced Obesity.” *Philosophical Transactions of the Royal Society of London. Series B, Biological Sciences* 361 (1471): 1159–85. doi:10.1098/rstb.2006.1855.

Beckwith, Esteban J, and M Fernanda Ceriani. 2015. “Communication between Circadian Clusters: The Key to a Plastic Network.” *FEBS Letters* 589 (22): 3336–42. doi:10.1016/j.febslet.2015.08.017.

Beshel, Jennifer, Josh Dubnau, and Yi Zhong. 2017. “A Leptin Analog Locally Produced in the Brain Acts via a Conserved Neural Circuit to Modulate Obesity-Linked Behaviors in Drosophila.” *Cell Metabolism* 25 (1): 208–17. doi:10.1016/j.cmet.2016.12.013.

Besing, Rachel C., Lauren M. Hablitz, Jodi R. Paul, Russell L. Johnson, Rebecca a. Prosser, and Karen L. Gamble. 2012. “Neuropeptide Y–Induced Phase Shifts of PER2::LUC Rhythms Are Mediated by Long-Term Suppression of Neuronal Excitability in a Phase-Specific Manner.” *Chronobiology International* 29 (2): 91–102. doi:10.3109/07420528.2011.649382.

Blanchard, Florence J, Ben Collins, Shawn A Cyran, Daniel H Hancock, Michael V Taylor, and Justin Blau. 2010. “The Transcription Factor Mef2 Is Required for Normal Circadian Behavior in Drosophila.” *The Journal of Neuroscience : The Official Journal of the Society for Neuroscience* 30 (17): 5855–65. doi:10.1523/JNEUROSCI.2688-09.2010.

Blau, Justin, and Michael W. Young. 1999. “Cycling Vrille Expression Is Required for a Functional Drosophila Clock.” *Cell* 99 (6): 661–71. doi:10.1016/S0092-8674(00)81554-8.

Borbély, Alexander A., Serge Daan, Anna Wirz-Justice, and Tom Deboer. 2016. “The Two-Process Model of Sleep Regulation: A Reappraisal.” *Journal of Sleep Research* 25 (2): 131–43. doi:10.1111/jsr.12371.

Bringmann, Henrik. 2018. “Sleep-Active Neurons: Conserved Motors of Sleep.” *Genetics* 208 (4). Genetics Society of America: 1279–89. doi:10.1534/genetics.117.300521.

Brown, Mark R., Joe W. Crim, Ryan C. Arata, Haini N. Cai, Cao Chun, and Ping Shen. 1999. “Identification of a Drosophila Brain-Gut Peptide Related to the Neuropeptide Y Family.” *Peptides* 20 (9): 1035–42. doi:10.1016/S0196-9781(99)00097-2.

Burke, Christopher J, Wolf Huetteroth, David Owald, Emmanuel Perisse, Michael J Krashes, Gaurav Das, Daryl Gohl, Marion Silies, Sarah Certel, and Scott Waddell. 2012. “Layered Reward Signalling through Octopamine and Dopamine in Drosophila.” *Nature* 492 (7429): 433–37. doi:10.1038/nature11614.

Bushey, Daniel, Giulio Tononi, and Chiara Cirelli. 2015. “Sleep- and Wake-Dependent Changes in Neuronal Activity and Reactivity Demonstrated in Fly Neurons Using in Vivo Calcium Imaging.” *Proceedings of the National Academy of Sciences of the United States of America* 112 (15): 4785–90. doi:10.1073/pnas.1419603112.

Cailotto, Cathy, Jun Lei, Jan van der Vliet, Caroline van Heijningen, Corbert G. van Eden, Andries Kalsbeek, Paul Pévet, and Ruud M. Buijs. 2009. “Effects of Nocturnal Light on (Clock) Gene Expression in Peripheral Organs: A Role for the Autonomic Innervation of the Liver.” *PLoS ONE* 4 (5): e5650. doi:10.1371/journal.pone.0005650.

Cannell, Elizabeth, Anthony J Dornan, Kenneth A Halberg, Selim Terhzaz, Julian A T Dow, and Shireen-A Davies. 2016. “The Corticotropin-Releasing Factor-like Diuretic Hormone 44 (DH44) and Kinin Neuropeptides Modulate Desiccation and Starvation Tolerance in Drosophila Melanogaster.” *Peptides* 80 (June): 96–107. doi:10.1016/j.peptides.2016.02.004.

Cao, Guan, and Michael N. Nitabach. 2008. “Circadian Control of Membrane Excitability in Drosophila Melanogaster Lateral Ventral Clock Neurons.” *The Journal of Neuroscience : The Official Journal of the Society for Neuroscience* 28 (25): 6493–6501. doi:10.1523/JNEUROSCI.1503-08.2008.

Cavanaugh, Daniel J., Jill D. Geratowski, Julian R. A. Wooltorton, Jennifer M. Spaethling, Clare E. Hector, Xiangzhong Zheng, Erik C. Johnson, James H. Eberwine, and Amita Sehgal. 2014. “Identification of a Circadian Output Circuit for Rest:Activity Rhythms in Drosophila.” *Cell* 157 (3). Elsevier Inc.: 689–701. doi:10.1016/j.cell.2014.02.024.

Cavanaugh, Daniel J, Abigail S Vigderman, Terry Dean, David S Garbe, and Amita Sehgal. 2016. “The Drosophila Circadian Clock Gates Sleep through Time-of-Day Dependent Modulation of Sleep-Promoting Neurons.” *Sleep* 39 (2): 345–56. doi:10.5665/sleep.5442.

Cavey, Matthieu, Ben Collins, Claire Bertet, and Justin Blau. 2016. “Circadian Rhythms in Neuronal Activity Propagate through Output Circuits.” *Nature Neuroscience* 19 (February 2016). Nature Publishing Group: 1–11. doi:10.1038/nn.4263.

Ceriani, M Fernanda, John B Hogenesch, Marcelo Yanovsky, Satchidananda Panda, Martin Straume, and Steve a Kay. 2002. “Genome-Wide Expression Analysis in Drosophila Reveals Genes Controlling Circadian Behavior.” *The Journal of Neuroscience : The Official Journal of the Society for Neuroscience* 22 (21): 9305–19. doi:22/21/9305 [pii].

Challet, E. 2015. “Keeping Circadian Time with Hormones.” *Diabetes, Obesity & Metabolism* 17 Suppl 1 (September): 76–83. doi:10.1111/dom.12516.

Challet, Etienne, Fred W Turek, Marie-Aline Laute, and Olivier Van Reeth. 2001. “Sleep Deprivation Decreases Phase-Shift Responses of Circadian Rhythms to Light in the Mouse:

Role of Serotonergic and Metabolic Signals." *Brain Research* 909 (1–2): 81–91. doi:10.1016/S0006-8993(01)02625-7.

Chen, Jiangtian, Wencke Reiher, Christiane Hermann-Luibl, Azza Sellami, Paola Cognigni, Shu Kondo, Charlotte Helfrich-Förster, Jan A. Veenstra, and Christian Wegener. 2016. "Allatostatin A Signalling in Drosophila Regulates Feeding and Sleep and Is Modulated by PDF." Edited by Paul H. Taghert. *PLOS Genetics* 12 (9): e1006346. doi:10.1371/journal.pgen.1006346.

Chen, Tsai-Wen, Trevor J. Wardill, Yi Sun, Stefan R. Pulver, Sabine L. Renninger, Amy Baohan, Eric R. Schreiter, et al. 2013. "Ultrasensitive Fluorescent Proteins for Imaging Neuronal Activity." *Nature* 499 (7458). Nature Research: 295–300. doi:10.1038/nature12354.

Chen, Yi, Orkun Akin, Aljoscha Nern, C Y Kimberly Tsui, Matthew Y Pecot, and S Lawrence Zipursky. 2014. "Cell-Type-Specific Labeling of Synapses in Vivo through Synaptic Tagging with Recombination." *Neuron* 81 (2): 280–93. doi:10.1016/j.neuron.2013.12.021.

Chiu, Cindy N., Jason Rihel, Daniel A. Lee, Chanpreet Singh, Eric A. Mosser, Shijia Chen, Viveca Sapin, et al. 2016. "A Zebrafish Genetic Screen Identifies Neuromedin U as a Regulator of Sleep/Wake States." *Neuron* 89 (4). Elsevier: 842–56. doi:10.1016/j.neuron.2016.01.007.

Choi, Charles, Guan Cao, Anne K Tanenhaus, Ellena V McCarthy, Misun Jung, William Schleyer, Yuhua Shang, Michael Rosbash, Jerry C P Yin, and Michael N. Nitabach. 2012. "Autoreceptor Control of Peptide/Neurotransmitter Corelease from PDF Neurons Determines Allocation of Circadian Activity in Drosophila." *Cell Reports* 2 (2): 332–44. doi:10.1016/j.celrep.2012.06.021.

Choi, Charles, Jean-Philippe Fortin, Ellena V McCarthy, Lea Oksman, Alan S Kopin, and Michael N. Nitabach. 2009. "Cellular Dissection of Circadian Peptide Signals with Genetically Encoded Membrane-Tethered Ligands." *Current Biology : CB* 19 (14). Elsevier Ltd: 1167–75. doi:10.1016/j.cub.2009.06.029.

Chung, Brian Y., Valerie L. Kilman, J. Russel Keath, Jena L. Pitman, and Ravi Allada. 2009. "The GABA(A) Receptor RDL Acts in Peptidergic PDF Neurons to Promote Sleep in Drosophila." *Current Biology : CB* 19 (5): 386–90. doi:10.1016/j.cub.2009.01.040.

Chung, Henry, Tamar Sztal, Shivani Pasricha, Mohan Sridhar, Philip Batterham, and Phillip J Daborn. 2009. "Characterization of Drosophila Melanogaster Cytochrome P450 Genes." *Proceedings of the National Academy of Sciences of the United States of America* 106 (14): 5731–36. doi:10.1073/pnas.0812141106.

Claridge-Chang, Adam, Herman Wijnen, Felix Naef, Catharine Boothroyd, Nikolaus Rajewsky, and Michael W Young. 2001. "Circadian Regulation of Gene Expression Systems in the Drosophila Head." *Neuron* 32 (4): 657–71. doi:10.1016/S0896-6273(01)00515-3.

Collins, Ben, Elizabeth A. Kane, David C. Reeves, Myles H. Akabas, and Justin Blau. 2012. "Balance of Activity between LN(v)s and Glutamatergic Dorsal Clock Neurons Promotes Robust Circadian Rhythms in Drosophila." *Neuron* 74 (4). Elsevier Inc.: 706–18. doi:10.1016/j.neuron.2012.02.034.

Crocker, Amanda, Mohammad Shahidullah, Irwin B Levitan, and Amita Sehgal. 2010. "Identification of a Neural Circuit That Underlies the Effects of Octopamine on Sleep:Wake Behavior." *Neuron* 65 (5): 670–81. doi:10.1016/j.neuron.2010.01.032.

Curie, Thomas, Stephanie Maret, Yann Emmenegger, and Paul Franken. 2015. "In Vivo Imaging of the Central and Peripheral Effects of Sleep Deprivation and Suprachiasmatic Nuclei Lesion on PERIOD-2 Protein in Mice." *Sleep* 38 (9): 1381–94. doi:10.5665/sleep.4974.

Dallmann, Robert, Steven A. Brown, and Frédéric Gachon. 2014. "Chronopharmacology: New

Insights and Therapeutic Implications." *Annual Review of Pharmacology and Toxicology* 54 (1): 339–61. doi:10.1146/annurev-pharmtox-011613-135923.

Damiola, F. 2000. "Restricted Feeding Uncouples Circadian Oscillators in Peripheral Tissues from the Central Pacemaker in the Suprachiasmatic Nucleus." *Genes & Development* 14 (23): 2950–61. doi:10.1101/gad.183500.

Davis, Shaun M, Amanda L Thomas, Krystle J Nomie, Longwen Huang, and Herman A. Dierick. 2014. "Tailless and Atrophin Control Drosophila Aggression by Regulating Neuropeptide Signalling in the Pars Intercerebralis." *Nature Communications* 5 (January). Nature Publishing Group: 3177. doi:10.1038/ncomms4177.

de Velasco, Begona, Ted Erclik, Diana Shy, Joey Sclafani, Howard Lipshitz, Roderick McInnes, and Volker Hartenstein. 2007. "Specification and Development of the Pars Intercerebralis and Pars Lateralis, Neuroendocrine Command Centers in the Drosophila Brain." *Developmental Biology* 302 (1): 309–23. doi:10.1016/j.ydbio.2006.09.035.

Deboer, Tom. 2018. "Sleep Homeostasis and the Circadian Clock: Do the Circadian Pacemaker and the Sleep Homeostat Influence Each Other's Functioning?" *Neurobiology of Sleep and Circadian Rhythms*, March. doi:10.1016/j.nbscr.2018.02.003.

Deboer, Tom, László Détári, and Johanna H Meijer. 2007. "Long Term Effects of Sleep Deprivation on the Mammalian Circadian Pacemaker." *Sleep* 30 (3): 257–62.

del Valle Rodríguez, Alberto, Dominic Didiano, and Claude Desplan. 2011. "Power Tools for Gene Expression and Clonal Analysis in Drosophila." *Nature Methods* 9 (1): 47–55. doi:10.1038/nmeth.1800.

Depetris-Chauvin, Ana, Jimena Berni, Ezequiel J Aranovich, Nara I Muraro, Esteban J Beckwith, and María Fernanda Ceriani. 2011. "Adult-Specific Electrical Silencing of Pacemaker Neurons Uncouples Molecular Clock from Circadian Outputs." *Current Biology : CB* 21 (21): 1783–93. doi:10.1016/j.cub.2011.09.027.

Depetris-Chauvin, Ana, Agata Fernández-Gamba, E Axel Gorostiza, Anastasia Herrero, Eduardo M Castaño, and M Fernanda Ceriani. 2014. "Mmp1 Processing of the PDF Neuropeptide Regulates Circadian Structural Plasticity of Pacemaker Neurons." *PLoS Genetics* 10 (10). Public Library of Science: e1004700. doi:10.1371/journal.pgen.1004700.

Dierick, Herman A., and Ralph J. Greenspan. 2007. "Serotonin and Neuropeptide F Have Opposite Modulatory Effects on Fly Aggression." *Nature Genetics* 39 (5): 678–82. doi:10.1038/ng2029.

Donlea, Jeffrey M. 2017. "Neuronal and Molecular Mechanisms of Sleep Homeostasis." *Current Opinion in Insect Science* 24 (December). Elsevier: 51–57. doi:10.1016/J.COIS.2017.09.008.

Donlea, Jeffrey M., Diogo Pimentel, and Gero Miesenbock. 2014. "Neuronal Machinery of Sleep Homeostasis in Drosophila." *Neuron* 81 (4): 860–72. doi:10.1016/j.neuron.2013.12.013.

Donlea, Jeffrey M., Diogo Pimentel, Clifford B. Talbot, Anissa Kempf, Jaison J. Omoto, Volker Hartenstein, and Gero Miesenböck. 2018. "Recurrent Circuitry for Balancing Sleep Need and Sleep." *Neuron*, 1–12. doi:10.1016/j.neuron.2017.12.016.

Donlea, Jeffrey M., Matthew S Thimgan, Yasuko Suzuki, Laura Gottschalk, and Paul J Shaw. 2011. "Inducing Sleep by Remote Control Facilitates Memory Consolidation in Drosophila." *Science (New York, N.Y.)* 332 (6037): 1571–76. doi:10.1126/science.1202249.

Donlea, Jeffrey M, Narendrakumar Ramanan, and Paul J Shaw. 2009. "Use-Dependent Plasticity in Clock Neurons Regulates Sleep Need in Drosophila." *Science (New York, N.Y.)* 324

(5923): 105–8. doi:10.1126/science.1166657.

Dubowy, Christine, and Amita Sehgal. 2017. “Circadian Rhythms and Sleep in Drosophila Melanogaster.” *Genetics* 205 (4): 1373–97. doi:10.1534/genetics.115.185157.

Dus, Monica, Jason Sih-Yu Lai, Keith M. Gunapala, Soohong Min, Timothy D. Tayler, Anne C. Hergarden, Eliot Geraud, Christina M. Joseph, and Greg S B Suh. 2015. “Nutrient Sensor in the Brain Directs the Action of the Brain-Gut Axis in Drosophila.” *Neuron* 87 (1). Elsevier Inc.: 139–51. doi:10.1016/j.neuron.2015.05.032.

Duvall, Laura B., and Paul H. Taghert. 2013. “E and M Circadian Pacemaker Neurons Use Different PDF Receptor Signalosome Components in Drosophila.” *Journal of Biological Rhythms* 28 (4). SAGE PublicationsSage CA: Los Angeles, CA: 239–48. doi:10.1177/0748730413497179.

Enriquez, Jonathan, Lalanti Venkatasubramanian, Myungin Baek, Meredith Peterson, Ulkar Aghayeva, and Richard S Mann. 2015. “Specification of Individual Adult Motor Neuron Morphologies by Combinatorial Transcription Factor Codes.” *Neuron* 86 (4): 955–70. doi:10.1016/j.neuron.2015.04.011.

Erion, Renske, Anna N King, Gang Wu, John B Hogenesch, and Amita Sehgal. 2016. “Neural Clocks and Neuropeptide F/Y Regulate Circadian Gene Expression in a Peripheral Metabolic Tissue.” *ELife* 5 (April). doi:10.7554/eLife.13552.

Feinberg, Evan H, Miri K Vanhoven, Andres Bendesky, George Wang, Richard D Fetter, Kang Shen, and Cornelia I Bargmann. 2008. “GFP Reconstitution Across Synaptic Partners (GRASP) Defines Cell Contacts and Synapses in Living Nervous Systems.” *Neuron* 57 (3): 353–63. doi:10.1016/j.neuron.2007.11.030.

Fernández, María de la Paz, Jessie Chu, Adriana Villella, Nigel Atkinson, Steve A Kay, and María Fernanda Ceriani. 2007. “Impaired Clock Output by Altered Connectivity in the Circadian Network.” *Proceedings of the National Academy of Sciences of the United States of America* 104 (13). National Academy of Sciences: 5650–55. doi:10.1073/pnas.0608260104.

Fernández, María Paz, Jimena Berni, and María Fernanda Ceriani. 2008. “Circadian Remodeling of Neuronal Circuits Involved in Rhythmic Behavior.” *PLoS Biology* 6 (3): e69. doi:10.1371/journal.pbio.0060069.

Flourakis, Matthieu, Elzbieta Kula-Eversole, Alan L Hutchison, Tae Hee Han, Kimberly Aranda, Devon L Moose, Kevin P White, et al. 2015. “A Conserved Bicycle Model for Circadian Clock Control of Membrane Excitability.” *Cell* 162 (4): 836–48. doi:10.1016/j.cell.2015.07.036.

Foltenyi, Krisztina, Ralph J. Greenspan, and John W Newport. 2007. “Activation of EGFR and ERK by Rhomboid Signaling Regulates the Consolidation and Maintenance of Sleep in Drosophila.” *Nature Neuroscience* 10 (9). Nature Publishing Group: 1160–67. doi:10.1038/nn1957.

Fouquet, Wernher, David Owald, Carolin Wichmann, Sara Mertel, Harald Depner, Marcus Dyba, Stefan Hallermann, Robert J Kittel, Stefan Eimer, and Stephan J Sigrist. 2009. “Maturation of Active Zone Assembly by Drosophila Bruchpilot.” *The Journal of Cell Biology* 186 (1): 129–45. doi:10.1083/jcb.200812150.

Frenkel, Lia, Nara I. Muraro, Andrea N. Beltrán González, María S. Marcora, Guillermo Bernabó, Christiane Hermann-Luibl, Juan I. Romero, et al. 2017. “Organization of Circadian Behavior Relies on Glycinergic Transmission.” *Cell Reports* 19 (1): 72–85. doi:10.1016/j.celrep.2017.03.034.

Fujii, Shinsuke, and Hubert Amrein. 2002. “Genes Expressed in the Drosophila Head Reveal a

Role for Fat Cells in Sex-Specific Physiology." *The EMBO Journal* 21 (20): 5353–63. doi:10.1093/emboj/cdf556.

———. 2010. "Ventral Lateral and DN1 Clock Neurons Mediate Distinct Properties of Male Sex Drive Rhythm in Drosophila." *Proceedings of the National Academy of Sciences of the United States of America* 107 (23): 10590–95. doi:10.1073/pnas.0912457107.

Fujii, Shinsuke, Patrick Emery, and Hubert Amrein. 2017. "SIK3-HDAC4 Signaling Regulates Drosophila Circadian Male Sex Drive Rhythm via Modulating the DN1 Clock Neurons." *Proceedings of the National Academy of Sciences of the United States of America* 114 (32). National Academy of Sciences: E6669–77. doi:10.1073/pnas.1620483114.

Fujii, Shinsuke, Akemi Toyama, and Hubert Amrein. 2008. "A Male-Specific Fatty Acid Hydroxylase, SXE1, Is Necessary for Efficient Male Mating in Drosophila Melanogaster." *Genetics* 180 (September): 179–90. doi:10.1534/genetics.108.089177.

Furuyama, Kazumichi, Kiriko Kaneko, and Patrick D Vargas. 2007. "Heme as a Magnificent Molecule with Multiple Missions: Heme Determines Its Own Fate and Governs Cellular Homeostasis." *The Tohoku Journal of Experimental Medicine* 213 (1): 1–16. doi:10.1620/tjem.213.1.

Gachon, Frédéric, Fabienne Fleury Olela, Olivier Schaad, Patrick Descombes, and Ueli Schibler. 2006. "The Circadian PAR-Domain Basic Leucine Zipper Transcription Factors DBP, TEF, and HLF Modulate Basal and Inducible Xenobiotic Detoxification." *Cell Metabolism* 4 (1): 25–36. doi:10.1016/j.cmet.2006.04.015.

Garczynski, Stephen F., Mark R. Brown, Ping Shen, Thomas F. Murray, and Joe W. Crim. 2002. "Characterization of a Functional Neuropeptide F Receptor from Drosophila Melanogaster." *Peptides* 23: 773–80. doi:10.1016/S0196-9781(01)00647-7.

Gautier, Laurent, Leslie Cope, Benjamin M. Bolstad, and Rafael A. Irizarry. 2004. "Affy--Analysis of Affymetrix GeneChip Data at the Probe Level." *Bioinformatics (Oxford, England)* 20 (3): 307–15. doi:10.1093/bioinformatics/btg405.

Ghezzi, Alfredo, Benjamin J Liebeskind, Ammon Thompson, Nigel S Atkinson, and Harold H Zakon. 2014. "Ancient Association between Cation Leak Channels and Mid1 Proteins Is Conserved in Fungi and Animals." *Frontiers in Molecular Neuroscience* 7: 15. doi:10.3389/fnmol.2014.00015.

Giebultowicz, J M, R Stanewsky, J C Hall, and D M Hege. 2000. "Transplanted Drosophila Excretory Tubules Maintain Circadian Clock Cycling out of Phase with the Host." *Current Biology : CB* 10 (2): 107–10.

Gilestro, Giorgio F, and Chiara Cirelli. 2009. "PySolo: A Complete Suite for Sleep Analysis in Drosophila." *Bioinformatics (Oxford, England)* 25 (11): 1466–67. doi:10.1093/bioinformatics/btp237.

Gill, Shubhroz, Hiep D. Le, Girish C. Melkani, Satchidananda Panda, and Panda S. Gill S, Le HD, Melkani GC. 2015. "Time-Restricted Feeding Attenuates Age-Related Cardiac Decline in Drosophila." *Science* 347 (6227): 1265–69. doi:10.1126/science.1256682.

Glynn, Earl F., Jie Chen, and Arcady R. Mushegian. 2006. "Detecting Periodic Patterns in Unevenly Spaced Gene Expression Time Series Using Lomb-Scargle Periodograms." *Bioinformatics (Oxford, England)* 22 (3): 310–16. doi:10.1093/bioinformatics/bti789.

Gorostiza, E Axel, Ana Depetris-Chauvin, Lia Frenkel, Nicolás Pírez, and María Fernanda Ceriani. 2014. "Circadian Pacemaker Neurons Change Synaptic Contacts across the Day." *Current Biology : CB* 24 (18): 2161–67. doi:10.1016/j.cub.2014.07.063.

Górska-Andrzejak, Jolanta, Milena Damulewicz, and Elżbieta Pyza. 2015. “Circadian Changes in Neuronal Networks.” *Current Opinion in Insect Science* 7 (February): 76–81. doi:10.1016/j.cois.2015.01.005.

Górska-Andrzejak, Jolanta, Renata Makuch, Joanna Stefan, Alicja Görlich, Danuta Semik, and Elzbieta Pyza. 2013. “Circadian Expression of the Presynaptic Active Zone Protein Bruchpilot in the Lamina of Drosophila Melanogaster.” *Developmental Neurobiology* 73 (1): 14–26. doi:10.1002/dneu.22032.

Gratz, Scott J, Fiona P Ukken, C Dustin Rubinstein, Gene Thiede, Laura K Donohue, Alexander M Cummings, and Kate M O’Connor-Giles. 2014. “Highly Specific and Efficient CRISPR/Cas9-Catalyzed Homology-Directed Repair in Drosophila.” *Genetics* 196 (4): 961–71. doi:10.1534/genetics.113.160713.

Grima, Brigitte, Elisabeth Chélot, Ruohan Xia, and François Rouyer. 2004. “Morning and Evening Peaks of Activity Rely on Different Clock Neurons of the Drosophila Brain.” *Nature* 431 (7010). Nature Publishing Group: 869–73. doi:10.1038/nature02935.

Gunawardhana, Kushan L., and Paul E. Hardin. 2017. “VRILLE Controls PDF Neuropeptide Accumulation and Arborization Rhythms in Small Ventrolateral Neurons to Drive Rhythmic Behavior in Drosophila.” *Current Biology : CB* 27 (22). Cell Press: 3442–3453.e4. doi:10.1016/j.cub.2017.10.010.

Guo, Fang, Isadora Cerullo, Xiao Chen, and Michael Rosbash. 2014. “PDF Neuron Firing Phase-Shifts Key Circadian Activity Neurons in Drosophila.” *ELife* 2014 (June). eLife Sciences Publications Limited: 1–21. doi:10.7554/eLife.02780.

Guo, Fang, Junwei Yu, Hyung Jae Jung, Katharine C Abruzzi, Weifei Luo, Leslie C. Griffith, and Michael Rosbash. 2016. “Circadian Neuron Feedback Controls the Drosophila Sleep--Activity Profile.” *Nature* 536 (7616). Nature Research: 292–97. doi:10.1038/nature19097.

Hamasaka, Yasutaka, Dirk Rieger, Marie-Laure Parmentier, Yves Grau, Charlotte Helfrich-Förster, and Dick R Nässel. 2007. “Glutamate and Its Metabotropic Receptor in Drosophila Clock Neuron Circuits.” *The Journal of Comparative Neurology* 505 (1): 32–45. doi:10.1002/cne.21471.

Harris, David T., Benjamin R. Kallman, Brendan C. Mullaney, and Kristin Scott. 2015. “Representations of Taste Modality in the Drosophila Brain.” *Neuron* 86 (6): 1449–60. doi:10.1016/j.neuron.2015.05.026.

Harrisingh, Marie C, Ying Wu, Gregory A Lnenicka, and Michael N Nitabach. 2007. “Intracellular Ca2+ Regulates Free-Running Circadian Clock Oscillation in Vivo.” *The Journal of Neuroscience* 27 (46). Society for Neuroscience: 12489–99. doi:10.1523/JNEUROSCI.3680-07.2007.

Haynes, Paula R, Bethany L Christmann, and Leslie C. Griffith. 2015. “A Single Pair of Neurons Links Sleep to Memory Consolidation in Drosophila Melanogaster.” *ELife* 4 (January). eLife Sciences Publications Limited: e03868. doi:10.7554/eLife.03868.

He, C., X. Cong, R. Zhang, D. Wu, C. An, and Z. Zhao. 2013. “Regulation of Circadian Locomotor Rhythm by Neuropeptide Y-like System in Drosophila Melanogaster.” *Insect Molecular Biology* 22 (4): 376–88. doi:10.1111/imb.12027.

He, Chunxia, Yunyan Yang, Mingming Zhang, Jeffrey L. Price, and Zhangwu Zhao. 2013. “Regulation of Sleep by Neuropeptide Y-Like System in Drosophila Melanogaster.” *PLoS ONE* 8 (9): e74237. doi:10.1371/journal.pone.0074237.

Hector, Clare E., Colin A. Bretz, Yan Zhao, and Erik C. Johnson. 2009. “Functional Differences between Two CRF-Related Diuretic Hormone Receptors in Drosophila.” *The Journal of*

Experimental Biology 212 (19): 3142–47. doi:10.1242/jeb.033175.

Hege, David M, Ralf Stanewsky, Jeffrey C. Hall, and Jadwiga M Giebultowicz. 1997. “Rhythmic Expression of a PER-Reporter in the Malpighian Tubules of Decapitated Drosophila: Evidence for a Brain-Independent Circadian Clock.” *Journal of Biological Rhythms* 12 (4): 300–308. doi:10.1177/074873049701200402.

Helfrich-Förster, C. 1998. “Robust Circadian Rhythmicity of Drosophila Melanogaster Requires the Presence of Lateral Neurons: A Brain-Behavioral Study of Disconnected Mutants.” *Journal of Comparative Physiology. A, Sensory, Neural, and Behavioral Physiology* 182 (4): 435–53.

Helfrich-Förster, Charlotte. 1995. “The Period Clock Gene Is Expressed in Central Nervous System Neurons Which Also Produce a Neuropeptide That Reveals the Projections of Circadian Pacemaker Cells within the Brain of Drosophila Melanogaster.” *Proceedings of the National Academy of Sciences of the United States of America* 92 (2): 612–16.

Helfrich-Förster, Charlotte, Orie T Shafer, Corinna Wülbeck, Eva Grieshaber, Dirk Rieger, and Paul Taghert. 2007. “Development and Morphology of the Clock-Gene-Expressing Lateral Neurons of Drosophila Melanogaster.” *The Journal of Comparative Neurology* 500 (1): 47–70. doi:10.1002/cne.21146.

Helfrich-Förster, Charlotte, M Täuber, Jae H Park, M Mühlig-Versen, S Schneuwly, and A Hofbauer. 2000. “Ectopic Expression of the Neuropeptide Pigment-Dispersing Factor Alters Behavioral Rhythms in Drosophila Melanogaster.” *The Journal of Neuroscience : The Official Journal of the Society for Neuroscience* 20 (9): 3339–53.

Helfrich-Förster, Charlotte, T Yoshii, C Wülbeck, E Grieshaber, D Rieger, W Bachleitner, P Cusamano, and François Rouyer. 2007. “The Lateral and Dorsal Neurons of Drosophila Melanogaster: New Insights about Their Morphology and Function.” *Cold Spring Harbor Symposia on Quantitative Biology* 72 (January): 517–25. doi:10.1101/sqb.2007.72.063.

Hendricks, J C, Julie a Williams, K Panckeri, D Kirk, M Tello, Jerry C.P. Yin, and Amita Sehgal. 2001. “A Non-Circadian Role for CAMP Signaling and CREB Activity in Drosophila Rest Homeostasis.” *Nature Neuroscience* 4 (11): 1108–15. doi:10.1038/nn743.

Hermann-Luibl, Christiane, Taishi Yoshii, Pingkalai R. Senthilan, Heinrich Dircksen, and Charlotte Helfrich-Förster. 2014. “The Ion Transport Peptide Is a New Functional Clock Neuropeptide in the Fruit Fly Drosophila Melanogaster.” *The Journal of Neuroscience : The Official Journal of the Society for Neuroscience* 34 (29): 9522–36. doi:10.1523/JNEUROSCI.0111-14.2014.

Hermann, Christiane, Taishi Yoshii, Verena Dusik, and Charlotte Helfrich-Förster. 2012. “Neuropeptide F Immunoreactive Clock Neurons Modify Evening Locomotor Activity and Free-Running Period in Drosophila Melanogaster.” *The Journal of Comparative Neurology* 520 (5): 970–87. doi:10.1002/cne.22742.

Herrero, Anastasia, José M Duhart, and Maria F Ceriani. 2017. “Neuronal and Glial Clocks Underlying Structural Remodeling of Pacemaker Neurons in Drosophila.” *Frontiers in Physiology* 8: 918. doi:10.3389/fphys.2017.00918.

Howard, A D, R Wang, S S Pong, T N Mellin, A Strack, X M Guan, Z Zeng, et al. 2000. “Identification of Receptors for Neuromedin U and Its Role in Feeding.” *Nature* 406 (6791). Macmillian Magazines Ltd.: 70–74. doi:10.1038/35017610.

Hughes, Michael E., John B. Hogenesch, and Karl Kornacker. 2010. “JTK_CYCLE: An Efficient Nonparametric Algorithm for Detecting Rhythmic Components in Genome-Scale Data Sets.” *Journal of Biological Rhythms* 25 (5): 372–80. doi:10.1177/0748730410379711.

Hughes, Michael E., Hee-Kyung Kyung Hong, Jason L. Chong, Alejandra a. Indacochea, Samuel

S. Lee, Michael Han, Joseph S. Takahashi, and John B. Hogenesch. 2012. “Brain-Specific Rescue of Clock Reveals System-Driven Transcriptional Rhythms in Peripheral Tissue.” *PLoS Genetics* 8 (7). Public Library of Science: e1002835. doi:10.1371/journal.pgen.1002835.

Hyun, Seogang, Youngseok Lee, Sung-Tae Hong, Sunhoe Bang, Donggi Paik, Jongkyun Kang, Jinwhan Shin, et al. 2005. “Drosophila GPCR Han Is a Receptor for the Circadian Clock Neuropeptide PDF.” *Neuron* 48 (2): 267–78. doi:10.1016/j.neuron.2005.08.025.

Ikeda, Masayuki. 2004. “Calcium Dynamics and Circadian Rhythms in Suprachiasmatic Nucleus Neurons.” *The Neuroscientist* 10 (4). Sage PublicationsSage CA: Thousand Oaks, CA: 315–24. doi:10.1177/10738584031262149.

Im, Seol Hee, and Paul H. Taghert. 2010. “PDF Receptor Expression Reveals Direct Interactions between Circadian Oscillators in Drosophila.” *The Journal of Comparative Neurology* 518 (11): 1925–45. doi:10.1002/cne.22311.

Irizarry, Rafael A., Bridget Hobbs, Francois Collin, Yasmin D Beazer-Barclay, Kristen J Antonellis, Uwe Scherf, and Terence P Speed. 2003. “Exploration, Normalization, and Summaries of High Density Oligonucleotide Array Probe Level Data.” *Biostatistics (Oxford, England)* 4 (2): 249–64. doi:10.1093/biostatistics/4.2.249.

Itskov, Pavel M., and Carlos Ribeiro. 2013. “The Dilemmas of the Gourmet Fly: The Molecular and Neuronal Mechanisms of Feeding and Nutrient Decision Making in Drosophila.” *Frontiers in Neuroscience* 7 (7 FEB): 12. doi:10.3389/fnins.2013.00012.

Izumo, Mariko, Martina Pejchal, Andrew C Schook, Ryan P Lange, Jacqueline A Walisser, Takashi R Sato, Xiaozhong Wang, Christopher A Bradfield, and Joseph S. Takahashi. 2014. “Differential Effects of Light and Feeding on Circadian Organization of Peripheral Clocks in a Forebrain Bmal1 Mutant.” *ELife* 3 (January). eLife Sciences Publications Limited: e04617. doi:10.7554/eLife.04617.

Jenett, Arnim, Gerald M Rubin, Teri-T B Ngo, David Shepherd, Christine Murphy, Heather Dionne, Barret D Pfeiffer, et al. 2012. “A GAL4-Driver Line Resource for Drosophila Neurobiology.” *Cell Reports* 2 (4): 991–1001. doi:10.1016/j.celrep.2012.09.011.

Jepson, James E C, Mohammad Shahidullah, Angelique Lamaze, Drew Peterson, Huihui Pan, and Kyunghee Koh. 2012. “Dyschronic, a Drosophila Homolog of a Deaf-Blindness Gene, Regulates Circadian Output and Slowpoke Channels.” *PLoS Genetics* 8 (4): e1002671. doi:10.1371/journal.pgen.1002671.

Johard, Helena A.D., Taishi Yoishii, Heinrich Dircksen, Paola Cusumano, Francois Rouyer, Charlotte Helfrich-Förster, and Dick R. Nässel. 2009. “Peptidergic Clock Neurons in Drosophila: Ion Transport Peptide and Short Neuropeptide F in Subsets of Dorsal and Ventral Lateral Neurons.” *The Journal of Comparative Neurology* 516 (1): 59–73. doi:10.1002/cne.22099.

Johnson, Erik C., Laura M Bohn, and Paul H. Taghert. 2004. “Drosophila CG8422 Encodes a Functional Diuretic Hormone Receptor.” *The Journal of Experimental Biology* 207 (Pt 5): 743–48. doi:10.1242/jeb.00818.

Joiner, William J. 2016. “Unraveling the Evolutionary Determinants of Sleep.” *Current Biology : CB* 26 (20): R1073–87. doi:10.1016/j.cub.2016.08.068.

Joiner, William J, Amanda Crocker, Benjamin H White, and Amita Sehgal. 2006. “Sleep in Drosophila Is Regulated by Adult Mushroom Bodies.” *Nature* 441 (7094): 757–60. doi:10.1038/nature04811.

Kaneko, Haruna, Lauren M Head, Jinli Ling, Xin Tang, Yilin Liu, Paul E. Hardin, Patrick Emery,

and Fumika N. Hamada. 2012. “Circadian Rhythm of Temperature Preference and Its Neural Control in Drosophila.” *Current Biology : CB* 22 (19): 1851–57. doi:10.1016/j.cub.2012.08.006.

Kaneko, Maki, and Jeffrey C. Hall. 2000. “Neuroanatomy of Cells Expressing Clock Genes in Drosophila: Transgenic Manipulation of the Period and Timeless Genes to Mark the Perikarya of Circadian Pacemaker Neurons and Their Projections.” *The Journal of Comparative Neurology* 422 (1). John Wiley & Sons, Inc.: 66–94. doi:10.1002/(SICI)1096-9861(20000619)422:1<66::AID-CNE5>3.0.CO;2-2.

Karl, Tim, Liesl Duffy, and Herbert Herzog. 2008. “Behavioural Profile of a New Mouse Model for NPY Deficiency.” *European Journal of Neuroscience* 28 (1): 173–80. doi:10.1111/j.1460-9568.2008.06306.x.

Kim, Woo Jae Jae, Lily Yeh Yeh Jan, and Yuh Nung Nung Jan. 2013. “A PDF/NPF Neuropeptide Signaling Circuitry of Male Drosophila Melanogaster Controls Rival-Induced Prolonged Mating.” *Neuron* 80 (5): 1190–1205. doi:10.1016/j.neuron.2013.09.034.

King-Jones, Kirst, Michael a. Horner, Geanette Lam, and Carl S. Thummel. 2006. “The DHR96 Nuclear Receptor Regulates Xenobiotic Responses in Drosophila.” *Cell Metabolism* 4 (July): 37–48. doi:10.1016/j.cmet.2006.06.006.

King, Anna N., Annika F. Barber, Amelia E. Smith, Austin P. Dreyer, Divya Sitaraman, Michael N. Nitabach, Daniel J. Cavanaugh, and Amita Sehgal. 2017. “A Peptidergic Circuit Links the Circadian Clock to Locomotor Activity.” *Current Biology*, June. doi:10.1016/j.cub.2017.05.089.

Kitamoto, Toshihiro. 2001. “Conditional Modification of Behavior in Drosophila by Targeted Expression of a Temperature-Sensitive Shibire Allele in Defined Neurons.” *Journal of Neurobiology* 47 (2): 81–92.

Klose, Markus, Laura B. Duvall, Weihua Li, Xitong Liang, Chi Ren, Joe Henry Henry Steinbach, and Paul H. H Taghert. 2016. “Functional PDF Signaling in the Drosophila Circadian Neural Circuit Is Gated by Ral A-Dependent Modulation.” *Neuron* 90 (4): 781–94. doi:10.1016/j.neuron.2016.04.002.

Kornmann, Benoît, Olivier Schaad, Hermann Bujard, Joseph S. Takahashi, and Ueli Schibler. 2007. “System-Driven and Oscillator-Dependent Circadian Transcription in Mice with a Conditionally Active Liver Clock.” *PLoS Biology* 5 (2). Public Library of Science: e34. doi:10.1371/journal.pbio.0050034.

Kornmann, Benoît, Olivier Schaad, H. Reinke, C. Saini, and Ueli Schibler. 2007. “Regulation of Circadian Gene Expression in Liver by Systemic Signals and Hepatocyte Oscillators.” *Cold Spring Harbor Symposia on Quantitative Biology* 72: 319–30. doi:10.1101/sqb.2007.72.041.

Krashes, Michael J, Shamik DasGupta, Andrew Vreede, Benjamin White, James Douglas Armstrong, and Scott Waddell. 2009. “A Neural Circuit Mechanism Integrating Motivational State with Memory Expression in Drosophila.” *Cell* 139 (2): 416–27. doi:10.1016/j.cell.2009.08.035.

Krupp, Joshua J., Clement Kent, Jean Christophe Billeter, Reza Azanchi, Anthony K C So, Julia a. Schonfeld, Benjamin P. Smith, Christophe Lucas, and Joel D. Levine. 2008. “Social Experience Modifies Pheromone Expression and Mating Behavior in Male Drosophila Melanogaster.” *Current Biology* 18 (18): 1373–83. doi:10.1016/j.cub.2008.07.089.

Krupp, Joshua J, Jean-Christophe Billeter, Amy Wong, Charles Choi, Michael N Nitabach, and Joel D Levine. 2013. “Pigment-Dispersing Factor Modulates Pheromone Production in Clock Cells That Influence Mating in Drosophila.” *Neuron* 79 (1). Cell Press: 54–68. doi:10.1016/j.neuron.2013.05.019.

Kula, Elzbieta, Edwin S. Levitan, Elzbieta Pyza, and Michael Rosbash. 2006. “PDF Cycling in the Dorsal Protocerebrum of the Drosophila Brain Is Not Necessary for Circadian Clock Function.” *Journal of Biological Rhythms* 21 (2): 104–17. doi:10.1177/0748730405285715.

Kunst, Michael, Michael E. Hughes, Davide Raccuglia, Mario Felix, Michael Li, Gregory Barnett, Janelle Duah, and Michael N. Nitabach. 2014. “Calcitonin Gene-Related Peptide Neurons Mediate Sleep-Specific Circadian Output in Drosophila.” *Current Biology* 24 (22). Elsevier: 2652–64. doi:10.1016/j.cub.2014.09.077.

Kvon, Evgeny Z, Tomas Kazmar, Gerald Stampfel, J Omar Yáñez-Cuna, Michaela Pagani, Katharina Schernhuber, Barry J. Dickson, and Alexander Stark. 2014. “Genome-Scale Functional Characterization of Drosophila Developmental Enhancers in Vivo.” *Nature* 512 (June). Nature Publishing Group, a division of Macmillan Publishers Limited. All Rights Reserved.: 91–95. doi:10.1038/nature13395.

Lamia, Katja A, Kai-Florian Storch, and Charles J Weitz. 2008. “Physiological Significance of a Peripheral Tissue Circadian Clock.” *Proceedings of the National Academy of Sciences of the United States of America* 105 (39): 15172–77. doi:10.1073/pnas.0806717105.

Lear, Bridget C, Jui-Ming Lin, J Russel Keath, Jermaine J McGill, Indira M Raman, and Ravi Allada. 2005. “The Ion Channel Narrow Abdomen Is Critical for Neural Output of the Drosophila Circadian Pacemaker.” *Neuron* 48 (6): 965–76. doi:10.1016/j.neuron.2005.10.030.

Lear, Bridget C, C Elaine Merrill, Jui-Ming Lin, Analyne Schroeder, Luoying Zhang, and Ravi Allada. 2005. “A G Protein-Coupled Receptor, Groom-of-PDF, Is Required for PDF Neuron Action in Circadian Behavior.” *Neuron* 48 (2): 221–27. doi:10.1016/j.neuron.2005.09.008.

Lee, Gyunghee, Jae Hoon Bahn, and Jae H Park. 2006. “Sex- and Clock-Controlled Expression of the Neuropeptide F Gene in Drosophila.” *Proceedings of the National Academy of Sciences of the United States of America* 103 (33): 12580–85. doi:10.1073/pnas.0601171103.

Lee, Ivan T, Alexander S Chang, Manabu Manandhar, Yongli Shan, Junmei Fan, Mariko Izumo, Yuichi Ikeda, et al. 2015. “Neuromedin S-Producing Neurons Act as Essential Pacemakers in the Suprachiasmatic Nucleus to Couple Clock Neurons and Dictate Circadian Rhythms.” *Neuron* 85 (5): 1086–1102. doi:10.1016/j.neuron.2015.02.006.

Lee, Kang-Min, Ivana Daubnerová, R. Elwyn Isaac, Chen Zhang, Sekyu Choi, Jongkyeong Chung, and Young-Joon Kim. 2015. “A Neuronal Pathway That Controls Sperm Ejection and Storage in Female Drosophila.” *Current Biology : CB* 25 (6): 790–97. doi:10.1016/j.cub.2015.01.050.

Li, Qian, Yi Li, Xiao Wang, Junxia Qi, Xi Jin, Huawei Tong, Zikai Zhou, Zi Chao Zhang, and Junhai Han. 2017. “Fbxl4 Serves as a Clock Output Molecule That Regulates Sleep through Promotion of Rhythmic Degradation of the GABAA Receptor.” *Current Biology : CB* 27 (23): 3616–3625.e5. doi:10.1016/j.cub.2017.10.052.

Li, Weizhe, Yufeng Pan, Zhipeng Wang, Haiyun Gong, Zhefeng Gong, and Li Liu. 2009. “Morphological Characterization of Single Fan-Shaped Body Neurons in Drosophila Melanogaster.” *Cell and Tissue Research* 336 (3). Springer-Verlag: 509–19. doi:10.1007/s00441-009-0781-2.

Liang, Xitong, Timothy E. Holy, and Paul H. Taghert. 2016. “Synchronous Drosophila Circadian Pacemakers Display Nonsynchronous Ca^{2+} Rhythms in Vivo.” *Science (New York, N.Y.)* 351 (6276). American Association for the Advancement of Science: 976–81. doi:10.1126/science.aad3997.

Liang, Xitong, Timothy E. Holy, and Paul H. Taghert. 2017. “A Series of Suppressive Signals

within the Drosophila Circadian Neural Circuit Generates Sequential Daily Outputs." *Neuron* 94 (6): 1173–1189.e4. doi:10.1016/j.neuron.2017.05.007.

Lima, Susana Q., and Gero Miesenböck. 2005. "Remote Control of Behavior through Genetically Targeted Photostimulation of Neurons." *Cell* 121 (1): 141–52. doi:10.1016/j.cell.2005.02.004.

Lin, Yiing, Gary D. Stormo, and Paul H. Taghert. 2004. "The Neuropeptide Pigment-Dispersing Factor Coordinates Pacemaker Interactions in the Drosophila Circadian System." *The Journal of Neuroscience : The Official Journal of the Society for Neuroscience* 24 (36). Society for Neuroscience: 7951–57. doi:10.1523/JNEUROSCI.2370-04.2004.

Lingo, P.R., Z Zhao, and P Shen. 2007. "Co-Regulation of Cold-Resistant Food Acquisition by Insulin- and Neuropeptide Y-like Systems in Drosophila Melanogaster." *Neuroscience* 148 (2): 371–74. doi:10.1016/j.neuroscience.2007.06.010.

Liu, Qili, Sha Liu, Lay Kodama, Maria R Driscoll, and Mark N. Wu. 2012. "Two Dopaminergic Neurons Signal to the Dorsal Fan-Shaped Body to Promote Wakefulness in Drosophila." *Current Biology : CB* 22 (22): 2114–23. doi:10.1016/j.cub.2012.09.008.

Liu, Sha, Angelique Lamaze, Qili Liu, Masashi Tabuchi, Yong Yang, Melissa Fowler, Rajnish Bharadwaj, et al. 2014. "WIDE AWAKE Mediates the Circadian Timing of Sleep Onset." *Neuron* 82 (1): 151–66. doi:10.1016/j.neuron.2014.01.040.

Liu, Sha, Qili Liu, Masashi Tabuchi, and Mark N. Wu. 2016. "Sleep Drive Is Encoded by Neural Plastic Changes in a Dedicated Circuit." *Cell* 165 (6): 1347–60. doi:10.1016/j.cell.2016.04.013.

Lu, Yuan-Fu, Tao Jin, Yasha Xu, Dan Zhang, Qin Wu, Yu-Kun Jennifer Zhang, and Jie Liu. 2013. "Sex Differences in the Circadian Variation of Cytochrome P450 Genes and Corresponding Nuclear Receptors in Mouse Liver." *Chronobiology International* 30 (9): 1135–43. doi:10.3109/07420528.2013.805762.

Luo, Wenyu, and Amita Sehgal. 2012. "Regulation of Circadian Behavioral Output via a MicroRNA-JAK/STAT Circuit." *Cell* 148 (4). Elsevier Inc.: 765–79. doi:10.1016/j.cell.2011.12.024.

Macpherson, Lindsey J, Emanuela E Zaharieva, Patrick J Kearney, Michael H Alpert, Tzu-Yang Lin, Zeynep Turan, Chi-Hon Lee, and Marco Gallio. 2015. "Dynamic Labelling of Neural Connections in Multiple Colours by Trans-Synaptic Fluorescence Complementation." *Nature Communications* 6 (December): 10024. doi:10.1038/ncomms10024.

Mahr, Andrea, and Hermann Aberle. 2006. "The Expression Pattern of the Drosophila Vesicular Glutamate Transporter: A Marker Protein for Motoneurons and Glutamatergic Centers in the Brain." *Gene Expression Patterns : GEP* 6 (3): 299–309. doi:10.1016/j.modgep.2005.07.006.

Marcheva, Biliana, Kathryn M Ramsey, Clara B Peek, Alison Affinati, Eleonore Maury, and Joseph Bass. 2013. "Circadian Clocks and Metabolism." *Handbook of Experimental Pharmacology*, no. 217: 127–55. doi:10.1007/978-3-642-25950-0_6.

Marcheva, Biliana, Kathryn Moynihan Ramsey, Ethan D. Buhr, Yumiko Kobayashi, Hong Su, Caroline H. Ko, Ganka Ivanova, et al. 2010. "Disruption of the Clock Components CLOCK and BMAL1 Leads to Hypoinsulinaemia and Diabetes." *Nature* 466 (7306): 627–31. doi:10.1038/nature09253.

Marchler-Bauer, Aron, Myra K Derbyshire, Noreen R Gonzales, Shennan Lu, Farideh Chitsaz, Lewis Y Geer, Renata C Geer, et al. 2015. "CDD: NCBI's Conserved Domain Database." *Nucleic Acids Research* 43 (Database issue). Oxford University Press: D222-6.

doi:10.1093/nar/gku1221.

Masuyama, Kaoru, Yi Zhang, Yi Rao, and Jing W Wang. 2012. “Mapping Neural Circuits with Activity-Dependent Nuclear Import of a Transcription Factor.” *Journal of Neurogenetics* 26 (1). Informa Healthcare New York: 89–102. doi:10.3109/01677063.2011.642910.

Matsui, Takaaki, Tomohisa Matsumoto, Naoyuki Ichihara, Tsubasa Sakai, Honoo Satake, Yasuhiko Watari, and Makio Takeda. 2009. “The Pars Intercerebralis as a Modulator of Locomotor Rhythms and Feeding in the American Cockroach, Periplaneta Americana.” *Physiology & Behavior* 96 (4–5): 548–56. doi:10.1016/j.physbeh.2008.12.009.

Maywood, Elizabeth S, Hitoshi Okamura, and Michael H Hastings. 2002. “Opposing Actions of Neuropeptide Y and Light on the Expression of Circadian Clock Genes in the Mouse Suprachiasmatic Nuclei.” *The European Journal of Neuroscience* 15 (1): 216–20. doi:10.1046/j.0953-816x.2001.01852.x.

McDonald, Michael J, and Michael Rosbash. 2001. “Microarray Analysis and Organization of Circadian Gene Expression in Drosophila.” *Cell* 107 (5): 567–78. doi:10.1016/S0092-8674(01)00545-1.

McGuire, Sean E., Phuong T Le, Alexander J Osborn, Kunihiro Matsumoto, and Ronald L. Davis. 2003. “Spatiotemporal Rescue of Memory Dysfunction in Drosophila.” *Science* 302 (5651). American Association for the Advancement of Science: 1765–68. doi:10.1126/science.1089035.

McKellar, Claire E. 2016. “Motor Control of Fly Feeding.” *Journal of Neurogenetics* 30 (2): 101–11. doi:10.1080/01677063.2016.1177047.

Melcher, Christoph, Rüdiger Bader, Steffen Walther, Oleg Simakov, and Michael J. Pankratz. 2006. “Neuromedin U and Its Putative Drosophila Homolog Hugin.” *PLoS Biology* 4 (3): e68. doi:10.1371/journal.pbio.0040068.

Melcher, Christoph, and Michael J. Pankratz. 2005. “Candidate Gustatory Interneurons Modulating Feeding Behavior in the Drosophila Brain.” *PLoS Biology* 3 (9): e305. doi:10.1371/journal.pbio.0030305.

Mertens, Inge, Anick Vandingenen, Erik C. Johnson, Orie T. Shafer, W Li, Jennifer S Trigg, Arnold De Loof, Liliane Schoofs, and Paul H. Taghert. 2005. “PDF Receptor Signaling in Drosophila Contributes to Both Circadian and Geotactic Behaviors.” *Neuron* 48 (2): 213–19. doi:10.1016/j.neuron.2005.09.009.

Mezan, Shaul, Jean Daniel Feuz, Bart Deplancke, and Sebastian Kadener. 2016. “PDF Signaling Is an Integral Part of the Drosophila Circadian Molecular Oscillator.” *Cell Reports* 17 (3). Cell Press: 708–19. doi:10.1016/J.CELREP.2016.09.048.

Mistlberger, Ralph E., Glenn J Landry, and Elliott G Marchant. 1997. “Sleep Deprivation Can Attenuate Light-Induced Phase Shifts of Circadian Rhythms in Hamsters.” *Neuroscience Letters* 238 (1–2): 5–8. doi:10.1016/S0304-3940(97)00815-X.

Miyasako, Yoko, Yujiro Umezaki, and Kenji Tomioka. 2007. “Separate Sets of Cerebral Clock Neurons Are Responsible for Light and Temperature Entrainment of Drosophila Circadian Locomotor Rhythms.” *Journal of Biological Rhythms* 22 (2): 115–26. doi:10.1177/0748730407299344.

Mohawk, Jennifer A., Carla B. Green, and Joseph S. Takahashi. 2012. “Central and Peripheral Circadian Clocks in Mammals.” *Annual Review of Neuroscience* 35 (1): 445–62. doi:10.1146/annurev-neuro-060909-153128.

Monyak, Rachel E., Danielle Emerson, Brian P. Schoenfeld, Xiangzhong Zheng, Daniel B.

Chambers, Cory Rosenfelt, Steven Langer, et al. 2017. “Insulin Signaling Misregulation Underlies Circadian and Cognitive Deficits in a Drosophila Fragile X Model.” *Molecular Psychiatry* 22 (8): 1140–48. doi:10.1038/mp.2016.51.

Muraro, N.I., N. Pírez, and M.F. Ceriani. 2013. “The Circadian System: Plasticity at Many Levels.” *Neuroscience* 247 (September): 280–93. doi:10.1016/j.neuroscience.2013.05.036.

Myers, Edith M, Jiujiu Yu, and Amita Sehgal. 2003. “Circadian Control of Eclosion: Interaction between a Central and Peripheral Clock in Drosophila Melanogaster.” *Current Biology : CB* 13 (6): 526–33.

Nakahara, Keiko, Reiko Hanada, Noboru Murakami, Hitoshi Teranishi, Hideko Ohgusu, Nobuhiro Fukushima, Maiko Moriyama, Takanori Ida, Kenji Kangawa, and Masayasu Kojima. 2004. “The Gut-Brain Peptide Neuromedin U Is Involved in the Mammalian Circadian Oscillator System.” *Biochemical and Biophysical Research Communications* 318 (1): 156–61. doi:10.1016/j.bbrc.2004.04.014.

Nässel, Dick R. 2018. “Substrates for Neuronal Cotransmission With Neuropeptides and Small Molecule Neurotransmitters in Drosophila.” *Frontiers in Cellular Neuroscience* 12 (March). doi:10.3389/fncel.2018.00083.

Nässel, Dick R., Olga I. Kubrak, Yiting Liu, Jiangnan Luo, and Oleh V. Lushchak. 2013. “Factors That Regulate Insulin Producing Cells and Their Output in Drosophila.” *Frontiers in Physiology* 4 (September): 252. doi:10.3389/fphys.2013.00252.

Nässel, Dick R., and Christian Wegener. 2011. “A Comparative Review of Short and Long Neuropeptide F Signaling in Invertebrates: Any Similarities to Vertebrate Neuropeptide Y Signaling?” *Peptides* 32 (6): 1335–55. doi:10.1016/j.peptides.2011.03.013.

Ng, Fanny S, and F Rob Jackson. 2015. “The ROP Vesicle Release Factor Is Required in Adult Drosophila Glia for Normal Circadian Behavior.” *Frontiers in Cellular Neuroscience* 9. Frontiers Media SA: 256. doi:10.3389/fncel.2015.00256.

Ng, Fanny S, Michelle M Tangredi, and F Rob Jackson. 2011. “Glial Cells Physiologically Modulate Clock Neurons and Circadian Behavior in a Calcium-Dependent Manner.” *Current Biology : CB* 21 (8): 625–34. doi:10.1016/j.cub.2011.03.027.

Nicolaï, Laura J J, Ariane Ramaekers, Tim Raemaekers, Andrzej Drozdzecki, Alex S Mauss, Jiekun Yan, Matthias Landgraf, Wim Annaert, and Bassem A Hassan. 2010. “Genetically Encoded Dendritic Marker Sheds Light on Neuronal Connectivity in Drosophila.” *Proceedings of the National Academy of Sciences of the United States of America* 107 (47): 20553–58. doi:10.1073/pnas.1010198107.

Nishiitsutsuji-Uwo, Junko, Stephen F. Petropulos, and Colin S. Pittendrigh. 1967. “Central Nervous System Control of Circadian Rhythmicity in the Cockroach. I. Role of the Pars Intercerebralis.” *The Biological Bulletin* 133 (3): 679–96. doi:10.2307/1539928.

Nitabach, Michael N., Justin Blau, and Todd C Holmes. 2002. “Electrical Silencing of Drosophila Pacemaker Neurons Stops the Free-Running Circadian Clock.” *Cell* 109 (4): 485–95.

Nusbaum, Michael P, Dawn M Blitz, and Eve Marder. 2017. “Functional Consequences of Neuropeptide and Small-Molecule Co-Transmission.” *Nature Reviews. Neuroscience* 18 (7): 389–403. doi:10.1038/nrn.2017.56.

Oh, Yangkyun, Sung-Eun Yoon, Qi Zhang, Hyo-Seok Chae, Ivana Daubnerová, Orie T. Shafer, Joonho Choe, and Young-Joon Kim. 2014. “A Homeostatic Sleep-Stabilizing Pathway in Drosophila Composed of the Sex Peptide Receptor and Its Ligand, the Myoinhibitory Peptide.” Edited by Paul Shaw. *PLoS Biology* 12 (10). Public Library of Science: e1001974. doi:10.1371/journal.pbio.1001974.

Ohhara, Yuya, Satoru Kobayashi, Kimiko Yamakawa-Kobayashi, and Naoki Yamanaka. 2018. “Adult-Specific Insulin-Producing Neurons in *Drosophila Melanogaster*.” *Journal of Comparative Neurology*, no. September 2017: 1–17. doi:10.1002/cne.24410.

Oishi, Katsutaka, Noriko Amagai, Hidenori Shirai, Koji Kadota, Naoki Ohkura, and Norio Ishida. 2005. “Genome-Wide Expression Analysis Reveals 100 Adrenal Gland-Dependent Circadian Genes in the Mouse Liver.” *DNA Research : An International Journal for Rapid Publication of Reports on Genes and Genomes* 12 (3): 191–202. doi:10.1093/dnares/dsi003.

Oishi, Katsutaka, Masayuki Shiota, Katsuhiko Sakamoto, Manami Kasamatsu, and Norio Ishida. 2004. “Feeding Is Not a More Potent Zeitgeber than the Light-Dark Cycle in Drosophila.” *Neuroreport* 15 (4): 739–43. doi:10.1097/01.wnr.00001.

Olsen, Shawn R, and Rachel I Wilson. 2008. “Cracking Neural Circuits in a Tiny Brain: New Approaches for Understanding the Neural Circuitry of Drosophila.” *Trends in Neurosciences* 31 (10): 512–20. doi:10.1016/j.tins.2008.07.006.

Parisky, Katherine M, José Agosto, Stefan R Pulver, Yuhua Shang, Elena Kuklin, James J L Hodge, Kyeongjin Kang, et al. 2008. “PDF Cells Are a GABA-Responsive Wake-Promoting Component of the Drosophila Sleep Circuit.” *Neuron* 60 (4): 672–82. doi:10.1016/j.neuron.2008.10.042.

Parisky, Katherine M, José L Agosto Rivera, Nathan C Donelson, Sejal Kotecha, and Leslie C. Griffith. 2016. “Reorganization of Sleep by Temperature in Drosophila Requires Light, the Homeostat, and the Circadian Clock.” *Current Biology : CB* 26 (7): 882–92. doi:10.1016/j.cub.2016.02.011.

Park, Jae H., Charlotte Helfrich-Förster, Gyunghee Lee, Li. Liu, Michael Rosbash, and Jeffrey C. Hall. 2000. “Differential Regulation of Circadian Pacemaker Output by Separate Clock Genes in Drosophila.” *Proceedings of the National Academy of Sciences* 97 (7). National Academy of Sciences: 3608–13. doi:10.1073/pnas.97.7.3608.

Peng, Ying, Dan Stoleru, Joel D. Levine, Jeffrey C. Hall, and Michael Rosbash. 2003. “Drosophila Free-Running Rhythms Require Intercellular Communication.” *PLoS Biology* 1 (1): E13. doi:10.1371/journal.pbio.0000013.

Petsakou, Afroditi, Themistoklis P. Sapsis, and Justin Blau. 2015. “Circadian Rhythms in Rho1 Activity Regulate Neuronal Plasticity and Network Hierarchy.” *Cell* 162 (4): 823–35. doi:10.1016/j.cell.2015.07.010.

Pfeiffer, Barret D, Teri-T B Ngo, Karen L Hibbard, Christine Murphy, Arnim Jenett, James W Truman, and Gerald M Rubin. 2010. “Refinement of Tools for Targeted Gene Expression in Drosophila.” *Genetics* 186 (2). Genetics Society of America: 735–55. doi:10.1534/genetics.110.119917.

Pfeiffer, Barret D, James W Truman, and Gerald M Rubin. 2012. “Using Translational Enhancers to Increase Transgene Expression in Drosophila.” *Proceedings of the National Academy of Sciences of the United States of America* 109 (17): 6626–31. doi:10.1073/pnas.1204520109.

Pimentel, Diogo, Jeffrey M. Donlea, Clifford B Talbot, Seoho M Song, Alexander J F Thurston, and Gero Miesenböck. 2016. “Operation of a Homeostatic Sleep Switch.” *Nature* 536 (7616): 333–37. doi:10.1038/nature19055.

Pírez, Nicolás, Bethany L Christmann, and Leslie C. Griffith. 2013. “Daily Rhythms in Locomotor Circuits in Drosophila Involve PDF.” *Journal of Neurophysiology* 110 (3): 700–708. doi:10.1152/jn.00126.2013.

Pitman, Jena L, Jermaine J McGill, Kevin P Keegan, and Ravi Allada. 2006. “A Dynamic Role for the Mushroom Bodies in Promoting Sleep in Drosophila.” *Nature* 441 (7094): 753–56. doi:10.1038/nature04739.

Plautz, Jeffrey D, Maki Kaneko, Jeffrey C. Hall, and Steve A Kay. 1997. “Independent Photoreceptive Circadian Clocks throughout Drosophila.” *Science (New York, N.Y.)* 278 (5343): 1632–35. doi:10.1126/science.278.5343.1632.

Port, Fillip, Hui-Min Chen, Tzumin Lee, and Simon L Bullock. 2014. “Optimized CRISPR/Cas Tools for Efficient Germline and Somatic Genome Engineering in Drosophila.” *Proceedings of the National Academy of Sciences of the United States of America* 111 (29). National Academy of Sciences: E2967-76. doi:10.1073/pnas.1405500111.

Pulver, Stefan R, Stanislav L Pashkovski, Nicholas J Hornstein, Paul A Garrity, and Leslie C. Griffith. 2009. “Temporal Dynamics of Neuronal Activation by Channelrhodopsin-2 and TRPA1 Determine Behavioral Output in Drosophila Larvae.” *Journal of Neurophysiology* 101 (6): 3075–88. doi:10.1152/jn.00071.2009.

Qian, Yongjun, Yue Cao, Bowen Deng, Guang Yang, Jiayun Li, Rui Xu, Dandan Zhang, Juan Huang, and Yi Rao. 2017. “Sleep Homeostasis Regulated by 5HT2b Receptor in a Small Subset of Neurons in the Dorsal Fan-Shaped Body of Drosophila.” *ELife* 6 (October). doi:10.7554/eLife.26519.

Rao, Sujata, Cynthia Lang, Edwin S. Levitan, and David L. Deitcher. 2001. “Fast Track: Visualization of Neuropeptide Expression, Transport, and Exocytosis in Drosophila Melanogaster.” *Journal of Neurobiology* 49 (3): 159–72. doi:10.1002/neu.1072.

Reddy, Akhilesh B., Elizabeth S. Maywood, Natasha a. Karp, Verdun M. King, Yusuke Inoue, Frank J. Gonzalez, Kathryn S. Lilley, Charalambos P. Kyriacou, and Michael H. Hastings. 2007. “Glucocorticoid Signaling Synchronizes the Liver Circadian Transcriptome.” *Hepatology* 45 (6): 1478–88. doi:10.1002/hep.21571.

Renn, Susan C., Jae H Park, Michael Rosbash, Jeffrey C. Hall, and Paul H. Taghert. 1999. “A Pdf Neuropeptide Gene Mutation and Ablation of PDF Neurons Each Cause Severe Abnormalities of Behavioral Circadian Rhythms in Drosophila.” *Cell* 99 (7): 791–802. doi:10.1016/S0092-8674(00)81676-1.

Ro, Jennifer, Zachary M. Harvanek, and Scott D. Pletcher. 2014. “FLIC: High-Throughput, Continuous Analysis of Feeding Behaviors in Drosophila.” *PloS One* 9 (6). Public Library of Science: e101107. doi:10.1371/journal.pone.0101107.

Roenneberg, Till, and Martha Merrow. 2016. “The Circadian Clock and Human Health.” *Current Biology* 26 (10): R432–43. doi:10.1016/j.cub.2016.04.011.

Ryder, Edward, Fiona Blows, Michael Ashburner, Rosa Bautista-Llacer, Darin Coulson, Jenny Drummond, Jane Webster, et al. 2004. “The DrosDel Collection: A Set of P-Element Insertions for Generating Custom Chromosomal Aberrations in Drosophila Melanogaster.” *Genetics* 167 (2): 797–813. doi:10.1534/genetics.104.026658.

Sakai, Takaomi, and Norio Ishida. 2001. “Circadian Rhythms of Female Mating Activity Governed by Clock Genes in Drosophila.” *Proceedings of the National Academy of Sciences* 98 (16): 9221–25. doi:10.1073/pnas.151443298.

Schindelin, Johannes, Ignacio Arganda-Carreras, Erwin Frise, Verena Kaynig, Mark Longair, Tobias Pietzsch, Stephan Preibisch, et al. 2012. “Fiji: An Open-Source Platform for Biological-Image Analysis.” *Nature Methods* 9 (7): 676–82. doi:10.1038/nmeth.2019.

Schlegel, Philipp, Michael J Texada, Anton Miroschnikow, Andreas Schoofs, Sebastian Hückesfeld, Marc Peters, Casey M Schneider-Mizell, et al. 2016. “Synaptic Transmission

Parallels Neuromodulation in a Central Food-Intake Circuit." *ELife* 5 (November). eLife Sciences Publications Limited: 462–65. doi:10.7554/eLife.16799.

Schmid, Andreas, Stefan Hallermann, Robert J Kittel, Omid Khorramshahi, Andreas M J Frölich, Christine Quentin, Tobias M Rasse, Sara Mertel, Manfred Heckmann, and Stephan J Sigrist. 2008. "Activity-Dependent Site-Specific Changes of Glutamate Receptor Composition in Vivo." *Nature Neuroscience* 11 (6): 659–66. doi:10.1038/nn.2122.

Seay, Daniel J., and Carl S. Thummel. 2011. "The Circadian Clock, Light, and Cryptochrome Regulate Feeding and Metabolism in Drosophila." *Journal of Biological Rhythms* 26 (6): 497–506. doi:10.1177/0748730411420080.

Seidner, Glen, James E. Robinson, Meilin Wu, Kurtresha Worden, Pavel Masek, Stephen W. Roberts, Alex C. Keene, and William J. Joiner. 2015. "Identification of Neurons with a Privileged Role in Sleep Homeostasis in Drosophila Melanogaster." *Current Biology* 25 (22). Elsevier: 2928–38. doi:10.1016/j.cub.2015.10.006.

Selcho, Mareike, Carola Millán, Angelina Palacios-Muñoz, Franziska Ruf, Lilian Ubillo, Jiangtian Chen, Gregor Bergmann, et al. 2017. "Central and Peripheral Clocks Are Coupled by a Neuropeptide Pathway in Drosophila." *Nature Communications* 8 (May). Nature Publishing Group: 15563. doi:10.1038/ncomms15563.

Seluzicki, Adam, Matthieu Flourakis, Elzbieta Kula-Eversole, Luoying Zhang, Valerie Kilman, and Ravi Allada. 2014. "Dual PDF Signaling Pathways Reset Clocks via TIMELESS and Acutely Excite Target Neurons to Control Circadian Behavior." *PLoS Biology* 12 (3): e1001810. doi:10.1371/journal.pbio.1001810.

Shafer, Orie T., Dong Jo Kim, Richard Dunbar-Yaffe, Viacheslav O Nikolaev, Martin J Lohse, and Paul H. Taghert. 2008. "Widespread Receptivity to Neuropeptide PDF throughout the Neuronal Circadian Clock Network of Drosophila Revealed by Real-Time Cyclic AMP Imaging." *Neuron* 58 (2): 223–37. doi:10.1016/j.neuron.2008.02.018.

Shafer, Orie T., and Paul H. Taghert. 2009. "RNA-Interference Knockdown of Drosophila Pigment Dispersing Factor in Neuronal Subsets: The Anatomical Basis of a Neuropeptide's Circadian Functions." Edited by Michael N. Nitabach. *PloS One* 4 (12). Public Library of Science: e8298. doi:10.1371/journal.pone.0008298.

Shafer, Orie T., and Zepeng Yao. 2014. "Pigment-Dispersing Factor Signaling and Circadian Rhythms in Insect Locomotor Activity." *Current Opinion in Insect Science* 1 (July). Elsevier: 73–80. doi:10.1016/j.cois.2014.05.002.

Shakiryanova, Dinara, Arvonn Tully, Randall S Hewes, David L. Deitcher, and Edwin S. Levitan. 2005. "Activity-Dependent Liberation of Synaptic Neuropeptide Vesicles." *Nature Neuroscience* 8 (2). Nature Publishing Group: 173–78. doi:10.1038/nn1377.

Shang, Yuhua, Nathan C. Donelson, Christopher G. Vecsey, Fang Guo, Michael Rosbash, and Leslie C. Griffith. 2013. "Short Neuropeptide F Is a Sleep-Promoting Inhibitory Modulator." *Neuron* 80 (1): 171–83. doi:10.1016/j.neuron.2013.07.029.

Shang, Yuhua, Leslie C. Griffith, and Michael Rosbash. 2008. "Light-Arousal and Circadian Photoreception Circuits Intersect at the Large PDF Cells of the Drosophila Brain." *Proceedings of the National Academy of Sciences of the United States of America* 105 (50): 19587–94. doi:10.1073/pnas.0809577105.

Shearin, Harold K., Alisa R. Dvarishkis, Craig D. Kozeluh, and R. Steven Stowers. 2013. "Expansion of the Gateway Multisite Recombination Cloning Toolkit." *PloS One* 8 (10). Public Library of Science: e77724. doi:10.1371/journal.pone.0077724.

Sheeba, Vasu, Keri J Fogle, Maki Kaneko, Saima Rashid, Yu-Ting Chou, Vijay K Sharma, and

Todd C Holmes. 2008. “Large Ventral Lateral Neurons Modulate Arousal and Sleep in Drosophila.” *Current Biology : CB* 18 (20): 1537–45. doi:10.1016/j.cub.2008.08.033.

Sheeba, Vasu, Huaiyu Gu, Vijay K Sharma, Diane K. O’Dowd, and Todd C. Holmes. 2008. “Circadian- and Light-Dependent Regulation of Resting Membrane Potential and Spontaneous Action Potential Firing of Drosophila Circadian Pacemaker Neurons.” *Journal of Neurophysiology* 99 (2): 976–88. doi:10.1152/jn.00930.2007.

Sitaraman, Divya, Yoshinori Aso, Xin Jin, Nan Chen, Mario Felix, Gerald M. Rubin, and Michael N. Nitabach. 2015. “Propagation of Homeostatic Sleep Signals by Segregated Synaptic Microcircuits of the Drosophila Mushroom Body.” *Current Biology* 25 (22). Elsevier Ltd: 2915–27. doi:10.1016/j.cub.2015.09.017.

Sivachenko, Anna, Yue Li, Katharine C Abruzzi, and Michael Rosbash. 2013. “The Transcription Factor Mef2 Links the Drosophila Core Clock to Fas2, Neuronal Morphology, and Circadian Behavior.” *Neuron* 79 (2). Elsevier Inc.: 281–92. doi:10.1016/j.neuron.2013.05.015.

Spandidos, Athanasia, Xiaowei Wang, Huajun Wang, Stefan Dragnev, Tara Thurber, and Brian Seed. 2008. “A Comprehensive Collection of Experimentally Validated Primers for Polymerase Chain Reaction Quantitation of Murine Transcript Abundance.” *BMC Genomics* 9: 633. doi:10.1186/1471-2164-9-633.

Spandidos, Athanasia, Xiaowei Wang, Huajun Wang, and Brian Seed. 2010. “PrimerBank: A Resource of Human and Mouse PCR Primer Pairs for Gene Expression Detection and Quantification.” *Nucleic Acids Research* 38 (Database issue): D792-9. doi:10.1093/nar/gkp1005.

Spina, M., E. Merlo-Pich, R K Chan, A. M. Basso, J. Rivier, W. Vale, and G. F. Koob. 1996. “Appetite-Suppressing Effects of Urocortin, a CRF-Related Neuropeptide.” *Science (New York, N.Y.)* 273 (5281). American Association for the Advancement of Science: 1561–64. doi:10.1126/science.273.5281.1561.

Stengel, Andreas, and Yvette Taché. 2014. “CRF and Urocortin Peptides as Modulators of Energy Balance and Feeding Behavior during Stress.” *Frontiers in Neuroscience* 8 (January): 52. doi:10.3389/fnins.2014.00052.

Stoleru, Dan, Ying Peng, José Agosto, and Michael Rosbash. 2004. “Coupled Oscillators Control Morning and Evening Locomotor Behaviour of Drosophila.” *Nature* 431 (7010). Nature Publishing Group: 862–68. doi:10.1038/nature02926.

Stoleru, Dan, Ying Peng, Pipat Nawathean, and Michael Rosbash. 2005. “A Resetting Signal between Drosophila Pacemakers Synchronizes Morning and Evening Activity.” *Nature* 438 (7065): 238–42. doi:10.1038/nature04192.

Suh, Joowon, and F Rob Jackson. 2007. “Drosophila Ebony Activity Is Required in Glia for the Circadian Regulation of Locomotor Activity.” *Neuron* 55 (3): 435–47. doi:10.1016/j.neuron.2007.06.038.

Talay, Mustafa, Ethan B. Richman, Nathaniel J. Snell, Griffin G. Hartmann, John D. Fisher, Altar Sorkaç, Juan F. Santoyo, et al. 2017. “Transsynaptic Mapping of Second-Order Taste Neurons in Flies by Trans-Tango.” *Neuron* 96 (4). Cell Press: 783–795.e4. doi:10.1016/J.NEURON.2017.10.011.

Tang, Xin, Sanne Roessingh, Sean E Hayley, Michelle L Chu, Nobuaki K Tanaka, Werner Wolfgang, Seongho Song, Ralf Stanewsky, and Fumika N. Hamada. 2017. “The Role of PDF Neurons in Setting the Preferred Temperature before Dawn in Drosophila.” *ELife* 6 (May). eLife Sciences Publications Limited: e23206. doi:10.7554/eLife.23206.

Tanoue, Shintaro, Parthasarathy Krishnan, Balaji Krishnan, Stuart E. Dryer, and Paul E. Hardin.

2004. “Circadian Clocks in Antennal Neurons Are Necessary and Sufficient for Olfaction Rhythms in Drosophila.” *Current Biology* 14: 638–49. doi:10.1016/j.cub.2004.04.009.

Terhzaz, Selim, Philippe Rosay, Stephen F Goodwin, and Jan A Veenstra. 2007. “The Neuropeptide SIFamide Modulates Sexual Behavior in Drosophila.” *Biochemical and Biophysical Research Communications* 352 (2): 305–10. doi:10.1016/j.bbrc.2006.11.030.

Thevenaz, P., U.E. Ruttimann, and M. Unser. 1998. “A Pyramid Approach to Subpixel Registration Based on Intensity.” *IEEE Transactions on Image Processing* 7 (1): 27–41. doi:10.1109/83.650848.

Turek, Fred W., Corinne Joshu, Akira Kohsaka, Emily Lin, Ganka Ivanova, Erin McDearmon, Aaron Laposky, et al. 2005. “Obesity and Metabolic Syndrome in Circadian Clock Mutant Mice.” *Science (New York, N.Y.)* 308 (5724): 1043–45. doi:10.1126/science.1108750.

Ueno, Taro, Jun Tomita, Hiromu Tanimoto, Keita Endo, Kei Ito, Shoen Kume, and Kazuhiko Kume. 2012. “Identification of a Dopamine Pathway That Regulates Sleep and Arousal in Drosophila.” *Nature Neuroscience* 15 (11): 1516–23. doi:10.1038/nn.3238.

Urban, J H, A C Bauer-Dantoin, and J E Levine. 1993. “Neuropeptide Y Gene Expression in the Arcuate Nucleus: Sexual Dimorphism and Modulation by Testosterone.” *Endocrinology* 132 (1): 139–45. doi:10.1210/endo.132.1.8419120.

Vecsey, Christopher G., Nicolás Pírez, and Leslie C. Griffith. 2014. “The Drosophila Neuropeptides PDF and SNPF Have Opposing Electrophysiological and Molecular Effects on Central Neurons.” *Journal of Neurophysiology* 111 (5): 1033–45. doi:10.1152/jn.00712.2013.

Vollmers, Christopher, Shubhroz Gill, Luciano DiTacchio, Sandhya R Pulivarthy, Hiep D Le, and Satchidananda Panda. 2009. “Time of Feeding and the Intrinsic Circadian Clock Drive Rhythms in Hepatic Gene Expression.” *Proceedings of the National Academy of Sciences of the United States of America* 106 (50): 21453–58. doi:10.1073/pnas.0909591106.

Wang, Xiaowei, and Brian Seed. 2003. “A PCR Primer Bank for Quantitative Gene Expression Analysis.” *Nucleic Acids Research* 31 (24): 154–61. doi:10.1093/nar/gng154.

Weber, Paweł, Elzbieta Kula-Eversole, and Elzbieta Pyza. 2009. “Circadian Control of Dendrite Morphology in the Visual System of Drosophila Melanogaster.” *PloS One* 4 (1): e4290. doi:10.1371/journal.pone.0004290.

White, Kristin, Elvan Tahaoglu, and Hermann Steller. 1996. “Cell Killing by the Drosophila Gene Reaper.” *Science* 271 (5250). American Association for the Advancement of Science: 805–7. doi:10.1126/science.271.5250.805.

Wijnen, Herman, Felix Naef, Catharine Boothroyd, Adam Claridge-Chang, and Michael W. Young. 2006. “Control of Daily Transcript Oscillations in Drosophila by Light and the Circadian Clock.” *PLoS Genetics* 2 (3): e39. doi:10.1371/journal.pgen.0020039.

Wijnen, Herman, and Michael W. Young. 2006. “Interplay of Circadian Clocks and Metabolic Rhythms.” *Annual Review of Genetics* 40 (1): 409–48. doi:10.1146/annurev.genet.40.110405.090603.

Williams, Julie A., Henry S Su, Andre Bernards, Jeffrey Field, and Amita Sehgal. 2001. “A Circadian Output in Drosophila Mediated by Neurofibromatosis-1 and Ras/MAPK.” *Science (New York, N.Y.)* 293 (5538): 2251–56. doi:10.1126/science.1063097.

Wu, Qi, Tieqiao Wen, Gyunghee Lee, Jae H. Park, Haini N. Cai, and Ping Shen. 2003. “Developmental Control of Foraging and Social Behavior by the Drosophila Neuropeptide Y-like System.” *Neuron* 39 (1): 147–61. doi:10.1016/S0896-6273(03)00396-9.

Wu, Qi, Zhangwu Zhao, and Ping Shen. 2005. “Regulation of Aversion to Noxious Food by Drosophila Neuropeptide Y- and Insulin-like Systems.” *Nature Neuroscience* 8 (10): 1350–55. doi:10.1038/nn1540.

Wülbeck, Corinna, Eva Grieshaber, and Charlotte Helfrich-Förster. 2008. “Pigment-Dispersing Factor (PDF) Has Different Effects on Drosophila’s Circadian Clocks in the Accessory Medulla and in the Dorsal Brain.” *Journal of Biological Rhythms* 23 (5): 409–24. doi:10.1177/0748730408322699.

Xu, Kanyan, Justin R. DiAngelo, Michael E. Hughes, John B. Hogenesch, and Amita Sehgal. 2011. “The Circadian Clock Interacts with Metabolic Physiology to Influence Reproductive Fitness.” *Cell Metabolism* 13 (6). Elsevier Inc.: 639–54. doi:10.1016/j.cmet.2011.05.001.

Xu, Kanyan, Xiangzhong Zheng, and Amita Sehgal. 2008. “Regulation of Feeding and Metabolism by Neuronal and Peripheral Clocks in Drosophila.” *Cell Metabolism* 8 (4): 289–300. doi:10.1016/j.cmet.2008.09.006.

Yadlapalli, Swathi, Chang Jiang, Andrew Bahle, Pramod Reddy, Edgar Meyhofer, and Orie T Shafer. 2018. “Circadian Clock Neurons Constantly Monitor Environmental Temperature to Set Sleep Timing.” *Nature* 555 (7694): 98–102. doi:10.1038/nature25740.

Yannielli, P., and M.E. Harrington. 2004. “Let There Be ‘More’ Light: Enhancement of Light Actions on the Circadian System through Non-Photic Pathways.” *Progress in Neurobiology* 74 (1): 59–76. doi:10.1016/j.pneurobio.2004.06.001.

Yao, Zepeng, Ann Marie Macara, Katherine R Lelito, Tamara Y Minosyan, and Orie T. Shafer. 2012. “Analysis of Functional Neuronal Connectivity in the Drosophila Brain.” *Journal of Neurophysiology* 108 (2): 684–96. doi:10.1152/jn.00110.2012.

Yao, Zepeng, and Orie T. Shafer. 2014. “The Drosophila Circadian Clock Is a Variably Coupled Network of Multiple Peptidergic Units.” *Science (New York, N.Y.)* 343 (6178): 1516–20. doi:10.1126/science.1251285.

Yap, Melvyn H W, Martyna J Grabowska, Chelsie Rohrscheib, Rhiannon Jeans, Michael Troup, Angelique C Paulk, Bart van Alphen, Paul J Shaw, and Bruno van Swinderen. 2017. “Oscillatory Brain Activity in Spontaneous and Induced Sleep Stages in Flies.” *Nature Communications* 8 (1): 1815. doi:10.1038/s41467-017-02024-y.

Yasuyama, Kouji, and Ian A. Meinertzhagen. 2010. “Synaptic Connections of PDF-Immunoreactive Lateral Neurons Projecting to the Dorsal Protocerebrum of Drosophila Melanogaster.” *The Journal of Comparative Neurology* 518 (3). Wiley-Blackwell: 292–304. doi:10.1002/cne.22210.

Yoshii, Taishi, Christiane Hermann-Luibl, and Charlotte Helfrich-Förster. 2016. “Circadian Light-Input Pathways in Drosophila.” *Communicative & Integrative Biology* 9 (1): e1102805. doi:10.1080/19420889.2015.1102805.

Yoshii, Taishi, Christiane Hermann, and Charlotte Helfrich-Förster. 2010. “Cryptochrome-Positive and -Negative Clock Neurons in Drosophila Entrain Differentially to Light and Temperature.” *Journal of Biological Rhythms* 25 (6): 387–98. doi:10.1177/0748730410381962.

Yoshii, Taishi, Corinna Wülbeck, Hana Sehadova, Shobi Veleri, Dominik Bichler, Ralf Stanewsky, and Charlotte Helfrich-Förster. 2009. “The Neuropeptide Pigment-Dispersing Factor Adjusts Period and Phase of Drosophila’s Clock.” *The Journal of Neuroscience : The Official Journal of the Society for Neuroscience* 29 (8): 2597–2610. doi:10.1523/JNEUROSCI.5439-08.2009.

Zerr, Danielle M., Jeffrey C. Hall, Michael Rosbash, and Kathleen K. Siwicki. 1990. “Circadian Fluctuations of Period Protein Immunoreactivity in the CNS and the Visual System of

Drosophila." *The Journal of Neuroscience* 10 (8): 2749–62. doi:10.1523/JNEUROSCI.10-08-02749.1990.

Zhan, Yin Peng, Li Liu, and Yan Zhu. 2016. "Taotie Neurons Regulate Appetite in Drosophila." *Nature Communications* 7 (December). Nature Publishing Group: 13633. doi:10.1038/ncomms13633.

Zhang, Luoying, Brian Y. Chung, Bridget C. Lear, Valerie L. Kilman, Yixiao Liu, Guruswamy Mahesh, Rose-Anne Anne Meissner, Paul E. Hardin, and Ravi Allada. 2010. "DN1p Circadian Neurons Coordinate Acute Light and PDF Inputs to Produce Robust Daily Behavior in Drosophila." *Current Biology* 20 (7): 591–99. doi:10.1016/j.cub.2010.02.056.

Zhang, Ray, Nicholas F. Lahens, Heather I. Ballance, Michael E. Hughes, and John B. Hogenesch. 2014. "A Circadian Gene Expression Atlas in Mammals: Implications for Biology and Medicine." *Proceedings of the National Academy of Sciences* 111 (45): 16219–24. doi:10.1073/pnas.1408886111.

Zhang, Shirley L, Zhifeng Yue, Denice M Arnold, Gregory Artiushin, and Amita Sehgal. 2018. "A Circadian Clock in the Blood-Brain Barrier Regulates Xenobiotic Efflux." *Cell* 173 (1): 130–139.e10. doi:10.1016/j.cell.2018.02.017.

Zhang, Yong, Yixiao Liu, Diana Bilodeau-Wentworth, Paul E. Hardin, and Patrick Emery. 2010. "Light and Temperature Control the Contribution of Specific DN1 Neurons to Drosophila Circadian Behavior." *Current Biology : CB* 20 (7): 600–605. doi:10.1016/j.cub.2010.02.044.

Zhang, Yong Q, Christopher K Rodesch, and Kendal Broadie. 2000. "Living Synaptic Vesicle Marker: Synaptotagmin-GFP." *Genesis* 34 (1–2): 142–45. doi:10.1002/gene.10144.

Zheng, Xiangzhong, and Amita Sehgal. 2012. "Speed Control: Cogs and Gears That Drive the Circadian Clock." *Trends in Neurosciences* 35 (9): 574–85. doi:10.1016/j.tins.2012.05.007.